Uranium and Thorium Complexes with Aroylbis(*N*,*N*-dialkylthioureas)

Inaugural-Dissertation

to obtain the academic degree

Doctor rerum naturalium (Dr. rer. nat.)

submitted to the Department of Biology, Chemistry and Pharmacy
of Freie Universität Berlin

by

CHRISTELLE NJIKI NOUFELE

from Bangwa (Cameroon)

2018

1. Gutachter: Prof. Dr. Ulrich Abram

2. Gutachter: Prof. Dr. Nora Kulak

Disputation am: 19.02.2018

"You do not shoot at a flower to grow it.

You water it and watch it grow ... patiently. "

African proverb.

Acknowledgment

First and foremost, I would like to thank my doctoral supervisor Prof. Dr. Ulrich Abram for the interesting and challenging topic. During this research time, he had been a great support in both domain, professional and extra-professional endeavors, offering valuable expertise support and advices.

I thank Prof. Dr. Nora Kulak for the willingness to prepare and conduct the second appraisal.

Several people have made a great contribution to the completion of this work and I would like to thank them. First, I would like to thank Dr. Adelheid Hagenbach for the countless hours of work and her great patience, in the measurement and refinement of my crystals, and her assistance addressing all my concerns. Thank you, Detlef Wille for measuring my samples using elemental analysis and for the introduction to LSC measurements. I cordially thank Jacqueline Grewe "the queen of Google" for her energetic support during the past years, especially during the writing phase. Her stories and exhilarating humor have often conjured a laugh in my face.

I would also like to thank the HZDR (Helmholtz-Zentrum Dresden-Rossendorf) for welcoming me and the privileged working conditions that were offered to me, especially Dr. Juliane März for her constant support and availability and Dr. Michael Patzschke for the informative discussions on DFT calculations.

I thank the former and current members of the AG Abram, who have provided a cooperative, friendly and familial working atmosphere. Special thanks go to Dr. Jecob Jegatesh and Dr. Pham Chien Thang for the introduction into the chemistry of aroylthioureas, and Clemens Scholtysik for the valuable discussions on NMR spectroscopy. Particular Thanks to Dr. Janine Ackermann and Sarah Hildebrandt for the permanent support in the extra-university matters.

I thank my research students, Dennis Schulze, Simon Suhr, Yogita Joshi and Sandra Mierschink for their interest, cooperation and support to my research topic.

This work could not have been completed without financial support, which went far beyond my expectations. A big thank you to the Rosa Luxemburg Foundation for giving me material and financial support.

A big thank you to my friends, Cynthia Kembuan, Monique and Norbert Anselm, Patrick Ngono Abe and Sandra Foso Noukele. What would I be without you?

I thank the Insearch Network, particularly, Dr. Babila Tachu for his great support.

My special thanks go to my family, those people who believed in me and who allowed me to attain the end of this work. Thank you, Bonie, you are my mentor and idol. Joyce, no words can describe your amazing contribution in my life, be blessed. Naily S, Yves-Kevin, Gaëlle and Mary, thank you

for your unconditional support from near and far. Papa and Maman, thank you for all your sacrifices, to make me what I am today, I hope I have made you proud.

I cannot close this chapter of my life without thanking God Almighty, for giving me the necessary strength and the audacity to overcome the difficulties faced in the past years

To my husband, Thierry Djoumatchoua and our children Lakisha, Ayanna and Kesaiah.

You are my inexhaustible sources of inspiration and energy.

Danksagung

An erster Stelle, möchte ich meinem Doktorvater Prof. Dr. Ulrich Abram für die interessante und herausfordernde Themenstellung danken. Während dieser Forschungsarbeit stand er mir, durch ständige Unterstützung, Verfügbarkeit und Beratung sachkundig und wertvoll zur Seite.

Ich danke Prof. Dr. Nora Kulak für die Bereitschaft zur Anfertigung des Zweitgutachtens.

Mehrere Personen haben einen großen Beitrag zur Vervollständigung dieser Arbeit geleistet und ich möchte mich hier dafür herzlichst bedanken. Zuallererst möchte ich Dr. Adelheid Hagenbach für die unzähligen Stunden und ihre große Geduld bei der Messung und Verfeinerung meiner Kristalle sowie ihre Hilfestellung in all meinen Belangen danken. Bei Herrn Detlef Wille möchte ich mich für das Messen meiner Proben mittels Elementaranalyse und die Einführung in die LSC Messtechnik bedanken. Jacqueline Grewe, der „Königin des Googlen" danke ich von Herzen für die tatkräftige Unterstützung in all den vergangenen Jahren, vor allem in der Schreibphase. Ihre Geschichten und erheiternder Humor haben mir des Öfteren ein Lachen ins Gesicht gezaubert.

Ich möchte mich auch beim HZDR (Helmholtz-Zentrum Dresden-Rossendorf) für die Möglichkeit zur Arbeit und die hervorragenden Arbeitsbedingungen, bedanken. Insbesondere danke ich Dr. Juliane März für ihre ständige Unterstützung und Verfügbarkeit, sowie Dr. Michael Patzschke für die lehrreichen Diskussionen zu DFT-Berechnungen.

Den ehemaligen und aktuellen Mitgliedern der AG Abram danke ich für die kollegiale, freundliche und familiäre Arbeitsatmosphäre. Mein besonderer Dank gilt Dr. Jecob Jegatesh und Dr. Pham Chien Thang für die Einführung in die Chemie der Aroylthioharnstoffe. Clemens Scholtysik danke ich für die lehrreichen Diskussionen über NMR Spektroskopie. Dr. Janine Ackermann und Sarah Hildebrandt danke ich besonders für die immer vorhandene Unterstützung vor allen in außeruniversitären Belangen.

Meinen Forschungspraktikanten Dennis Schulze, Yogita Joshi, Simon Suhr und Sandra Mierschink danke ich für deren Interesse, Mitarbeit und Unterstützung an meinem Forschungsthema.

Diese Arbeit hätte ohne finanzielle Unterstützung nicht abgeschlossen werden können. Ein großes Dankeschön an die Rosa-Luxemburg-Stiftung für ihre großzügige materielle und finanzielle Förderung.

Ein großes Dankeschön an meine Freunde, Cynthia Kembuan, Monique und Norbert Anselm, Patrick Ngono Abe und Sandra Foso Noukele. Was wäre ich ohne euch?

Ich danke dem Insearch Network, insbesondere Dr. Babila Tachu für seine großartige Unterstützung.

Mein Dank gilt vor allem meiner Familie, jenen Menschen, die an mich geglaubt haben und die es mir erlaubt haben, das Ende dieser Arbeit zu erreichen. Danke dir, Bonie, du bist mein Mentor und Idol. Joyce, keine Worte können deinen Beitrag in meinem Leben beschreiben, sei gesegnet. Naily S, Yves-Kevin, Gaëlle und Mary, danke für eure bedingungslose Unterstützung von nah und fern. Papa und Maman, für all euer Opfer, um mich zu dem zu machen, was ich heute bin, ich hoffe, ihr seid stolz auf mich.

Ich kann dieses Kapitel meines Lebens nicht beenden, ohne dem allmächtigen Gott zu danken, dass er mich mit genug Kraft und Mut belohnt hat, um die Hürde der letzten Jahre zu überwinden.

Für meinen Mann, Thierry Djoumatchoua und unsere Kindern Lakisha, Ayanna und Kesaiah

Ihr seid für mich unerschöpfliche Quellen an Inspiration und Energie.

Remerciements

Je tiens premièrement à exprimer mes plus vifs remerciements à Prof. Dr. Ulrich Abram qui fut pour moi un directeur de thèse attentif et disponible malgré ses nombreuses charges. Tout au long de ce travail de recherche, sa compétence, sa rigueur scientifique ainsi que ses précieux conseils m'ont beaucoup appris, surtout à devenir plus autonome tout au long de ce travail de recherche.

Je remercie également Prof. Dr. Nora Kulak, pour avoir accepté d'établir la seconde évaluation de cette thèse.

J'adresse toute ma gratitude à toutes les personnes qui m'ont aidé dans la réalisation de ce travail. Je remercie particulièrement Madame Adelheid Hagenbach pour sa grande patience et les innombrables heures passées pour l'analyse structurelle de mes cristaux et pour son aide dans toutes mes préoccupations, académiques et personnelles. Je remercie Monsieur Detlef Wille pour les mesures d'analyse élémentaire et pour l'introduction à la technique LSC. Un grand Merci à Madame Jacqueline Grewe, „la reine de Google" pour m'avoir permis de travailler dans d'aussi bonnes conditions et spécialement pour son soutien énergique au cours de ces dernières années, particulièrement dans la phase de rédaction. Ses anecdotes et son humour exaltant m'ont très souvent arrachée un fou rire.

Je tiens également à remercier le HZDR (Helmholtz-Zentrum Dresden-Rossendorf) pour l'accueil et les conditions de travail privilégiées qui m'y ont été offertes. Plus particulièrement, Dr. Juliane März pour son appui, son temps et ses conseils ainsi que Dr. Michael Patzschke pour les discussions concernant les calculs DFT.

Je remercie tous les membres et ex-membres du groupe AG Abram pour le climat de travail sympathique et convivial. Particulièrement Dr. Jecob Jegatesh et Dr. Pham Chien Thang pour l'introduction dans le passionnant domaine des molécules Aroylbisthioureas. Merci à Clemens Scholtysik pour nos échanges instructifs concernant la spectroscopie NMR. Un grand Merci á Dr. Janine Ackermann et Sarah Hildebrandt pour leur incroyable soutien surtout dans les questions para-universitaires.

Je remercie mes étudiants, Dennis Schulze, Simon Suhr, Yogita Joshi et Sandra Mierschink pour leurs support et intérêt pour mes travaux de recherche.

Ce travail n'aurait pu être mené à bien sans l'aide d'un financement qui, pour ma part est allé bien au-delà de mes expectations. Un grand Merci à la Rosa-Luxemburg-Stiftung pour leur soutien matériel et financier.

Un grand Merci à mes amis, Cynthia Kembuan, Monique et Norbert Anselm, Patrick Abe, Sandra Foso. Que serais-je sans vous ?

Mes remerciements s'adressent aussi à l'association Insearch Network, notamment au Dr. Babila Tachu pour son aide précieuse lors de la rédaction de cette thèse.

Mes remerciements vont surtout à ma famille, ces personnes qui ont cru en moi et qui m'ont permis d'arriver au bout de cette thèse. Merci à toi Bonie, tu es mon mentor et mon idole. Joyce, aucun mot ne peut décrire ton apport dans ma vie, soit bénie. Naily S, Yves-Kevin, Gaëlle et Mary, merci pour votre soutien inconditionnel, de près comme de loin. Papa et Maman, un grand Merci pour tous vos sacrifices pour faire de moi ce que je suis aujourd'hui, j'espère vous avoir rendu fier.

Je ne saurai clôturer ce chapitre de ma vie sans remercier le bon Dieu, tout puissant, de m'avoir gratifié d'assez de force et d'audace pour surpasser les difficultés affrontées ces dernières années.

À mon mari, Thierry Djoumatchoua et nos enfants Lakisha, Ayanna et Kesaiah.

Vous êtes mes sources intarissables d'inspiration et d'énergie.

Table of contents

1 Introduction 1

1.1 Fundamentals of uranium and thorium chemistry 1

1.2 The chemistry of aroylthioureas 2

2 Results and Discussion 7

2.1 Aroylbis(*N*,*N*-dialkylthioureas) 7

2.2 Uranyl complexes with aroylbis(*N*,*N*-dialkylthioureas), H_2L^1, H_2L^2 and H_2L^3 10

2.2.1 Complexes with isophthaloylbis(*N*,*N*-diethylthiourea), H_2L^1 11

2.2.2 Complexes with pyridine-2,6-dicarbonylbis(*N*,*N*-dialkylthioureas), H_2L^{2a} and H_2L^{2a} 18

2.2.3 Synthesis and structure of $[UO_2(L^3)]$ 24

2.2.4 Stability tests of the complexes obtained from H_2L^1, H_2L^2 and H_2L^3 25

2.3 Oligonuclear uranyl complexes with H_2L^2 30

2.4 Mixed-metal complexes of H_2L^2 with uranyl and transition or post-transition metal ions 50

2.4.1 A uranyl complex with H_2L^{2a} and gold(I) 50

2.4.2 A uranyl complex with H_2L^{2a} and lead(II) 53

2.4.3 Uranyl complexes with H_2L^2 and divalent transition metal ions (Zn^{2+}, Ni^{2+}, Co^{2+}, Fe^{2+}, Mn^{2+} and Cd^{2+}). 56

2.5 Complexes of H_2L^{2a} and H_2L^3 with Thorium(IV) and Uranium(IV). 67

2.5.1 Thorium(IV) complexes with H_2L^{2a} 67

2.5.2 Uranium(IV) complexes with H_2L^{2a} 70

2.5.3 Thorium(IV) complexes with H_2L^3 73

3 Experimental section 76

3.1 Starting materials 76

3.2 Analytical methods 76

3.3 Crystal structure determination 77

3.4 Syntheses 79

3.4.1 Ligands 79

3.4.2 Uranyl complexes 85

3.4.3 Mixed-metal complexes of uranium with transition and post-transition metals 96

3.4.4 Complexes with Uranium(IV) and Thorium (IV) 104

3.5 Stability and hydrolysis studies 106

4 Summary 107
5 Zusammenfassung 111
6 References 115
Appendix 123
Crystallographic data 125
Cartesian coordinates of the calculated molecules 261

Symbols and Abbreviations

AcOH	Acetic acid
bipy	Bipyridine
BTP	2,6-Bis(5,6-dialkyl-1,2,4-triazin-3-yl)pyridine
BTBP	6,6'-Bis(5,6-dialkyl-1,2,4-triazin-3-yl)-2,2'-bipyridine
Calcd.	calculated
d; q; t	Doublet; Quartet; Triplet (NMR)
DFT	Density Functional Theory
DIDPA	**D**i**i**so**d**ecyl**p**hosphoric **a**cid
DME	1,2-Dimethoxyethane
DMF	Dimethylformamid
DMSO	Dimethylsulfoxid
ε	Molar extinction coefficient [$M^{-1}cm^{-1} = Lmol^{-1}cm^{-1}$]
ESI	Electron spray ionization
Et	Ethyl
EtOH	Ethanol
Hartree	1 Hartree = 2625.5 kJ/mol = 627.503 kcal/mol
IR	Infrared
m	Medium (IR), Multiplett (NMR)
Me	Methyl
MeOH	Methanol
org	Organic
ph	Phenyl
PUREX	**P**lutonium-**U**ranium **R**ecovery by **E**xtraction
py	Pyridine
r. t.	Room temperature
s	Strong (IR), Singulett (NMR)
SANEX	**S**elective **A**cti**n**ide **Ex**traction
S. A. V.	Solvent Accessible Voids
solv	solvent
TALSPEAK	**T**rivalent **A**ctinide **L**anthanide **S**eparation by **P**hosphorus-Reagent **E**xtraction from **A**queous **C**omplexes
tht	Tetrahydrothiophen
UV/Vis	Ultraviolet/Visible
vs	Very strong (IR)
vw	Very weak (IR)
w	Weak(IR)

1 Introduction

1.1 Fundamentals of uranium and thorium chemistry

Uranium and thorium are the heaviest naturally occurring elements, since they are the only actinides, which occur with a relatively high abundance in our environment, mainly in rocks and minerals. Both elements are exclusively radioactive and emit alpha particles with low specific activities. Uranium has three naturally occurring isotopes; the fertile ^{238}U (99.275 %), the fissile ^{235}U (0.720 %) and ^{234}U (0.005 %). Because of these properties and the related potential for energy production in nuclear reactors, uranium is the most relevant and best studied element of the actinides series. Naturally occurring thorium on the other hand has only one isotope, ^{232}Th, which is fertile.

Since the discovery of nuclear fission in 1938 by Hahn, Meitner and Strassman,[1,2] scientific research on uranium with focus on its application in nuclear technology was almost exclusively dominated by the aspects of exploration, exploitation, nuclear fuel production, reprocessing and disposal of nuclear waste. These applications, however, produce a substantial amount of radioactive waste, which bear the risk of a release of the element in soluble form into the biosphere.

The coordination chemistry of uranium and thorium is relatively poor developed compared to the chemistry of the transition metals and the lanthanides. The common valences of uranium are II to VI, where the most stable ones are IV and VI. The valences of thorium are II to IV, with Th(IV) being the most stable one. Because of their relatively small ionic radii and their high charges, uranium and thorium ions are hard Lewis acids according to the HSAB principle.[3] Consequently, they favor the coordination with hard Lewis bases such as oxygen or nitrogen donor atoms. In an aqueous environment, uranium as well as thorium tend to hydrolyze and are found essentially in their highest valences. The chemistry of hexavalent uranium is dominated by its dioxido cation $[UO_2]^{2+}$ also called “uranyl cation”. It is a linear unit, in which the uranium ion is connected to two axial oxygen atoms, forcing any other donor atom to coordinate equatorially to the metal center.[4-6]

During the past three decades, significant progress has been made in the molecular chemistry of the actinides with the perspective to elucidate the reactions, coordination behavior and physicochemical properties of the elements. The motivation behind this is the improvement and development of separation techniques for the actinides regarding the management and processing of nuclear waste, but also to understand the increasing bioavailability of the elements in mining

regions. Although ligand systems combining 'hard' and "soft" donor atoms have been proven to increase and control the selectivity of the complexation of metal ions, the coordination chemistry of uranium and thorium with such ligands is still less explored. Nevertheless, over the recent years significant efforts have been made, with a range of complexes of uranium (mostly U(IV) and U(III)) have been synthetized and characterized with sulfur containing ligands.[7] Meanwhile, only a few complexes with uranyl units and thorium have been reported so far. Some examples are illustrated in Figure 1.1.

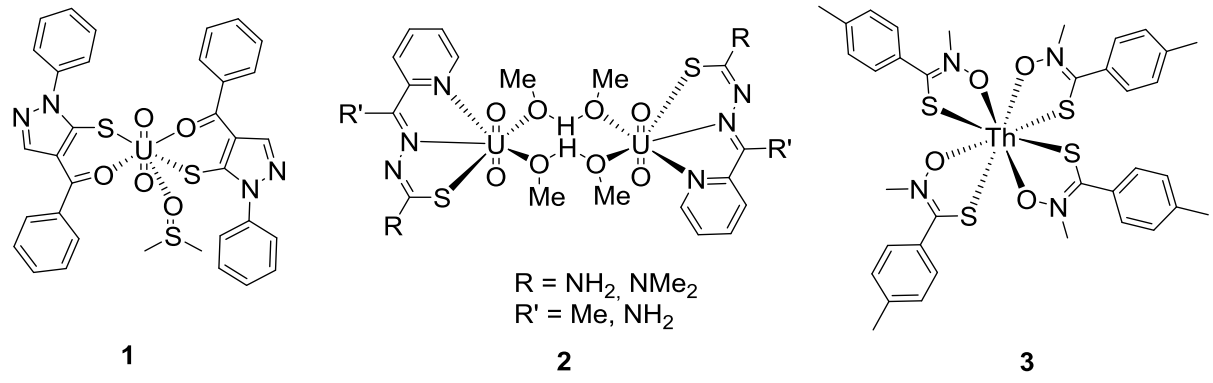

Figure 1.1: Previously reported complexes of uranyl units and thorium with sulfur containing ligands.[8–12]

1.2 The chemistry of aroylthioureas

The fundamental unit of the ligand systems used in the present thesis is the aroylthiourea. This class of compounds is known for more than 100 years. The first acetylthiourea was synthesized in 1873 by Nencki et al., followed by the synthesis of the first benzoylthiourea by Pike et al. in the same year.[13,14] The coordination chemistry of aroylthioureas has been extensively studied since the sixties.[15,16] The chemical properties of the thioureas is determined by these three groups: an amide, a thiooxoketone and a thiourea group, so that these ligands possess at least three potential donor atoms, the "hard" *O*, the "weak" *S* and the "borderline" *N*, which is protonated (see Figure *1.2*).

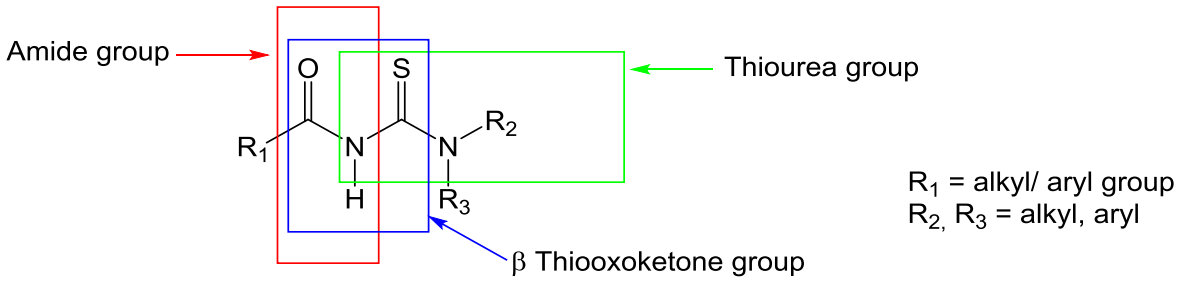

Figure 1.2: Structural groups of the alkyl/aroylthioureas.

In general, aroyl(*N*,*N*-dialkylthioureas) have two main coordination modes: the monodentate (*S*) and the bidentate (*S*,*O*) coordination as is shown in Figure 1.3. Monodentate coordinated ligands have been observed with thiophilic metal ions such as Au(I), Ag(I) and Pd(II) (**4**).[17–19] The bidentate coordination is frequently observed with divalent metal ions such as Ni(II) Cd(II) or Cu(II) in square planar complexes (**5**), and with trivalent metal ions such as Fe(III), Tc(III) or Co(III) as octahedral complexes (**6**).[20–28] Aroylthioureas can also stabilize metal ions in higher oxidation states, when co-ligands such as oxido- or phenylimido are involved (**7**).[29,30] So far, the literature on transition metal chemistry of aroylthioureas is dominated by reports on "soft" or "borderline" metal ions. Some of the complexes have been successfully applied in material chemistry and in environmental sciences as ionophores or selective extraction agents.[12,31–36] The activity of such thiourea derivatives and their metal complexes frequently depends on the functionalization of the different organic residues in the periphery of the molecules. This has been demonstrated for some antibacterial and antifungal activities of thiourea derivatives and complexes.[16,37–40] Merdivan et al. and Zhao et al. showed that the functionalization of adsorbent materials such as activated carbon and resin with benzoylthiourea can selectively enhance the solid phase extraction of uranyl ions, but there is no information on the chemical processes involved in the mechanism.[41,42]

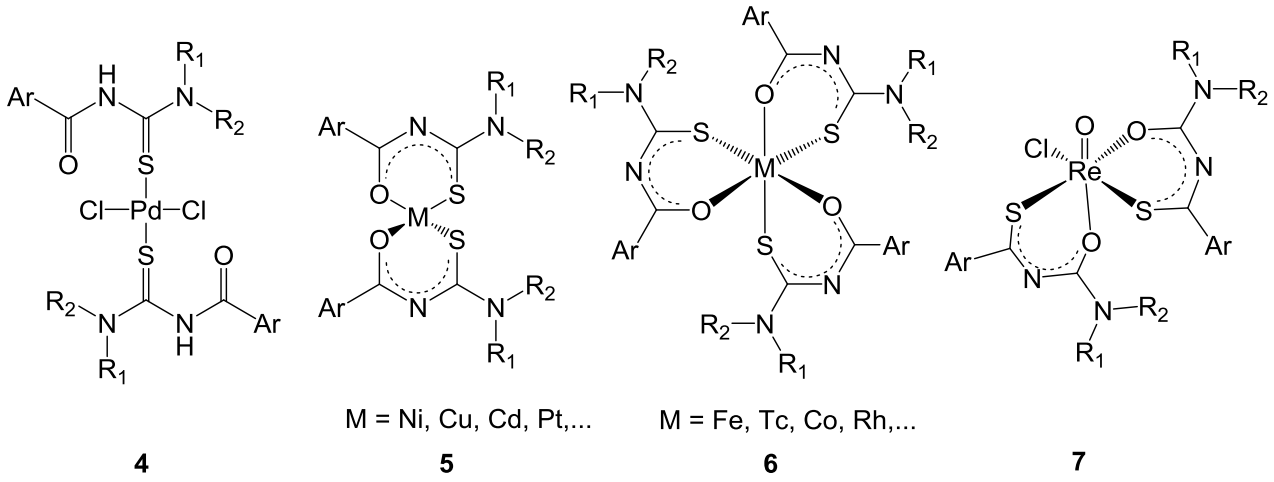

Figure 1.3: Coordination modes found in transition metal complexes with aroyl(*N*,*N*-dialkyl-thioureas).

More interesting compounds are bipodal aroylthioureas. They are characterized by the presence of two thiourea groups, which are linked through a "spacer" molecule and therefore allow the formation of multinuclear complexes. Meta-substituted benzoylbis(*N*,*N*-dialkylthioureas) form binuclear complexes (**8**) while para-substituted benzoylbis(*N*,*N*-dialkylthioureas) form trinuclear

complexes (**9**). [43–46] The variation of the central "spacer" molecule can increase the flexibility of the ligand framework and the denticity of the ligand, which can be used for the modeling of supramolecular building blocks. Such supramolecules have been reported in the literature with a wide range of metal ions. Generally, the thiourea groups coordinate "soft" metal ions and, depending on the nature of the spacer, a guest cation (generally a "hard" metal ion or organic cations) can be encapsulated in the formed metallamacrocycles or cryptates, see compounds **10** and **11** of Figure 1.4.[47–50]

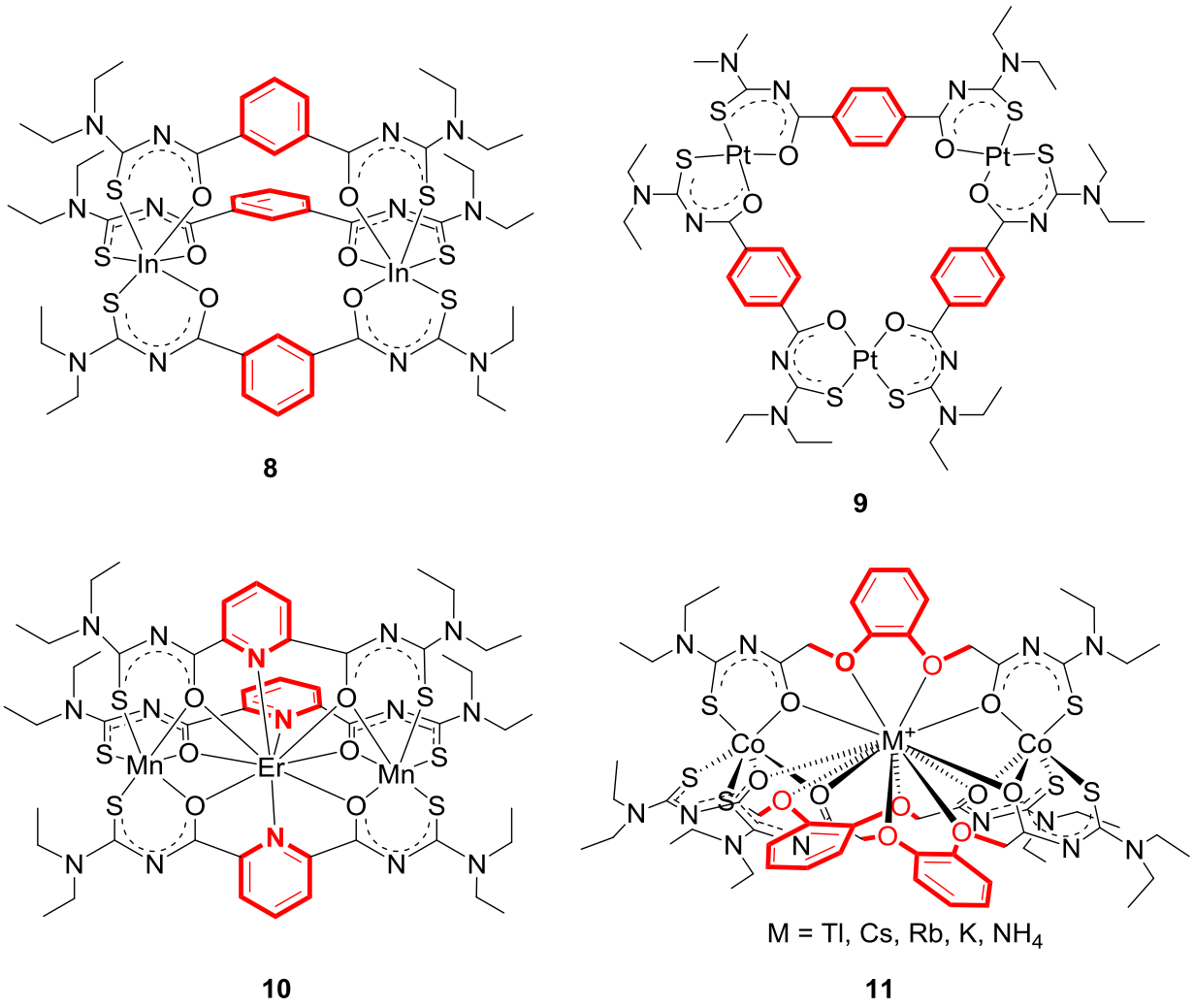

Figure 1.4: Structures of complexes of different aroylbis(*N*,*N*)-dialkylthioureas.

The goal of the present work is the synthesis and characterization of uranium and thorium complexes with multidentate ligand systems containing mixed "hard" and "soft" donor sites in order to increase and control the selectivity of the complexation of the metal ions.

This thesis presents novel uranyl complexes with isophthaloylbis(*N*,*N*–diethylthiourea), H_2L^1, pyridine-2,6-dicarbonylbis(*N*,*N*–dialkylthioureas), H_2L^{2a}, H_2L^{2b} and 2,2'-bipyridine-6,6'-dicarbonylbis(*N*,*N*-diethylthiourea), H_2L^3.

Heterometallic complexes with uranyl and transition as well as post-transition metal ions have been synthesized with pyridine-2,6-dicarbonylbis(*N*,*N*–dialkylthioureas). Structural studies of such mixed-metal uranyl complexes might contribute to a better understanding of the migration processes of the metal ion in the biosphere.

The last part of this work describes complexes of tetravalent uranium and thorium ions with aroylbis(*N*,*N*-dialkylthioureas).

A summary of all the ligands used in this dissertation is give in Figure 1.5.

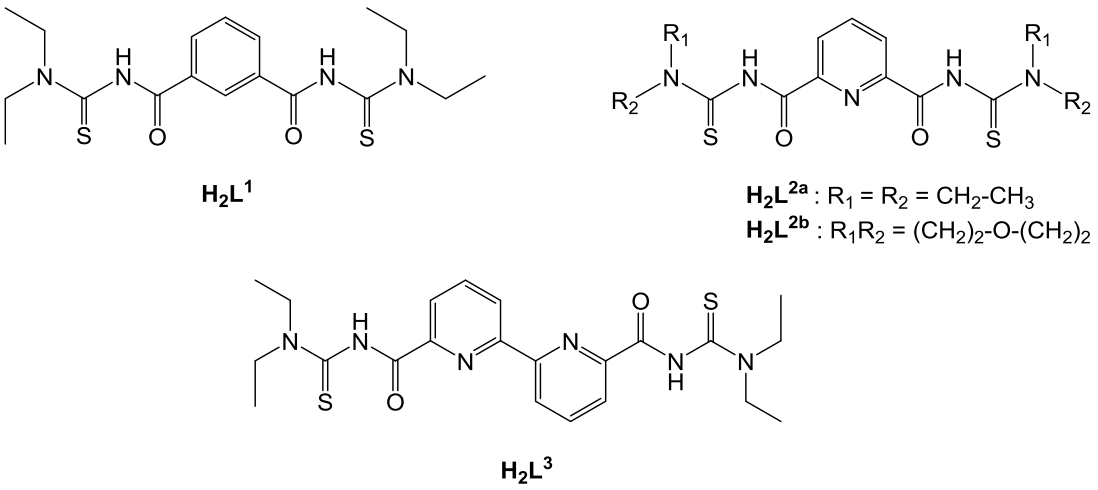

Figure 1.5: Structures of isophthaloylbis(*N*,*N*-diethylthiourea), H_2L^1; pyridine-2,6-dicarbonylbis-(*N*,*N*-dialkylthioureas), H_2L^{2a} and H_2L^{2b}, and 2,2'-bipyridine-6,6'-dicarbonylbis-(*N*,*N*-diethyl-thiourea), H_2L^3.

2 Results and Discussion

Although the coordination chemistry of aroylthioureas is widely reported in the literature, there are so far, no publications reporting molecular complexes of these ligand systems with the early actinides uranium and thorium. Aroylthioureas form stable complexes with metal ions in oxidations states from (+1) up to (+5) and stabilize metal cores such as the oxido and phenylimido cores of rhenium and technetium. This feature makes this ligand class also interesting for the uranium dioxido cation with a total charge of (+2). Until now, there are only two publications reporting the uranyl extraction behavior of different materials functionalized with benzoyl(*N*,*N*-dialkylthioureas), but there is no structural information about the product. Thus, the chemical mechanisms behind these experiments are practically unknown.[41,42]

2.1 Aroylbis(*N*,*N*-dialkylthioureas)

The syntheses of bipodal aroylthioureas are well established in the literature. The central "spacer" unit as well as the side chains can be modified in order to improve or change the properties of the ligands. The one-pot synthesis of isophthaloylbis(*N*,*N*-diethylthiourea), H_2L^1, has been reported by Koch et al. (see Scheme 2.1).[43] In the first step, one equivalent of isophthaloyl dichloride was added to two equivalents of NH_4SCN in dry acetone. The intermediate isophthaloylbis(isothiocyanate) is formed and after cooling of the reaction mixture to room temperature, two equivalents of diethyl amine were added, and the mixture was heated again under reflux. The product is obtained in a pure form with yields between 80 and 90 %. The analytical data are in consistence with the reported data.[51,52]

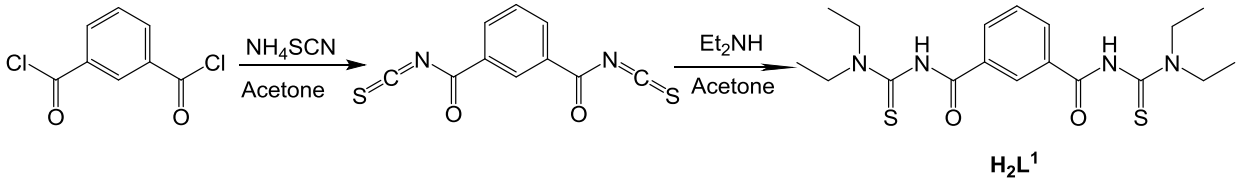

Scheme 2.1: Synthesis of isophthaloylbis(*N*,*N*-diethylthiourea), H_2L^1.

Since this synthetic route is not appropriate for pyridine-2,6-dicarbonylbis(*N*,*N*-dialkyl-thioureas), another procedure, requiring a pre-synthesis of *N*,*N*-dialkylthioureas has been described by Schröder et al.[53] *N*,*N*-Dialkylthioureas are synthesized from reactions of

chloroformic acid ethylester with potassium thiocyanate and the corresponding amine in acetone (see Scheme 2.2).[54] Pure products of Et_2tu and Mortu are obtained as microcrystalline white precipitates with yields of about 50 %.

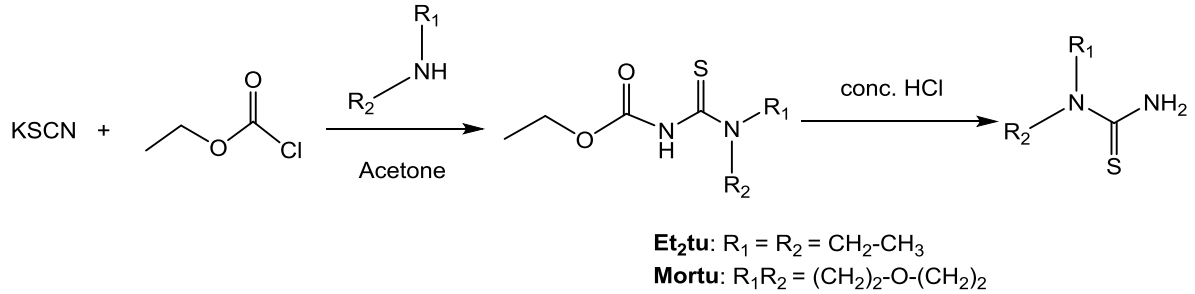

Scheme 2.2: Synthesis of *N*,*N*-dialkylthioureas

The ligands H_2L^{2a} and H_2L^{2b} were obtained after coupling reactions of one equivalent of pyridine-2,6-dicarbonyl dichloride with two equivalents of Et_2tu or Mortu in the presence of triethylamine. The reaction is illustrated in Scheme 2.3. Performing the reaction in THF instead of acetone as described by Schröder et al., improved the yield up to 90 %, since the ligands H_2L^{2a} and H_2L^{2b} are slightly soluble in acetone.[53] The analytical data are in consistence with the literature values.[53] A variation of the substituents of the lateral nitrogen atoms can have an influence on the complexation behavior of the ligand framework or the stability of the formed metal complexes. Morpholine has been included as a side-unit in this work, since the additional terminal *O* donor atoms may generate interesting inter- or intramolecular interactions.[49]

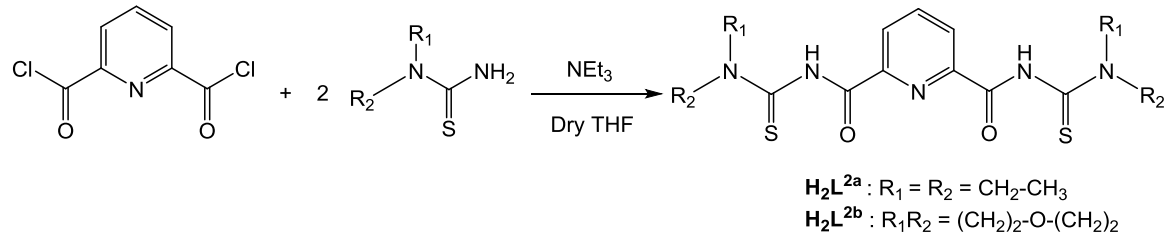

Scheme 2.3: Synthesis of pyridine-2,6-dicarbonylbis(*N*,*N*-diethylthiourea), H_2L^{2a}, and pyridine-2,6-dicarbonylbis(morpholinethiourea), H_2L^{2b}.

2,2'-Bipyridine-6,6'-dicarbonylbis(*N*,*N*-diethylthiourea), H_2L^3, can be prepared following the same route described for H_2L^{2a} and H_2L^{2b} according to the same standard procedure. Since 6,6'-dicarboxy-2,2'-bipyridine (**14**) is not commercially available, it had to be synthesized prior to the coupling reaction with Et_2tu as is shown in Scheme 2.4. First, 2,2-bipyridine was converted into 2,2'-bipyridine-*N,N'*-dioxide (**12**), followed by its functionalization with cyanide groups.

The resulting 6,6'-dicyanido-2,2'-bipyridine (**13**) was then hydrolyzed and compound **14** was obtained as a colorless precipitate with a final yield of 51 %.

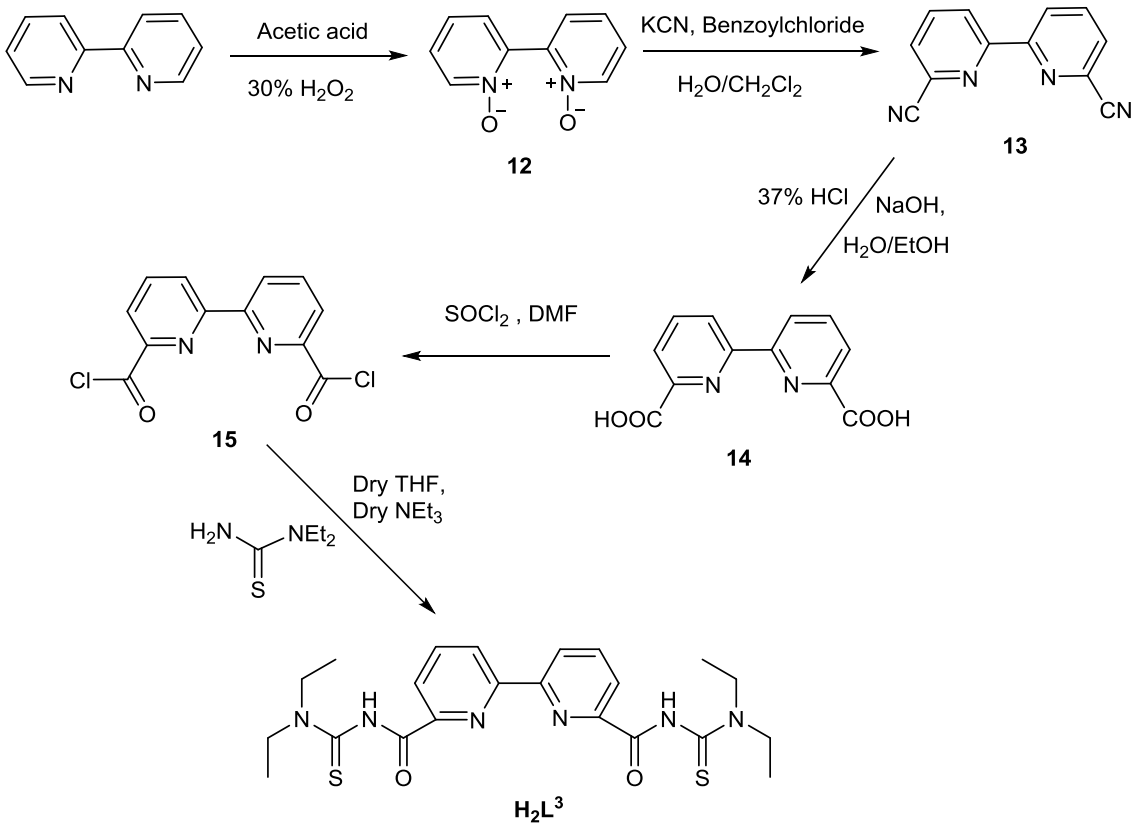

Scheme 2.4: Synthesis of 2,2'-bipyridine-6,6'dicarbonylbis(*N*,*N*-diethylthiourea), H_2L^3.

The dicarboxylic acid **14** was converted to the corresponding dichloride (**15**) by heating with an excess of thionyl chloride. H_2L^3 was obtained from the reaction of **15** with two equivalents of Et_2tu in the presence of triethylamine. The colorless product is soluble in solvents such as THF, acetone, CH_2Cl_2 or $CHCl_3$. The IR spectrum of H_2L^3 shows a band at 3375 cm^{-1}, which corresponds to the N-H stretching frequency. The strong absorption band at 1707 cm^{-1} can be assigned to the carbonyl stretch. The ^{1}H-NMR spectrum in $CDCl_3$ is characterized by a singlet at 10.21 ppm belonging to the N-H protons. The resonances of the aromatic protons are observed at 8.56, 8.26 and 8.08 ppm. The hindered rotation around the C(*S*)-NEt_2 bond , which is found in many benzoylthioureas, [30] is also observed in H_2L^3. This results in a magnetic inequivalence of the two diethyl residues. Two multipletts at 4.04 and 3.68 ppm for the CH_2 protons and one multiplett at 1.20 ppm for the CH_3 protons are observed. The composition of the ligand is also confirmed by its +ESI mass spectrum with the molecular ion $[M+H]^+$ peak at m/z = 473.1806.

Single crystals of H_2L^3 could be obtained after recrystallization from a CH_2Cl_2/diethylether (1:5) mixture. Figure 2.1 shows the molecular structure of H_2L^3. Selected bond lengths and angles are given in Table 2.1. The compound crystallizes in the triclinic space group $P\overline{1}$. Only half of the molecule is contained in the asymmetric unit. The complete ligand is produced by an inversion center being located between C25 and C25'. The C-O bond length of 1.214(2) and the C-S bond length of 1.673(2) Å are within the expected ranges of corresponding double bonds. The C2-N3 and C4-N3 bond lengths are 1.406(2) and 1.380(2) Å and reflect a partial double bond character suggesting a delocalization of π-electron density. Similarities with these observed values have been previously reported for other bipodal aroylthioureas.[50,53]

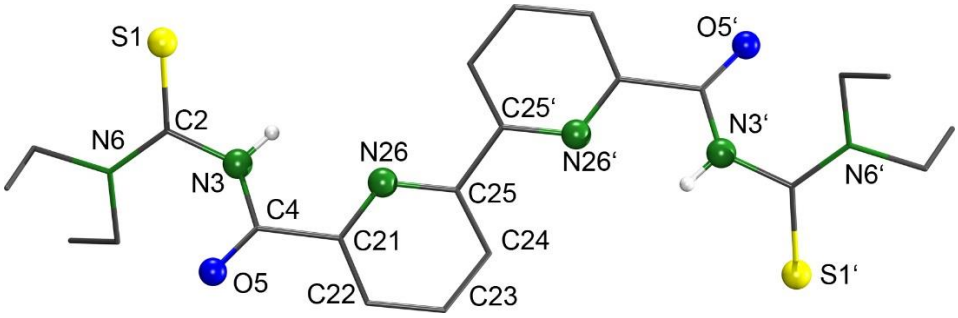

Figure 2.1: Molecular structure of H_2L^3. Symmetry related atoms are produced by an inversion center between C25 and C25' (symmetry operator -x, 1-y, 1-z). Hydrogen atoms of the ethyl and bipyridine groups have been omitted for clarity.[55]

Table 2.1: Selected bond lengths (Å) and angles (°) in H_2L^3.

Bond lengths			
C4–O5	1.214(2)	C2–S1	1.673(2)
C4–N3	1.380(2)	C2–N3	1.406(2)
Angles			
O5–C4–N3	124.3(2)	O5–C4-C21	122.9(2)
C2–N3–C4	124.4(1)	N3–C2–N6	117.1(2)
N3–C2–S1	117.3(1)	N6–C2–S1	125.6(2)
N3–C4-C21	112.8(1)		

2.2 Uranyl complexes with aroylbis(*N*,*N*-dialkylthioureas), H_2L^1, H_2L^2 and H_2L^3

Attempted reactions with potentially bidentate benzoyl(*N*,*N*-dialkylthioureas), the ligand type shown in the complexes **4**-**7** of Figure 1.3, with the $UO_2(CH_3COO)_2 \cdot 2H_2O$, $UO_2(NO_3)_2 \cdot 6H_2O$

or $(NBu_4)_2[UO_2Cl_4]$ in different solvents such as H_2O, MeOH, acetone or THF were not successful and no crystalline products could be isolated from such experiments. Only in the cases of the reactions in acetone and THF, were changes in color observed in the reaction mixture, though no pure products were obtained from such solutions.

More successful were the reactions with the bipodal aroylthioureas shown in Figure 1-5.

2.2.1 Complexes with isophthaloylbis(*N*,*N*-diethylthiourea), H_2L^1

Isophthaloylbis(*N*,*N*-diethylthiourea), H_2L^1, is a versatile ligand due to the free rotation around the C-C bond between the central phenyl ring and the amide groups. The ligand can adopt different conformations leading to the formation of various macrocyclic compounds. This is the reason why some considerations about the stability of relevant conformations of this compound have been performed. They are shown in Figure 2.2. Experimentally, H_2L^1 was isolated as orthorhombic crystals, adopting the conformation **D.** It shows intermolecular hydrogen bonds in the crystal packing.[56]

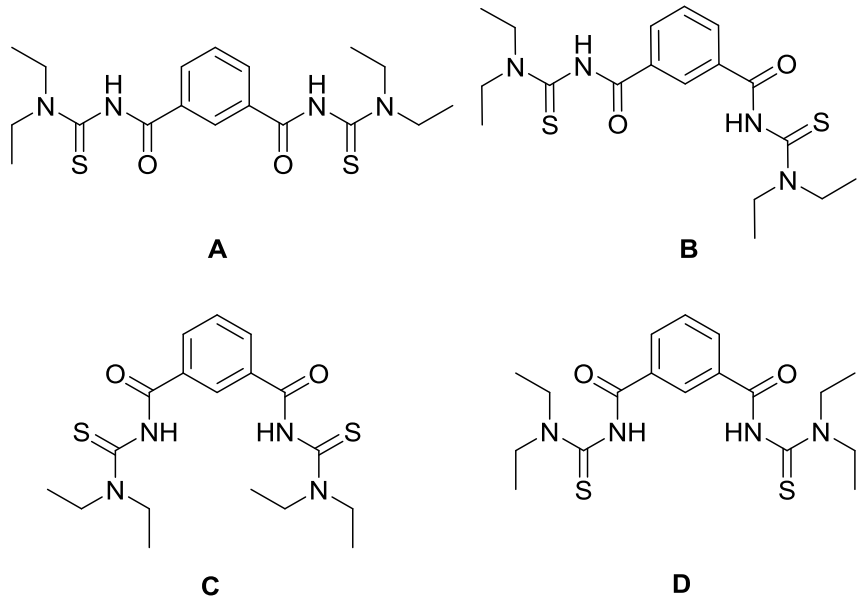

Figure 2.2: Possible models for the molecular conformation of H_2L^1.

These intermolecular hydrogen bonds are the driving forces for the stability of this conformation by maintaining the C(*O*) and the C(*S*) bonds perpendicular to each other. In coordination compounds, the most reported conformation of H_2L^1 is the conformation **A**, where the ligand adopts a linear configuration and all the *O* and *S* donor atoms point to the same

direction. With divalent metal ions, the ligand in the conformation **A** produces mostly *cis*-coordinated 2:2 metallamacrocycles, while trivalent metal ions form usually 2:3 metallamacrocycles.[15] The formation of polymers is also possible, as described by Schwade et al.[44] The conformation **B**, which is formed after the rotation of the C-C bond on one side of the ligand by 180 °, was observed in reactions with $[Au(PPh_3)]^+$, Pb^{2+} and oxidorhenium(V) complexes.[44,57] The additional rotation of the C-C bond of the second side of the ligand also by 180 ° leads to the conformation **C**. So far, no structure with the conformation **C** has been reported.

In order to estimate, whether the geometry of H_2L^1 has an influence on its stability and reactivity, DFT calculations of the different conformations (see Table 2.2) were performed. The structural parameters were taken from the literature and adapted with GaussView.[56,58] The geometry optimization of the four conformations of H_2L^1 shows that the conformation **A** is the thermodynamically most stable one with an energy difference of 23.8 kJ/mol to the conformation **B,** and 28.0 kJ/mol to the conformations **C** and **D**. The optimized structure of conformation **C** converges in structure to that of conformation **D**, implying that both structures have the same energy after optimization. The results from the DFT calculations show that geometrical fluctuations of the active sites cannot significantly affect the overall energetic barrier, which is needed for the complexation of different metal ions, and that significant conformational changes mostly occur during the reaction, depending on the used metal ions.

Table 2.2: DFT calculations on H_2L^1. Level of theory: B3LYP; basis sets: 6-311G.

	Conformation **A**		Conformation **B**		Conformation **C**		Conformation **D**
Energy [Hartree]	-1867.4179	<	-1867.4088	<	-1867.4072	=	-1867.4072
ΔE [kJ/mol]		23.8		4.2		0	

Treatment of $UO_2(CH_3COO)_2 \cdot 2\ H_2O$ with an equivalent amount of H_2L^1 in EtOH at room temperature gave an orange-red solution. The addition of two drops of NEt_3 accelerated the formation of an orange-red precipitate and increased the yield of the reaction up to 70 %. The product was isolated by filtration and characterized as $(HNEt_3)_2[\{UO_2(L^1)\}_4(OAc)_2]$ (Scheme 2.5).

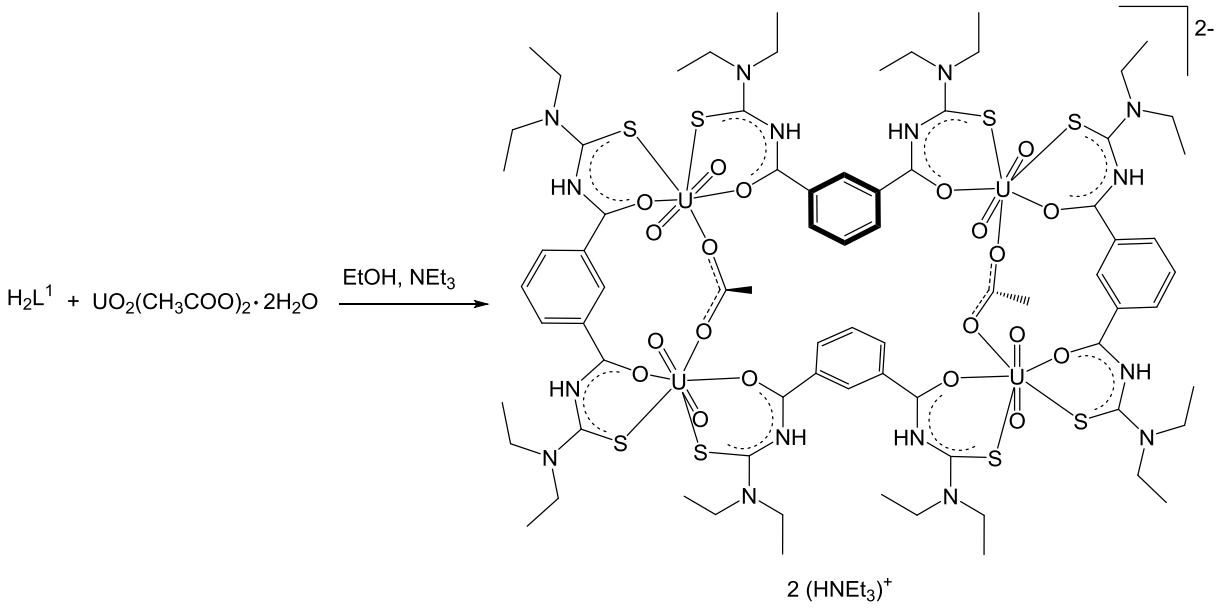

Scheme 2.5: Synthesis of $(HNEt_3)_2[\{UO_2(L^1)\}_4(OAc)_2]$.

Yellow crystals of $(HNEt_3)_2[\{UO_2(L^1)\}_4(OAc)_2] \cdot CH_2Cl_2$ were obtained after recrystallization from CH_2Cl_2/EtOH. The IR spectrum of the complex shows an asymmetric $\nu_{U=O}$ band at 910 cm^{-1}. A weak band at 1680 cm^{-1} can be assigned as the $\nu_{C=O}$ stretch of the acetato bridges. The $\nu_{C=O}$ stretching frequency of the organic ligand appears in the complex at 1500 cm^{-1}. A bathochromic shift of 180 cm^{-1} is observed in comparison to the position of this band in the uncoordinated ligand. This indicates a chelate formation with a strong degree of electron delocalization. Such strong bathochromic shifts of the carbonyl frequencies have also been observed in benzoyl(*N*,*N*-dialkylthioureato) complexes with other heavy metal ions.[15,16,44,57] The absence of a band above 3000 cm^{-1} indicates the deprotonation of the ligands during the complex formation, which is confirmed by the ^{1}H-NMR spectrum of the compound, where no signals for the N-H protons have been observed. The molecular structure of the compound was confirmed by X-ray diffraction. The compound crystallizes in the triclinic space group $P\overline{1}$. The asymmetric unit contains half of the molecule, one triethylammonium cation and a half dichloromethane molecule. Figure 2.3 shows the molecular structure of the $[\{UO_2(L^1)\}_4(OAc)_2]^{2-}$ anion. Selected bond lengths and angles are listed in Table 2.3.

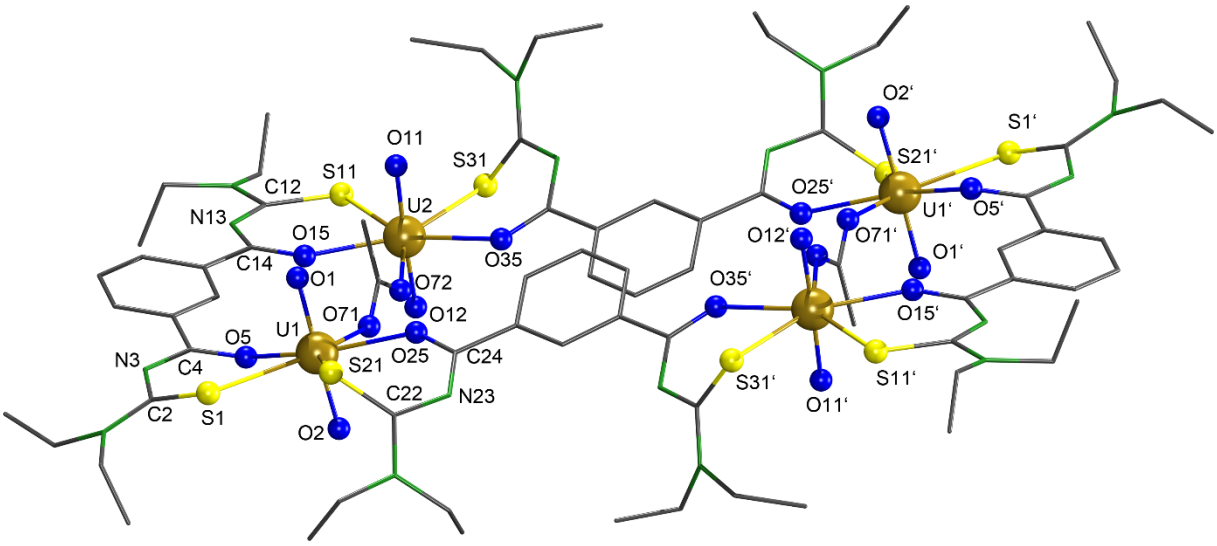

Figure 2.3: Representation of the molecular structure of $[\{UO_2(L^1)\}_4(OAc)_2]^{2-}$. Symmetry related atoms are produced by an inversion center (symmetry operator -x, -y+1, -z+1). Hydrogen atoms have been omitted for clarity.[55]

Table 2.3: Selected bond lengths (Å), distances (Å), bond angles and torsion angles (°) in $(HNEt_3)_2[\{UO_2(L^1)\}_4(OAc)_2]$. Symmetry operator: -x+1,-y+1,-z+1.

Distances					
U1–O1	1.776(9)	C2–N3	1.38(2)	U2–O11	1.76(1)
U1–O2	1.788(9)	N3–C4	1.31(2)	U2–O12	1.78(1)
U1–S1	2.844(4)	C4–O5	1.27(2)	U2–S11	2.847(4)
U1–S21	2.841(4)	C22–S21	1.71(2)	U2–S31	2.844(8)
U1–O5	2.275(8)	C22–N23	1.36(2)	U2–O15	2.286(8)
U1–O25	2.339(8)	N23’–C24	1.28(2)	U2–O35	2.336(8)
U1–O71	2.402(8)	C24’–O25	1.26(2)	U2–O72	2.415(8)
C2–S1	1.70(1)	U1···U2	6.85(1)	U1···U2’	11.74(1)
Angles					
O1–U1–O2	178.5(4)	O1–U1–O25	88.9(4)	O1–U1–S1	90.3(4)
O1–U1–O5	90.8(4)	O2–U1–O25	90.8(3)	O2–U1–S1	90.9(4)
O1–U1–O71	92.9(4)	O2–U1–O5	90.8(4)	O1–U1–S21	88.7(7)
O11–U2–O12	177.3(5)				
Torsion angles					
C4–N3–C2–S1		29.3(2)	C24–N23–C22–S21		-32.1(2)
C2–N3–C4–O5		4.0(2)	C22–N23–C24–O25		-17.4(3)
C14–N13–C12–S11		-11.4(2)	C34–N33–C32–S31		-13.4(2)
C12–N13–C14–O15		1.1(2)	C32–N33–C34–O35		-37.1(2)

The compound exhibits a tetranuclear unit containing four uranyl units, 4 deprotonated $\{L^1\}^{2-}$ ligands and two acetato ligands, indicating a net charge of the complex of -2. The charge is compensated by two triethylammonium cations. Each uranyl moiety is coordinated equatorially with two bidentate thiourea units coming from different ligands. The isophthaloylbis(thiourea) ligand shows in this structure its flexibility in order to optimize the coordination environment for the uranyl cation. Two conformation types of the ligand are established in the $[\{UO_2(L^1)\}_4(OAc)_2]^{2-}$ anion: the linear conformation **A** and the unprecedented conformation **C** (see Figure 2.3). The coordination environment of the uranium atom is a pentagonal-bipyramid resulting from the *cis S,O* coordination of two deprotonated ligands $\{L^1\}^{2-}$ and an additional acetato ligand. The uranyl bond lengths are between 1.76(1) and 1.788(9) Å with angles of 178.6(4) ° and 177.3(5) °. The bond lengths between the uranium atoms and the oxygen donor atoms of the organic ligand with the conformation **A** are around 2.28 (1) Å and slightly shorter than the bond lengths between uranium and the oxygen atoms belonging to the ligand with the conformation **C** with approximately 2.34(1) Å. The U-S bonds are almost equal with approximately 2.74 Å. The *S,O* chelate rings exhibit the typical extended delocalized π-systems with a slight elongation of the C-O and C-S bonds and a shortening of the C-N bonds, reflecting some double bond character.[30,44,59] As illustrated in Figure 2.4, the *S,O* chelate rings in the compound of the ligands with the conformation **C**, when compared to the situation in the chelate rings, which adopt the conformation **A**, show significant deviations from the planarity (see also Table *2.3*).

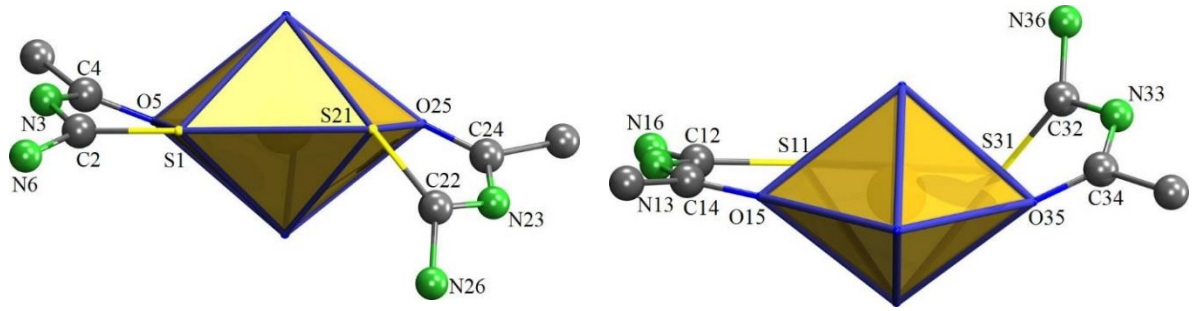

a) b)

Figure 2.4: The coordination environment around the uranium atoms U1 and U2, showing the deviations from planarity for the chelate rings.

Interestingly, this tetranuclear complex is stabilized in the solid state by weak intramolecular π-π interactions between the co-planar central phenyl units with a C53-C53' distance of 3.31(3) Å (see Figure 2.5a). Additionally, hydrogen bonds and cation-π interactions with a

distance of 3.47(3) Å are observed between the acetato ligand and the triethylammonium ion.[60] The bonding situation and the bonding parameters of these cation-anion interactions are summarized in Figure 2.5b and in Table 2.4.

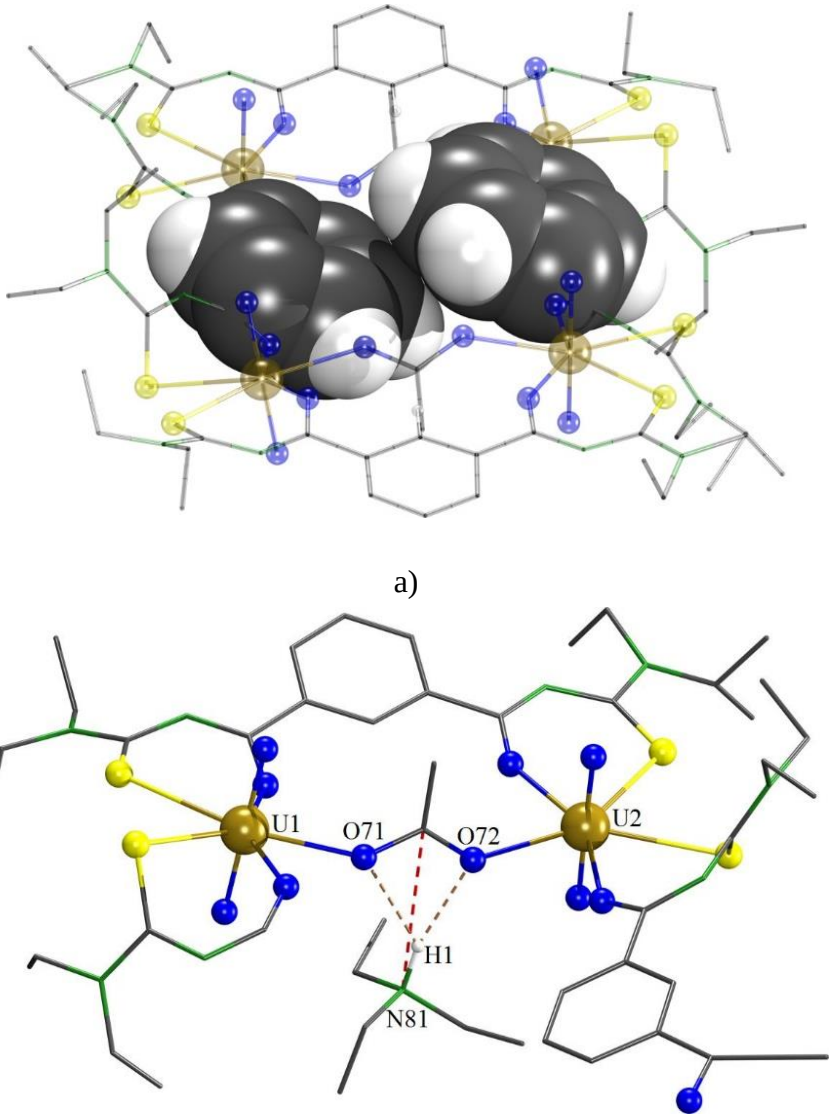

a)

b)

Figure 2.5: Structure of a) the complex anion $[\{UO_2(L^1)\}_4(OAc)_2]^{2-}$ and b) the asymmetric unit of $(HNEt_3)_2[\{UO_2(L^1)\}_4(OAc)_2]$ showing the different weak interactions in the molecule.

Table 2.4: Hydrogen bond parameters in $(HNEt_3)_2[\{UO_2(L^1)\}_4(OAc)_2]$.

D–H···A	d(D–H) (Å)	d(H···A) (Å)	d(D···A) (Å)	<(DHA) (°)
N81–H1···O71	0.981(2)	2.272(8)	3.037(2)	134.1(1)
N81–H1···O72	0.981(2)	2.038(9)	2.996(2)	165.0(1)

The reaction of $(NBu_4)_2[UO_2Cl_4]$ with H_2L^1 in EtOH gives a product similar to that described previously. The obtained orange-red precipitate has a composition of $(NBu_4)_2[\{UO_2(L^1)\}_4(OEt)_2(HOEt)_2]$. The IR spectrum of the product shows a broad signal at 3446 cm^{-1}, which can be assigned to O-H vibrations. The absence of a vibration at 3100 cm^{-1} indicates the deprotonation of H_2L^1. The formation of a uranyl complex is confirmed by the presence of the strong band at 910 cm^{-1}. As in the compound $(HNEt_3)_2[\{UO_2(L^1)\}_4(OAc)_2]$, a bathochromic shift of the $\nu_{C=O}$ stretch is observed. The presence of two (O-H) protons was confirmed by their ^{1}H-NMR signal at 11.30 ppm. Single crystals of $(NBu_4)_2[\{UO_2(L^1)\}_4(OEt)_2(HOEt)_2]$ were obtained from a CH_2Cl_2/EtOH mixture. The quality of the single crystals however, was not suitable for a detailed discussion of the bond lengths and angles. Thus, only general bonding features shall be discussed here. The molecular structure of the compound can certainly be derived from the crystal data. It is illustrated in Figure 2.6. The coordination sphere of each uranyl moiety is completed by two *S,O* chelates of the benzoylthiourea unit and each one ethanolato and one ethanol ligands. The previously discussed intramolecular π-π interactions between the central phenyl units are also found in the $[\{UO_2(L^1)\}_4(OEt)_2(HOEt)_2]^{2-}$ anion.

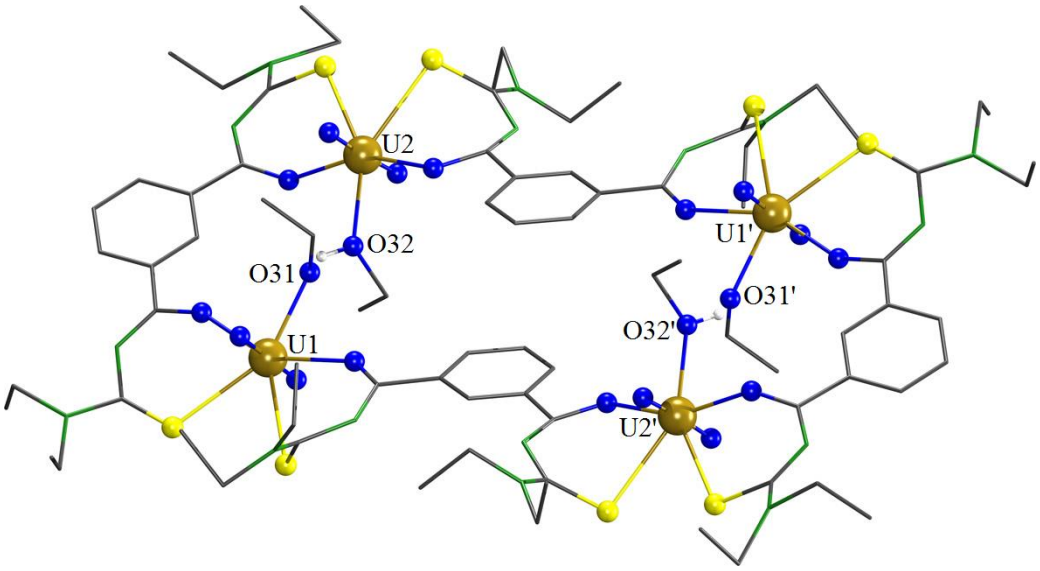

Figure 2.6: Molecular structure of the $[\{UO_2(L^1)\}_4(OEt)_2(HOEt)_2]^{2-}$ anion. Symmetry related atoms are produced by an inversion center (symmetry operator -x, 1-y, 1-z). Hydrogen atoms bonded to the carbon atoms have been omitted for clarity.

2.2.2 Complexes with pyridine-2,6-dicarbonylbis(*N*,*N*-dialkylthioureas), H_2L^{2a} and H_2L^{2a}

As mentioned earlier, the introduction of an additional donor atom in the spacer moiety can increase the flexibility as well as the denticity of the aroylbis(dialkylthiourea) ligands. This may result in the formation of different coordination patterns. The introduction of a pyridine molecule as "spacer" can lead to the formation of five different conformations of the ligand as is shown in Figure 2.7 for H_2L^{2a}. They all have been found in metal complexes, where the coordination to suitable metal ions is the determining factor for the complexation. The conformation **A** is the most reported one and it is frequently observed in oligonuclear "host-guest" coordination compounds with "hard" metal ions being "guests" in bimetallic metal chelates.[47,49,61] Conformation **D** was observed in mononuclear complexes of rhenium and technetium.[62,63] Here, the ligand coordinates pentadentate via an *S*,*N*,*N*,*N*,*S* donor set and the oxygen atoms do not participate in the coordination of the metal ion. Nguyen et al. have reported an example of the conformation **C**, which presents the possibility of a tridentate *N*,*N*,*N* coordination and two additional bidentate *S*,*O* coordinations. In the same publication, they also reported the conformation **B** in a dimeric nickel complex. The ligands coordinate in this case tridentate over *O*,*N*,*N* to one Ni^{2+} ion and bidentate over *S*,*O* to a second Ni^{2+} ion.[49] The conformation **E,** which differs from the conformation **B** only by the orientation of the sulfur atoms, has been reported by Pham in a polymeric $[TlFe(L^2)_2]$ complex. Here, the orientation of the sulfur atom out of the plane of oxygen allowed the latter one to act as a monodentate ligand and the formation of a polymeric chain was observed.[61]

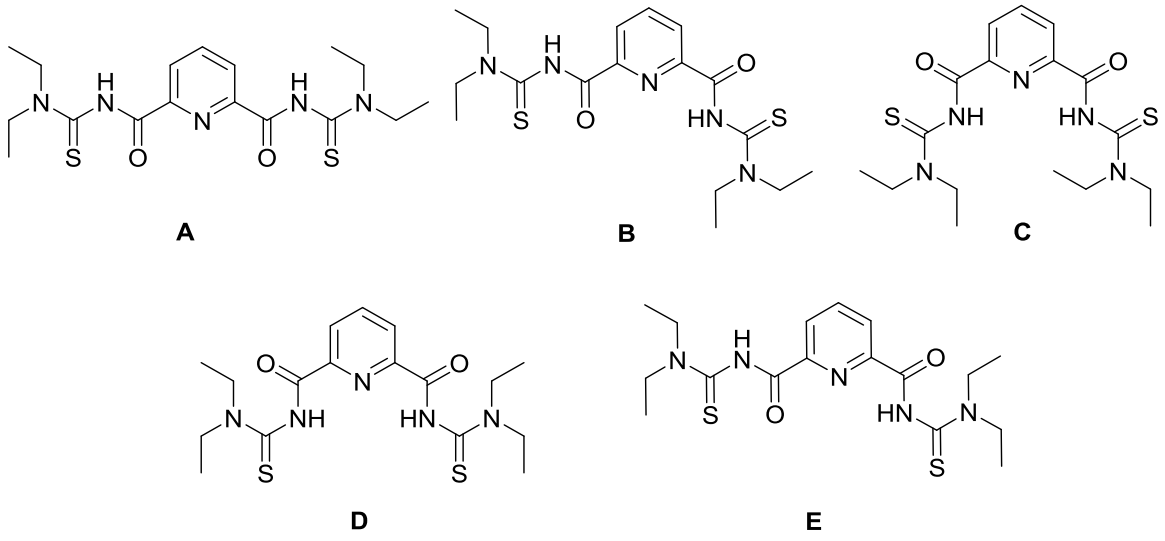

Figure 2.7: Possible models for the molecular conformations of H_2L^{2a}.

In order to determine which conformation of H_2L^{2a} is the most stable one, DFT calculations have been carried out and the conformation geometries were optimized. The structures were modeled with the program GaussView and the structural parameters were taken from the literature.[47] The results are summarized in Table 2.5. According to the DFT calculations, configuration **D** is the thermodynamically most stable one with an energy difference of 10.9 kJ/mol to the second most stable configuration **C** and 67.4 kJ/mol to the unfavorable conformation **A**. In comparison to H_2L^1, the linear conformation, of H_2L^{2a} is the less stable one. This may emphasize the fact, that the linear confirmation of H_2L^{2a} is exclusively found in supramolecular host-guest compounds. Also here, the type of the metal ions and their preferred coordination modes, play the predominant role in the conformation, that the ligand adopts during the complexation reactions.

The variation of the alkyl moiety of the thiourea group may influence the stability of the different conformations of the ligand. The steric effect of the substituents might obstruct the formation of the desired coordination compound. In this work, the chosen substituents were diethyl and morpholine. Morpholine is a less flexible substituent than the diethyl amine one, and provides an additional "hard" donor atom (*O*) in its periphery, which can allow intermolecular interactions in solid state structures as has been reported by Nguyen et al.[49] The geometry optimizations of the earlier mentioned conformations (Figure 2.7) with morpholine instead of diethyl as substituents reveal that only three conformations of the non-coordinated ligand are stable (conformation **B**, **D** and **E**). The conformation **A** converges to conformation **E** and conformation **C** converges to conformation **D**. Conformation **D** is also here the energetically most favorable conformation, followed by conformation **E** and conformation **B**.

Table 2.5: DFT calculations of the different conformations of H_2L^{2a} and H_2L^{2b}. Level of theory: B3LYP; basis sets: 6-311G.

H_2L^{2a}	Conformation **A**	Conformation **B**	Conformation **C**	Conformation **D**	Conformation **E**
Energy [Hartree]	-1883.4307	-1883.4388	-1883.4522	-1883.4564	-1883.4461
H_2L^{2b}					
Energy [Hartree]	-2031.4304	-2031.4216	-2031.4439	-2031.4439	-2031.4304

First, reactions of H_2L^{2a} and H_2L^{2b} with uranyl nitrate hexahydrate or uranyl acetate dihydrate were performed in MeOH at 50 °C without the addition of a supporting base. Such reactions ended in a decomposition of the ligands and the formation of pyridine dicarboxylic acid. This hydrolysis product finally forms a uranyl complex (see Scheme 2.6), which has already been described by Immirizi et al.[64] Obviously, the thiourea derivatives are sensitive against the strong acidic conditions in such solutions.

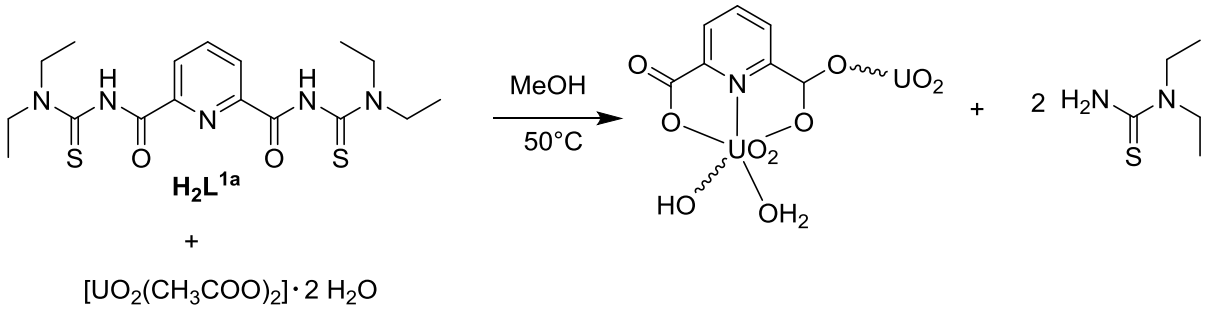

Scheme 2.6: Cleavage and hydrolysis of H_2L^{2a} during the reaction with $[UO_2(CH_3COO)_2]\cdot 2\ H_2O$.

A similar observation has been made by Gatto during the reaction of a mono-substituted diacetylresorcinol thiosemicarbazone ligand and uranyl nitrate.[65] During the reaction, the C=N bond was cleaved. The remaining ligand partially hydrolyzed under formation of 4,6-diacetylresorcinol, which coordinated to the uranyl ions under the formation of a tetrameric, macrocyclic compound.

The decomposition of H_2L^{2a} and H_2L^{2b} can be avoided, when a supporting base is added. This allows the deprotonation of the ligands and their coordination in favor to their hydrolysis. Chelate coordination of $\{L^{2a}\}^{2-}$ and $\{L^{2b}\}^{2-}$ with uranyl ions was obtained when two drops of triethylamine were added to the reaction mixtures.

A compound of the composition $[UO_2(L^{2a})(MeOH)]$ was obtained from the reaction of H_2L^{2a}, a uranyl source ($[UO_2(CH_3COO)_2]\cdot 2\ H_2O$, $(NBu_4)_2[UO_2Cl_4]$ or $[UO_2(NO_3)_2]\cdot 6\ H_2O$) and NEt_3 in methanol. Slow evaporation of the reaction mixture at room temperature gave single crystals of the compound (Scheme 2.7). Dissolution of the compound in a coordinating solvent such as DMF led to an exchange of the coordinated methanol ligand and $[UO_2(L^{2a})(DMF)]\cdot(DMF)$ was obtained after the slow evaporation of the solvent at room temperature. The IR spectrum of the complex $[UO_2(L^{2a})(MeOH)]$ shows the strong asymmetric $\nu_{U=O}$ band at 912 cm^{-1} and the ν_{OH} band at 3211 cm^{-1}. The IR spectrum of the complex $[UO_2(L^{2a})(DMF)]\cdot(DMF)$ shows the $\nu_{U=O}$ stretch at 904 cm^{-1}. The carbonyl bands appear at 1654 cm^{-1} for $[UO_2(L^{2a})(MeOH)]$ and at 1629

cm^{-1} for $[UO_2(L^{2a})(DMF)]\cdot(DMF)$. This corresponds to a bathochromic shift of only 26 and 51 cm^{-1} with respect to the values in H_2L^{2a}. These values strongly indicate, that the C=O functionality is not involved in the coordination. The absence of the N-H vibration suggests the deprotonation of the ligand, which is confirmed by the ^{1}H-NMR spectrum. The ESI^+ mass spectra show the fragment $[\{M\text{-}MeOH\}+K]^+$ at m/z = 702.1331 and $[\{M\text{-}DMF\}+Na]^+$ at m/z = 686.1625. The solvent ligands were abstracted during the measurement. Interestingly, the cluster fragments $[\{M\text{-}MeOH\}_2+K]^+$ at 1365.3036 and $[\{M\text{-}DMF\}_2+Na]^+$ at 1365.3322 were observed, which indicates a dimerization of the complex in solution, which also resists the transfer into the gasphase.

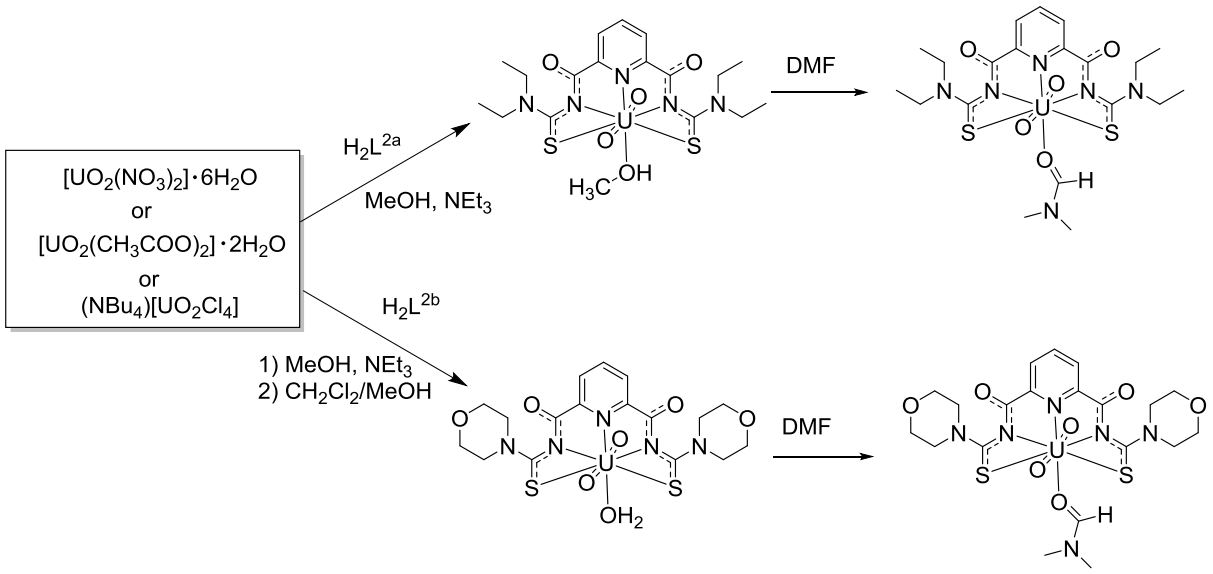

Scheme 2.7: Reactions of H_2L^{2a} and H_2L^{2b} with uranyl salts.

Figure 2.8 shows the molecular structures of $[UO_2(L^{2a})(MeOH)]$ and $[UO_2(L^{2a})(DMF)]$. The uranium atoms in both structures have a distorted hexagonal-bipyramidal coordination sphere with the oxido ligands in the axial positions. The ligands $\{L^2\}^{2-}$ coordinate pentadentate with three nitrogen and two sulfur atoms. The hexagonal base is completed by the coordination of a solvent molecule. Selected bond lengths and angles are given in Table 2.6. The uranyl bond lengths with values between 1.747(7) and 1.782(2) Å and with O=U=O bond angles of 178.1(10) and 178.2(3) are in agreement with the literature. The U-N bond lengths are in the range of 2.438(2) – 2.514(8) Å for the thiourea site and between 2.600(3) and 2.624(7) Å for the pyridine ring. The distances between U1 and O31 are 2.490(2) Å for MeOH and 2.441(6) Å for DMF.

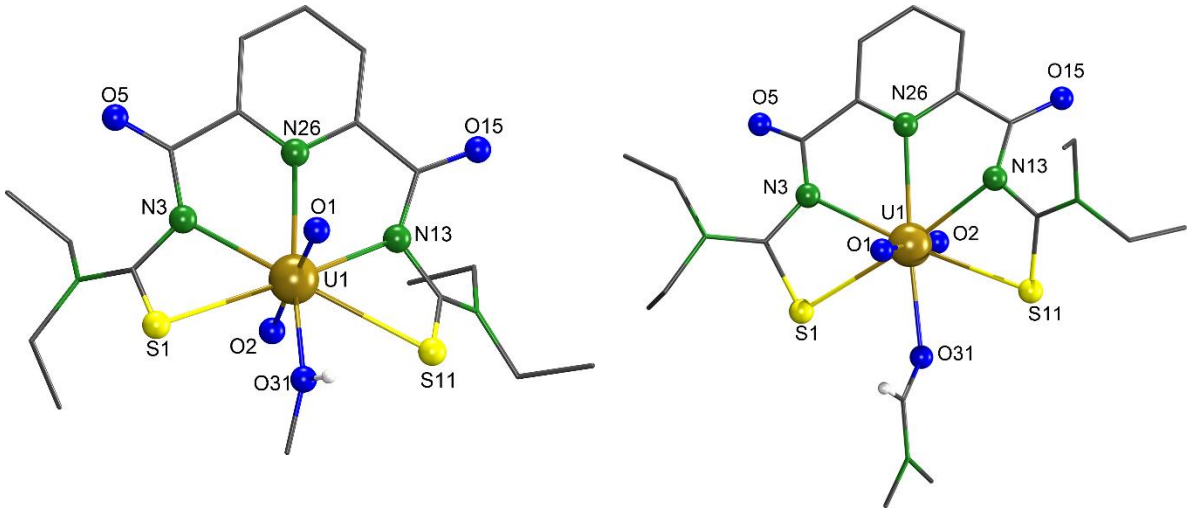

a) b)

Figure 2.8: Molecular structures of a) $[UO_2(L^{2a})(MeOH)$ and b) $[UO_2(L^{2a})(DMF)]$. Hydrogen atoms except for the coordinated solvents have been omitted for clarity.

Table 2.6: Selected bond lengths (Å) and bond angles (°) in $[UO_2(L^{2a})(MeOH)]$ (**1**) and $[UO_2(L^{2a})(DMF)]\cdot(DMF)$ (**2**).

Bond lengths	(**1**)	(**2**)	Bond lengths	(**1**)	(**2**)
U1–O1	1.776(2)	1.747(7)	U1–O31	2.490(2)	2.441(6)
U1–O2	1.782(2)	1.760(6)	C2–S1	1.705(3)	1.723(9)
U1–S1	2.979(9)	2.939(2)	C12–S11	1.721(3)	1.720(9)
U1–S11	2.969(9)	2.913(3)	C4–O5	1.242(4)	1.22(1)
U1–N3	2.508(3)	2.514(8)	C14–O15	1.223(4)	1.23(1)
U1–N13	2.438(3)	1.37(1)	C2–N3	1.384(4)	1.35(1)
U1–N26	2.600(3)	2.514(8)	C4–N3	1.339(4)	1.36(1)
C14–N13	1.360(4)	2.624(7)	C12–N13	1.371(4)	1.37(1)
Bond angles	(**1**)	(**2**)	Bond angles	(**1**)	(**2**)
O1–U1–O2	178.1(9)	178.2(3)	N3–U1-N26	60.3(8)	60.4(2)
O31–U1-N26	161.6(8)	168.8(2)	O1–U1–O31	96.3(9)	88.2(3)
N3–U1–S11	168.7(6)	173.4(2)	O2–U1-N26	102.1(9)	101.1(2)
O2–U1-N13	85.4(9)	86.0(2)	O1–U1-N26	79.7(9)	80.6(2)
N13–U1–S1	168.3(6)	173.1(2)	O1–U1-N13	94.8(9)	94.2(3)

Reactions of H_2L^{2b} with uranyl acetate or $(NBu_4)_2[UO_2Cl_4]$ in the presence of 2 drops of triethylamine give yellow precipitates, which could be recrystallized from a 1:1 mixture of

CH_2Cl_2/MeOH (v/v) and characterized as $[UO_2(L^{2b})(H_2O)]$ (Scheme 2.7). $[UO_2(L^{2b})(H_2O)]$ shows the same coordination mode as is observed in $[UO_2(L^{2a})(MeOH)]$ with a coordinating water molecule instead of methanol. $[UO_2(L^{2b})(H_2O)]$ crystallizes in the orthorhombic space group Pbca. Also here, the water molecule could be replaced by the dissolution of the compound in DMF. The resulting $[UO_2(L^{2b})(DMF)]$ crystallizes in the monoclinic space group $P2_1/c$. Figure 2.9 shows the molecular structures of $[UO_2(L^{2b})(H_2O)]$ and $[UO_2(L^{2b})(DMF)]$.

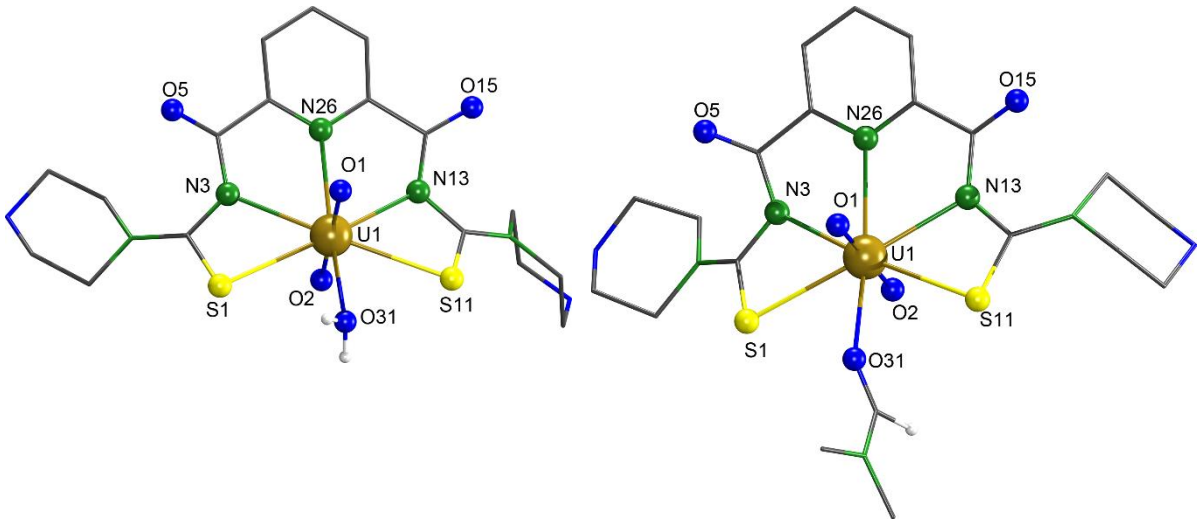

a) b)

Figure 2.9: Molecular structures of a) $[UO_2(L^{2b})(H_2O)]$ and b) $[UO_2(L^{2b})(DMF)]$. Hydrogen atoms except for the coordinated solvents have been omitted for clarity.

The analyses of the mass spectra indicate the loss of the solvent molecules during the measurements and the formation of dimeric fragments $[2\{M\text{-}(solv)\} + Na]^+$ with a mass peak at m/z = 1405.2538 and even trimeric fragments $[3\{M\text{-}(solv)\} + Na]^+$ (m/z = 2096.3828). Obviously, the removal of the solvent ligands gives access to the formation of oligonuclear compounds.

Such an effect might be avoided by a hexadentate ligand, which was synthesized by changing the "pyridine-spacer" of H_2L^{2a} into a 2,2'-bipyridine unit, which resulted in the formation of 2,2'-bipyridine-6,6'-dicarbonylbis(*N*,*N*-diethylthiourea), H_2L^3.

2.2.3 Synthesis and structure of $[UO_2(L^3)]$

Reactions of H_2L^3 with uranyl acetate or $(NBu_4)_2[UO_2Cl_4]$ in the presence of 2 drops of triethylamine give yellow precipitates of $[UO_2(L^3)]$ with yields of about 90 %. The IR spectrum of the product shows a strong $\nu_{U=O}$ vibration at 908 cm^{-1} and the $\nu_{C=O}$ stretch is detected at 1637 cm^{-1}. The latter frequency corresponds to a bathochromic shift of 70 cm^{-1} with respect to the value in H_2L^3, which is slightly more than the shift observed between $[UO_2(L^{2a})(MeOH)]$ and H_2L^{2a}. The observed shift does not necessarily imply that the coordination is established via the carbonyl group, since in such cases the bathochromic shift of the carbonyl band is more considerable with values larger 100 cm^{-1}.[47,48] Nevertheless, a strong electron delocalization involving the C=O group is indicated. The absence of a NH vibration suggests the deprotonation of the coordinated ligand. The positive ESI mass spectrum shows the expected molecular fragments $[M+H]^+$ at 741.1991, $[M+Na]^+$ at 763.1816 and $[M+K]^+$ at 779.1550. No dimerization or trimerization was detected, indicating a high stability of the compound.

Single crystals suitable for X-ray analysis were obtained from a solution of a 1:1 mixture of CH_2Cl_2/MeOH (v/v). Figure 2.10 shows the molecular structure of $[UO_2(L^3)]$. Selected bond lengths and angles are listed in Table 2.7.

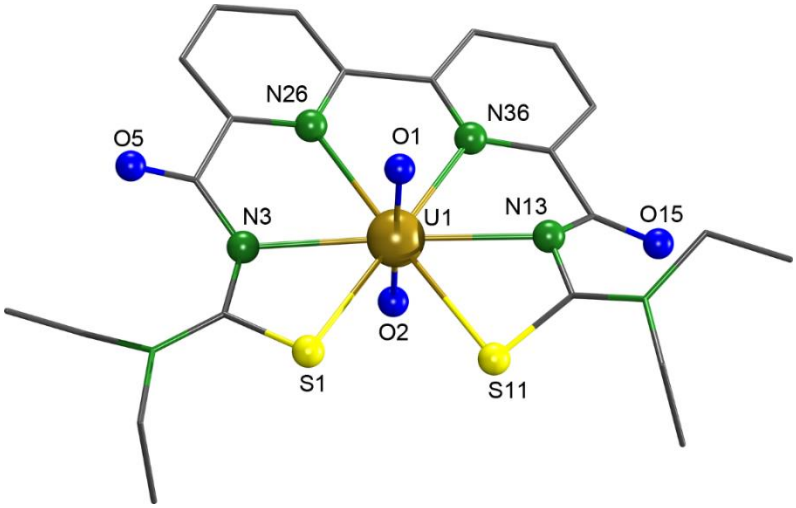

Figure 2.10: Molecular structure of $[UO_2(L^3)]$. Hydrogen atoms have been omitted for clarity.

Expectedly, the organic ligand coordinates hexadentate to the uranyl moiety via four nitrogen and two sulfur atoms giving a hexagonal-bipyramidal coordination of the metal ion. The uranyl bond lengths are 1.769(2) and 1.772(2) Å and the O=U=O bond angle is 176.0(1). The

hexagonal plane of $[UO_2(L^3)]$ is almost perfectly planar, with a maximum deviation of 0.17 Å for atom N3 from the mean least-square plane formed by the donor atoms of the equatorial plane of U1. The U-N bond lengths are between 2.517(3) and 2.518(3) Å for the thiourea sites and 2.609(3) and 2.610(3) Å for the bipyridine nitrogen atoms. The U-S distances are 2.88(1) Å. This value is by 0.05 Å shorter than the value of the U-S bond lengths observed in $[UO_2(L^{2a})(MeOH)]$, where $\{L^{2a}\}^{2-}$ shows the same coordination pattern as $\{L^3\}^{2-}$. However it is equal to the value of the U-S distances observed in the compound $(NBu_4)_2[\{(UO_2(L^1)\}_4(OAc)_2]$, with $\{L^1\}^{2-}$ showing the *S,O* coordination pattern.

Table 2.7: Selected bond lengths (Å), bond angles (°) and torsion angles (°) in $[UO_2(L^3)]$.

Bond lengths					
U1–O1	1.769(2)	U1–N13	2.518(3)	C4–O5	1.232(4)
U1–O2	1.772(3)	U1–N26	2.609(3)	C14–O15	1.229(4)
U1–S1	2.88(1)	U1–N36	2.610(3)	C2–N3	1.380(5)
U1–S11	2.88(1)	C2–S1	1.706(4)	C4–N3	1.346(5)
U1–N3	2.517(3)	C12–S11	1.718(4)	C12–N13	1.370(5)
C14–N13	1.353(5)				
Bond angles					
O1–U1–O2	176.0(1)	N13–U1–S1	120.0(7)	O1–U1-N13	87.0(1)
O1–U1–N36	92.0(1)	O1–U1–N26	83.0(1)	O2–U1-N13	92.0(1)
O2–U1–N36	85.0(1)	O2–U1–N26	93.0(1)	N13–U1-N36	61.8(9)
N3–U1–S11	119.9(7)	O1–U1–S1	88.9(9)	O1–U1–S11	94.5(9)
N3–U1–N26	62.0(9)	O2–U1–S1	93.9(8)	O2–U1–S11	89.4(9)
Torsion angles					
U1–N3–C4–O5		-144.6(1)	U1–N13–C14–O15		-144.8(1)

2.2.4 Stability tests of the complexes obtained from H_2L^1, H_2L^2 and H_2L^3

Liquid-liquid extraction processes play an important role in the treatment of actinides and other heavy metals in waste solutions and in recovery procedures. A conventional solvent extraction method for nuclear fuel recovery is the PUREX (**P**lutonium and **U**ranium **R**ecovery by **Ex**traction) process, which is based on the extraction of uranyl ions from an nitric acid environment into an organic phase by using tri-*n*-butyl phosphate (TBP) as complexation agent.[66] Next to the PUREX process, other liquid-liquid extraction methods have been developed such as the TALSPEAK (Trivalent Actinides Lanthanides Separation by

Phosphorus-reagent Extraction from Aqueous Complexes), the DIDPA (**D**i**i**so**d**ecyl**p**hosphoric **a**cid) and the SANEX (**S**elective **A**cti**n**ide **Ex**traction) processes. [67,68] Most of the ligands used in such separation processes are phosphorus based derivatives, but research on the development of new ligand systems in order to optimize selective extraction and back extraction of actinides from their lanthanide counter parts is still ongoing. Recently, a variety of ligand systems based on the 2,6-pyridine and 6,6'-(2,2'-bipyridine) scaffolds (see Figure 2.11) have been successfully studied as extractants in the above mentioned methods.[69,70]

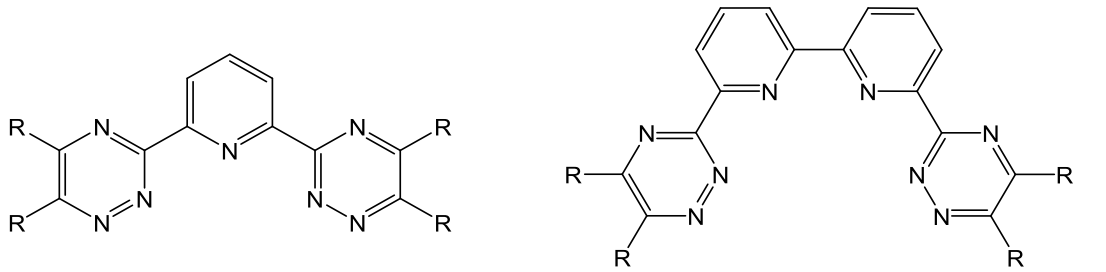

Figure 2.11: Ligand systems used in the liquid-liquid extraction of actinides from lanthanides.

In order to verify the potential suitability of the ligands discussed in this thesis as possible extraction agents for uranyl, and keeping in mind the propensity of H_2L^2 to decompose under acidic conditions (see Chapter 2.2.2), a stability study of the complexes $(HNEt_3)_2[\{UO_2(L^1)\}_4(OAc)_2]$, $[UO_2(L^{2a})(MeOH)]$, $[UO_2(L^{2b})(H_2O)]$ and $[UO_2(L^3)]$ in aqueous solutions at different pH values was done. The pH values were adjusted with nitric acid. As expected, the complexes $(HNEt_3)_2[\{UO_2(L^1)\}_4(OAc)_2]$, $[UO_2(L^{2a})(MeOH)]$ and $[UO_2(L^{2b})(H_2O)]$ are not stable in acidic aqueous solutions. They decompose and the released uranyl ions from the respective complex solutions in dichloromethane can be detected radiometrically in the aqueous phases using a liquid scintillation counter. Optically, in the case of the complexes $[UO_2(L^{2a})(MeOH)]$ and $[UO_2(L^{2b})(H_2O)]$, the solvent mixtures became turpid, which indicates the formation of less soluble hydrolyzed species (see Figure 2.12).

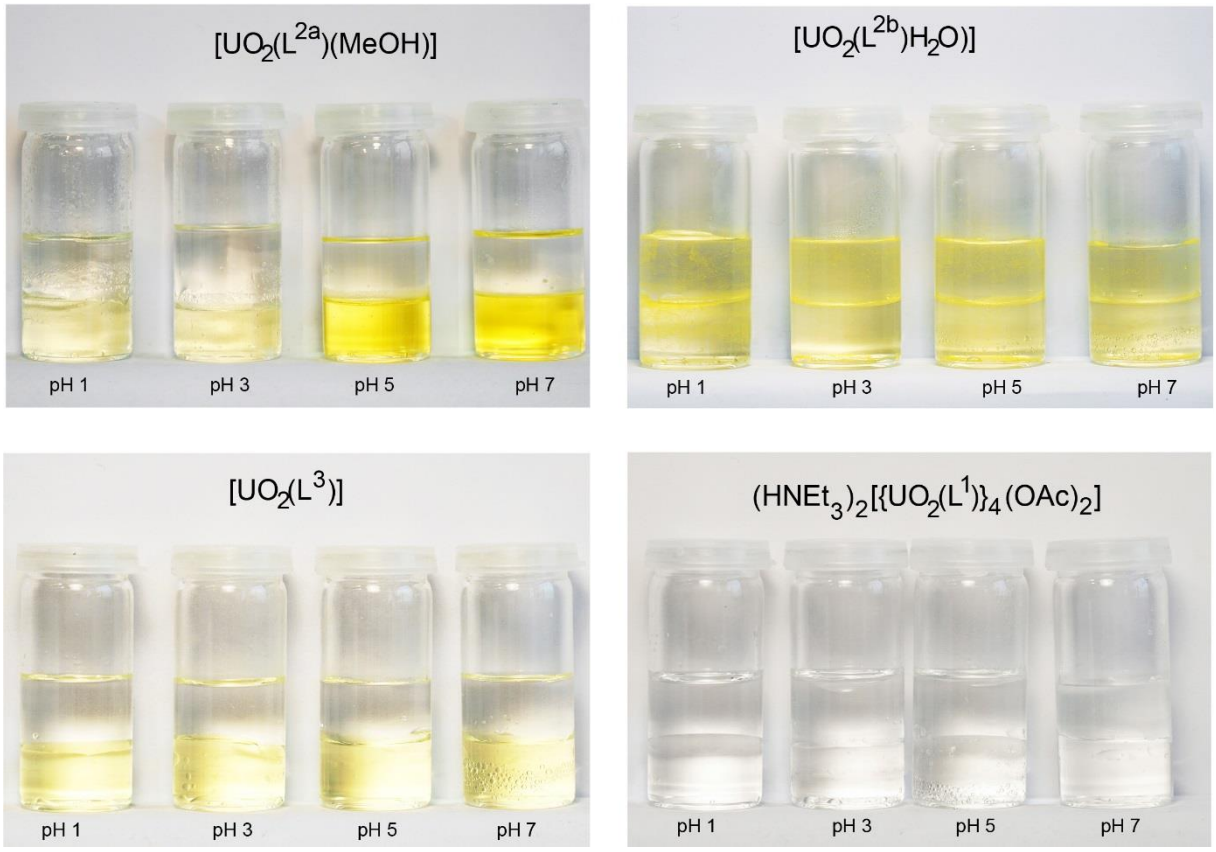

Figure 2.12: Two phase stability study of the synthesized uranyl complexes at various pH values. Concentration of the complexes: 0.4 mM in CH_2Cl_2, t = 60 min, T = 23 °C.

The extraction of uranyl ions into the aqueous phase increases with decreasing pH. The compound $(HNEt_3)_2[\{UO_2(L^1)\}_4(OAc)_2]$, where the uranyl ion is bounded via the bidentate *S,O* coordination, is the most unstable complex with a uranyl extraction of 60 % already at pH 7 and 98% at pH 1. The monomeric complexes $[UO_2(L^{2a})(MeOH)]$ and $[UO_2(L^{2b})(H_2O)]$ show a similar behavior with extraction rates at neutral pH of around 20 % and > 70 % at pH 1. $[UO_2(L^3)]$ shows no eviction of the metal ion from pH 7 to pH 1 with extraction values ≤ 1 % (see Figure 2.13a). The depletion of uranyl ions from the organic phase of $[UO_2(L^3)]$ was only observed with high acid concentrations. In half-concentrated HNO_3 solution, a uranyl extraction of 80 % was observed after 30 min. A total extraction of the uranyl ions from $[UO_2(L^3)]$ was reached in concentrated nitric acid (see Figure 2.13b).

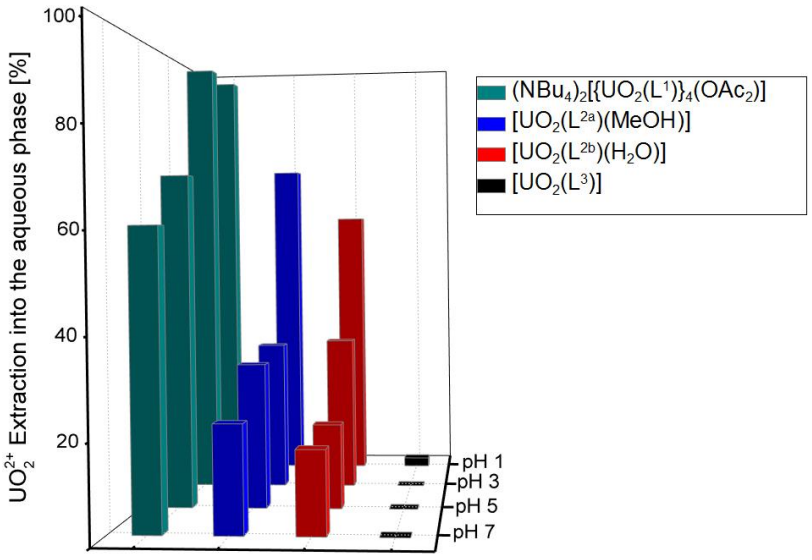

a)

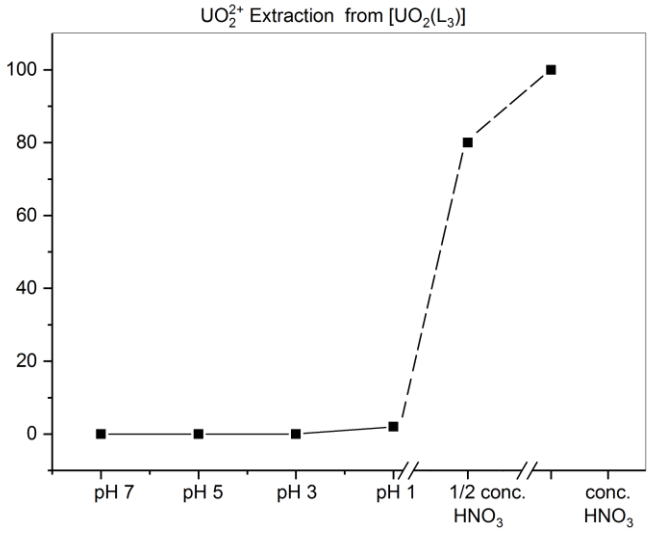

b)

Figure 2.13: a) $[UO_2]^{2+}$ extraction from the synthesized complexes in an aqueous nitric acid solution at different pH values. Concentration of the complexes: 0.4 mM (in CH_2Cl_2); t = 60 min, T = 23 °C. b) pH dependence of the $[UO_2]^{2+}$ extraction from $[UO_2(L^3)]$ at high acidic concentrations.

The separation of the uranyl ions from the ligand framework were also monitored spectroscopically with ^{1}H-NMR and UV/Vis. The UV/Vis spectra of the organic phases before and after the extraction procedure are compared in Figure 2.14. It clearly shows that the extracted uranium species are not identical with the used chelates $(HNEt_3)_2$-$[\{UO_2(L^1)\}_4(OAc)_2]$, $[UO_2(L^{2a})(MeOH)]$ or $[UO_2(L^{2b})(H_2O)]$. The organic phase of the extraction experiments with $(HNEt_3)_2[\{UO_2(L^1)\}_4(OAc)_2]$ contain more or less the intact aroylthiourea, while the experiments with $[UO_2(L^{2a})(MeOH)]$ or $[UO_2(L^{2b})(H_2O)]$ indicate the

decomposition of the complexes and the formation of unknown species. The observations from the UV/Vis spectroscopy study were confirmed by ^{1}H-NMR analyses.

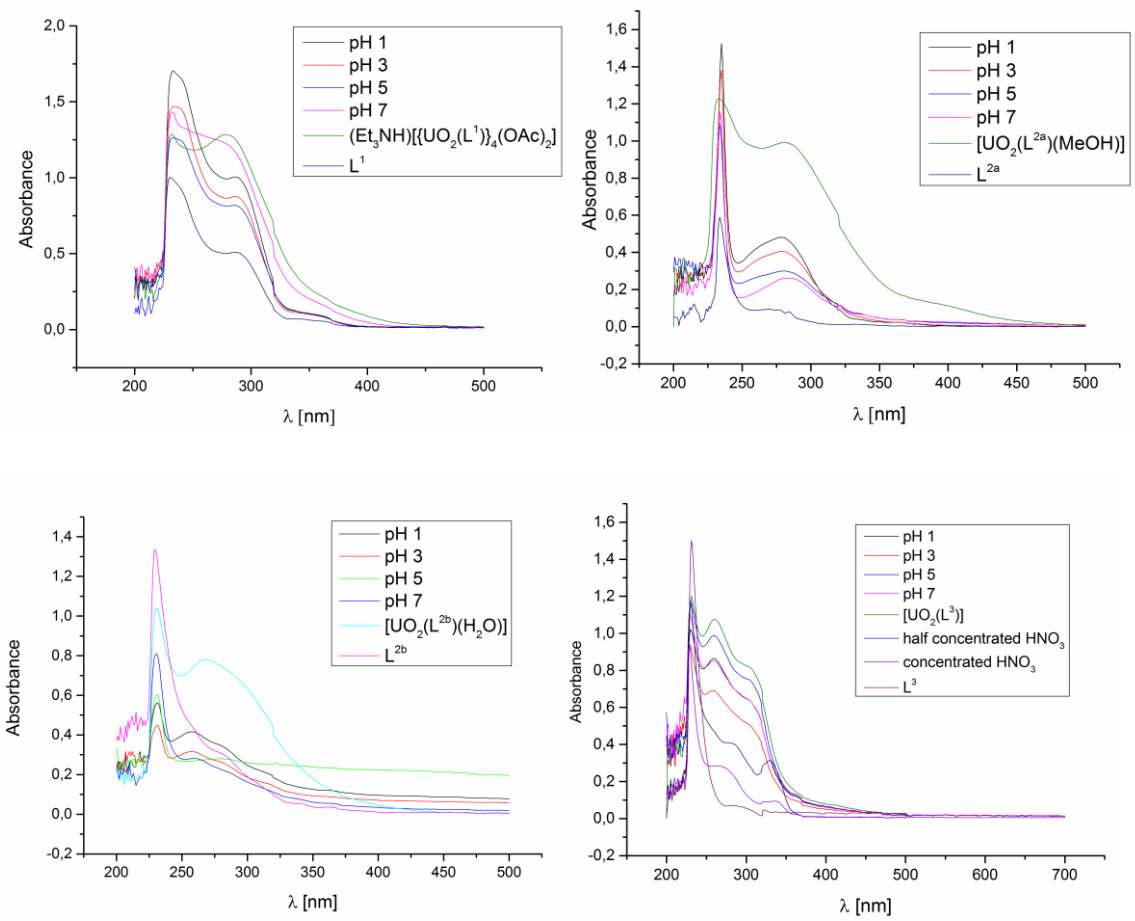

Figure 2.14: UV/Vis spectra in CH_2Cl_2 of the synthesized complexes, the deprotonated ligands and the remaining extracted complex solution at different pH values. Concentrations: complexes = 0.01 – 0.06 mM, ligands = 0.008 – 0.02 mM.

In contrast, the spectra of the extracted organic phase of $[UO_2(L^3)]$ from pH 7 to pH 1 show no differences to the spectrum of the $[UO_2(L^3)]$. Decomposition was only observed in the spectra of solutions with high acid concentrations. Also here, a comparison of the extracted organic phases to the deprotonated ligand was made using both UV/Vis and ^{1}H-NMR spectroscopy.

2.3 Oligonuclear uranyl complexes with H_2L^2

As mentioned in the Chapters 2.2.3 and 2.2.4, the monomeric uranyl complexes with H_2L^{2a} and H_2L^{2b} are instable in solution due to the ready release of the coordinated solvent molecules, which stabilize the hexagonal-bipyramidal coordination environments of the uranyl ions. In the presence of water, the formation of some products resulting from the hydrolysis of the uranyl complexes is observed. The pH-dependent hydrolysis of uranyl complexes is not unusual and typical products are illustrated in Figure 2.15. The diagram shows that aqueous solutions of uranyl ions with increasing pH tends to the formation of oligonuclear species.[71,72] Mononuclear, dinuclear, trinuclear and tetranuclear species coexist in aqueous solutions in the pH range between 2.5 and 5 with oligomers dominating in solution with pH above 3.[73–76] De Stefano et al. studied the kinetic effect of the variation of the ionic strength of the solution on the hydrolysis constants for dioxido uranium compounds in weakly acidic NaCl and $NaNO_3$ solutions.[77] They could show that the formation of one specific hydrolysis product of uranium, mentioned in Figure 2.15 is strongly dependent on the pH of the solution and the nature of the ionic media, since the ions present in the solution can stabilized some of the formed species. At lower pH value, the formation of mononuclear species is preferred. In the pH range between 3.5 and 4.5, binuclear and trinuclear species are formed in NaCl solution and only binuclear species could be observed in $NaNO_3$ solution. At higher pH values the formation of the trinuclear species in both media is predominant.[77]

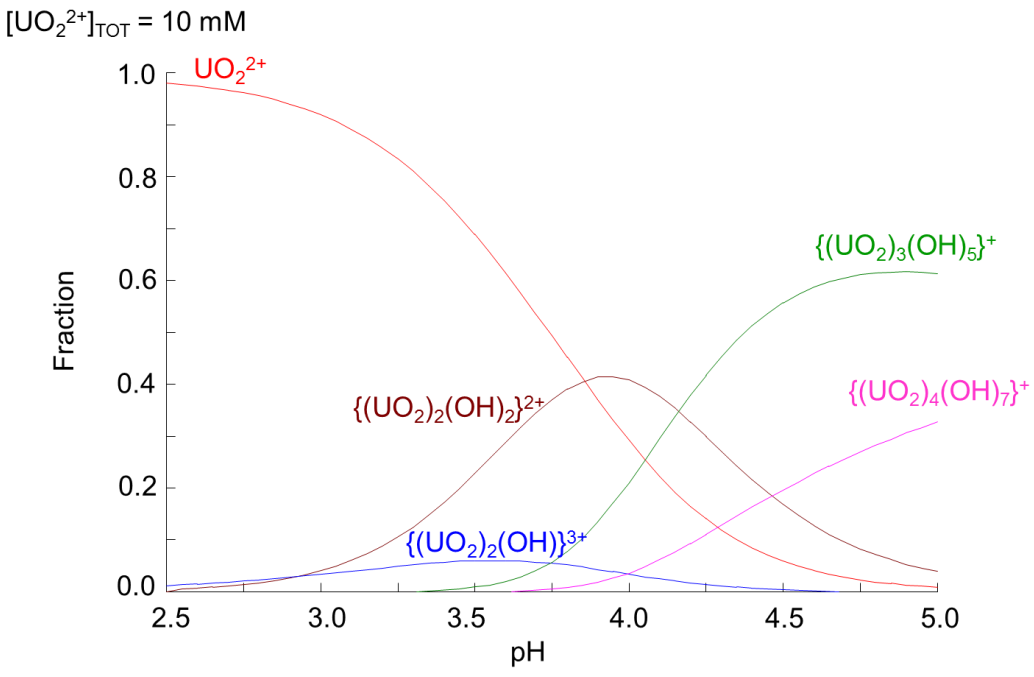

Figure 2.15: Speciation diagram of uranyl hydrolysis product adapted from ref. [72].

Such oligomerizations are not restricted to aqueous solutions, but can also be observed in organic solvents and/or mixtures of water and alcohols. In the following sections, the synthesis and characterization of oligonuclear uranyl complexes will be discussed.

Treatment of H_2L^{2a} with a uranyl salt and four drops of NEt_3 in methanol at room temperature gave instantly a yellow precipitate. Independently of the uranyl starting materials used, the products were identified to be an identical dimeric complex of the composition $(HNEt_3)_2$-$[\{UO_2(L^{2a})(\mu_2\text{-}OMe)\}_2]$ (Scheme 2.8).

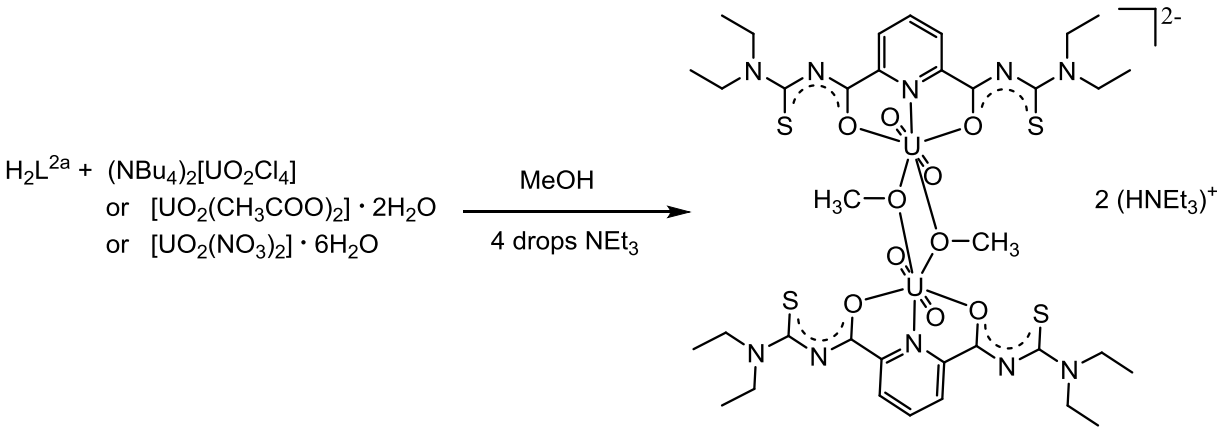

Scheme 2.8: Synthesis of $(HNEt_3)_2[\{UO_2(L^{2a})(\mu_2\text{-}OMe)\}_2]$.

The IR spectra of the obtained precipitates show the absence of NH vibrations, which confirms the deprotonation of the organic ligand in the compound. A strong absorption observed at 1589 cm^{-1} can be assigned to the $\nu_{C=O}$ stretching vibration. In comparison, the $\nu_{C=O}$ stretch of the non-coordinated ligand is observed at 1680 cm^{-1} and the $\nu_{C=O}$ stretch of the monomeric complex $[(UO_2(L^{2a})(MeOH)]$ is observed at 1654 cm^{-1}. The significant bathochromic shift strongly suggests the coordination via the carbonyl oxygen atoms. Similar shifts have also been observed for other metal complexes after chelate formation of H_2L^{2a}, and it indicates strong electron delocalization inside the chelate rings.[47,48] The presence of uranyl ions is confirmed by $\nu_{U=O}$ stretching vibrations observed at 912 cm^{-1}.

The ^{1}H-NMR spectra of the compound in $CDCl_3$ and $(CD_3)_2SO$ indicate an interesting behavior of the complex in these two solvents. Beside the signals of the deprotonated ligand $\{L^{2a}\}^{2-}$, signals corresponding to the counter ions $\{HNEt_3\}^+$ were observed. But for the stabilization of the charge in the metal complex the additional methanolato ligand is required. However, the latter could not be detected with the conditions used for the ^{1}H-NMR measurements. This indicates a decomposition of the dimeric complex in solution. The labile U-O(Me)-U bonds are

broken and the monomeric units $[UO_2(L^{2a})(OMe)_{2-n}(solv)_n]$ are found. Here, the solvent acts as ligand and stabilizes the coordination environment of uranium. The missing signal for the coordinated methanolato ligands indicates a fast exchange with other donor ligands (e.g. OH^-/H_2O). The spectrum in $(CD_3)_2SO$ show a remaining signal observed at 3.13 ppm, which can be assigned to the free methanol molecules, resulting from the ligand exchange equilibrium in solution.

The $(CD_3)_2SO$ solution overlayered with methanol affords a crystalline product, which has been characterized as a neutral complex of the composition $[UO_2(L^{2a})(DMSO)_2]$. The quality of the single crystals, however, was not suitable for a detailed discussion of the bond lengths and angles. Thus, only general bonding features shall be discussed here. The molecular structure of the compound could be derived from the crystal data. It is illustrated in Figure 2.16. The ligand $\{L^{2a}\}^{2-}$ coordinates tridentate to the uranyl unit through *O,N,O* and the coordination environment of the metal center is completed by two dimethyl sulfoxide ligands.

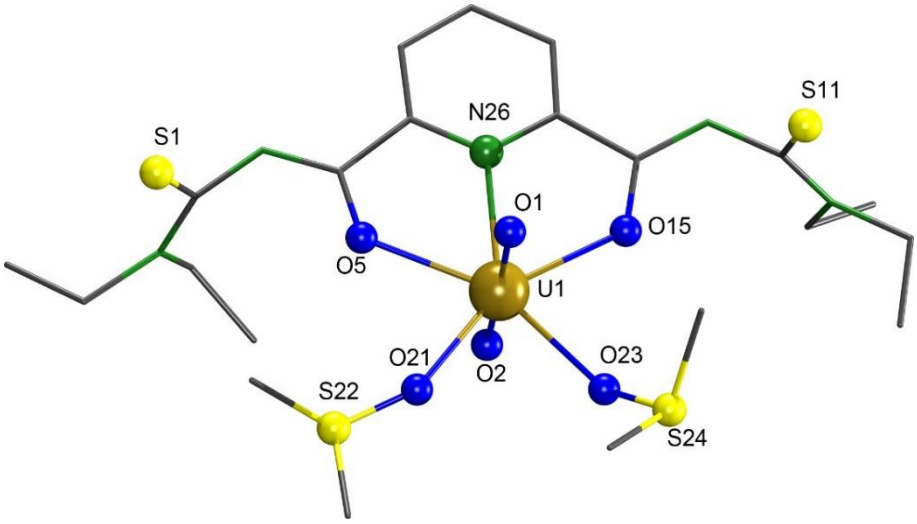

Figure 2.16: Molecular structure of $[UO_2(L^{2a})(DMSO)_2]$. Hydrogen atoms have been omitted for clarity.

The molecular decomposition of the dimeric compound in solution has also been observed in the negative-mode ESI mass spectrum of the complex, which has been measured in $CHCl_3$/MeOH. The peak of the molecular ion $[\{UO_2(L^{2a})(\mu_2\text{-}OMe)\}_2]^{2-}$ was not observed, but different peaks, which indicate the decomposition of the complex. The two main peaks observed at m/z = 680.1775 and 694.1932 can be assigned to the monomeric anions $[UO_2(L^{2a})(OH)]^-$ and $[UO_2(L^{2a})(OMe)]^-$. A part of this spectrum is shown in Figure 2.17.

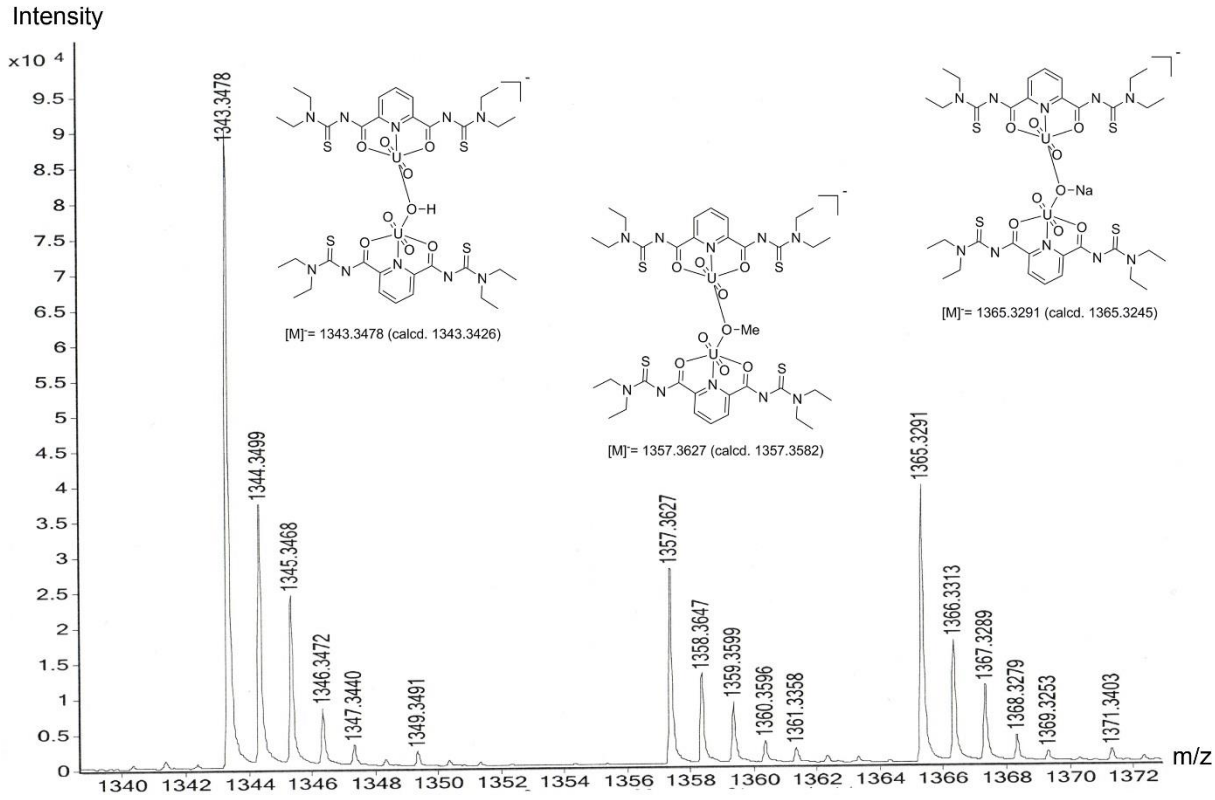

Figure 2.17: Molecular fragments observed in the negative-mode ESI-MS spectrum of $(HNEt_3)_2[\{UO_2(L^{2a})(\mu_2\text{-}OMe)\}_2]$.

Yellow crystals suitable for X-ray diffraction analysis were obtained from a 1:1 mixture of CH_2Cl_2/MeOH (v:v) at room temperature. The analysis of the X-ray data as well as the results of the elemental analysis confirm the composition of the complex as $(HNEt_3)_2[\{UO_2(L^{2a})(\mu_2\text{-}OMe)\}_2]$. Interestingly, recrystallization of the complex from a $CDCl_3$/MeOH solution at room temperature gave another isomer of $(HNEt_3)_2[\{UO_2(L^{2a})\text{-}(\mu_2\text{-}OMe)\}_2]$.

Figure 2.18 and Figure 2.19 show the representations of the two isomeric structures of $(HNEt_3)_2[\{UO_2(L^{2a})(\mu_2\text{-}OMe)\}_2]$. Selected bond lengths and angles are listed in Table 2.8. The *syn,syn*-isomer, based on the orientation of the sulfur atoms and of the bridging methanolato ligands crystallizes in the triclinic space group $P\overline{1}$ and the *anti,anti*-isomer crystallizes in the monoclinic space group C2/c, the latter one with one half of the molecule in the asymmetric unit.

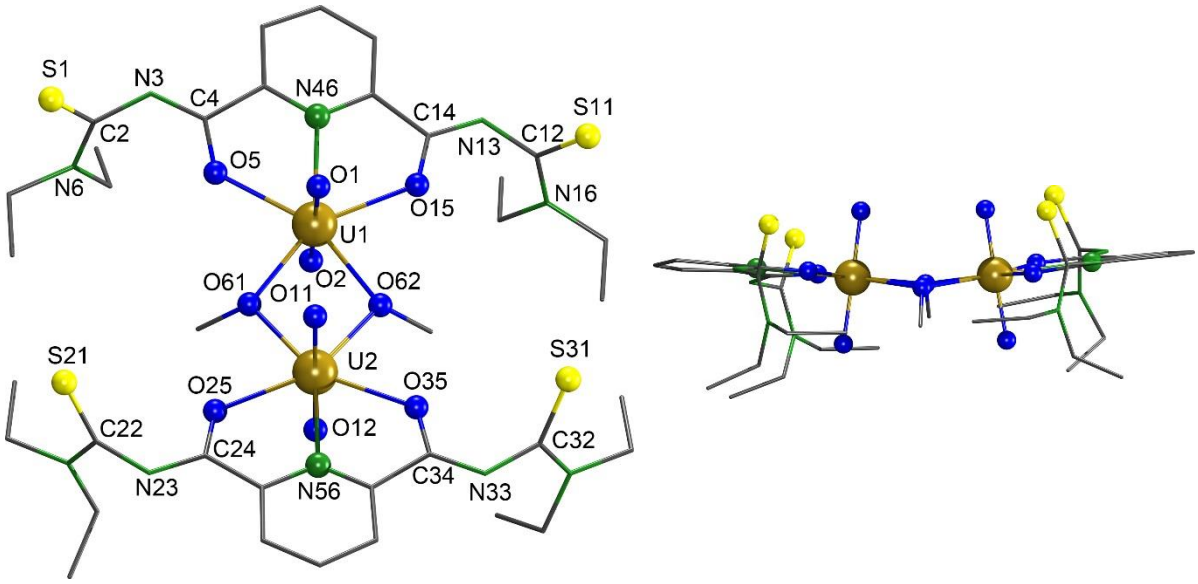

a) b)

Figure 2.18: a) Molecular structure of the anion *syn,syn*-[{$UO_2(L^{2a})(\mu_2\text{-}OMe)\}_2$]$^{2-}$. b) View along the [1,1,1] direction. Hydrogen atoms have been omitted for clarity.

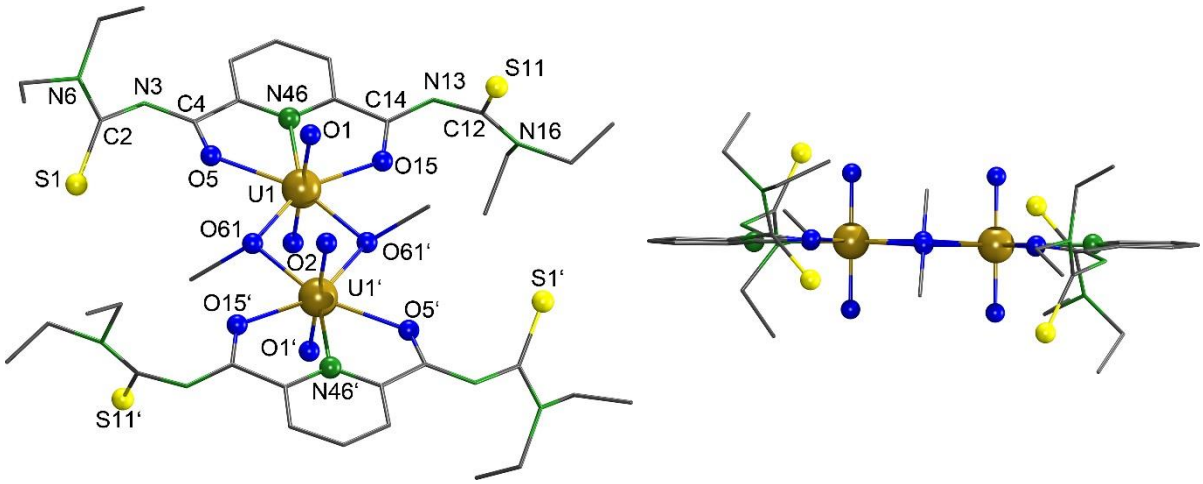

a) b)

Figure 2.19: a) Molecular structure of the anion *anti,anti*-[{$UO_2(L^{2a})(\mu_2\text{-}OMe)\}_2$]$^{2-}$. b) View along the [1,1,1] direction. Symmetry related atoms are produced by the symmetry operator -x+1/2, -y+3/2, -z. Hydrogen atoms have been omitted for clarity.

Table 2.8: Selected bond lengths (Å), distances (Å), bond angles (°) and torsion angles (°) in *syn,syn*-$(HNEt_3)_2[\{UO_2(L^{2a})(\mu_2\text{-}OMe)\}_2]$ (**3**) and *anti,anti*-$(HNEt_3)_2[\{UO_2(L^{2a})(\mu_2\text{-}OMe)\}_2]$ (**4**) (symmetry operator -x+1/2,-y+3/2,-z).

Bond lengths	(**3**)	(**4**)	Distances	(**3**)	(**4**)
U1–O1	1.765(6)	1.769(5)	U2–O35	2.372(6)	–
U1–O2	1.770(6)	1.778(5)	U2–N56	2.564(7)	–
U1–O5	2.357(6)	2.354(5)	U2–O61	2.336(6)	–
U1–O15	2.376(5)	2.348(5)	U2–O62	2.344(5)	–
U1–N46	2.579(7)	2.530(5)	C2–S1	1.68(1)	1.656(8)
U1–O61	2.348(6)	2.344(4)	C2–N3	1.39(1)	1.409(9)
U1–O62(O61')	2.365(5)	2.357(5)	C4–N3	1.29(1)	1.229(9)
U2–O11	1.776(6)	–	O5–C4	1.31(1)	1.289(6)
U2–O12	1.783(6)	–	C2–N6	1.34(1)	1.33(1)
U2–O25	2.380(6)	–	U1···U2(U1')	3.772(5)	3.783(4)
Bond angles	(**3**)	(**4**)	Bond angles	(**3**)	(**4**)
O1–U1–O2	178.5(3)	179.6(3)	O11–U2–O12	179.0(3)	–
O1–U1–N46	90.7(3)	91.1(2)	O11–U2–N46	91.4(3)	–
O1–U1–O5	89.1(3)	88.3(3)	O11–U2–O25	88.2(3)	–
O1–U1–O15	89.6(3)	90.8(3)	O11–U2–O35	91.6(3)	–
O1–U1–O61	91.2(3)	91.6(2)	O11–U2–O61	91.7(3)	–
O1–U1–O62	89.5(3)	89.7(3)	O11–U2–O62	90.4(2)	–
Torsion angles	(**3**)	(**4**)	Torsion angles	(**3**)	(**4**)
S1–C2–N3–C4	100.3(1)	-66.2(9)	S21–C22–N23–C24	-96.8(2)	–
S11–C12–N13–C14	-95.7(1)	-73.6(1)	S31–C32–N33–C34	85.8(1)	–

Both structures of $(HNEt_3)_2[\{UO_2(L^{2a})(\mu_2\text{-}OMe)\}_2]$ are built up from two units of a uranyl cation coordinated by one $\{L^{2a}\}^{2-}$ ligand, which is bonded through *O,N,O*. The subunits are connected by two methanolato ligands. Thus, each uranium atom is 7-fold coordinated with a pentagonal-bipyramidal geometry. The axial uranyl bond lengths are observed in the range of 1.765(6) – 1.783(6) Å. The U-O bond lengths in the equatorial plane are in the range of 2.348(6) – 2.376(5) Å for the *syn,syn*-isomer and in a range of 2.344(4) – 2.354(5) Å for the *anti,anti*-isomer. The U-N bond distances are between 2.579(7) and 2.564(7) Å for the *syn,syn*-isomer and slightly shorter with 2.530(5) Å for the *anti,anti*-isomer. The carbonyl bond lengths are 1.31(1) Å for the *syn,syn*-isomer and between 1.283(5) and 1.289(6) Å for the *anti,anti*-isomer. They are significantly longer than the distance of 1.223(5) Å, which is observed in the

non-coordinated ligand H_2L^{2a} and therefore in the expected range for chelate complexes. The C-S bonds of 1.658(8) to 1.68(1) Å are nearly equal to the corresponding distances in H_2L^{2a}. For the *anti,anti*-isomer, the C4-N3 and the C2-N3 bond lengths are by 0.111 Å and 0.018 Å shorter, and the C2-S1 bond length is with 1.656(6) Å identical with the corresponding distances observed in H_2L^{2a}.[47] The bond lengths in the molecular structure of the complexes indicate the π-electron delocalization in the thiourea chelates. The nearly perfect pentagonal-bipyramidal coordination geometry of the uranium ions in both conformers is described by angles between the two mean least-square planes of the bipyramides and the uranyl oxygen atoms of 88.77 ° and 89.46 ° for the *anti,anti*-isomer and 89.90 ° for the *syn,syn*-isomer. The maximum deviation from the equatorial mean least-square plane is observed for N46 with 0.04 Å for the *anti,anti*-isomer and 0.142 Å for the *syn,syn*-isomer. The distinguishing feature in these structures is the orientation of the sulfur atoms with regard to the equatorial plane, which can be determined by the torsion angle of the thiourea groups. The structure of the *syn,syn*-isomer shows two positive and two negative torsion angles, while the *anti,anti*-isomer shows three negative and one positive torsion angles.

Similar reactions of H_2L^{2b} with two equivalents of a uranyl salt in methanol result in the analogous product $(HNEt_3)_2[\{UO_2(L^{2b})(\mu_2\text{-}OMe)\}_2]$. The IR spectrum shows the $\nu_{C=O}$ vibration at 1587 cm^{-1} and the uranyl vibration at 901 cm^{-1}. The structure of $(HNEt_3)_2[\{UO_2(L^{2b})(\mu_2\text{-}OMe)\}_2]$ could be confirmed by an X-ray diffraction analysis of the yellow crystals, which were obtained from a CH_2Cl_2/MeOH solution. Because of the low crystal quality, the data set is not suitable for a detailed analysis and discussion of bond lengths and angles. The molecular structure of the formed complex, however, could be derived unambiguously. It is the *anti,anti*-isomer of the dimeric complex. Single crystals of better quality were obtained by the replacement of the $(HNEt_3)^+$ counter ions.

Addition of $(EtPPh_3)Cl$ to a CH_2Cl_2/MeOH solution of $(HNEt_3)_2[\{UO_2(L^{2b})(\mu_2\text{-}OMe)\}_2]$ lead to the exchange of the cations and the product $(EtPPh_3)_2[\{UO_2(L^{2b})(\mu_2\text{-}OMe)\}_2]$ was isolated. The IR spectrum shows the $\nu_{C=O}$ vibration at 1585 cm^{-1} and the uranyl vibration at 906 cm^{-1}. The NMR analysis confirms the presence of two $(EtPPh_3)^+$ cations. Figure 2.20 represents the molecular structure of the anion $[\{UO_2(L^{2b})(\mu_2\text{-}OMe)\}_2]^{2-}$, which also crystallized as an *anti,anti*-isomer in the triclinic space group $P\bar{1}$ with one half of the molecule in the asymmetric unit. Selected bond lengths and angles are listed in the Table 2.9.

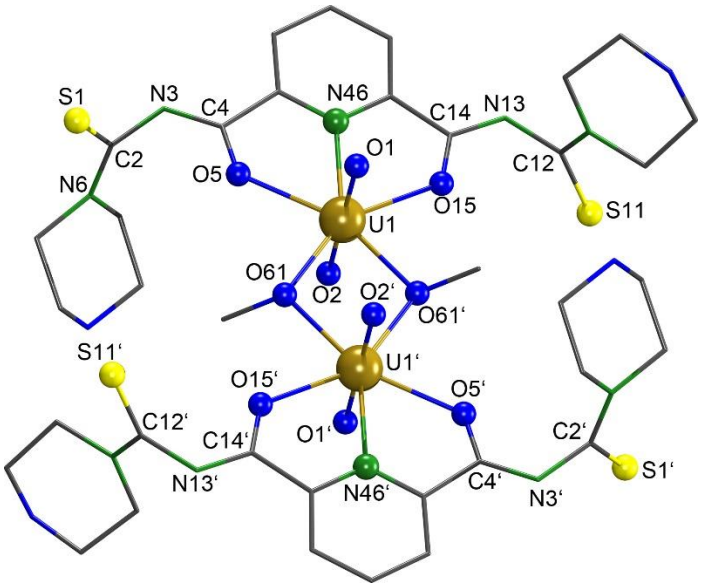

Figure 2.20: Structure of the anion of *anti,anti*-$(EtPPh_3)_2[\{UO_2(L^{2b})(\mu_2\text{-}OMe)\}_2]$. Symmetry related atoms are produced by the symmetry operator -x+1, -y+2, -z+1. Hydrogen atoms have been omitted for clarity.

Table 2.9: Selected bond lengths (Å), bond angles (°) and torsion angles (°) in *anti,anti*-$(EtPPh_3)_2[\{UO_2(L^{2b})(\mu_2\text{-}OMe)\}_2]$ (symmetry operator –x+1, -y+2, -z+1).

Bond lengths					
U1–O1	1.787(3)	U1–N46	2.558(4)	C2–S1	1.664(5)
U1–O2	1.793(3)	U1–O61	2.343(3)	C2–N3	1.405(6)
U1–O5	2.375(3)	U1–O61’	2.363(3)	C4–N3	1.306(6)
U1–O15	2.361(3)	C2–N6	1.330(9)	O5–C4	1.289(5)
Bond angles					
O1–U1–O2	178.8(1)	O1–U1–O5	89.1(1)	O1–U1–O61	86.2(1)
O1–U1-N46	89.3(1)	O1–U1–O15	89.1(1)	O1–U1–O61’	93.5(2)
Torsion angles					
S1–C2–N3–C4		-96.7(1)	S1’–C2’–N3’–C4’		-83.7(1)
S11–C12–N13–C14		-83.7(1)	S11’–C32’–N33’–C34’		96.7(1)

An attempt to exchange the cations of the complex $(HNEt_3)_2[\{UO_2(L^{2a})(\mu_2\text{-}OMe)\}_2]$ in a similar manner with $(EtPPh_3)Cl$ in CH_2Cl_2/MeOH solution led to the precipitation of two types of yellow crystals, blocks and needles. The yellow blocks with a yield of 12 % were characterized as the dimeric compound $(EtPPh_3)_2$ *anti,syn*-$[\{UO_2(L^{2a})(\mu_2\text{-}OMe)\}_2]$. The IR spectrum shows the $\nu_{C=O}$ vibration at 1591 cm^{-1} and the asymmetric uranyl vibration at 905 cm^{-1}. NMR analyses confirm the presence of the $(EtPPh_3)^+$ cations. Figure 2.21 represents

the molecular structure of the anion *anti,syn*-[{$UO_2(L^{2a})(\mu_2\text{-OMe})\}_2]^2$. Selected bond lengths and angles are listed in Table 2.10.

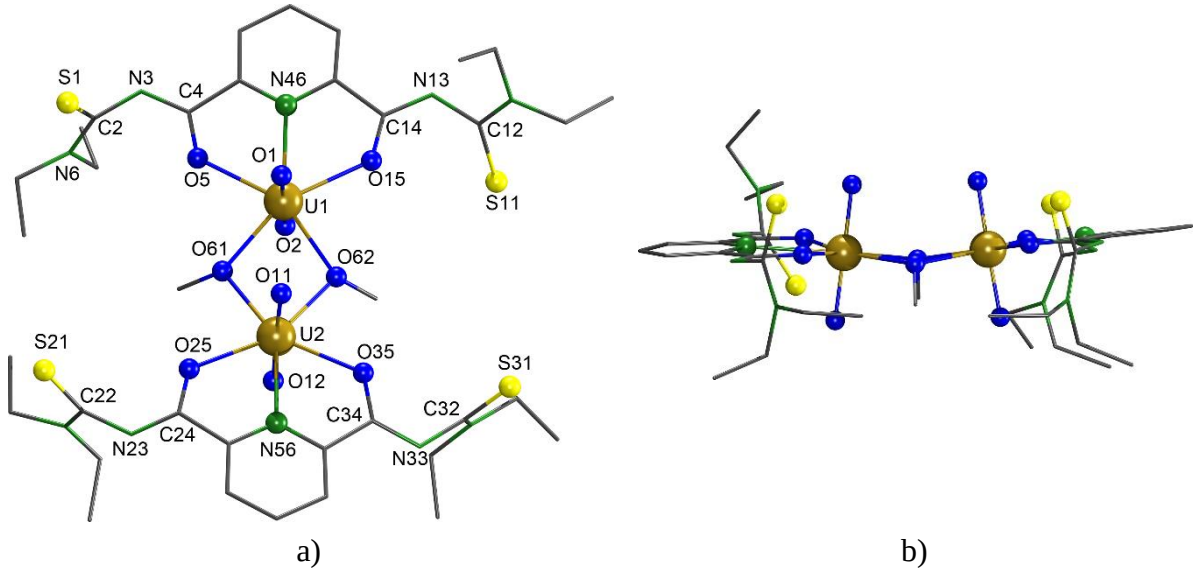

a) b)

Figure 2.21: a) Molecular structure of the anion *anti,syn*-$[\{UO_2(L^{2a})(\mu_2\text{-OMe})\}_2]^{2-}$. b) View along the [1,1,1] direction. Hydrogen atoms have been omitted for clarity.

Table 2.10: Selected bond lengths (Å), bond angles (°) and torsion angles (°) in *anti,syn*-$(EtPPh_3)_2[\{UO_2(L^{2a})(\mu_2\text{-OMe})\}_2]$

Bond lengths					
U1–O1	1.782(3)	U2–O11	1.791(3)	C2–S1	1.687(5)
U1–O2	1.786(3)	U2–O12	1.788(3)	C2–N3	1.380(6)
U1–O5	2.359(3)	U2–O25	2.357(3)	C4–N3	1.297(6)
U1–O15	2.362(3)	U2–O35	2.365(3)	O5–C4	1.284(5)
U1–N46	2.537(4)	U2–N56	2.531(4)	C2–N6	1.337(6)
U1–O61	2.332(3)	U2–O61	2.351(3)		
U1–O62	2.350(3)	U2–O62	2.341(3)		
Bond angles					
O1–U1–O2	179.4(1)	O1–U1–O61	88.8(1)	O11–U2–O25	89.8(2)
O1–U1–N46	86.2(2)	O1–U1–O62	91.8(1)	O11–U2–O35	90.6(1)
O1–U1–O5	91.2(2)	O11–U2–O12	177.8(2)	O11–U2–O61	90.2(2)
O1–U1–O15	90.2(1)	O11–U2–N46	87.1(2)	O11–U2–O62	90.4(2)
Torsion angles					
S1–C2–N3–C4		67.3(5)	S21–C22–N23–C24		98.7(4)
S11–C12–N13–C14		88.8(4)	S31–C32–N33–C34		-99.6(5)

In this isomer, the sulfur atoms are oriented in different directions, while the methanolato ligands are oriented in the same direction. The bond distances and angles are in the same range as observed in the *anti,anti*-isomer.

Interestingly, the addition of excess amounts of NEt_3 to reaction mixtures of a uranyl salt and one molar equivalent of H_2L^{2a} in methanol or ethanol results in the formation of the identical trinuclear uranyl complex, $(HNEt_3)[(UO_2)_3(L^{2a**})_2(\mu_2\text{-}OH)(\mu_3\text{-}O)]$ independent of the uranyl starting material used (see Scheme 2.9).

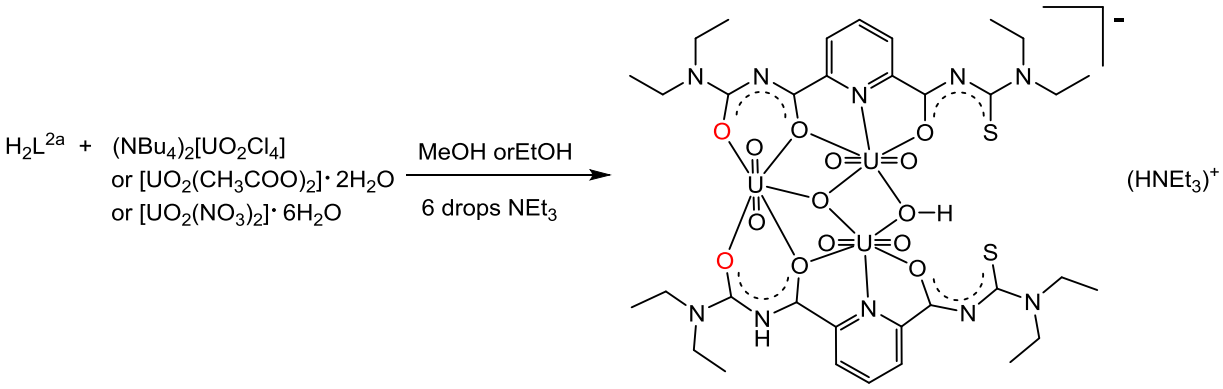

Scheme 2.9: Synthesis of $(HNEt_3)[(UO_2)_3(L^{2a**})_2(\mu_2\text{-}OH)(\mu_3\text{-}O)]$.

IR spectra of the products show the $\nu_{U=O}$ stretch at 902 cm^{-1} and the $\nu_{C=O}$ vibrations at 1597 cm^{-1}. The ^{1}H-NMR spectrum in $(CD_3)_2SO$, which is shown in Figure 2.22, indicates the formation of a monoanionic complex with one triethylammonium counter ion. In the aromatic region, two signals with six protons are observed. They indicate the presence of two ligands $\{L^{2a**}\}^{2-}$. The methylene protons of $\{L^{2a**}\}^{2-}$ show two identical quartets at 3.95 and 3.53 ppm and the methyl groups show two identical triplets at 1.25 and 1.02 ppm. $(HNEt_3)^+$ shows two signals at 2.37 and 0.87 ppm, which correspond to its methylene and methyl groups. The signal for the μ_2-hydroxido and the NH groups could not be observed with the conditions used for the NMR measurements. The formation of the trinuclear uranyl complex is confirmed by ESI mass spectrum in the negative mode, which show the fragment for the molecular anion at m/z =1597.4242, (Calcd. 1597.4238).

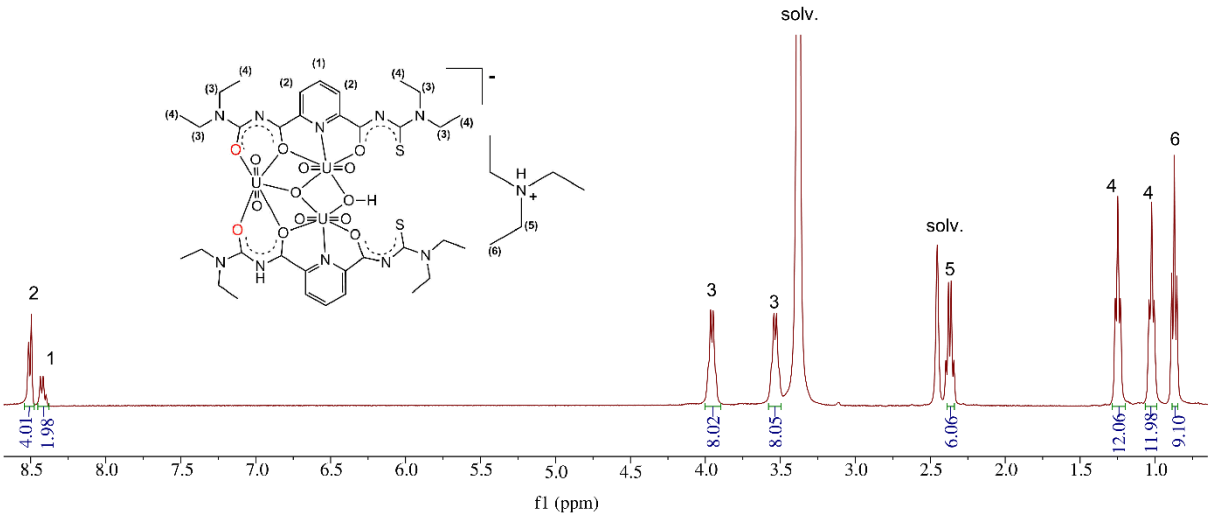

Figure 2.22: ^{1}H-NMR spectrum of $(HNEt_3)[(UO_2)_3(L^{2a**})_2(\mu_2\text{-}OH)(\mu_3\text{-}O)]$ in $(CD_3)_2SO$.

Single crystals of $(HNEt_3)[(UO_2)_3(L^{2a**})_2(\mu_2\text{-}OH)(\mu_3\text{-}O)]$ were obtained from CH_2Cl_2/EtOH. The compound crystallizes in the monoclinic space group C2/c and its asymmetric unit contains one complex anion, one triethylammonium cation as well as one water solvent. The molecular structure of the complex anion $[(UO_2)_3(L^{2a**})_2(\mu_2\text{-}OH)(\mu_3\text{-}O)]^-$ is shown in Figure 2.23. Selected bond lengths and angles are summarized in the Table 2.11.

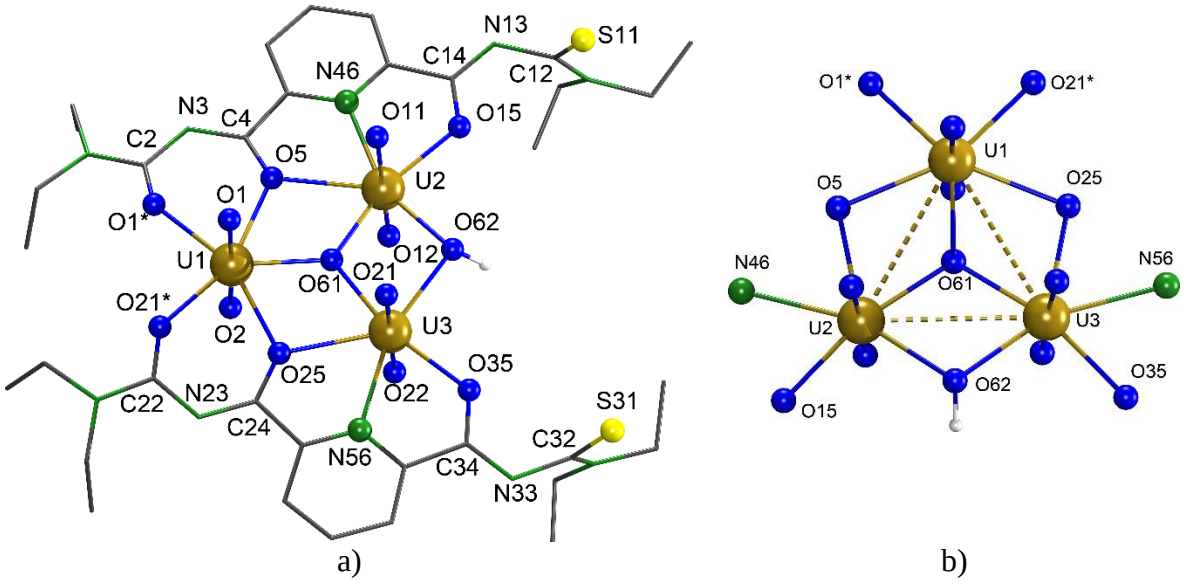

Figure 2.23: a) Molecular structure of the anion $[(UO_2)_3(L^{2a**})_2(\mu_2\text{-}OH)(\mu_3\text{-}O)]^-$. Hydrogen atoms bonded to the carbon atoms have been omitted for clarity. b) Coordination environment of the uranium triangle in $[(UO_2)_3(L^{2a**})_2(\mu_2\text{-}OH)(\mu_3\text{-}O)]^-$.

Table 2.11: Selected bond lengths (Å), distances (Å), bond angles (°) and torsion angles (°) in $(HNEt_3)[(UO_2)_3(L^{2a})_2(\mu_2\text{-}OH)(\mu_3\text{-}O)]$.

Distances					
U1–O1	1.753(8)	U2–O11	1.769(7)	U3-O21	1.769(7)
U1–O2	1.777(8)	U2–O12	1.774(8)	U3-O22	1.774(8)
U1–O5	2.526(7)	U2–O5	2.483(7)	U3-O25	2.494(7)
U1–O25	2.503(7)	U2–O15	2.346(7)	U3-O35	2.346(7)
U1–O1*	2.341(8)	U2–N46	2.536(8)	U3-N56	2.535(8)
U1–O21*	2.302(7)	U2–O61	2.213(7)	U3-O61	2.239(7)
U1–O61	2.200(8)	U2–O62	2.389(7)	U3-O62	2.389(7)
U1⋯U2	3.735(6)	U2⋯U3	3.876(6)	U1⋯U3	3.897(5)
C2–O1*	1.25(1)	C2–N3	1.39(1)	C2–N6	1.33(1)
C4–N3	1.30(1)	O5–C4	1.29(1)	C12–S11	1.68 (2)
C12–N13	1.41(2)	C14–N13	1.29(1)	O15–C14	1.29(1)
Bond angles					
O1–U1–O2	177.2(3)	O1–U1–O61	90.1(3)	O1–U1–O5	93.2(3)
O1–U1–O1*	89.1(3)	O1–U1–O21*	88.1(2)	O1–U1–O25	93.4(2)
O11–U2–O5	90.9(3)	O11–U2–O15	88.6(2)	O11–U2–O12	176.1(3)
O11–U2–O61	90.8(3)	O11–U2–O62	92.9(3)	O11–U2–N46	89.8(3)
O21–U3-O25	91.8(2)	O21–U3-O35	88.5(3)	O21–U3-O22	176.3(2)
O21–U3-O61	91.5(3)	O21–U3-O62	94.4(3)	O21–U3-N56	87.7(2)
U1–O61–U2	122.9(3)	U1–O61–U3	122.8(3)	U2–O61–U3	114.1(3)
U2⋯U3⋯U1	61.6(2)	U3⋯U1⋯U2	57.4(2)	U1⋯U2⋯U3	61.0(2)
Torsion angles					
O1*–C2–N3–C4		6.9(2)	O21*–C22–N23–C24		-3.8(2)
S11–C12–N13–C14		-77.6(2)	S31–C32–N33–C34		100.3(2)

The complex anion is composed of two ligands $\{L^{2a**}\}^{2-}$, three uranyl units, one μ_3-oxido ligand and one μ_2-hydroxido ligand, indicating a net charge of the complex of -1. Both ligands $\{L^{2a**}\}^{2-}$ coordinate each two uranyl ions in a tetradentate *O,O,N,O,* fashion. The three uranium atoms are connected to each other via the central μ_3-oxido ligand. U2 and U3 are connected to each other via the μ_2-hydroxido ligand. This results in the formation of a regular triangle of the uranium atoms as is shown in Figure 2.23. The angles between the uranium atoms are 57.4(2), 61.0(2) and 61.6(2) ° and the U-U distances are 3.735(6), 3.876(6) and 3.897(5) Å. Each uranium ion is 7-fold coordinated and shows a typical pentagonal-bipyramidal geometry. The uranyl bond lengths are unexceptional. The uranium atoms U2 and U3 are coordinated by two

oxygen and the pyridine nitrogen atoms of $\{L^{2a**}\}^{2-}$. The third uranium atom, U1, is coordinated by the remaining two oxygen atoms from each ligand $\{L^{2a**}\}^{2-}$. The pentagonal base of the uranyl bipyramid is completed in the case of U1 by the μ_3-oxygen atom and in the case of U2 and U3 additionally by the μ_2-hydroxido ligand. The U-O61 distances have values between 2.213(7) and 2.239(7) Å and are shorter than those to the other equatorial donor atoms. Interestingly, the distances of the uranium atoms to the μ_2-oxygen atoms O5 and O25 are longer than to the mono-coordinated oxygen atoms of $\{L^{2a**}\}^{2-}$ (O1*, O15, O21* and O35). The equatorial planes of the uranyl ions are almost perfectly planar. The largest distortion in the coordination environment of the uranium atoms is observed for U3 with an angle between the two mean least-square planes of the pentagonal-bipyramide of 86.56 °.

The most interesting features in this structure are the hydrolysis of the organic ligands and the condensation reaction of the uranyl ions. The partial hydrolysis of the ligand occurred during the complex formation reaction. Condensation reactions of uranyl species have been widely reported in the literature, showing that in aqueous solutions with a pH values between 2.5 and 5 various mono-, bi- and trinuclear species coexists. A small change in the pH of the aqueous solution can influence the nuclearity of the uranyl species and favors the oligomerization of the compound as was shown in Figure 2.15.[72,77–79] Less common is the observed partial hydrolysis of $\{L^{2a}\}^{2-}$. Here, during the complex formation, the sulfur atoms of the coordinating sides of the ligands were replaced by oxygen atoms. A similar reaction has been observed by Rodenstein et al. during the reaction of the unstable isophthaloylbis(*N*,*N*-diethylselenourea) with Cu(II) ions in an excess of aqueous pyridine.[45] They observed the hydrolysis of the ligand and the formation of the isophthaloylbis(*N*,*N*-diethylurea) ligand, which coordinated the Cu(II) ions in a bidentate *O*,*O* fashion. Since the ligand H_2L^{2a} and its complexes are relatively stable compounds, a replacement of the sulfur atoms has never been reported before. A plausible reason for the partial hydrolysis of the sulfur atoms of the ligand is the influence of the hard uranyl ion, which forces the replacement of the "*soft*" sulfur atoms in favor of the "*hard*" oxygen atoms. Metal induced hydrolysis of (unsubstituted) thiourea ligands in basic aqueous solutions has been studied and reported in the literature. Some examples have been reported for compounds containing hard metal ions with a high hydrolysis affinity such as Cr(VI), Fe(V), Ru(III) and Co(II).[80–85] In general, the proposed mechanisms indicate, that the elimination process of the sulfur atom occurs over the formation and the decomposition of an intermediate $[R_2CS–M^{n+}–(OH)_n^-]$ complex.

A similar trinuclear complex was obtained from the addition of a solution of $(EtPPh_3)Cl$ in aqueous MeOH to a solution of the dimeric complex $(HNEt_3)_2[\{UO_2(L^{2a})(\mu_2\text{-}OMe)\}_2]$ in CH_2Cl_2. The yellow needles, which were isolated with a yield of 60 % as the main product of the reaction (see Scheme 2.10) were characterized as $(EtPPh_3)[(UO_2)_3(L^{2a**})_2(\mu_2\text{-}OMe)(\mu_3\text{-}O)]$, while the additionally formed yellow blocks were characterized as $(EtPPh_3)_2[\{UO_2(L^{2a})(\mu_2\text{-}OMe)\}_2]$. The latter compound has already been described above. The IR spectrum of $(EtPPh_3)[(UO_2)_3(L^{2a**})_2(\mu_2\text{-}OMe)(\mu_3\text{-}O)]$ show the $\nu_{U=O}$ stretch at 902 cm^{-1} and the $\nu_{C=O}$ vibrations at 1593 cm^{-1}. Also here, partial hydrolysis of $\{L^{2a}\}^{2-}$ was only observed in the product, in which the corresponding position is involved into the coordination of uranium, while in $(EtPPh_3)_2[\{UO_2(L^{2a})(\mu_2\text{-}OMe)\}_2]$, the (uncoordinated) sulfur atoms resist such reactions.

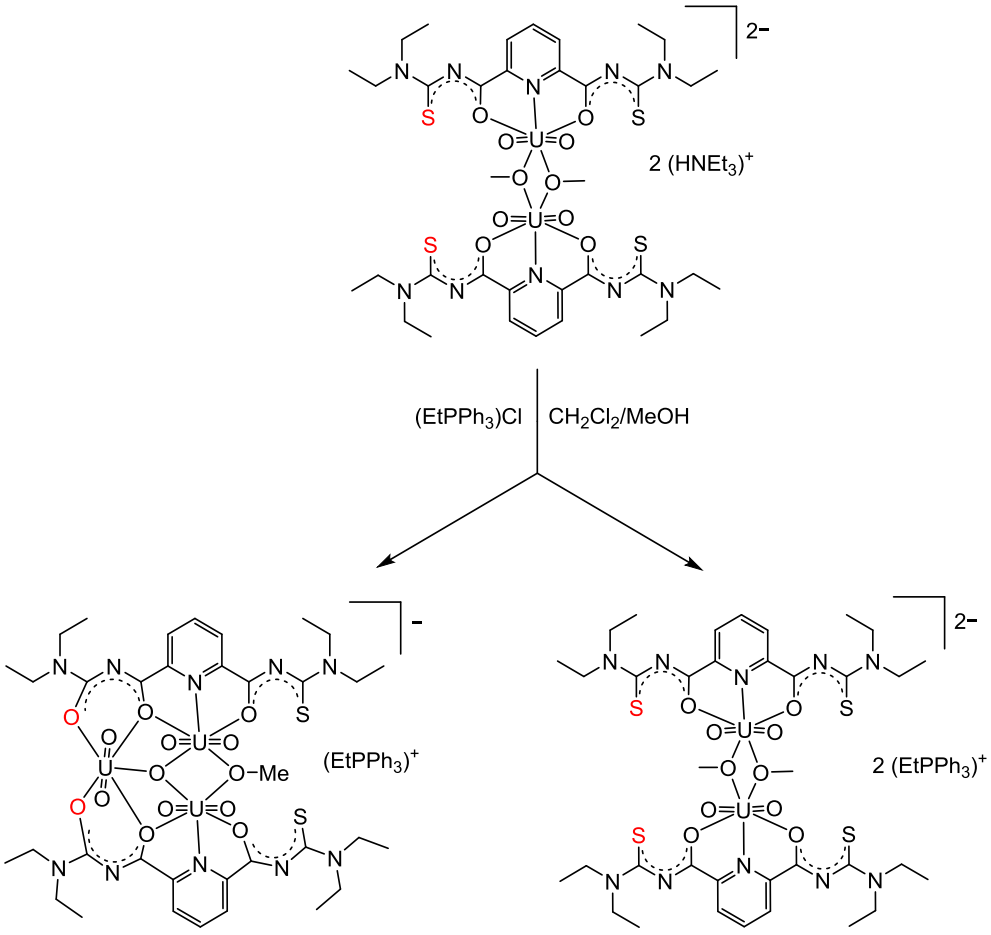

Scheme 2.10: Synthesis of $(EtPPh_3)[(UO_2)_3(L^{2a**})_2(\mu_2\text{–}OMe)(\mu_3\text{-}O)]$ and $(EtPPh_3)_2[\{UO_2(L^{2a})\text{-}(\mu_2\text{–}OMe)\}_2]$ from $(HNEt_3)_2[\{UO_2(L^{2a})(\mu_2\text{-}OMe)\}_2]$.

The analysis of the X-ray data confirms the composition of the complex as $(EtPPh_3)[(UO_2)_3(L^{2a**})_2(\mu_2\text{-}OMe)(\mu_3\text{-}O)]$. It crystallizes in the monoclinic space group P $2_1/c$ The structure of the molecular anion $\{[(UO_2)_3(L^{2a**})_2(\mu_2\text{-}OMe)(\mu_3\text{-}O)]\}^-$ is shown in Figure

2.24. It is very similar to the previously described trimeric complex with exception of the μ_2-coordinated ligand, which in this case is a methanolato ligand, provided by the methanol solvent. The asymmetric unit of the compound contains one complex anion and one ethyl-triphenyl phosphonium cation, indicating a net charge of the complex anion of -1.

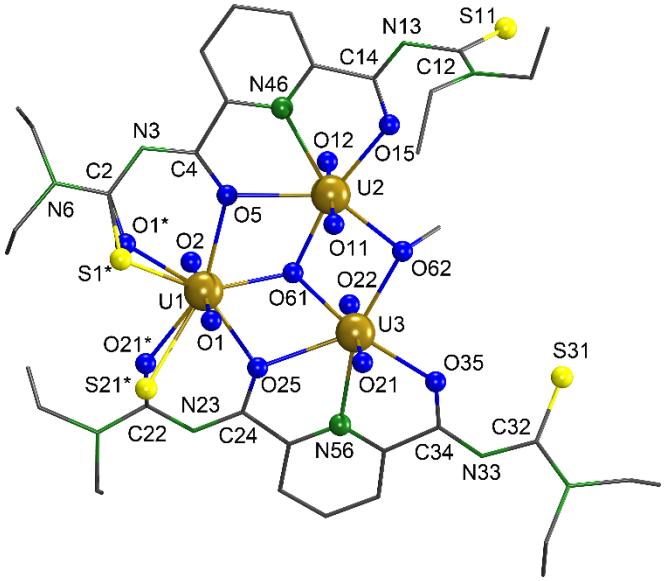

Figure 2.24: a) Molecular structure of the anion $[(UO_2)_3(L^{2a**})_2(\mu_2\text{-OMe})(\mu_3\text{-O})]^-$. Hydrogen atoms have been omitted for clarity.

The bond lengths in $(EtPPh_3)[(UO_2)_3(L^{2a})_2(\mu_2\text{-OMe})(\mu_3\text{-O})]$ do not show significant differences to those observed in $(HNEt_3)[(UO_2)_3(L^{2a})_2(\mu_2\text{-OMe})(\mu_3\text{-O})]$. The most interesting feature in this structure is the parallel presence of co-crystallized complexes with hydrolyzed and non-hydrolyzed ligands in the single crystals of the compounds. They occupy disordered positions with the oxygen atoms O1* and O21* having an occupancy of 90 %, and the sulfur atoms S1* and S21* having an occupancy of 10 %. Selected bond lengths and angles are summarized in the Table 2.12. Analysis of the bond lengths and the angles around the thiourea units shows that the C2-O1* bond length is 1.258(6) Å and the C2-S1* bond length is 1.543(3) Å. Interestingly, the laterally coordinated donor atoms O1*, O21*, S1* and S21* of $\{L^{2a**}\}^{2-}$ show the largest deviations from the equatorial mean least-square plane.

The complete hydrolysis of the ligands was obtained, when the CH_2Cl_2/MeOH reaction mixture was stirred for 1 h at room temperature before it was slowly evaporated for crystallization. Indeed, the same complex was obtained with 72 % yield and crystallized in the same monoclinic space group as the previous compound.

Table 2.12: Selected bond lengths (Å), bond angles and torsion angles (°) in $(EtPPh_3)[(UO_2)_3(L^{2a})_2(\mu_2\text{-}OMe)(\mu_3\text{-}O)]$.

Bond lengths					
U1–O1*	2.337(4)	U1–O21*	2.342(4)	C2–S1*	1.543(3)
U1–S1*	2.723(3)	U1–S21*	2.607(2)	C2–O1*	1.258(6)
Bond angles					
O1–U1–O2	175.9(2)	O1–U1–O61	91.8(2)	O1–U1–O5	89.7(1)
O1–U1–S1*	105.5(7)	O1–U1–S21*	105.5(5)	O1–U1–O25	86.7(1)
O1–U1–O1*	85.8(2)	O1–U1–O21*	89.2(2)	O11–U2–O12	178.0(2)
Torsion angles					
S1*–C2–N3–C4		35.7(1)	S21*–C22–N23–C24		-47.7(1)
O1*–C2–N3–C4		6.0(1)	O21*–C22–N23–C24		-4.0(1)
S11–C12–N13–C14		88.1(1)	S31–C32–N33–C34		-41.9(1)

Interestingly, the coordination of a μ_2-ethanolato ligand in the trinuclear complex could be obtained, when aqueous ethanol was used as solvent. An ethanolic solution of NEt_4Cl was added to the dimeric complex $(HNEt_3)_2[\{UO_2(L^{2a})(\mu_2\text{-}OMe)\}_2]$, which was previously dissolved in CH_2Cl_2 and the reaction mixture was stirred for 1 h. Also here, yellow needles precipitated with a yield of 70 %. The analysis of the X-ray data reveals a trinuclear complex with the composition $(HNEt_3)[(UO_2)_3(L^{2a})_2(\mu_2\text{-}OEt)(\mu_3\text{-}O)]$. It crystallizes in the orthorhombic space group Pnma. The asymmetric unit contains one half complex anion consisting of one ligand $\{L^{2a}\}^{2-}$, 1.5 uranyl atoms, one μ_3-oxido ligand with an occupational factor of 0.5 and one μ_2-ethanolato ligand with an occupational factor of 0.5. The charge is compensated by a disordered $(HNEt_3)^+$ ion.

More information about the behavior of the trinuclear complex $(HNEt_3)[(UO_2)_3(L^{2a})_2(\mu_2\text{-}OEt)(\mu_3\text{-}O)]$ in solution was obtained by the analysis of the ESI^- mass spectra of a solution of the complex in CH_2Cl_2/MeOH. Besides the peak of the molecular anion $[(UO_2)_3(L^{2a})_2(\mu_2\text{-}OEt)(\mu_3\text{-}O)]^-$, which is observed at m/z = 1627.4068, two fragments corresponding to the anions $[(UO_2)_3(L^{2a})_2(\mu_2\text{-}OMe)(\mu_3\text{-}O)]^-$ and $[(UO_2)_3(L^{2a})_2(\mu_2\text{-}OH)(\mu_3\text{-}O)]^-$ were detected at respectively m/z = 1611.4307 and 1597.4153. It indicates the lability of the μ_2-bonded ligand, which can readily be replaced by the dominant solvent present in the environment of the complex.

UV/Vis spectral analysis

The UV/Vis spectra of the non-coordinated ligand, H_2L^{2a}, the dimeric $(HNEt_3)_2[UO_2(L^{2a})(\mu_2\text{-}OMe)]_2$ and the trimeric $(HNEt_3)[(UO_2)_3(L^{2a**})_2(\mu_2\text{-}OH)(\mu_3\text{-}O)]$ were measured in CH_2Cl_2. The results are shown in Figure 2.25.

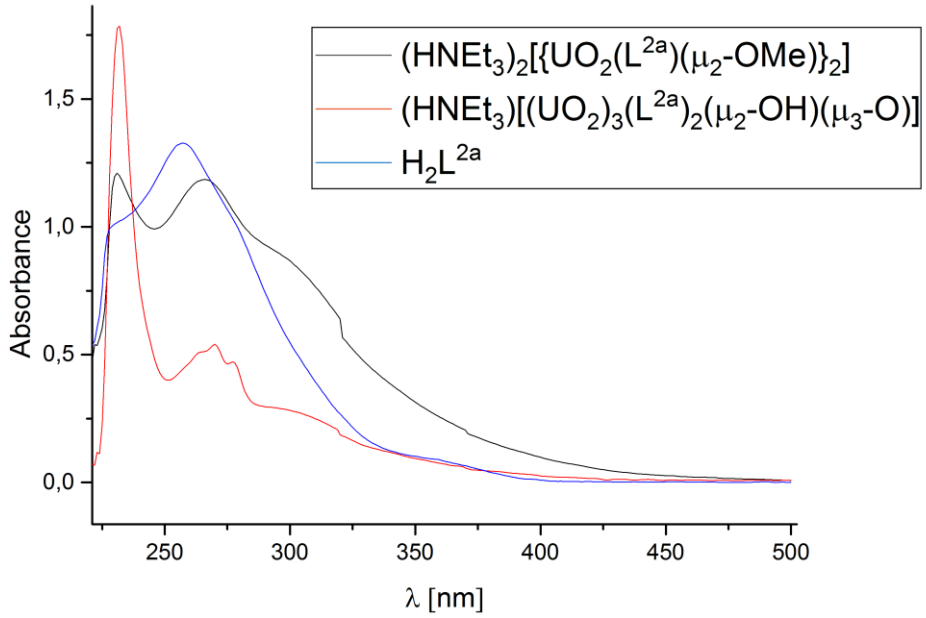

Figure 2.25: UV/Vis spectra of H_2L^{2a} and the uranyl complexes $(HNEt_3)_2[\{UO_2(L^{2a})\text{-}(\mu_2\text{-}OMe)\}_2]$ and $(HNEt_3)[(UO_2)_3(L^{2a**})_2(\mu_2\text{-}OH)(\mu_3\text{-}O)]$ in CH_2Cl_2. $C_{Complexes}$ = 0.03 mM, C_{Ligand} = 0.02 mM.

The absorption bands for the ligand, resulting from π-π* and n-π* transitions are observed around 224, 263 and 357 nm. In both uranyl complexes, a small red shift for all the absorption bands of the ligand is observed. The band at 224 nm shows an increase in intensity and the band at 263 nm a decrease in intensity in both complexes with the shifts in the trimeric complex being stronger. The broad band at 305 nm arises from a ligand-to-metal charge transfer (LMCT) transition from the equatorial bounded oxygen donor atoms to the uranyl cations.

Ligand hydrolysis study

In order to determine the influence of the pH in the observed partial hydrolysis reaction of the sulfur donor atoms of H_2L^{2a} and if the reaction also proceeds without metal ions, a hydrolysis study of the pure ligand was performed at different pH values. The organic phases containing each 0.01M H_2L^{2a} in CH_2Cl_2 were shaken with the same volume of water. The pH of the

aqueous phase was adjusted with HNO_3 or NaOH. After 1 h, the organic phases were separated from the aqueous ones and ^{1}H-NMR spectra were recorded. The results indicate the stability of the organic ligand at a broad pH range. The signal for the NH protons, which appears at 8.9 ppm at neutral pH disappears under acidic and basic conditions towards the formation of a protonated NH_2^+ conjugate. The broad signal for the NH_2 protons are observed around 5 ppm. A hydrolysis of the sulfur atoms of H_2L^{2a} is generally not observed. No variations are observed in the spectra under acidic conditions. However, under basic conditions, the intensity of the NMR signals observed in the organic layer decrease with increasing pH until the decomposition of the ligand H_2L^{2a} is observed. At pH 14, no signals related to the ligand H_2L^{2a}, were detected in the spectrum of the organic layer. The resulting by-products were then found in the aqueous layer, as it is shown in Figure 2.26b. A possible mechanism of the decomposition of the ligand is illustrated in Figure 2.26a.

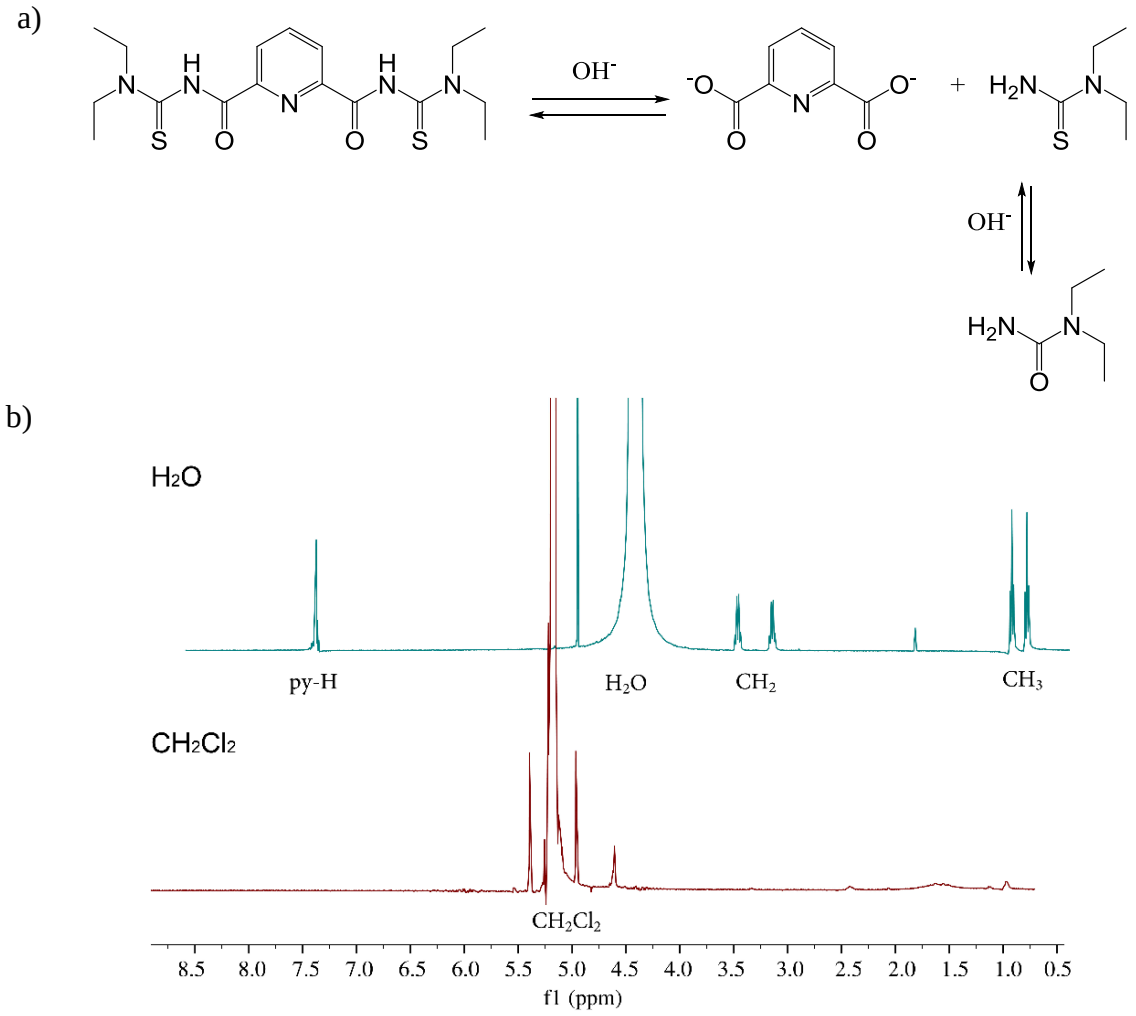

Figure 2.26: a) Hydrolysis reactions of H_2L^{2a} at pH 14. b) ^{1}H-NMR spectra of the extracted CH_2Cl_2 and H_2O phases of H_2L^{2a} at pH 14.

The excess of hydroxide ions induced the base catalyzed hydrolysis of the amide group in H_2L^{2a}, which is initiated by nucleophilic attack of a hydroxide ion on the carbon atom. The dissociation of H_2L^{2a} into 2,6-pyridine dicarboxylate and *N,N'*-diethylthiourea is observed. The latter one hydrolyzed at pH 14 under formation of *N,N*-diethylurea, which is soluble in water. The presence of 2,6-pyridine dicarboxylate and *N,N*-diethylurea in the water phase was confirmed by IR spectroscopy. The $\nu_{C=O}$ stretch was observed at 1776 cm^{-1} and vibrations of the aromatic ring at 2972, 2930 and 2872 cm^{-1}.

DFT Calculations

Experimentally, three different structural isomers of the $[\{UO_2(L^{2a})(\mu_2\text{-}OMe)\}_2]^{2-}$ anion and only one of the $[\{UO_2(L^{2b})(\mu_2\text{-}OMe)\}_2]^{2-}$ anion were isolated. In order to determine the most stable isomer, the compounds were modeled and their structures optimized using DFT calculations. The counter ions $(HNEt_3)^+$ or $(EtPPh_3)^+$ were not considered. The input coordinates were derived from X-ray data with the exception of the *syn,syn-* and *anti,syn-* $[\{UO_2(L^{2b})(\mu_2\text{-}OMe)\}_2]^{2-}$ anions, where the coordinates were adapted from the experimental data of the corresponding $[\{UO_2(L^{2a})(\mu_2\text{-}OMe)\}_2]^{2-}$ anions. The compounds were computed without any symmetry constraints at the density functional B3LYP level of theory. The optimized structure parameters are in good agreement with the experimental values for all structures. The bond lengths differ by less than 0.04 Å (except for the bond lengths between uranium and the oxygen atoms of $\{L^2\}^{2-}$, U-O5, U-O15, with a difference of 0.1 Å) and the deviation of the bond angles differ by less than 3 °. For $[\{UO_2(L^{2a})(\mu_2\text{-}OMe)\}_2]^{2-}$, the *anti,anti*-isomer was found to be most stable one, followed by the *anti,syn*-isomer (ΔE=5.4 kJ/mol) and the *anti,syn* by (ΔE=15.9 kJ/mol). A similar result has been obtained for the anion $[\{UO_2(L^{2b})(\mu_2\text{-}OMe)\}_2]^{2-}$ (see Table 2.13). Small energy differences found in the DFT calculations indicate that the isolation of the individual conformers is mainly determined by crystallographic packing effects.

Table 2.13: Computational results for the three isomers of $[\{UO_2(L^{2a})(\mu_2\text{-OMe})\}_2]^{2-}$ and $[\{UO_2(L^{2b})(\mu_2\text{-OMe})\}_2]^{2-}$.

	syn,syn		*anti,syn*		*anti,anti*
	$[\{UO_2(L^{2a})(\mu_2\text{-OMe})\}_2]^{2-}$		$\{[UO_2(L^{2a})(\mu_2\text{-OMe})\}_2]^{2-}$		$[\{UO_2(L^{2a})(\mu_2\text{-OMe})\}_2]^{2-}$
Energy [Hartree]	-4400.1782	>	-4400.1822	>	-4400.1847
ΔE [kJ/mol]		10.5		5.4	
	syn,syn		*anti,syn*		*anti,anti*
	$[\{UO_2(L^{2b})(\mu_2\text{-OMe})\}_2]^{2-}$		$[\{UO_2(L^{2b})(\mu_2\text{-OMe})\}_2]^{2-}$		$[\{UO_2(L^{2b})(\mu_2\text{-OMe})\}_2]^{2-}$
Energy [Hartree]	-4696.2683	>	-4696.2751	<	-4696.2727
ΔE [kJ/mol]		17.9		- 6.3	

2.4 Mixed-metal complexes of H_2L^2 with uranyl and transition or post-transition metal ions

Structural studies on heterometallic compounds containing the uranyl ion and transition metal ions are of interest because of their chemical properties and structural morphologies. Additionally, studies about the influence of additional transition metal ions on the complexation of the uranyl ions may help to elucidate the biodistribution of the metal ion and increase the selectivity of the complexation of uranyl ions during extraction and re-extraction processes. This may become important in spent nuclear fuel treatment, since the waste generated from spent nuclear fuel reprocessing contains besides the actinide elements, fission products such as lanthanides, molybdenum, technetium, palladium etc… as well as activation products, structural elements, and process chemicals.[86]

As described in the previous Chapters, pyridine-2,6-dicarbonylbis(*N,N'*-dialkylthioureas), H_2L^2; form dimeric uranyl complexes in a way that the ligands coordinate tridentate with their *O,N,O* donor atoms. The sulfur atoms of the ligands remain uncoordinated and offer the possibility of the coordination of additional metal ions. Since sulfur atoms are "soft" donors according to the HSAB principle, reactions with "soft" metal ions should be possible there, while the addition of a "hard" metal ion may compete with uranium. Jegathesh and Pham describe in their doctoral thesis the synthesis of several series of heterometallic host-guest compounds with the combination of "soft" and "hard" metal ions and H_2L^{2a}.[47,48] The hard metal ions are usually encapsulated in a central hole formed by a metallacryptate built by the softer metal ions and the deprotonated ligands $\{L^{2a}\}^{2-}$, which form chelates with the *S* and *O* donor atoms. As common for the synthesis of supramolecular complexes, the finding of appropriate chemical conditions for the isolation of the stable products is a big challenge.

2.4.1 A uranyl complex with H_2L^{2a} and gold(I)

A typical 'soft' and 'thiophilic' metal ion is Au(I), what make it favorable for the testing of the reactivity of the uncoordinated thiocarbonyl donor sites in the uranium complexes of the previous Chapter.

A 2-fold excess of $[Au(PPh_3)Cl]$ was added to the dimeric uranyl complex $(HNEt_3)_2$-$[\{UO_2(L^{2a})(\mu_2\text{-}OMe)\}_2]$ in CH_2Cl_2. Yellow needles of the composition $[\{UO_2(L^{2a})(OMe)\}_2$-$\{Au(PPh_3)\}_2]$ were isolated directly from a reaction mixture, which was overlayered with

MeOH. The same compound could be synthesized by a one-pot synthesis of equimolar amounts of H_2L^{2a}, $(NBu_4)_2[UO_2Cl_4]$ and $[Au(PPh_3)Cl]$ in MeOH. The use of an excess of $[Au(PPh_3)Cl]$ did not yield products with more than two sulfur atoms being coordinated to $\{Au(PPh_3)\}^+$ fragments. The IR spectrum of $[\{UO_2(L^{2a})(OMe)\}_2\{Au(PPh_3)\}_2]$ shows the $\nu_{C=O}$ band at 1587 cm^{-1} and the $\nu_{U=O}$ band at 914 cm^{-1}. The frequencies correspond to the values found in the dimeric complex $(HNEt_3)_2[\{UO_2(L^{2a})(\mu_2\text{-}OMe)\}_2]$. The presence of the triphenylphosphine ligands is confirmed by ^{31}P-NMR spectroscopy showing one broad signal at 36.1 ppm. This corresponds to the chemical shift which is observed for the $\{Au(PPh_3)\}^+$ unit in other triphenylphosphine gold(I) complexes.[87–89] The result of the elemental analysis supports the molecular composition of $[\{UO_2(L^{2a})(OMe)\}_2\{Au(PPh_3)\}_2]$. The crystal structure was solved and refined in the triclinic space group $P\overline{1}$. The centrosymmetric molecule contains two *O,N,O* coordinated $\{UO_2(L^{2a})\}$ units, which are connected by two $\{MeO\}^-$ ligands. Additionally, one $\{Au(PPh_3)\}^+$ is coordinated by one sulfur atom of each subunit (Figure 2.27). Selected bond lengths and angles are summarized in the Table 2.14.

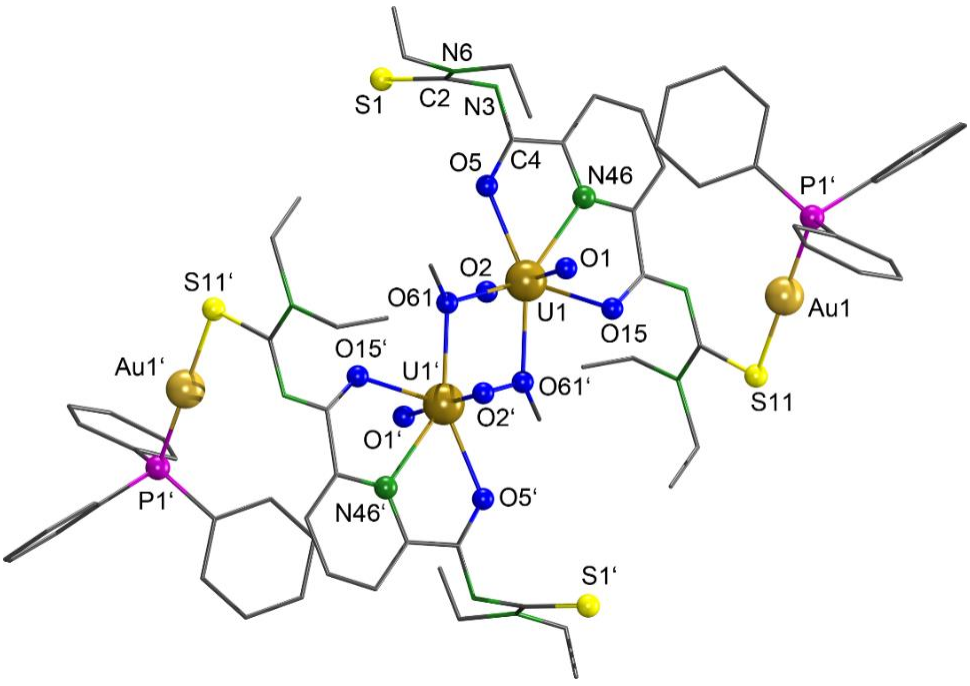

Figure 2.27: Molecular structure of $[\{UO_2(L^{2a})(OMe)\}_2\{Au(PPh_3)\}_2]$. Symmetry related atoms are reproduced by an inversion center (symmetry operator -x,-y+1,-z+1). Hydrogen atoms have been omitted for clarity.

The coordination of the sulfur atoms by the $\{Au(PPh_3)\}^+$ units does not affect the coordination environment of the uranium atoms. The bond lengths and angles around the uranium atoms are nearly identical to those observed in $(HNEt_3)_2[\{UO_2(L^{2a})(\mu_2\text{-}OMe)\}_2]$ with a maximum

deviation for the bond distances of 0.02 Å observed with O61' and a maximum bond angle deviation of 2 °observed for O1-U1-O61'.

Table 2.14: Selected bond lengths (Å), and bond angles (°) in $[\{UO_2(L^{2a})(OMe)\}_2\{Au(PPh_3)\}_2]$.

Bond lengths					
U1–O1	1.76(1)	U1-N46	2.531(13)	C2–S1	1.668(23)
U1–O2	1.77(1)	U1–O61	2.323(12)	C2–N3	1.352(21)
U1–O5	2.38(1)	U1–O61'	2.373(10)	C4–N3	1.319(19)
U1–O15	2.40(1)	C2–N6	1.347(21)	O5–C4	1.253(17)
Au1–S11	2.317(6)	Au1–P1	2.242(7)		
Bond angles					
O1–U1–O2	176.8(5)	O1–U1–O5	88.2(5)	O1–U1–O61	88.5(5)
O1–U1–N46	87.6(5)	O1–U1–O15	88.8(5)	O1–U1–O61'	93.8(4)
S11–Au1–P1	178.5(3)	S11–Au1–Au1'	83.9(2)	P1–Au1–Au1'	96.9(2)

Each Au(I) ion is coordinated with one sulfur atom of $\{L^{2a}\}^{2-}$ and the triphenylphosphine ligand. The S-Au-P bond angles are 178.5(3)°. The intermolecular organization in the solid state structure of $[\{UO_2(L^{2a})(OMe)\}_2\{Au(PPh_3)\}_2]$ is characterized by the presence of aurophilic interactions with Au-Au distances of 3.21(1) Å. The resulting one-dimensional polymeric chain is illustrated in Figure 2.28. In spite of the steric constraint imposed by the PPh_3 units, a coordination of all the sulfur atoms in this structure is hindered. The $\{Au(PPh_3)\}^+$ units coordinate two diagonally opposite sulfur atoms. This induce the presence of large voids between the molecules in the unit cell packing. The latter contributes to the fluctuation of the electrons near to these voids and leads to a poor crystal data quality.

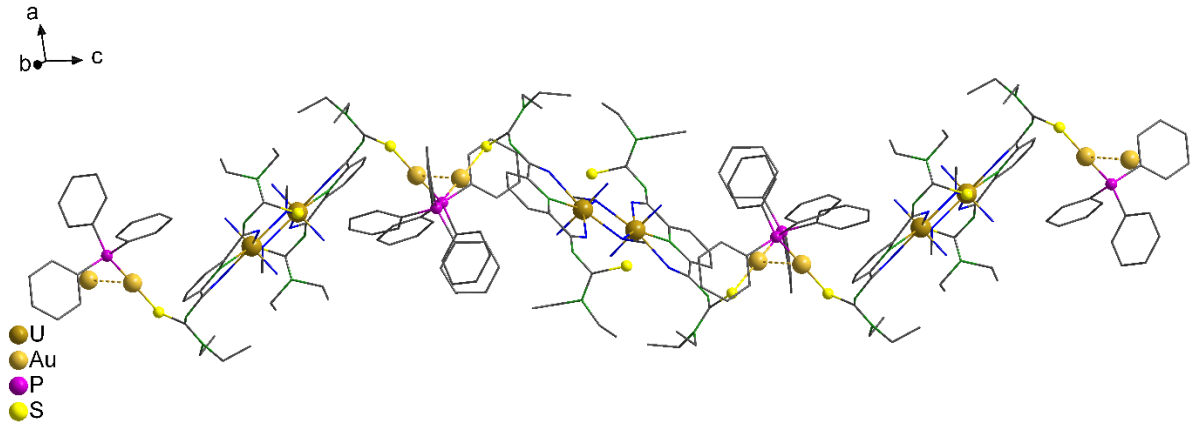

Figure 2.28: View along the crystallographic *b*-axis of the solid state structure of $[\{UO_2(L^{2a})(OMe)]\}_2\{Au(PPh_3)\}_2]$, showing the 1D polymeric chain. The Au-Au interactions are represented by the fragmented lines. Hydrogen atoms have been omitted for clarity.

2.4.2 A uranyl complex with H_2L^{2a} and lead(II)

Lead acetate reacts with each one equivalent of H_2L^{2a} and with uranyl acetate in methanol under formation of a yellow precipitate. The formation of the precipitate did not require the addition of NEt_3. The infrared spectrum of the product indicates the deprotonation of the organic ligand by the absence of the NH vibrations of H_2L^{2a} and a chelate formation by a significant bathochromic shift of the $\nu_{C=O}$ band of the ligand. It appears in the complex at 1597 cm^{-1}. The uranyl band appears at 916 cm^{-1}. Crystals suitable for X-ray analysis were obtained from a saturated CH_2Cl_2 solution of the yellow precipitate overlayered with MeOH. Figure 2.29 shows the molecular structure of the complex with the composition $[Pb_2(UO_2)_3(L^{2a})_3(\mu_2\text{-}OMe)_2(MeOH)_2]$.

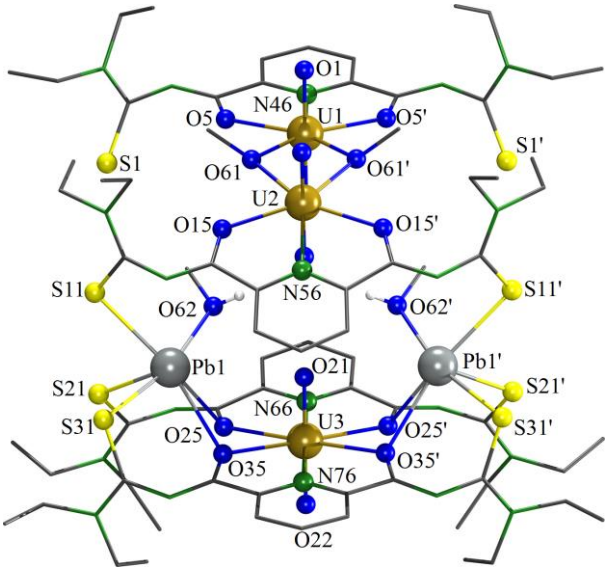

a)

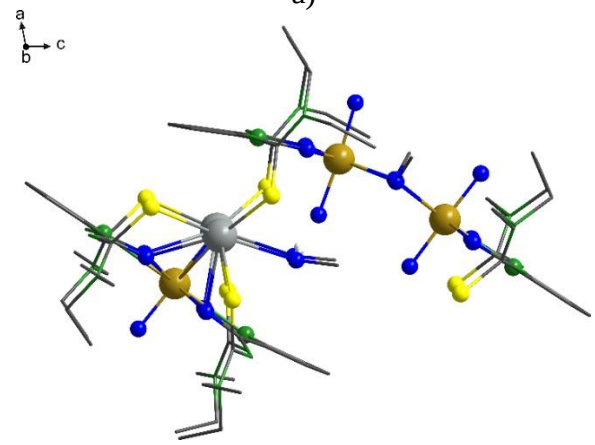

b)

Figure 2.29: a) Molecular structure of $[Pb_2(UO_2)_3(L^{2a})_4(\mu_2\text{-}OMe)_2(MeOH)_2]$. b) View along the crystallographic *b*-axis (symmetry operator -x, 3/2-y, z). Hydrogen atoms with the exception of the coordinated methanol have been omitted for clarity.

The X-ray data show that the asymmetric unit of the compound contains a half of the molecule and disordered methanol and water molecules. The complete complex molecule is obtained by a mirror plane, dividing the uranium atoms and the pyridine rings. The concerned atoms show an occupational factor of 0.5. The molecular structure is composed of four deprotonated ligands $\{L^{2a}\}^{2-}$, three uranyl ions, two Pb^{2+} ions, two methanolato ligands and two coordinated methanol molecules. This result in a neutral complex. All the four $\{L^{2a}\}^{2-}$ ligands are coordinated to the uranyl ions tridentate with their *O,N,O* donor atoms. Interestingly, the molecule is built up of two uranyl-containing subunits, which are connected by the Pb^{2+} ions as is shown in Figure 2.29. One subunit has the composition *syn,syn*-$[\{UO_2(L^{2a})(\mu^2\text{-}OMe)\}_2]^{2-}$, according to the orientation of the methanolato ligands and the sulfur atoms. The second subunit has the composition $\{UO_2(L^{2a})_2\}^{2-}$.

Table 2.15: Selected bond lengths (Å), distances (Å), bond angles (°) and dihedral angles (°) in $[Pb_2(UO_2)_3(L^{2a})_4(\mu_2\text{-}OMe)_2(MeOH)_2]$.

Distances					
U1–O1	1.773(5)	U2–O11	1.808(5)	U3–O21	1.774(5)
U1–O2	1.780(5)	U2–O12	1.784(5)	U3–O22	1.764(5)
U1–O5	2.346(3)	U2–O15	2.356(3)	U3–O25	2.471(3)
U1–O61	2.357(3)	U2–O61	2.294(3)	U3–O35	2.468(3
U1–N46	2.529(6)	U2–N56	2.544(5)	U3–N66	2.649(5)
Pb1–S11	2.795(2)	Pb1–S21	2.882(2)	U3–N76	2.656(5)
Pb1–S31	2.720(4)	Pb1–O62	2.685(4)	Pb1–O25	2.736(3)
Pb1–O35	2.709(3)	Pb1⋯U3	4.051(2)	U1⋯U2	3.711(1)
C2–S1	1.689(6)	C2–N3	1.364(6)	C4–N3	1.300(6)
O5–C4	1.284(6)	C2–N6	1.336(7)	C12–S11	1.701(5)
C12–N13	1.400(5)	C14–N13	1.301(5)	O15–C14	1.282(5)
C12–N16	1.316(5)	C22–S21	1.717(5)	C22–N23	1.371(6)
C24–N23	1.292(6)	O25–C24	1.291(5)	C22–N26	1.329(6)
Bond angles					
O1–U1–O2	176.3(2)	O11–U2–O12	178.9(2)	O21–U3-O22	179.7(2)
O62–Pb1–O35	115.9(1)	O35–Pb1–O25	53.9(1)	O62–Pb1–O25	71.4(1)
O62–Pb1–S21	88.7(1)	O35–Pb1–S21	106.7(1)	O62–Pb1–S11	86.5(1)
S21–Pb1–O25	76.8(1)	O35–Pb1–S11	157.4(1)	O62–Pb1–S31	166.8(1)
O25–Pb1–S11	144.8(1)	O25–Pb1–S31	117.2(1)	S21–Pb1–S11	75.6(1)
O35–Pb1–S31	76.9(1)	S21–Pb1–S31	83.9(1)	S11–Pb1–S31	81.1(1)

The lead ions are coordinated monodentate with the remaining sulfur atoms of the dimeric subunit $[\{UO_2(L^{2a})(\mu^2\text{-OMe})\}_2]^{2-}$, while with the monomeric subunit $[\{UO_2(L^{2a})_2]^{2-}$ a chelate formation of a *S,O* Pb^{2+} is established, sharing the oxygen atoms with uranium. In contrast to the five-coordinate uranyl ions of the *syn,syn*-$[\{UO_2(L^{2a})(\mu^2\text{-OMe})\}_2]^{2-}$ subunit, the monomeric subunit $[UO_2(L^{2a})_2]^{2-}$ shows a hexagonal-bipyramidal geometry around the uranium atom. The uranyl bond lengths are unexceptional. The distances between the uranyl ions and the equatorial donor atoms are in the range between 2.294(3) and 2.471(3) Å for the oxygen atoms and of 2.529(6) – 2.656(5) Å for the nitrogen atoms. The coordination environment of Pb is occupied by three sulfur atoms, and three oxygen atoms. The geometry of the lead ions can be described as monocapped square-pyramidal. If, the stereoactive 6s lone-pair electrons, which is indicated by the large void around the metal ions, are considered, the donor atoms are 'hemidirected' and the description of the coordination sphere (including this lone-pair) around Pb would correspond a monocapped octahedron (see Figure 2.30).[44,90,91] The Pb-S bond length are in the range of 2.720(6) – 2.882(5) Å and the Pb-O bond length are in the range between 2.685(6) – 2.736(5) Å. As generally observed in 'hemidirected' lead (II) compounds, the bond lengths of the donor atoms converging to the lone pair are somewhat elongated: in the present case, they are Pb-S21, Pb-S11 and Pb-O25. The two intra-ligand bond angles around Pb are similar with approximately 77 °. The interligand bond angles, however are very variable with values between 53.9(1) ° and 166.8(1) °. This indicates a highly distorted geometry. The *S,O* chelate rings of $\{L^{2a}\}^{2-}$ in the lead-containing subunit show an unprecedented deviation from the planarity in aroylbenzoylthioureato complexes. This is obviously due to the strong bond *O,N,O* chelate with uranium in the central parts of the corresponding subunits.

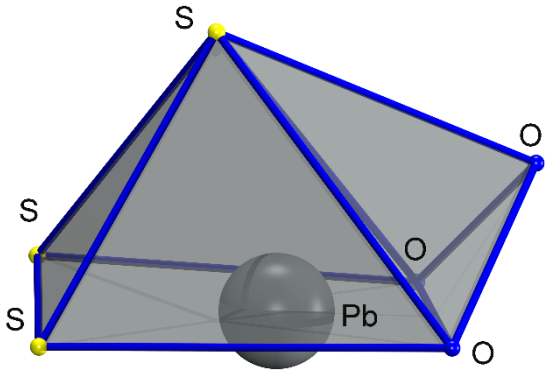

Figure 2.30: Coordination polyhedron of Pb^{2+} in $[Pb_2(UO_2)_3(L^{2a})_4(\mu_2\text{-OMe})_2(MeOH)_2]$.

The high resolution ESI+ mass spectra of the complex do not display the existence of the molecular ion peak. Instead, molecular fragments, which indicate the decomposition of the complex were detected. The observed base peak is illustrated in Figure 2.31. Interestingly, the decomposition happens preferably in the dimeric uranyl subunit of the complex and show the same pattern as observed in the negative mode of the ESI mass spectrum of $(HNEt_3)_2[\{UO_2(L^{2a})(\mu_2\text{-}OMe)\}_2]$, which is described in Chapter 2.3. The bond between the uranium atoms U1 and U2 and the methanolato ligands is cleaved and singly-bridged $[UO_2(L^{2a})]^{2-}$ units are observed at m/z = 2829.6021.

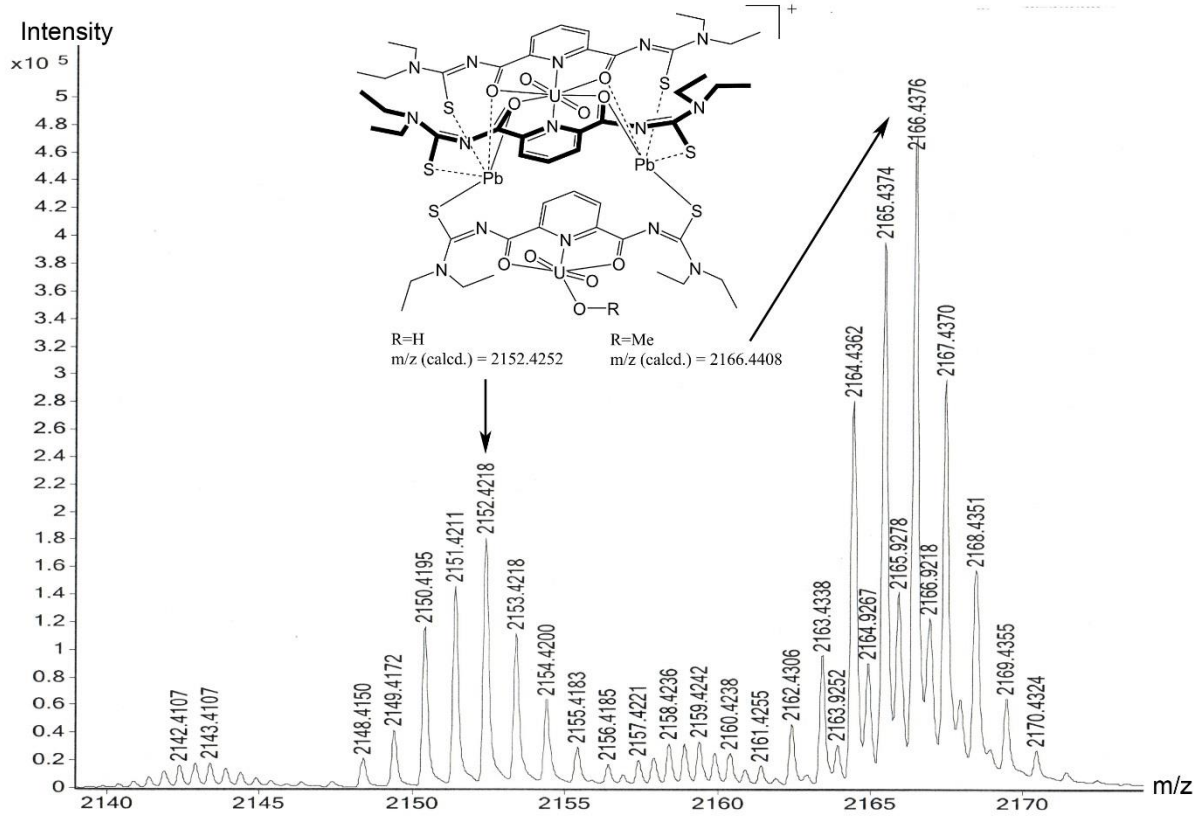

Figure 2.31: Base peaks observed in high resolution ESI+ mass spectra of $[Pb_2(UO_2)_3(L^{2a})_3\text{-}(\mu_2\text{-}OMe)_2(MeOH)_2]$.

2.4.3 Uranyl complexes with H_2L^2 and divalent transition metal ions (Zn^{2+}, Ni^{2+}, Co^{2+}, Fe^{2+}, Mn^{2+} and Cd^{2+}).

With respect to the previously described ready formation of heterometallic complexes between uranium and gold or lead by one-pot reactions, further reactions were performed using divalent transition metal ions as second metal source. Addition of a 2-fold excess of M(II) acetates (M =

Zn, Ni, Co, Fe, Mn or Cd), dissolved in methanol to a dichloromethane solution of $(HNEt_3)_2[\{UO_2(L^{2a})(\mu_2\text{-}OMe)\}_2]$ gave orange-red crystals. The obtained product is insoluble in common solvents, which restricts the analytical methods to IR, elemental analysis and X-ray crystallography. The IR and elemental analysis data reveal a compound with a composition, which is different from that of the dimeric starting complex.

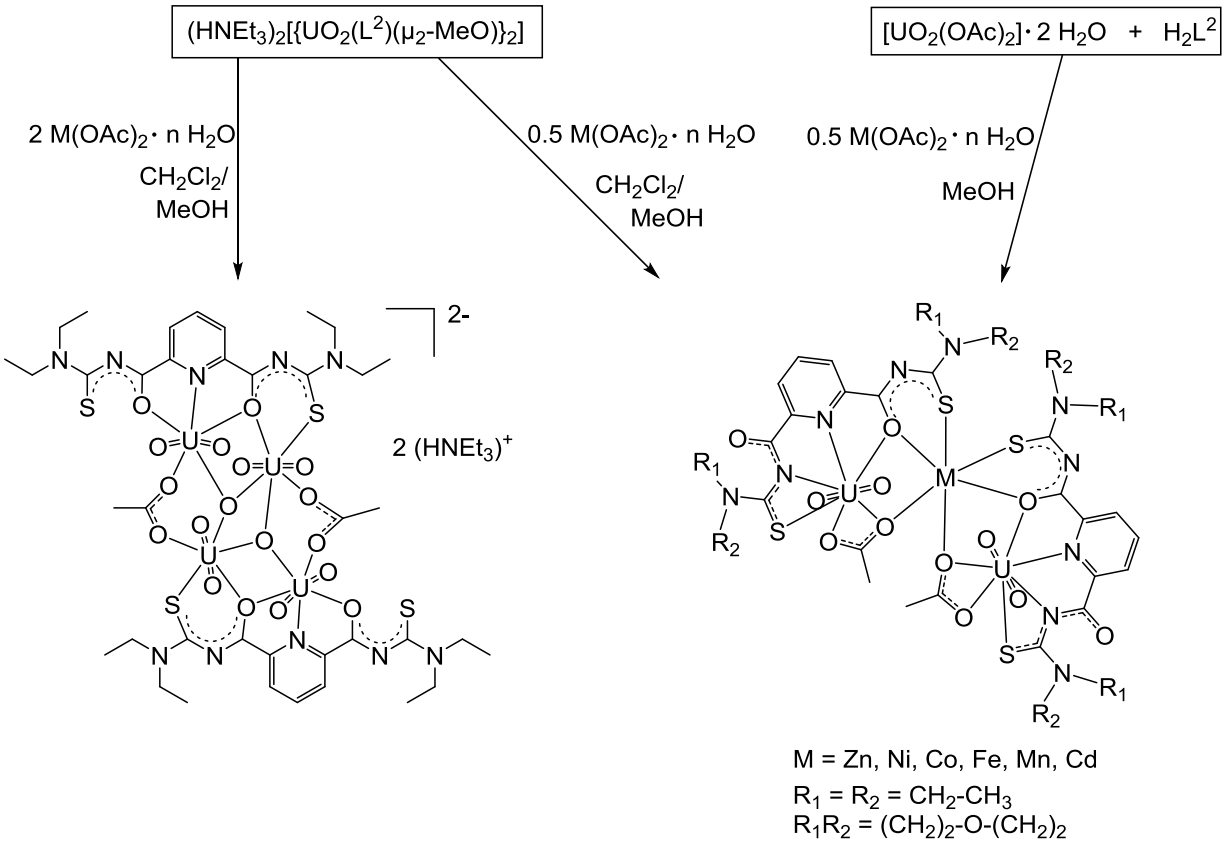

Scheme 2.11: Syntheses of the uranyl complex $(HNEt_3)_2[\{(UO_2)_2(L^{2a})(\mu_2\text{-}OAc)(\mu_3\text{-}O)\}_2]$ and of the heterometallic uranyl compounds of the type $[M\{UO_2(L^{2a})(OAc)\}_2]$ with M= Ni, Co, Fe, Mn, Zn, Cd.

The exact composition of the obtained product was determined by X-ray diffraction as $(HNEt_3)_2[\{(UO_2)_2(L^{2a})(\mu_2\text{-}OAc)(\mu_3\text{-}O)\}_2]$. Surprisingly, no mixed-metal complex was formed under the conditions applied. Obviously, the excess of metal acetate increased the pH of the reaction mixture to the level that the formation of oligonuclear uranyl aggregates is preferred and the sparingly soluble complex $(HNEt_3)_2[\{(UO_2)_2(L^{2a})(\mu_2\text{-}OAc)(\mu_3\text{-}O)\}_2]$ precipitated. The formation of heterometallic uranyl compounds was achieved by decreasing the amount of metal acetate to the required extent of 0.5 equivalent. Scheme 2.11 summarizes the syntheses of the oligomeric and heterometallic uranyl acetato complexes. Figure 2.32 shows the molecular structure of the anion $[\{(UO_2)_2(L^{2a})(\mu_2\text{-}OAc)(\mu_3\text{-}O)\}_2]^{2-}$.

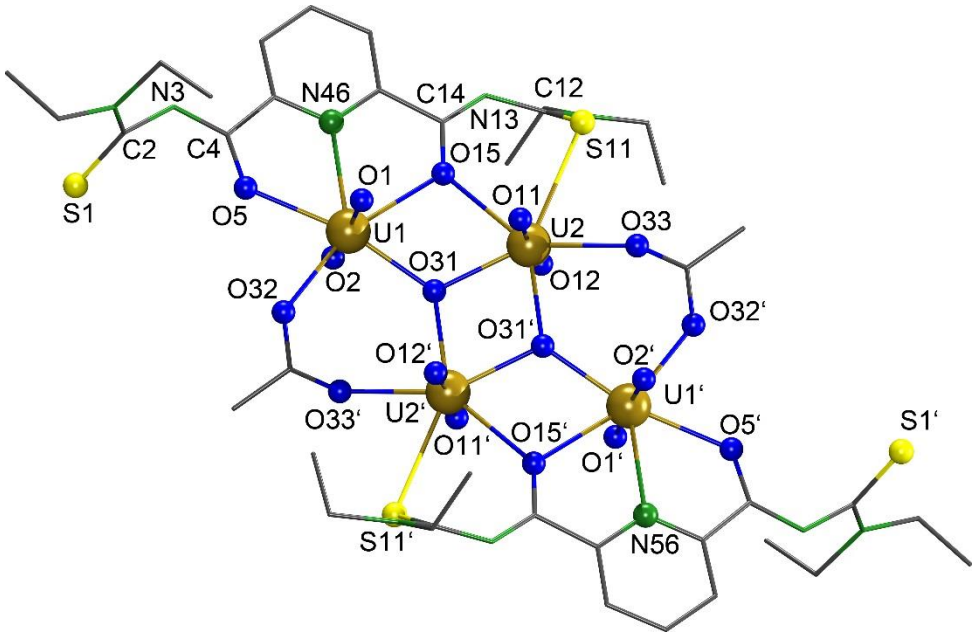

a)

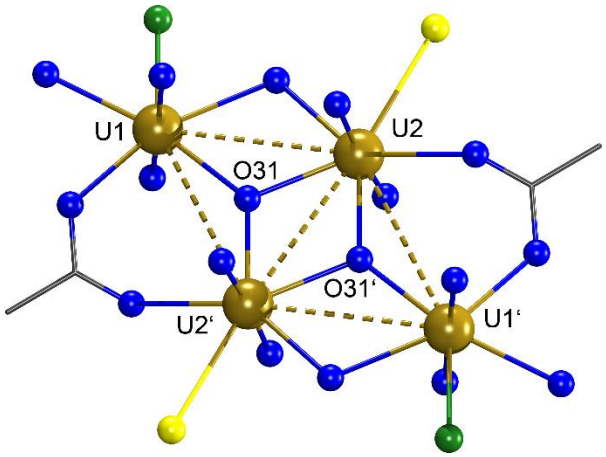

b)

Figure 2.32: a) Structures of the anion $[\{(UO_2)_2(L^{2a})(\mu_2\text{-}OAc)(\mu_3\text{-}O)\}_2]^{2-}$. b) Representation of the coordination environment of the uranium rhombus. Symmetry operator -x+2, -y+2,- z. Hydrogen atoms have been omitted for clarity.

Selected bond lengths and angles are summarized in Table 2.16. The compound crystallizes in the triclinic space group $P\bar{1}$ with one half of the molecule in the asymmetric unit. The $[\{(UO_2)_2(L^{2a})(\mu_2\text{-}OAc)(\mu_3\text{-}O)\}_2]^{2-}$ anion consists of four uranyl cations and two $\{L^{2a}\}^{2-}$ ligands, which are coordinated in a tetradentate *O,N,O,S* fashion. Each ligand coordinates two uranyl ions and the resulting sub-units are bridged by two μ_3-oxido and two bidentate coordinated acetato ligands. This results in a rhombus-like arrangement of the four uranium atoms as is shown in Figure 2.32. Each uranium atom exhibits a pentagonal-bipyramidal geometry. Two uranium atoms, U1 and U1', are coordinated by two oxygen atoms and the pyridine nitrogen

atoms of $\{L^{2a}\}^{2-}$, one oxygen atom of the acetato ligand and one μ_3-oxido ligand. The other uranium atoms, U2 and U2', are coordinated by the *S,O* chelate ring of the $\{L^{2a}\}^{2-}$ ligands, one oxygen atom of the acetato ligand and two μ_3-oxido ligands.

Table 2.16: Selected bond lengths (Å), distances (Å) and bond angles (°) in $(HNEt_3)_2$-$[\{(UO_2)_2(L^{2a})(\mu_2\text{-OAc})(\mu_3\text{-O})\}_2]$.

Distances					
U1–O1	1.768(7)	U1–O2	1.774(7)	U1–O5	2.385(6)
U1–O15	2.500(5)	U1–N26	2.558(7)	U1–O31	2.240(5)
U1–O32	2.374(7)	U2–O11	1.775(6)	U2–O12	1.801(6)
U1–S11	2.911(4)	U1–O15	2.509(6)	U1–O31	2.254(5)
U1–O31'	2.256(5)	U1–O33	2.370(6)	C2–S1	1.68(1)
C2–N3	1.39(1)	O5–C4	1.27(1)	C4–N3	1.30(1)
C2–N6	1.34(1)	C12–S11	1.70(1)	C12–O11	1.468(6)
C12–N13	1.37(1)	C14–N13	1.27(1)	O15–C14	1.30(1)
C12–N16	1.31(1)	U1···U2	3.872(5)	U1···U2'	4.101(6)
U2···U2'	3.656(8)	U1···U1'	7.089(8)		
Bond angles					
O1–U1–O2	176.5(3)	O1–U1–O31	90.7(3)	O1–U1–O32	89.9(3)
O1–U1–O5	90.6(3)	O1–U1–O15	90.6(3)	O1–U1–N26	84.6(3)
O11–U2–O12	174.8(3)	O11–U2–O31	89.5(2)	O11–U2–O31'	93.1(2)
O11–U2–O5	89.5(2)	O11–U2–O15	91.5(2)	O11–U2–N46	83.9(1)
O11–U2–O33	83.9(3)	O11–U2-O15	92.1(2)	O11–U2–S11	87.2(2)

As observed with the previously discussed trimeric complexes in Chapter 2.3, also in $(HNEt_3)_2[\{(UO_2)_2(L^{2a})(\mu_2\text{–OAc})(\mu_3\text{-O})\}_2]$ a partial hydrolysis of the sulfur atoms, which are coordinated to the uranium atoms is observed. The sulfur atom S11 is best refined with a S/O occupancy of 90/10 percent. This observation is supported by the deviations obtained from the elemental analysis. Since the percentage of the hydrolyzed species is small, it will not be regarded in the discussion of the structure. The distances between the uranium atoms and the central μ_3-O31 are between 2.240(5) and 2.256(5) Å and, thus, shorter than the distances of the equatorial oxygen atoms to the uranyl centers. The equatorial coordination spheres of the uranium atoms are almost perfectly planar.

The use of only 0.5 equivalents of metal acetate per equivalent of the uranyl source, leads to the formation of heterometallic complexes of the type $[M\{UO_2(L^{2a})(OAc)\}_2]$, M = Zn^{2+}, Ni^{2+}, Co^{2+}, Fe^{2+}, Mn^{2+} or Cd^{2+}. These neutral complexes were obtained directly from a

CH_2Cl_2/MeOH reaction mixture of the dimeric complex $(HNEt_3)_2[\{UO_2(L^{2a})(\mu_2\text{-}OMe)\}_2]$ with the transition metal acetates, as yellow crystals or they precipitated from reactions of uranyl acetate, M^{2+} acetate and H_2L^{2a} without the addition of NEt_3. The formed precipitates were recrystallized from CH_2Cl_2/MeOH. Interestingly, the addition of a base (e.g. NEt_3) to such reaction mixtures induces the formation of the previously described dimeric complex, $(HNEt_3)_2[\{UO_2(L^{2a})(\mu_2\text{-}OMe)\}_2]$. The formation of the heterometallic complexes was easily verified by elemental analysis and IR spectroscopy. In contrast to the dimeric complex, the heterometallic complexes show four carbonyl absorption bands, indicating the presence of different carbonyl units in the compound. The asymmetric uranyl stretches appear in a range between 916 – 924 cm^{-1} instead of at 910 cm^{-1} in the dimeric complex. Table 2.17 summarizes the carbonyl and uranyl stretches for the complexes obtained with H_2L^{2a}.

Table 2.17: Absorption band (in cm^{-1}) for the IR vibrations of the bimetallic uranyl complexes with H_2L^{2a} and the related monomeric and dimeric compounds.

Compound	**$\nu_{C=O}$ [cm^{-1}]**	**$\nu_{U=O}$ [cm^{-1}]**
H_2L^{2a}	1680	–
$[UO_2L^{2a}(MeOH)]$	1654	912
$(HNEt_3)_2[\{UO_2(L^{2a})(\mu^2\text{-}OMe)\}_2]$	1593	910
$[Cd\{UO_2(L^{2a})(OAc)\}_2]$	1649, 1599, 1566, 1518	916
$[Zn\{UO_2(L^{2a})(OAc)\}_2]$	1648, 1597, 1562, 1516	916
$[Ni\{UO_2(L^{2a})(OAc)\}_2]$	1653, 1597, 1558, 1518	922
$[Mn\{UO_2(L^{2a})(OAc)\}_2]$	1649, 1600, 1558, 1518	924
$[Fe\{UO_2(L^{2a})(OAc)\}_2]$	1647, 1599, 1562, 1518	924
$[Co\{UO_2(L^{2a})(OAc)\}_2]$	1651, 1597, 1560, 1516	922

The heterometallic compounds showed slight differences in their color depending on the transition metal contained. The complexes with Zn^{2+}, Cd^{2+} were pale yellow, complexes with Ni^{2+}, Mn^{2+} were deep yellow or light orange, while the complexes with Fe^{2+} and Co^{2+} were brownish. Electronic spectra of the complexes obtained from H_2L^{2a} were recorded in dichloromethane and are shown in Figure 2.33. For comparison, the electronic spectrum of the dimeric complex $(HNEt_3)_2[\{UO_2(L^{2a})(\mu_2\text{-}OMe)\}_2]$ is included in the Figure. The spectra of the heterometallic complexes with the transition metal ions Ni^{2+}, Mn^{2+}, Fe^{2+} and Co^{2+} are similar

with three main absorptions around 230, 290 and 370 nm. The complexes with the 'closed shell' metal ions Cd^{2+} and Zn^{2+} are slightly different with a red shift of the absorption at 290 nm, which appears around 305 nm in both complexes. The presence of the transition metal in the complexes is indicated by the absence of the absorption at 265 nm.

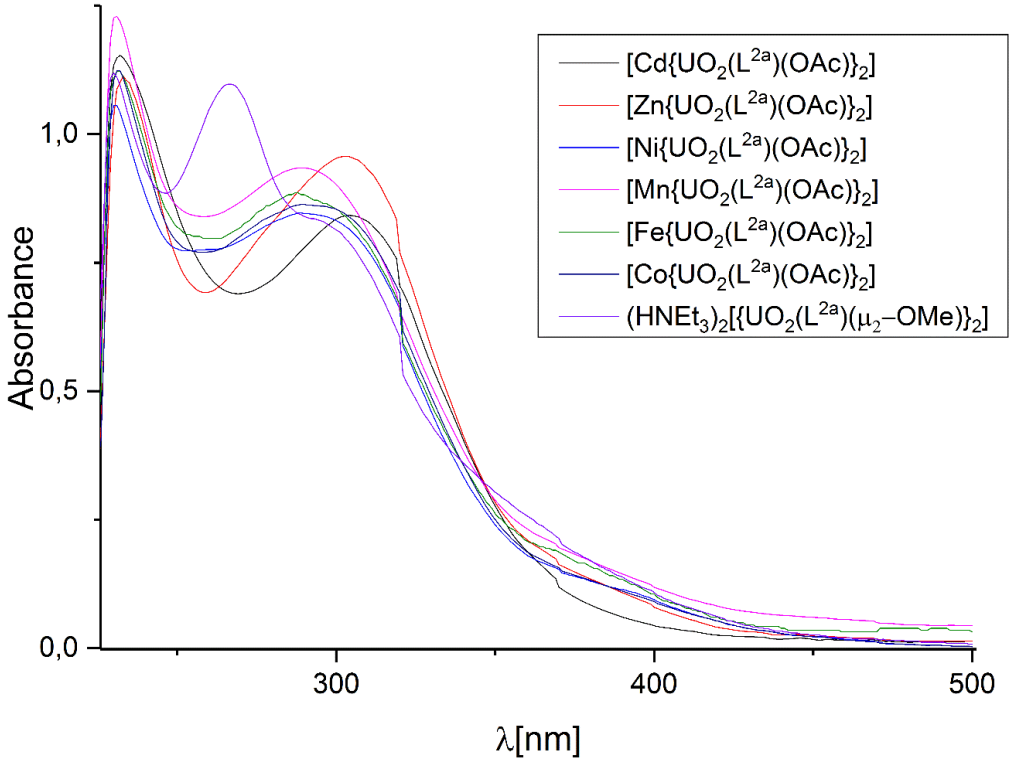

Figure 2.33: Absorption spectra of the heterometallic compounds $[M\{UO_2(L^{2a})(OAc)\}_2]$ (M = Cd, Zn, Ni, Mn, Fe, Co). The spectrum of the dimeric complex $(HNEt_3)_2[\{UO_2(L^{2a})(\mu_2\text{-}OMe)\}_2]$ is included for comparison.

NMR (in the case of the diamagnetic representatives) and ESI mass spectra are important tools to obtain information about the molecular dynamic in solution. Exemplary, Figure 2.34 shows the ^{1}H-NMR spectrum of $[Cd\{UO_2(L^{2b})(OAc)\}_2]$, which was recorded in CD_2Cl_2. The absence of the signal for NH protons, indicates the deprotonation of the ligands in the complex. The signal at 2.29 ppm corresponds to the methyl protons of the acetate groups.

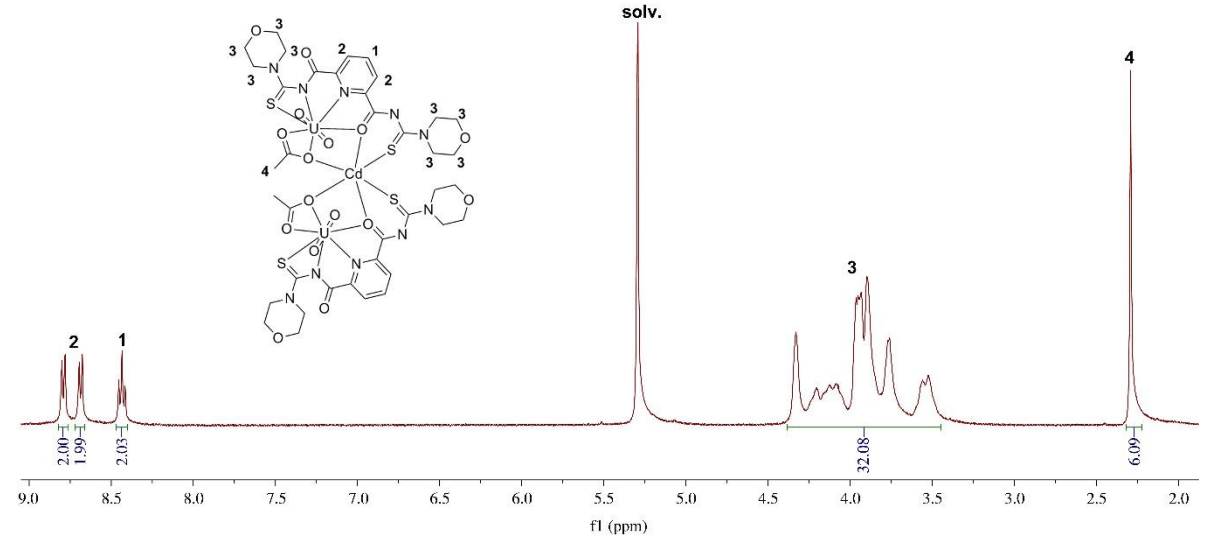

a)

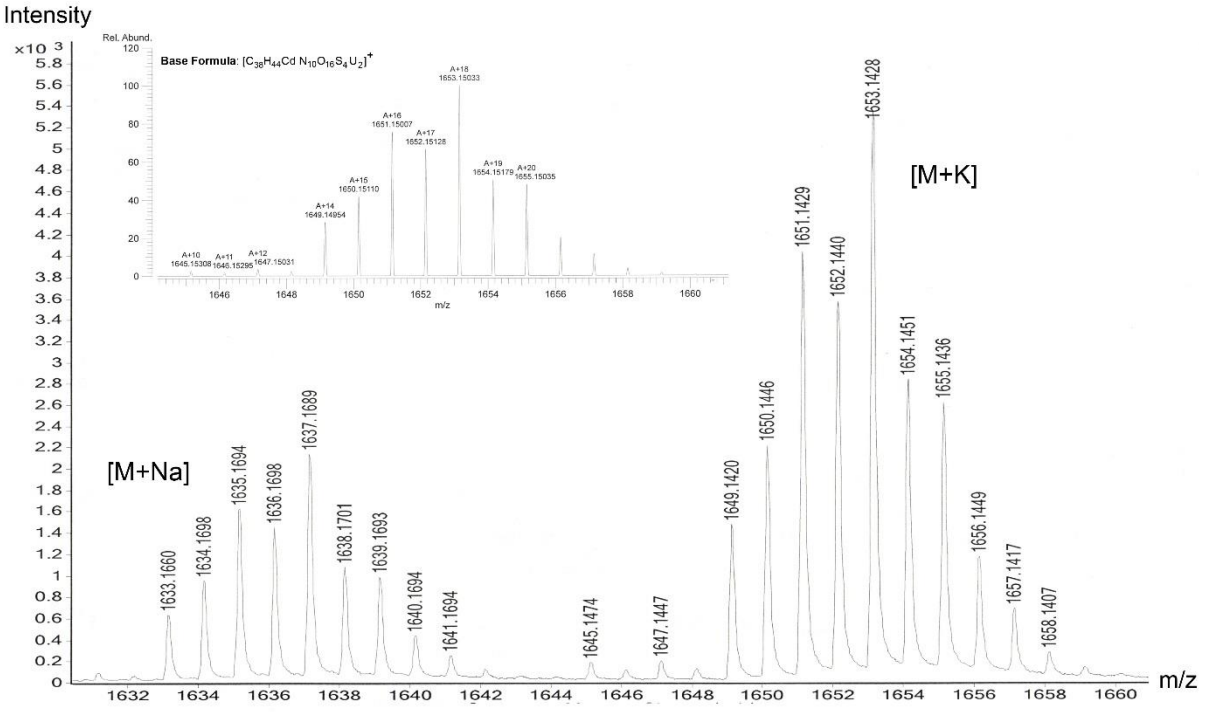

b)

Figure 2.34: a) ^{1}H-NMR spectrum and b) measured and simulated molecular ion peaks in high resolution ESI+ mass spectrum of [Cd{$UO_2(L^{2b})(OAc)$}$_2$].

High resolution ESI+ mass spectra of [Cd{$UO_2(L^{2b})(OAc)$}$_2$] display the molecular ion peak of the expected heterometallic complex as Na^+ and K^+ adducts. The measured isotopic patterns

and the simulated ones are in perfect agreement. This is demonstrated for $[Cd\{UO_2(L^{2b})(OAc)\}_2]$ in Figure 2.34. The observation of the molecular ion peaks of the heteronuclear complexes in the ESI+ measurement indicates their high stability in solution and in the gas phase.

Suitable single crystals for X-ray diffraction were obtained for the trinuclear complexes of Ni^{2+}, Co^{2+}, Fe^{2+} and Mn^{2+} with $\{L^{2a}\}^{2-}$. Additionally, the solid-state structures of such compounds with Ni^{2+}, Co^{2+} and Zn^{2+} containing H_2L^{2b} have been investigated.

The complexes with $[Ni\{UO_2(L^{2a})(OAc)\}_2]$, $[Fe\{UO_2(L^{2a})(OAc)\}_2]$ and $[Co\{UO_2(L^{2a})(OAc)\}_2]$ all crystallize in the centrosymmetric space group C2/c and with similar unit cell parameters. Their asymmetric units each show in a half complex molecule and co-crystallized solvent molecules. The transition metal ions have an occupational factor of 0.5. As a representative, the molecular structure of $[Ni\{UO_2(L^{2a})(OAc)\}_2]$ will be discussed. A molecular plot is shown in Figure 2.35. Selected bond lengths are listed in Table 2.18 together with the values of the compounds with Co^{2+}, Fe^{2+} and Mn^{2+}. The molecule is built up by two $\{UO_2(L^{2a})(OAc)\}^-$ units, which are linked to each other by the nickel ion. Each uranium atom is coordinated in a tetradentate manner with the *S,N,N,O* donor sets of $\{L^{2a}\}^{2-}$. The hexagonal coordination of the uranyl ion is completed by the acetato ligand. The axial U-O bond lengths are unexceptional. The equatorial U-O bond lengths are in the range of 2.434(5) to 2.519(5) Å. The U-N distances are 2.459(5) and 2.557(5) Å, while the U-S bond lengths are 2.841(4) Å. The bond angles between the uranyl oxygen atoms and the donor atoms of the equatorial plane differ in the case of the acetato ligand and the pyridine nitrogen slightly from the ideal 90° and cause a slight distortion of the equatorial plane.

The Ni^{2+} ion is coordinated with two *S,O* chelates of $\{L^{2a}\}^{2-}$ and two oxygen donor atoms of the acetato ligands. This results in a distorted octahedral coordination geometry for the Ni(II) ion. The Ni-O and Ni-S bond lengths are in the range of the values observed in other octahedral nickel (II) chelates with aroylbisthioureato ligands. [47,49] The metal ions (uranium and nickel) are connected to each via the carbonyl group of the *S,O* chelate of $\{L^{2a}\}^{2-}$ and the acetato ligands. This brings the uranium and nickel atoms relatively close to each other (3.683 Å).

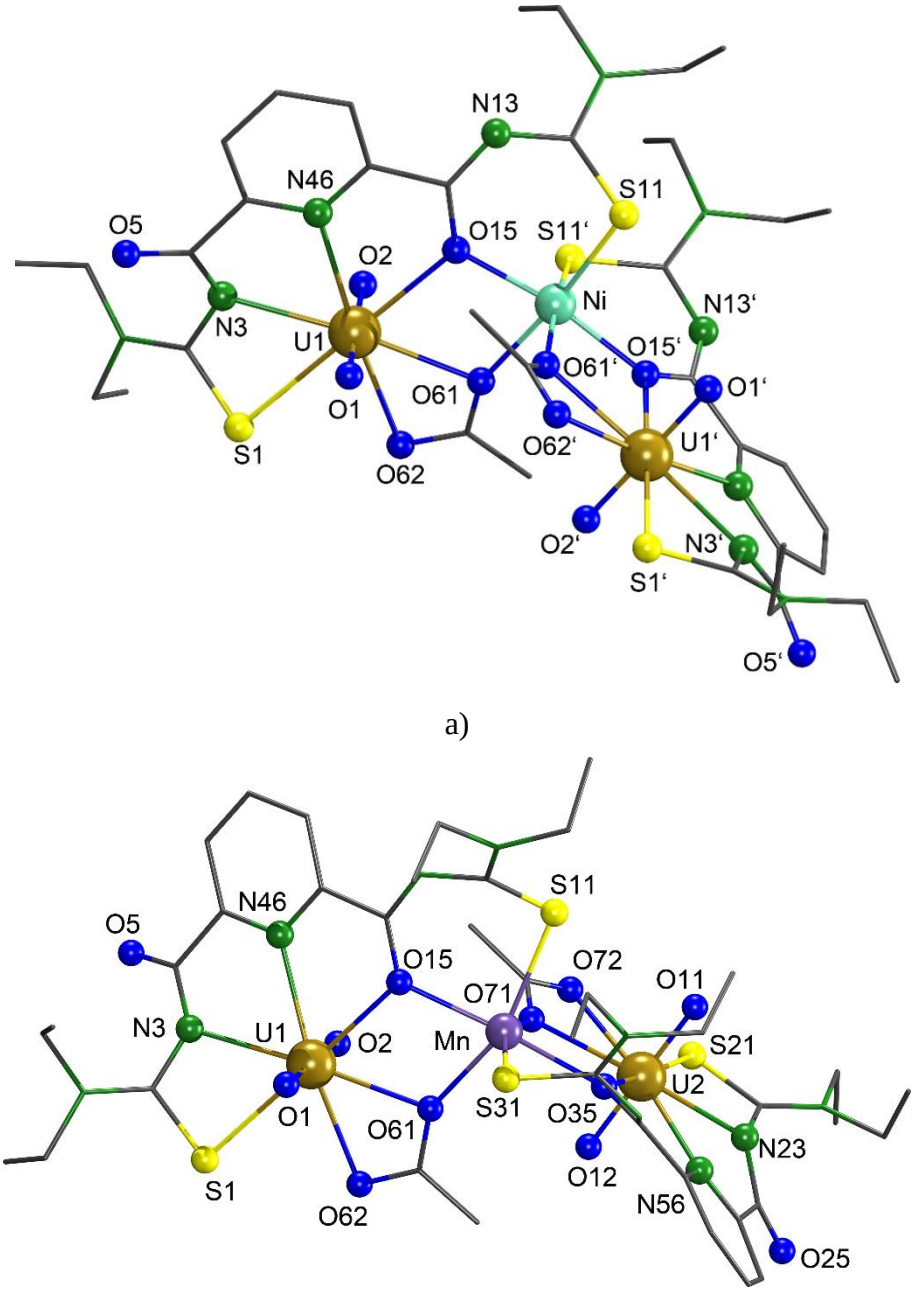

Figure 2.35: Structures of a) [Ni{$UO_2(L^{2a})(OAc)\}_2$], symmetry operator 1-x, y, 3/2-z and b) [Mn{$UO_2(L^{2a})(OAc)\}_2$]. Hydrogen atoms have been omitted for clarity.

The isostructural [Mn{$UO_2(L^{2a})(OAc)\}_2$] complex crystallizes in $P2_1/c$ with a complete complex molecule in the asymmetric unit. Its structure is illustrated in Figure 2.35. The bond lengths of the equatorial plane of the uranium atoms are slightly longer, than those observed for the nickel complex. The Mn(II) ion also shows a distorted octahedral geometry. The U-Mn distances are with 3.922(1) and 3.927(1) Å longer than the U-Ni distance. This is in accordance with the different ionic radii of both transition metal ions.[92]

Table 2.18: Selected bond lengths and distances (Å) in [M{$UO_2(L^{2a})(OAc)\}_2$] (M = Ni, Co, Mn and Fe).

	M = Ni	M = Co	M = Fe	M = Mn
Distances				
U1–O1	1.765(5)	1.762(3)	1.759(4)	1.772(3)
U1–O2	1.768(5)	1.764(3)	1.760(4)	1.777(3)
U1–S1	2.841(4)	2.855(2)	2.859(1)	2.887(1)
U1–N3	2.459(5)	2.477(4)	2.469(3)	2.480(2)
U1–N46	2.557(5)	2.564(3)	2.564(4)	2.559(3)
U1–O15	2.479(5)	2.493(2)	2.491(3)	2.522(2)
U1–O61	2.434(5)	2.447(4)	2.465(4)	2.475(4)
U1–O62	2.519(5)	2.526(3)	2.532(3)	2.519(3)
M–S11	2.339(5)	2.361(2)	2.411(2)	2.516(2)
M–O15	2.046(5)	2.134(3)	2.153(3)	2.227(3)
M–S31	_	_	_	2.540(3)
M–O35	_	_	_	2.216(2)
M–O61	2.048(5)	2.095(3)	2.118(4)	2.164(3)
M–O71	_	_	_	2.176(4)
U⋯⋯U	6.193(2)	6.367(1)	6.290(2)	6.542(1)
U⋯⋯M	3.683(2)	3.766(1)	3.779(1)	3.927(1)
				3.922(1)

As mentioned above, single crystals for three bimetallic complexes were obtained from reactions with H_2L^{2b}: $[Zn\{UO_2(L^{2b})(OAc)\}_2]$, $[Ni\{UO_2(L^{2b})(OAc)\}_2]$ and $[Co\{UO_2(L^{2b})(OAc)\}_2]$. All three compounds crystallizes in the monoclinic space group C2/c with similar unit cell parameters. As a representative, the molecular structure of $[Zn\{UO_2(L^{2b})(OAc)\}_2]$ will be discussed in detail. Its molecular plot is shown in Figure 2.36. Selected bond distances are mentioned in Table 2.19, together with the values of the compounds $[Ni\{UO_2(L^{2b})(OAc)\}_2]$ and $[Co\{UO_2(L^{2b})(OAc)\}_2]$.

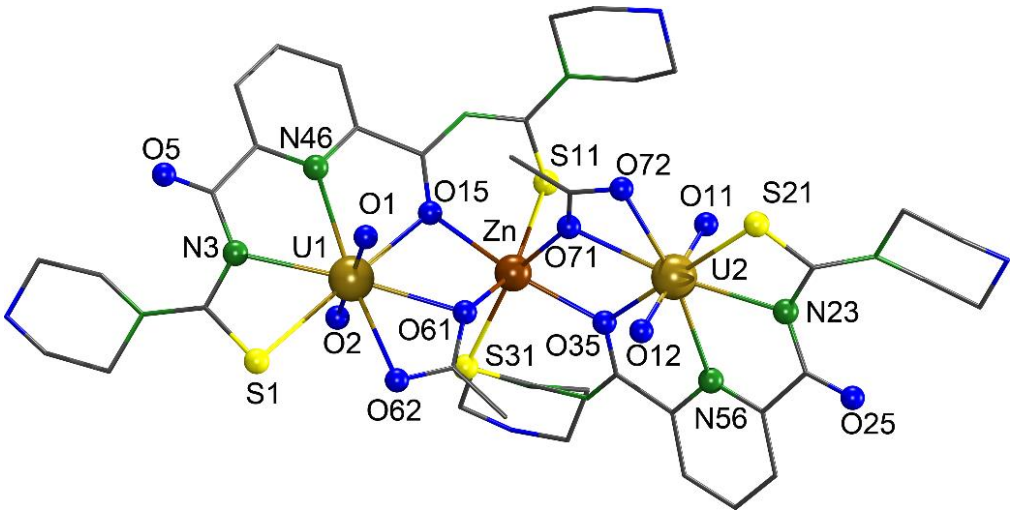

Figure 2.36: Molecular structure of $[Zn\{UO_2(L^{2b})(OAc)\}_2]$. Hydrogen atoms have been omitted for clarity.

The molecular structure of $[Zn\{UO_2(L^{2b})(OAc)\}_2]$ is built up of two $\{UO_2(L^{2b})(OAc\}^-$ units, which are linked to each via the Zn(II) ion. The coordination of the metal ions is similar to those observed in the complexes with $\{L^{2a}\}^{2-}$. The acetato ligands are coordinated *cis* to each other. The bond lengths around the metal atoms are similar to the bond lengths observed in the complexes with $\{L^{2a}\}^{2-}$. Interestingly, the U-U distance in this series of bimetallic complexes is longer. Good examples are the complexes of Ni(II): an elongation of 0.444 Å is observed for the $[Ni\{UO_2(L^{2b})(OAc)\}_2]$ compound to the complex with $\{L^{2a}\}^{2-}$.

Table 2.19: Selected bond lengths (Å) and distances (Å) in [M{$UO_2(L^{2b})(OAc)\}_2$] (M = Zn, Ni and Co).

	M = Zn	M = Ni	M = Co
Distances			
U1–O1	1.776(5)	1.776(3)	1.775(4)
U1–O2	1.769(5)	1.768(3)	1.768(4)
U1–S1	2.871(4)	2.876(2)	2.854(1)
U1–N3	2.479(5)	2.462(4)	2.464(3)
U1–N46	2.571(5)	2.552(3)	2.562(4)
U1–O15	2.482(5)	2.504(2)	2.491(3)
U1–O61	2.474(5)	2.458(4)	2.483(4)
U1–O62	2.477(5)	2.515(3)	2.505(3)
M–S11	2.474(5)	2.504(2)	2.441(2)
M–O15	2.183(5)	2.068(3)	2.140(3)
M–S31	2.505(5)	2.431(2)	2.397(2)
M–O35	2.172(5)	2.079(3)	2.169(3)
M–O61	2.146(5)	2.065(3)	2.121(4)
M–O71	2.109(3)	2.082(3)	2.074(4)
U⋯⋯U	6.745(5)	6.637(5)	6.759(2)
U⋯⋯M	3.840(2)	3.754(1)	3.760(1)
	3.776(2)	3.707(2)	3.812(1)

2.5 Complexes of H_2L^{2a} and H_2L^3 with Thorium(IV) and Uranium(IV).

2.5.1 Thorium(IV) complexes with H_2L^{2a}

The reaction of H_2L^{2a} with thorium nitrate forms a colorless precipitate. The infrared spectrum of the product shows two strong bands at 1635 and 1589 cm^{-1}, which can be assigned to carbonyl vibrations. At 3449 cm^{-1}, a strong and broad signal could be observed, indicating the presence of water in the compound. Crystals suitable for X-ray analysis were obtained by the slow diffusion of methanol into a saturated CH_2Cl_2 solution of the compound. An X-ray

diffraction study confirmed the hydrolysis of the ligand and the formation of the already known Th(IV) complex with 2,6-pyridine dicarboxylate: $[Th(L^{2a*})_2(H_2O)_4]$.[93] A similar hydrolysis of H_2L^{2a} was already observed with uranyl ions as described in Chapter 2.2.2 and could be avoid in that case by the addition of a supporting base in the reaction mixture. The addition of NEt_3 in the case of the thorium compound did not prevent the hydrolysis of H_2L^{2a}.

Therefore, a reaction of a water-free thorium starting material with H_2L^{2a} under water-free conditions was performed. Both reaction conditions and the obtained products are illustrated in Scheme 2.12.

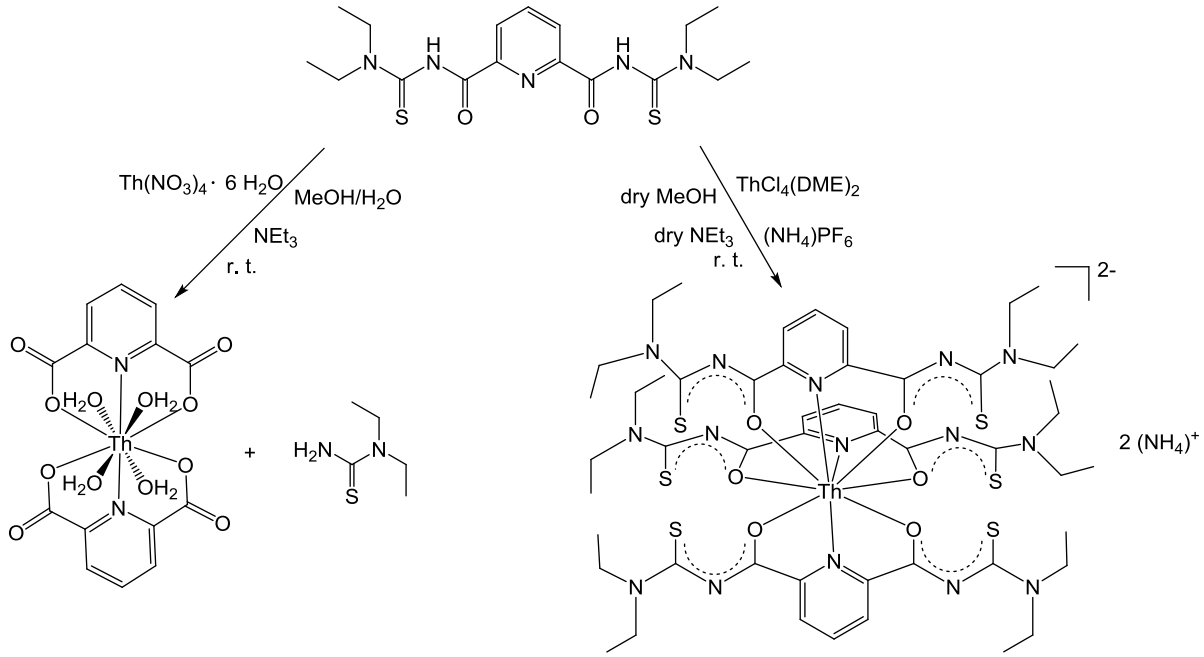

Scheme 2.12: Reactions of Th(IV) ions with H_2L^{2a}.

$[ThCl_4(DME)_2]$ (DME = 1,2-dimethoxyethane) was used as starting material and the reaction was performed in dry MeOH. The reaction solution turned green-yellow and even after the addition of 3 drops of dry NEt_3, no precipitate was formed. The addition of $NH_4(PF_6)$ induced a turbid reaction mixture and after filtration and concentration of the reaction mixture, crystals suitable for X-ray analysis were obtained. The molecular structure of the resulting $(NH_4)_2[Th(L^{2a})_3]$ is illustrated in Figure 2.37. Selected bond lengths are listed in Table 2.20. The compound crystallizes in the monoclinic space group $P2_1/c$ with one solvent methanol in the asymmetric unit. The complex is formed by one Th^{4+} ion and three deprotonated ligands

$\{L^{2a}\}^{2-}$. Two NH_4^+ counter ions provide charge compensation. The presence of the ammonium ions in the solid is confirmed by the observed broad band at 3202 cm^{-1} in IR spectrum.

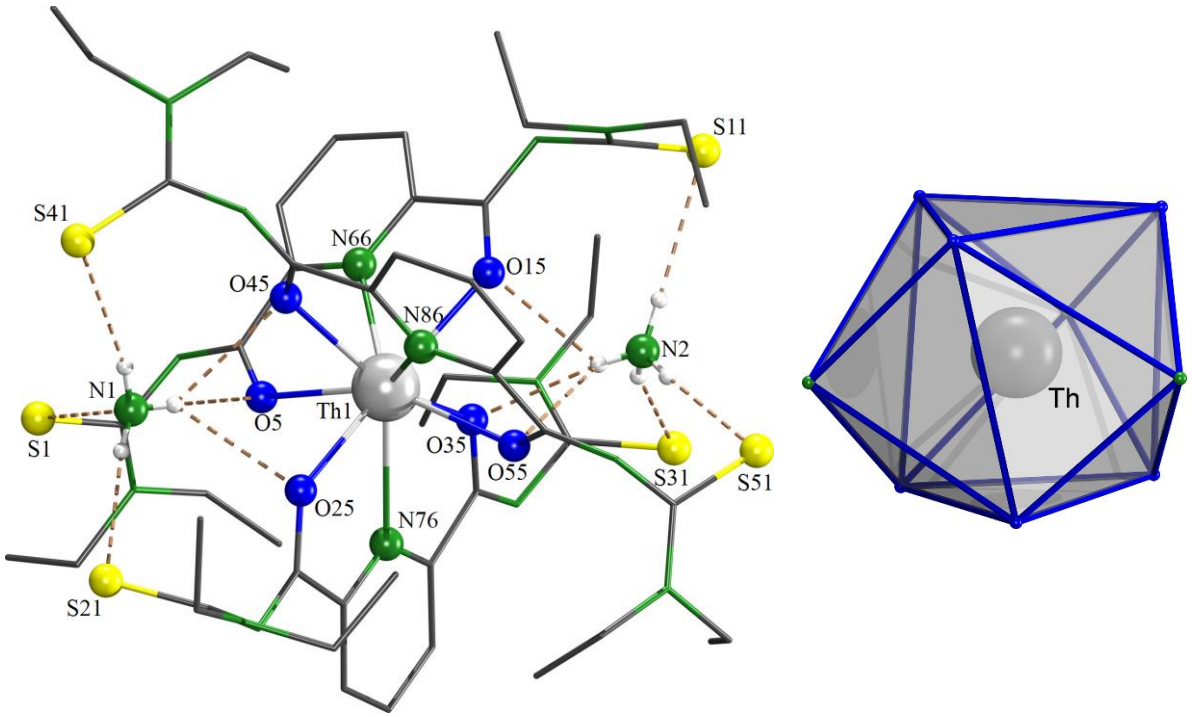

a) b)

Figure 2.37: a) Molecular structure of $(NH_4)_2[Th(L^{2a})_3]$. b) Coordination polyhedron around the thorium atom. Hydrogen atoms of $\{L^{2a}\}^{2-}$ are omitted for clarity.

Each of the $\{L^{2a}\}^{2-}$ ligands is coordinated in a tridentate fashion with the *O,N,O* donor sets of the organic ligand. This generates an elongated tricapped trigonal prism around the thorium atom. The trigonal faces of this prism are formed by two sets of the oxygen atoms O45, O5, O25, and O15, O35, O55. The three nitrogen atoms N66, N76 and N86 occupy the capping positions. The Th-O bonds are in the range of 2.403(1) – 2.432(1) Å. The Th-N bond lengths are between 2.597(1) and 2.615(1) Å. Interestingly, the ammonium ions establish intra-molecular hydrogen bonds to the oxygen and sulfur atoms of the $\{L^{2a}\}^{2-}$ ligands.

Table 2.20: Selected bond lengths (Å), distances (Å) and hydrogen bonds parameters in $(NH_4)_2[Th(L^{2a})_3]$.

Distances					
Th1–O5	2.428(1)	Th1–O15	2.427(1)	Th1–O25	2.432(1)
Th1–O35	2.403(1)	Th1–O45	2.407(1)	Th1–O55	2.419(1)
Th1–N66	2.615(1)	Th1–N76	2.599(1)	Th1–N86	2.597(2)
Th1 ⋯N1	4.107(2)	Th1 ⋯N2	4.193(1)		

D–H ⋯A	d(D–H) (Å)	d(H ⋯A) (Å)	d(D ⋯A) (Å)	<(DHA) (°)
N1–H2 ⋯S1	0.848(6)	2.452(4)	3.295(2)	172.5(1)
N1–H3 ⋯S21	0.849(7)	2.474(5)	3.317(2)	161.9(1)
N1–H4 ⋯S41	0.823(2)	2.513(6)	3.269(2)	168.3(1)
N1–H1 ⋯O5	0.747(2)	2.341(5)	2.851(2)	125.6(1)
N1–H1 ⋯O25	0.747(2)	2.463(2)	3.156(2)	138.2(1)
N1–H1 ⋯O45	0.747(2)	2.548(2)	3.053(2)	141.9(1)

2.5.2 Uranium(IV) complexes with H_2L^{2a}

The previous Subchapters described complexes of H_2L^{2a} with uranium(VI) and thorium(IV) ions. Low-valent uranium salts have hitherto not been considered. But it has previously been demonstrated by Jegathesh, that the trivalent lanthanides coordinate H_2L^{2a} under formation of host-guest compounds.[47]

The reaction of six equivalents of [Au(tht)Cl] (tht = tetrahydrothiophene) and one equivalent of $[U_2I_6(1,4\text{-dioxane})_3]$ with 6 equivalents of H_2L^{2a} in THF results in the formation of a brown-greenish reaction mixture with a brownish precipitate. The precipitate was filtered off and 3 drops of NEt_3 were added to the reaction mixture (see Scheme 2.13).

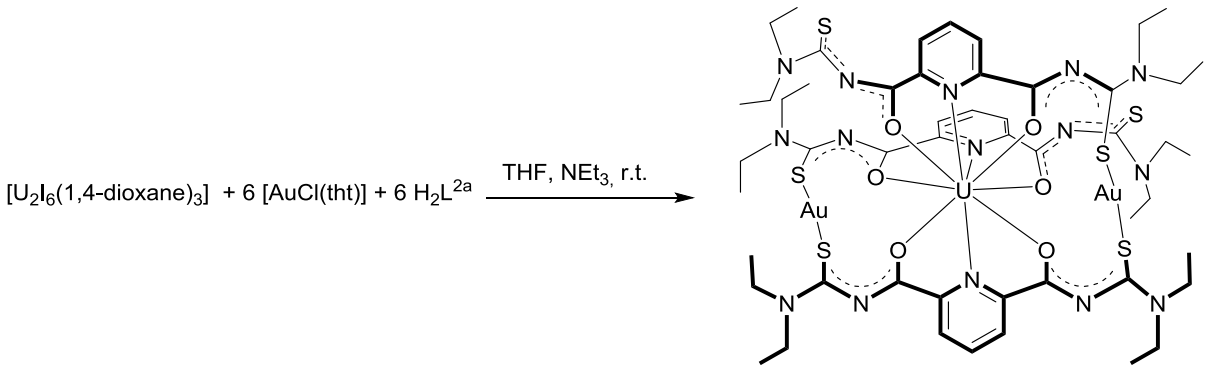

Scheme 2.13: Synthesis of $[Au_2\{U(L^{2a})_3\}]$.

Brownish crystals were obtained from a THF/diethyl ether mixture. The molecular composition of the product, $[Au_2\{U(L^{2a})_3\}]$, was confirmed spectroscopically and by X-ray diffraction. The IR spectrum of the compound shows two strong bands at 1582 cm^{-1} and 1560 cm^{-1}. These bands can be assigned to $\nu_{C=O}$ stretching frequencies of the organic ligand. The values correspond to bathochromic shifts of 98 and 120 cm^{-1} with respect to the spectrum of H_2L^{2a}. The observation of two different carbonyl bands reflects the presence of two chemically different carbonyl units and can be confirmed by the information derived from the X-ray diffraction study. The first carbonyl band can be assigned to the carbonyl unit of the ligand arms, where the sulfur atoms are not coordinated to Au. The additional coordination of Au atoms to the C(*S*) groups induce a stronger electron delocalization in the *S,O* chelate ring and, therefore, induces a stronger bathochromic shift of the carbonyl frequency. Nonetheless, the observed bathochromic shifts are low in comparison to those observed in previously described host-guest compounds with H_2L^{2a}.[47,48]

Figure 2.38 shows the molecular structure of $[Au_2\{U(L^{2a})_3\}]$. Selected bond lengths and angles are given in Table 2.21. The compound crystallizes in the monoclinic space group $P2_1/c$. The asymmetric unit shows one complex molecule with one THF solvent in the lattice. The molecular structure of $[Au_2\{U(L^{2a})_3\}]$ is built up of one uranium atom, two gold atoms and three deprotonated ligands $\{L^{2a}\}^{2-}$. There is no additional counter ion present. This means, a neutral complex can only be achieved when the uranium atom is oxidized from U(III) to U(IV). The oxidizing agent in this reaction is Au(I), which is partially reduced during the reaction to Au(0). Such one-electron oxidations of U(III) compounds are not unusual, but are mostly reported for organouranium species.[94–96] For the targeted oxidation of U(III), usually an excess of the oxidizing agent is required. In the described reaction, 3 equivalents of the Au(I) complex were used per equivalent uranium, as is required for the product $[Au_2\{U(L^{2a})_3\}]$. Nevertheless, a part of the Au(I) ions are reduced. This is reflected by the moderate yield of 40 %. Attempted reactions with an excess of uranium starting material or with very sandlow addition of [AuCl(tht)] could not avoid the oxidation of uranium. Reactions without the presence of Au(I) species did not give defined products.

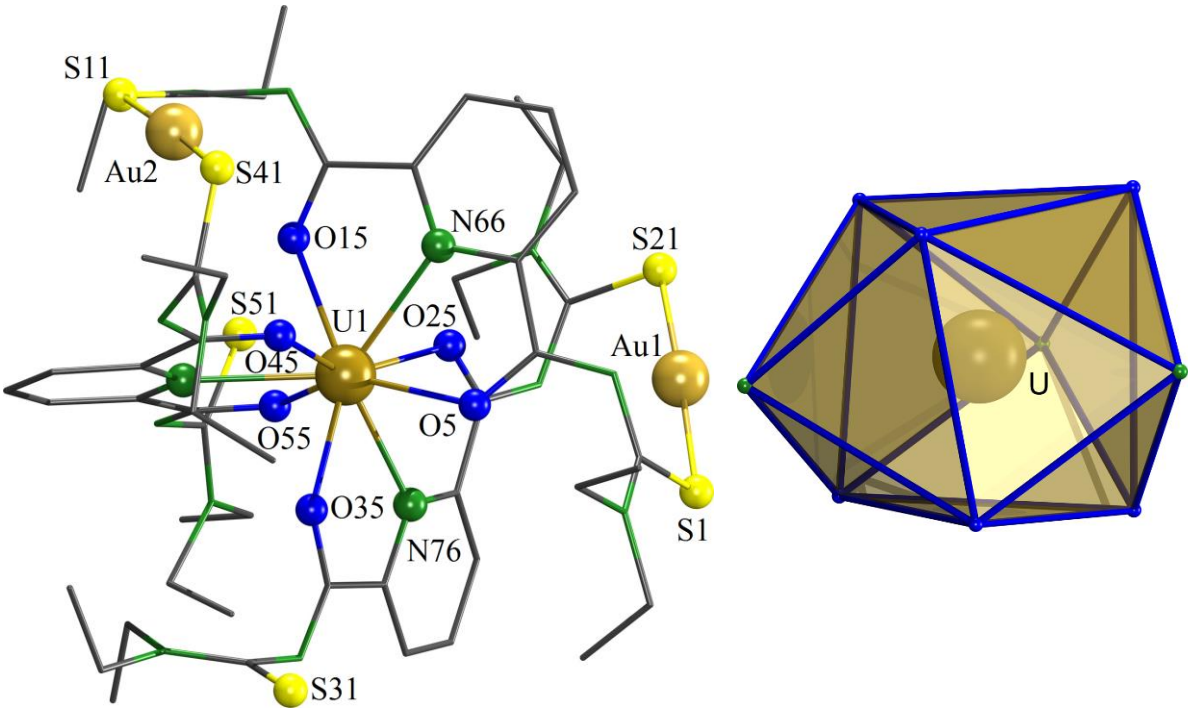

a) b)

Figure 2.38: a) Molecular structure of $[Au_2\{U(L^{2a})_3\}]$. b) Coordination polyhedron around the uranium atom. Hydrogen atoms are omitted for clarity.

Table 2.21: Selected bond lengths (Å), distances (Å) and bond angles (°) in $[Au_2\{U(L^{2a})_3\}]$.

Distances					
U1 – O5	2.337(5)	U1 – O15	2.382(5)	U1 – O25	2.412(5)
U1 – O35	2.349(5)	U1 – O45	2.375(5)	U1 – O55	2.331(5)
U1 – N66	2.575(6)	U1 – N76	2.542(7)	U1 – N86	2.551(7)
Au1 – S1	2.287(2)	Au1 – S21	2.293(2)	Au1 – S11	2.283(2)
Au1 – S41	2.282(2)	U1 ⋯ Au1	5.382(5)	U1 ⋯ Au2	5.143(6)
Bond angles					
S1 – Au1 –S21	175.3(8)	S11 – Au1 –S41	177.1(9)		

The coordination sphere of the oxophilic uranium atom is very similar to that of the thorium atom in $(NH_4)_2[Th(L^{2a})_3]$. Each $\{L^{2a}\}^{2-}$ ligand is coordinated in a tridentate fashion with the *O,N,O* donor set generating a tricapped trigonal-prismatic coordination sphere of the uranium atom as is shown in Figure 2.38b. The trigonal faces of the prism are formed by two sets of the oxygen atoms O45, O5, O25. The three nitrogen atoms N66, N76 and N86 occupy the capping positions. The observed U-O bond lengths are in the range of 2.331(5) – 2.412(5) Å. The U-N

bonds are between 2.542(7) and 2.575(6) Å. These values are similar to reported U(IV)-O and U(IV)-N bond lengths with other chelating ligands.[97,98]

The two gold atoms are coordinated linearly to the sulfur atoms of the thioureato side arms. This is not surprising with respect to the high thiophilicity of gold. The Au-S bonds show distances in the range of 2.282(2) – 2.293(2) Å.

2.5.3 Thorium(IV) complexes with H_2L^3

Attempted reactions of H_2L^3 with $ThNO_3 \cdot 4\ H_2O$ in different solvents such as MeOH, EtOH or H_2O were not successful and no solid products could be isolated. However, a light greenish precipitate was obtained after the addition of $Ni(CH_3COO)_2 \cdot 2\ H_2O$ at 50 °C. Yellow crystals of the composition $[Ni\{Th(L^3)_2(OAc)_2(MeOH)\}]$ were obtained after slow evaporation of the CH_2Cl_2/MeOH solvent mixture at room temperature. The IR spectrum of the crystals shows a broad band at 3443 cm^{-1}, which corresponds to O-H vibrations. The absence of NH vibrations suggests the deprotonation of the organic ligands. Two carbonyl bands are observed at 1591 and 1568 cm^{-1}. They indicate the presence of different carbonyl units in the molecule. The frequencies correspond to a strong bathochromic shift of the carbonyl stretch of $\{L^3\}^{2-}$ with regard to the value in the uncoordinated ligand. This proves a chelate formation with a strong electron delocalization and a coordination of the metal ion via the oxygen atoms. The molecular structure of the compound was determined by X-ray diffraction and is illustrated in Figure 2.39. Selected bond lengths and angles are summarized in Table 2.22. The compound crystallizes in the monclinic space group C2/c. The neutral complex is composed of two ligands $\{L^3\}^{2-}$, one Th^{4+} ion, one Ni^{2+} ion, two acetato ligands and one coordinated MeOH. The $\{L^3\}^{2-}$ ligands coordinate tetradentate to the thorium atom via the *O,N,N,O* donor atoms. The nickel ion is coordinated as *S,O* chelate by two of the aroylthiourea units and one methanol ligand. Both metal ions are linked through two oxygen atoms from $\{L^3\}^{2-}$ and one acetato ligand.

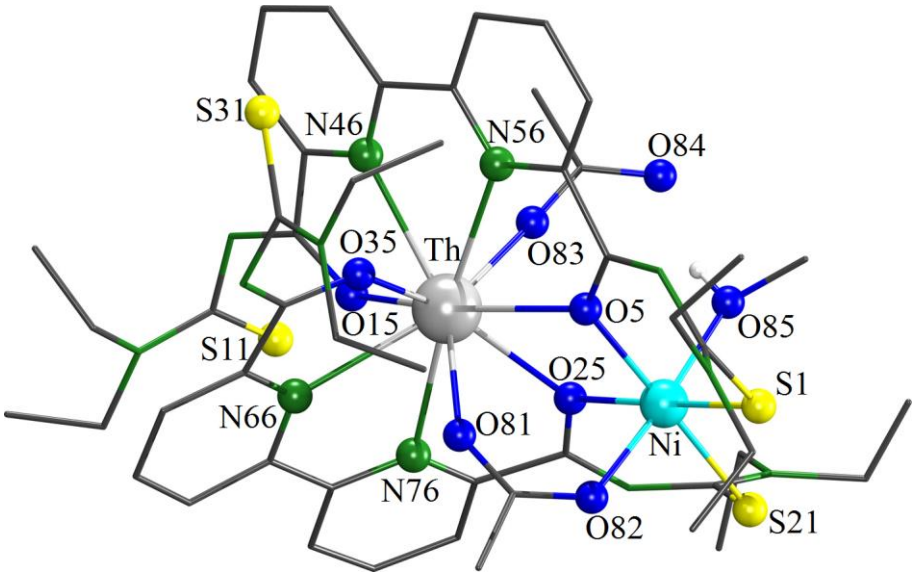

Figure 2.39: Molecular structure of [Ni{Th(L^3)$_2$(OAc)$_2$(MeOH)}]. Hydrogen atoms bonded to the carbon atoms have been omitted for clarity.

Table 2.22: Selected bond lengths (Å) and bond angles (°) in [Ni{Th(L^3)$_2$(OAc)$_2$(MeOH)}].

Bond lengths					
Th – O5	2.524(6)	Th – N46	2.715(7)	Th – O81	2.431(6)
Th – O15	2.354(6)	Th – N56	2.699(7)	Th – O83	2.320(7)
Th – O25	2.509(6)	Th – N66	2.724(7)	Th – N76	2.690(7)
Th – O35	2.383(6)	Ni – O5	2.0525(1)	Ni – S1	2.389(3)
Ni – O82	2.050(6)	Ni – S21	2.336(2)	Ni – O85	2.119(7)
Ni – O25	2.058(6)				
Bond angles					
S21 – Ni – O5	175.2(2)	O85 – Ni – O25	87.5(3)	O85 – Ni – S21	86.7(3)
O85 – Ni – O82	174.9(2)	O85 – Ni – O5	86.5(3)	O85 – Ni – S1	90.3(2)
S1 – Ni – O25	173.8(2)				

In the CSD database, there are no thorium compounds reported with substituted 2,2'-bipyridine ligands. Only 10 crystal structures of thorium complexes with unsubstituted 2,2'-bipyridine have been determined.[99–104] They are exclusively organometallic compounds, where the 2,2'-bipyridine ligand acts as a supporting ligand. The reported Th-N(bipy) bond lengths are in the range of 2.32 – 2.82 Å. However, a few thorium complexes with substituted 1,10-phenanthrolines are also known.[105–108] The 1,10-phenanthroline scaffold affords a similar coordination of the thorium ion over its two nitrogen atoms. The Th-N bond lengths in these compounds are in the range of 2.63 – 2.78 Å. The Th-N bond lengths observed in [Ni{Th(L^3)$_2$(OAc)$_2$(MeOH)}] are similar to those of the substituted 1,10-phenanthroline

complexes with values between 2.690(7) and 2.724(7) Å. The Th-O distances are in the range of 2.354(6) – 2.524(6) Å. The longest Th-O bonds belong to the bridging oxygen atoms O5 and O25 (2.524(6) and 2.509(6) Å). The Th···Ni distance is 3.66(1) Å. The Ni-S bond lengths are 2.336(2) and 2.389(3) Å. The Ni-O bond lengths have values between 2.050(6) and 2.119(7) Å.

The coordination sphere of thorium is completed by a mondentate acetato ligand, which results in a coordination number of ten. The octahedral environment of Ni^{2+} is obtained by the coordination of a methanol ligand. Commonly sphenocoronas or bicapped square antiprisms are used for the description of ten-coordinate metal centers with two tetradentate and two monodentate ligands.[109] Both polyhedra cannot be used for the description of the coordination polyhedron of the thorium atom in the present compound. A closer look at the coordination environment of the thorium atom shows a polyhedron, which can best be described as a distorted bi-edge-capped cube or a distorted bi-edge-capped antiprism as is shown in Figure 2.40. The distorted tetragonal faces of the cube are formed by sets of three oxygen atoms and one nitrogen atom. The capping positions are occupied by the remaining two nitrogen atoms. The large deviations in the edge lengths are due to the presence of the nickel atom in the molecule, which results in a compression of the faces of the cube.

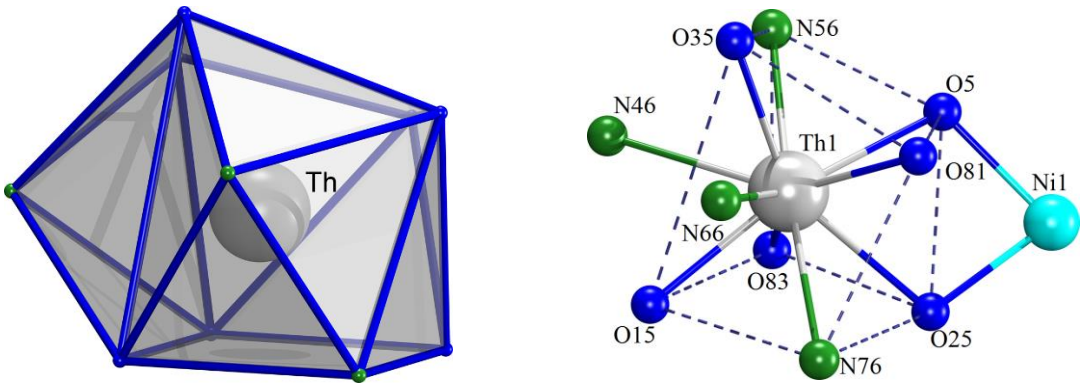

Figure 2.40: Coordination environment around the thorium atom in [Ni{Th(L^3)$_2$(OAc)$_2$-(MeOH)}].

The dihedral angle between the two mean least-square planes of the tetragonal faces of the polyhedron around thorium (O35, N56, O5, O81) and (O25, N76, O15, O83) is 21.99°. This is a clear sign of a strongly distorted coordination environment surrounding the thorium atom. It corresponds to a deviation of 49 % from the ideal cubic shape and of 51 % from the ideal antiprismatic shape.

3 Experimental section

3.1 Starting materials

All chemicals were reagent grade and used without further purification unless otherwise stated. $(NBu_4)_2[UO_2Cl_4]$ was prepared following a standard procedure from uranyl nitrate dissolved in aqueous HCl and NBu_4Cl.[110] $[U_2I_6(1,4\text{-dioxane})_3]$ was synthesized according to a literature procedure.[94] $[ThCl_4(DME)_2]$ was synthesized following the standard procedure[111] by Dr. Juliane März (Helmholtz-Zentrum Dresden-Rossendorf). $[AuCl(PPh_3)]$ and [AuCl(tht)] were synthesized according to a standard procedure from $HAuCl_4$ and PPh_3 or tetrahydrothiophene in ethanol.[112,113] THF was distilled from sodium wire and benzophenone and NEt_3 was distilled over CaH_2. All reactions with air- and moisture-sensitive compounds were performed under an argon atmosphere using standard Schlenk techniques unless otherwise stated.

3.2 Analytical methods

Infrared spectra were taken on a Shimadzu FTIR spectrometer between 400 and 4000 cm^{-1} from KBr pellets or on an Agilent Cary 630 FTIR spectrometer in an inert, water-free glove box filled with N_2 gas.

NMR spectra were recorded at 300 K on a JEOL- or ASC64- 400 MHz multinuclear spectrometers.

ESI mass spectra were measured with an Agilent 6210 ESI-TOF mass spectrometer (Agilent Technologies, Santa Clara, CA, USA). The solvent flow rate was adjusted to 4 µL/min. The spray voltage was set to 4 kV and the drying gas flow rate to 15 psi (1 bar). All other parameters were adjusted for a maximum abundance of the relative $[M+H]^+$ or $[M]^-$ ions. All MS results are given in the form: m/z, assignment. Because of radiation safety, not all the radioactive compounds were measured. For a series of complexes, some representatives were selected.

Elemental analyses of carbon, hydrogen, nitrogen and sulfur were determined using a Heraeus vario EL elemental analyzer.

UV/vis spectra were recorded at on a SPECORD 40 instrument (Analytik Jena).

Uranium contents were measured by a HIDEX 300 SL liquid scintillation counter. An aliquot (0.2 mL) of each sample was added to 10 mL of a scintillation cocktail (Rotiszint ecoplus, Carl Roth) and the net count rates were measured over 1024 channels with a counting time of 120 s.

DFT (Density Functional Theory) calculations were performed with the high-performance computing system of the ZEDAT (SOROBAN)[114] using the program packages GAUSSIAN 09 and GAUSSIAN 16. [115,116] The gas phase geometry optimizations were performed using coordinates derived from the X-ray crystal structures or by modification of the structures using GAUSSVIEW. Details are mentioned in the discussion part.[58] The calculations for the ligand molecules H_2L^1, H_2L^{2a} and H_2L^{2b} were performed without any restrictions on the structures by using the hybrid density functional B3LYP [117–119] together with the standard basis set 6-311G for all atoms. For molecules containing uranium, the calculations were also performed without any restrictions on the structures by using the hybrid density functional B3LYP [117–119] together with the basis sets obtained from the EMSL database 6-311++G for all atoms excluding uranium. For uranium the pseudopotential LANL2DZ was used.[120,121]

3.3 Crystal structure determination

The intensities for the X–ray determinations were collected on STOE IPDS 2T or Bruker D8 Venture instruments with Mo Kα or Cu Kα radiation. The crystals were fixed with KEL-F grease on a glass thread. The space groups were determined by the detection of systematical absences using CHECK–HKL.[122] Absorption corrections were carried out by SADABS[123] or X–RED32.[124] For some compounds, an absorption correction did not improve the quality of analyzed data. Some compounds crystallized with one or several highly disordered solvent molecules. In the compounds $(EtPPh_3)_2[\{UO_2(L^{2b})(\mu^2\text{-}OMe)\}_2]$, $[Pb_2(UO_2)_4(L^{2a})_4(MeOH)_2\text{-}(\mu_2\text{-}OMe)_2]$, $[Fe\{UO_2(L^{2a})(OAc)\}_2]$ and $[Ni\{Th(L^3)_2(OAc)_2(MeOH)\}]$, these solvent molecules could not be modeled properly. Therefore, parallel refinements were undertaken in order to: (1) better model the solvent disorders and (2) 'removal' of the disordered solvents by the SQUEEZE option installed in the program PLATON.[125] A comparison of the computed data is shown in Table 3.1. Structure solutions were performed with the programs SHELXS 86, SHELXS 97 and SHELXS 2014. Structure refinements were done with the SHELXL 2014 program.[126,127] Hydrogen atoms were placed at calculated positions and treated with the 'riding model' option of SHELXL 2014. For $[UO_2(L^{2a})(MeOH)]$, $[UO_2L^{2b}(H_2O)]$ and $(NH_4)_2\text{-}[Th(L^{2a})_3]$, the hydrogen atoms of the solvents (methanol and water) and of the ammonium cations were determined based on the electron density of the Fourier map and refined. The

representation of molecular structures was done using the programs DIAMOND 4.2.2[55] and POV-Ray V.3.6.[128]

Table 3.1: Comparison of the results of the structure refinement parameters for the compounds $(EtPPh_3)_2[\{UO_2(L^{2b})(\mu^2\text{-}OMe)\}_2]$, $[Pb_2(UO_2)_3(L^{2a})_4(MeOH)_2(\mu_2\text{-}OMe)_2]$, $[Fe\{UO_2(L^{2a})\text{-}(OAc)\}_2]$ and $[Ni\{Th(L^3)_2(OAc)_2(MeOH)\}]$, with and without the SQUEEZE calculations.

	$(EtPPh_3)_2[\{UO_2(L^{2b})(\mu^2\text{-}OMe)\}_2]$		$[Pb_2(UO_2)_3(L^{2a})_4(MeOH)_2(\mu_2\text{-}OMe)_2]$	
Solvents	2 H_2O, 2 MeOH	SQUEEZE	3 MeOH	SQUEEZE
S. A.V. [$Å^3$]	735.8		626.4	
GooF	1.086	1.095	1.200	1.119
R1(I>2σ)	0.0283	0.0242	0.0278	0.0250
R1(all data)	0.031	0.0266	0.0665	0.0544
wR2(I>2σ)	0.0687	0.0526	0.0336	0.0295
wR2(all data)	0.07	0.0535	0.0695	0.0563
Largest diff. peak [e. $Å^{-3}$]	1.831	1.142	3.186	1.598
Largest diff. hole[e. $Å^{-3}$]	-0.852	-0.798	-1.660	-1.564
	$[Fe\{UO_2(L^{2a})(OAc)\}_2]$		$[Ni\{Th(L^3)_2(OAc)_2(MeOH)\}]$	
Solvents	3 H_2O	SQUEEZE	CH_2Cl_2, 2.5 H_2O	SQUEEZE
S. A.V. [$Å^3$]	818.6		2076.8	
GooF	0.952	0.925	1.205	1.158
R1(I>2σ)	0.0340	0.0305	0.0583	0.0480
R1(all data)	0.0529	0.0486	0.0687	0.057
wR2(I>2σ)	0.0692	0.0565	0.1341	0.0936
wR2(all data)	0.0734	0.0598	0.1385	0.0961
Largest diff. peak [e. $Å^{-3}$]	1.143	0.689	2.56	2.393
Largest diff. hole[e. $Å^{-3}$]	-0.851	-0.898	-1.701	-1.584

3.4 Syntheses

3.4.1 Ligands

3.4.1.1 H_2L^1

H_2L^1 was synthesized according to a modified method with respect to the standard procedure by Douglas and Dains.[51,52] A solution of isophthaloyl dichloride (3.23 g, 16.25 mmol) dissolved in dry acetone was added dropwise to a warm solution of potassium thiocyanate (3.15 g, 32.50 mmol) in 50 mL dry acetone with stirring under an inert atmosphere. The resulting pale-yellow solution was heated for 30 min and allowed to cool to room temperature. Diethylamine (4.20 g, 32.50 mmol) dissolved in 30 mL dry acetone was added dropwise. The mixture was heated under reflux for 30 min, after which it was cooled to room temperature. The mixture was poured into 500 mL of 0.5 M HCl at 0 °C. A white precipitate was formed, which was recrystallized from methanol/acetone (5:1).

Yield: 81 % (6.7 g)

Elemental analysis: Calcd. for $C_{18}H_{26}N_4O_2S_2$: C, 54.80; H, 6.64; N, 14.20; S, 16.25 %. Found: C, 54.64; H, 6.62; N, 14.28; S, 16.26 %.

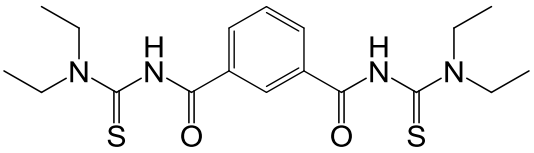

IR (KBr, cm^{-1}): 3119 (m), 2974 (m), 2938 (m), 2873 (m), 1693 (vs), 1533 (vs), 1452 (vs), 1429 (vs), 1379 (m), 1286 (s), 1217 (s), 1128 (s), 1101 (w), 1074 (m), 887 (m), 725 (m).

^{1}H NMR ($CDCl_3$, ppm): 9.46 (s, 2H, NH); 8.23 (s, 1H, ph), 7.91 (d, 2H, *J* = 8.0 Hz, ph), 7.47 (t, 1H, *J* = 8.0 Hz, ph); 3.97 (q, 4H, *J* = 7.0 Hz, CH_2); 3.55 (q, 4H, *J* = 7.0 Hz, CH_2), 1.28–1.23 (m, 12H, CH_3).

^{13}C NMR ($CDCl_3$, ppm): 179.2 (C=S); 163.5 (C=O); 132.8, 132.6, 129.4, 126.6 (ph); 47.8, 47.5 (CH_2); 13.3, 11.4 (CH_3).

+ESI MS **(**m/z): 433.1134 (calcd. 433.1134) $[M+K]^+$; 417.1404 (calcd. 417.1395) $[M+Na]^+$.

UV/Vis (CH_2Cl_2, nm): 236 ($\varepsilon = 33.9 \times 10^3$ L $mol^{-1}cm^{-1}$), 270 ($\varepsilon = 17.9 \times 10^3$ L $mol^{-1}cm^{-1}$), 289 ($\varepsilon = 16.1 \times 10^3$ L $mol^{-1}cm^{-1}$), 357 ($\varepsilon = 1.9 \times 10^3$ L $mol^{-1}cm^{-1}$).

3.4.1.2 H_2L^{2a} and H_2L^{2b}

a) Pyridine-2,6-dicarbonyl dichloride

Pyridine-2,6-dicarboxylic acid (5 g, 30 mmol) was added to freshly distilled thionyl chloride (30 mL, 0.4 mol) and two drops of DMF. After heating the mixture under reflux for 3 h under an inert atmosphere, residual $SOCl_2$ was removed under reduced pressure, which gave a colorless, solid residue of dipicolinoyl chloride.

Yield: 99 % (6 g)

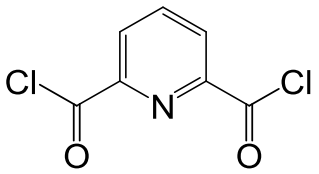

IR (KBr, cm^{-1}): 3084 (m), 1755 (vs), 1258 (vs), 1244 (vs), 871 (vs), 829 (vs), 735 (vs), 640 (vs), 625 (vs).

^1H NMR ($CDCl_3$, ppm): 8.33 (d, J = 8.0 Hz, 2H, py); 8.13 (t, J = 8.0 Hz, 1H, py).

^{13}C NMR ($CDCl_3$, ppm): 169.5 (C=O); 149.3, 139.5, 129.1 (py).

b) *N*,*N*-Diethylthiourea (Et_2tu), *N*-Morpholinethiourea (Mortu)

The synthesis of **Et_2tu** and **Mortu** was performed following the procedure of Yokoyama et al.[54] Ethyl chloroformate (10.8 g, 0.1 mol) was added dropwise to a warm solution of ammonium thiocyanate (9.8 g, 0.1 mol) in dry acetone (100 mL). The reaction mixture was heated under reflux for 2 h in an inert atmosphere. The formation of a colorless precipitate (NH_4Cl) was observed. It was cooled to 5 °C and the corresponding secondary amine (diethyl amine (9.2 g, 0.125 mol) or morpholine (10.9 g, 0.125 mol) was added dropwise. After being stirred at room temperature overnight, the mixture was poured into the double volume of 6M HCl and then extracted with ethyl acetate. The organic phase was dried with $MgSO_4$ and the solvent evaporated to yield the intermediate *N'*–ethoxycarbonyl *N*,*N*–diethylthiourea as a yellow oil.

Yield: 90 %.

Concentrated HCl (30 mL) was added to the product and heated as long as a gas evolution was observed. The resulting mixture was neutralized with $(NH_4)_2CO_3$ and extracted 5 times with ethyl acetate. The solvent of the extract was evaporated and the microcrystalline pure product was washed with diethyl ether.

Yield Et_2tu: 50 % (6.6 g)

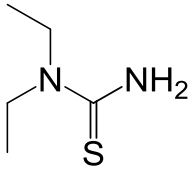

Elemental analysis : Calcd. for $C_5H_{12}N_2S$: C, 45.42; H, 9.15;
N, 21.19; S, 24.25 %. Found: C, 45.40; H, 9.16; N, 20.97; S, 23.52 %.
IR (KBr, cm^{-1}): 3375 (m), 3296 (m), 3190 (s), 3101 (w), 2974 (m), 2934 (w), 2895 (w), 1628 (vs), 1518 (vs), 1435 (m), 1360 (s), 1207 (w), 1074 (m), 843 (m), 667 (w).
^1H NMR ($CDCl_3$, ppm): 5.85 (s, 2H, NH_2); 3.65 (q, 4H, CH_2); 1.19 (t, 6H, J = 8.0 Hz, CH_3).
^{13}C NMR ($CDCl_3$, ppm): 180.8 (C=S); 45.8 (CH_2); 12.6 (CH_3).

Yield Mortu: 45 % (6.5 g)

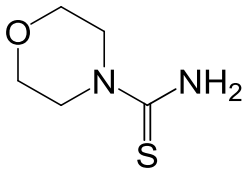

Elemental analysis: Calcd. for $C_5H_{10}N_2OS$: C, 41.07; H, 6.89;
N, 19.16; S, 21.93 %. Found: C, 41.10; H, 6.86; N, 18.91; S, 21.08 %.
IR (KBr, cm^{-1}): 3426 (m), 3327 (m), 3215 (m), 2970 (w), 2911 (w), 2872 (w), 1626 (vs), 1508 (vs), 1350 (vs), 1107 (vs), 1001 (vs), 833 (m), 590 (m).
^1H NMR ($CDCl_3$, ppm): 5.78 (s, 2H, NH_2); 3.74 (m, 8H, CH_2).
^{13}C NMR ($CDCl_3$, ppm): 179.3 (C=S); 66.1 (CH_2–O); 47.9 (CH_2–N).

c) H_2L^{2a}

A solution of Et_2tu (2.6 g, 20 mmol) in 100 mL dry THF was added dropwise to a solution of pyridine-2,6-dicarbonyl dichloride (2.3 g, 10 mmol) in 100 mL dry THF at room temperature. After stirring for 1 h, dry triethylamine (4.2 mL, 30 mmol) was added and the reaction mixture was stirred at 50 °C for additional 45 min. The formed colorless precipitate ($HNEt_3Cl$) was filtered off and the remaining solvent was removed under reduced pressure. The yellow product was recrystallized from methanol/chloroform (5:1).

Yield: 90 % (3.6 g)

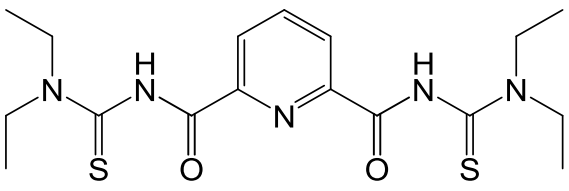

Elemental analysis: Calcd. for $C_{17}H_{25}N_5O_2S_2$: C, 51.62; H, 6.37; N, 17.71; S, 16.21 %. Found: C, 51.64; H, 6.05; N, 17.76; S, 16.34 %.
IR (KBr, cm^{-1}): 3269 (m), 2972 (w), 2934 (w), 2874 (w), 1680 (vs), 1518 (vs), 1440 (vs), 1421 (vs), 1274 (m), 1223 (vs), 1130 (m), 1101 (m), 1076 (m), 995 (w), 920 (w), 750 (m).

^{1}H NMR ($CDCl_3$, ppm): 9.90 (s, 2H, NH); 8.39 (d, 2H, *J* = 8.0 Hz, py); 8.07 (t, 1H, *J* = 8.0 Hz, py); 4.02 (q, 4H, *J* = 6.4 Hz, CH_2); 3.66 (q, 4H, *J* = 6.4 Hz, CH_2); 1.35–1.32 (m, 12H, CH_3).
^{13}C NMR ($CDCl_3$, ppm): 178.3 (C=S); 159.4 (C=O); 148.0, 139.7, 126.8 (py); 47.8, 47.4 (CH_2); 13.6, 11.5 (CH_3).
+ESI MS (m/z): 434.1097 (calcd. 434.1087) $[M+K]^+$; 418.1368 (calcd. 418.1347) $[M+Na]^+$.
UV/Vis (CH_2Cl_2, nm): 224 ($\varepsilon = 36.0 \times 10^3$ L mol^{-1}cm^{-1}), 263 ($\varepsilon = 34.6 \times 10^3$ L mol^{-1}cm^{-1}), 357 ($\varepsilon = 2.1 \times 10^3$ L mol^{-1}cm^{-1}).

d) H_2L^{2b}

The synthesis of H_2L^{2b} was carried out analogously to H_2L^{2b}. Mortu was used instead of Et_2tu.

Yield: 89 % (3.8 g)

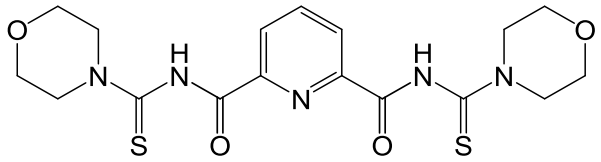

Elemental analysis: Calcd. for $C_{17}H_{21}N_5O_4S_2$: C, 48.21; H, 5.00; N, 16.54; S, 15.14 %.
Found: C, 47.61; H, 5.12; N, 16.23; S, 15.09 %.
IR (KBr, cm^{-1}): 3360 (m), 2978 (w), 2902 (w), 2854 (w), 1708 (vs), 1539 (vs), 1464 (vs) 1417 (vs), 1246 (vs), 1105 (vs), 1028 (m), 964 (m), 840 (m), 742 (m), 684 (m).
^{1}H NMR ($CDCl_3$, ppm): 10.04 (s, 2H, NH); 8.39 (d, 2H, *J* = 7.8 Hz, py); 8.10 (t, 2H, *J*= 7.8 Hz, py); 3.97–3.89 (m, 16H, CH_2).
^{13}C NMR ($CDCl_3$, ppm): 178.4 (C=S); 158.6 (C=O); 147.7, 139.9, 127.2 (py); 66.4 (CH_2–O); 52.5, 51.7 (CH_2–N).
+ESI MS (m/z): 462.0596 (calcd. 462.0672) $[M+K]^+$; 446.0856 (calcd. 446.0933) $[M+Na]^+$.
UV/Vis (CH_2Cl_2, nm): 258 ($\varepsilon = 28.0 \times 10^3$ L mol^{-1}cm^{-1}), 315 ($\varepsilon = 9.6 \times 10^3$ L mol^{-1}cm^{-1}), 366 ($\varepsilon = 2.1 \times 10^3$ L mol^{-1}cm^{-1}).

3.4.1.3 H_2L^3

a) 2,2'-Bipyridine-*N*,*N*'-dioxide

The synthesis was performed by the procedure of Skorka et al.[129] 2,2'-Bipyridine (10 g, 64 mmol) was dissolved in glacial acetic acid (75 mL). 30 % H_2O_2 (13 mL, 0.55 mol) was added dropwise and the reaction mixture was stirred at 80 °C. After 3h, another portion of 30 %

H_2O_2 (7 mL, 0.3 mol) was added dropwise. The light-yellow solution was stirred for additional 4 h at 80 °C. The reaction mixture was then cooled to room temperature and quenched with acetone (1 L). The obtained colorless precipitate was filtered off and dried in vacuum.

Yield: 93 % (11.2 g)

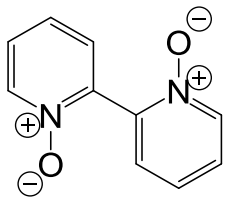

IR (KBr, cm^{-1}): 3038 (w), 2970 (w), 2835 (w), 1472 (m), 1426 (s), 1298 (m), 1253 (s), 1146 (m), 1020 (m), 959 (m), 837 (s), 766 (vs), 580 (s).
^{1}H NMR (D_2O, ppm): 8.29 (d, *J* = 8.0 Hz, 2H); 7.69–7.58 (m, 6H).
^{13}C NMR (D_2O, ppm): 139.6, 137.6, 129.3, 126.8, 126.4 (bipy).

b) 6,6'-Dicyano-2,2'-bipyridine

The synthesis was performed according to the procedure of Sharmoukh et al. with some modifications.[130] A solution of benzoyl chloride (24 mL, 208 mmol) in 80 mL dichloromethane was added dropwise during approximately 30 min to a cold mixture of 2,2'-bipyridine-*N,N'*-dioxid (11.2 g, 60 mmol) and potassium cyanide (22.5 g, 345 mmol) in 200 mL of deionized water. The reaction mixture was stirred for 4 h and the obtained precipitate was filtered off, thoroughly washed with ethanol and dried in vacuum.

Yield: 70 % (8.8 g)

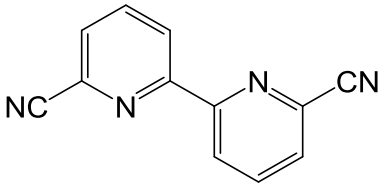

Elemental analysis: Calcd. for $C_{12}H_6N_4$: C, 69.90; H, 2.93; N 27.17 %. Found: C, 69.97; H, 2.80; N, 27.23 %.
IR (KBr, cm^{-1}): 3080 (w), 2972(w), 2929(w), 2236 (m), 2010(w), 1576 (s), 1433 (s), 1209 (w), 1156 (s), 1080 (m), 989 (s), 801 (s), 734 (m).
^{1}H NMR ($(CD_3)_2SO$, ppm): 8.03–7.98 (m, 2H, bipy); 7.78 (t, 2H, *J* = 7.2 Hz, bipy); 7.52–7.43 (m, 2H, bipy).
^{13}C NMR ($(CD_3)_2SO$, ppm): 154.9 (C=N); 138.7, 131.9, 128.9, 124.2 116.6 (bipy).

c) 6,6'-Dicarboxy-2,2'-bipyridine

6,6'-Dicyano-2,2'-bipyridine (5.5 g, 26.5 mmol) was added to a solution of NaOH (9.5 g, 238.3 mmol) in H_2O/EtOH (100 mL/100 mL) and stirred at 80 °C for 3 days. After cooling, the reaction mixture was neutralized with conc. HCl. The obtained precipitate was filtered off and washed thoroughly with EtOH. A pure product was obtained after recrystallization from EtOH/H_2O.

Yield: 80 % (5.1 g)

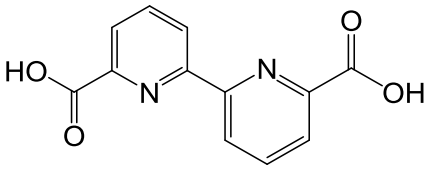

Elemental analysis: Calcd. for $C_{12}H_8N_2O_4$: C, 59.02 H, 3.30; N, 11.47 %. Found: C, 58.84; H, 3.36; N, 11.00 %.
IR (KBr, cm^{-1}): 3095(w), 2982(w), 2838(w), 2555(w), 1692(vs), 1583(s), 1452(m), 1398(s), 1313(s), 1265(m), 1172(w), 1080(m), 938(m), 824(m), 762(vs), 692(s).
^{1}H NMR ($(CD_3)_2SO$, ppm): 8.74 (d, 2H, *J* = 7.2 Hz, bipy); 8.19–8.13 (m, 4H, bipy).
^{13}C NMR ($(CD_3)_2SO$, ppm): 165.9 (C=O); 154.4, 148.1, 139.0, 125.3, 124.2 (bipy).

d) 2,2'-Bipyridine-6,6'-dicarbonyl dichloride

6,6'-Dicarboxy-2,2'-bipyridine (5 g, 20.5 mmol) was mixed with an excess of $SOCl_2$ (25 mL) and 2 drops of DMF and heated on reflux for 6 h. The solvent was then removed under reduced pressure and the resulting colorless solid was dried under vacuum.

Yield: 99 % (5.7 g)

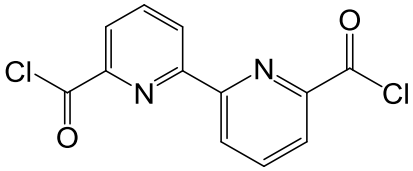

IR (KBr, cm^{-1}): 3085 (w), 2972(w), 2929(w), 1748 (vs), 1575 (w), 1439 (w), 1242 (s), 1157 (m), 954 (m), 864 (s), 733 (s), 623 (s).
^{1}H NMR ($CDCl_3$, ppm): 8.98 (dd, 2H, J_1 = 1.1 Hz, J_2 = 7.8 Hz, bipy); 8.18 (dd, 2H, J_1 = 1.1 Hz, J_2 = 7.8 Hz, bipy); 8.10 (t, 2H, *J* = 8.0 Hz, bipy).
^{13}C NMR ($CDCl_3$, ppm): 169.7 (C=O); 154.4, 149.3, 139.4, 125.3, 124.2 (bipy).

e) H_2L^3

The ligand H_2L^3 was synthesized in a similar manner like H_2L^{2a} and H_2L^{2b}.

A solution of Et_2tu (5.2 g, 40 mmol) in (100 mL) dry THF was added dropwise to a solution of 2,2'-bipyridine-6,6'-dicarbonyl dichloride (5.6 g, 20 mmol) in 100 mL dry THF at room temperature. After stirring for 1 h, dry triethylamine (4.2 mL, 30 mmol) was added and the reaction mixture was stirred at 50°C for additional 45 min. The formed colorless precipitate ($HNEt_3Cl$) was filtered off and the remaining solvent was removed under reduced pressure. The yellow product was recrystallized from methanol/chloroform (5:1).

Yield: 65 % (6.3 g)

Elemental analysis: Calcd. for $C_{22}H_{28}N_6O_2S_2$: C, 55.91; H, 5.97; N, 17.78; S, 13.57 %. Found: C, 55.92; H, 5.97; N, 17.72; S, 13.59 %.

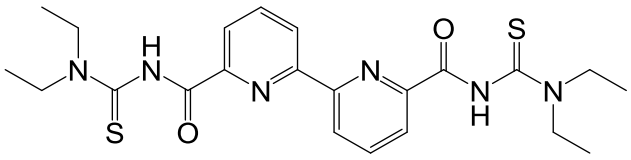

IR (KBr, cm^{-1}): 3375(m), 3318(m), 3190(m), 3082(w), 2972(m), 2929(w), 1707(vs), 1627(m), 1581(m), 1521(s), 1467(w), 1419(s), 1363(m), 1280(m), 1219(m), 1126(m), 1074(m), 1014(w), 931(w), 861(w), 756(m), 667(w).

^{1}H NMR ($CDCl_3$, ppm): 10.21 (s, 2H, NH); 8.54 (dd, 2H, J_1 = 1.2 Hz, J_2 = 8.0 Hz, bipy); 8.26 (dd, 2H, J_1 = 1.1 Hz, J_2 = 8.0 Hz, bipy), 8.08 (t, 2H, J = 8.0 Hz, bipy): 4.06–4.04 (m, 4H, CH_2); 3.71–3.68 (m, 4H, CH_2); 1.37–1.20 (m, 12H, CH_3).

^{13}C NMR ($(CD_3)_2SO$, ppm): 178.6 (C=S); 159.8 (C=O); 153.8, 148.1, 139.1, 124.7, 123.9 (bipy); 47.9, 45.6, (CH_2); 13.5, 12.5 (CH_3).

+ESI MS (m/z): 511.1364 (calcd. 511.1352) $[M+K]^+$; 495.1625 (calcd. 495.1613) $[M+Na]^+$; 473.1806 (calcd. 473.1793) $[M+H]^+$.

UV/Vis (CH_2Cl_2, nm): 218 (ε = 43.6 x 10^3 L $mol^{-1}cm^{-1}$), 246 (ε = 59.5 x 10^3 L $mol^{-1}cm^{-1}$), 280 (ε = 49.1 x 10^3 L $mol^{-1}cm^{-1}$), 354 (ε = 3.5 x 10^3 L $mol^{-1}cm^{-1}$).

3.4.2 Uranyl complexes

$(NBu_4)_2[\{UO_2(L^1)\}_4(OEt)_2(HOEt)_2]$

H_2L^1 (39.4 mg, 0.1 mmol) was dissolved in EtOH (3 mL) and added to a stirred solution of $(NBu_4)_2[UO_2Cl_4]$ (90 mg, 0.1 mmol) in EtOH (3 mL). After 10 min, 3 drops of NEt_3 were added and the reaction mixture was stirred at room temperature for 1 h. The orange-red precipitate was collected by filtration, washed with EtOH and dried in vacuum. Single crystals for X-ray diffraction were obtained after slow evaporation of a CH_2Cl_2/EtOH 1:1 (v/v) solution at room temperature.

Yield: 40 % (33 mg)

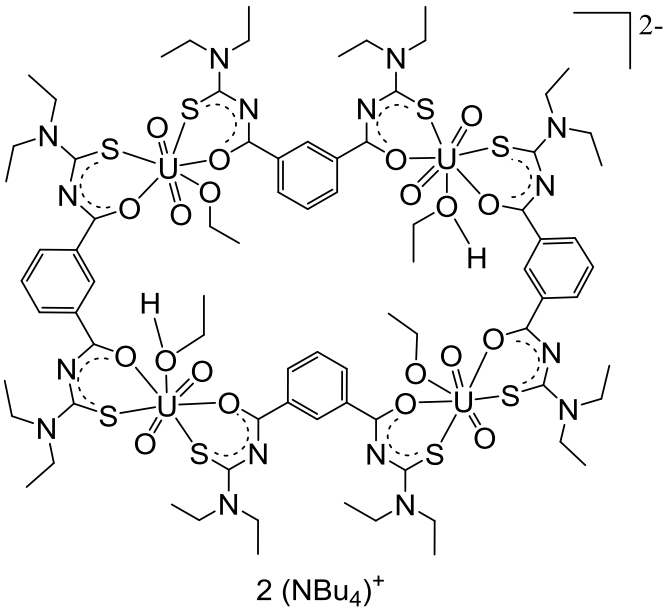

Elemental analysis: Calcd. for $C_{112}H_{190}N_{18}O_{20}S_8U_4$: C, 40.55; H, 5.77; N, 7.60; S, 7.73 %. Found: C, 40.54; H, 5.59 N, 7.88; S, 8.25 %.

IR (KBr, cm^{-1}): 3446 (m), 2966 (m), 2931 (m), 2873 (w), 1595 (w), 1500 (vs), 1423 (s), 1394 (s), 1309 (w), 1251 (w), 1140 (m), 1078 (m), 910 (s), 825 (m), 729 (m), 669 (w).

^{1}H NMR (CD_2Cl_2, ppm): 11.30 (s, 2H, OH_EtOH); 8.43 (m, 4H, Ph), 8.34 (d, 8H, *J* = 7.6 Hz, ph), 7.49 (m, 4H, ph); 4.26–4.05 (m, 32H, CH_2); 2.55–2.41 (m, 24H, CH_2_NBu_4, CH_2_EtOH), 1.48–1.24 (m, 32H, CH_2_NBu_4); 1.01–0.92 (m, 48H, CH_3); 0.82 (t, 12H, *J*=7.1 Hz, CH_3_EtOH); 0.65–0.61 (m, 18H, CH_3_NBu_4).

^{13}C NMR (CD_2Cl_2, ppm): 184.2 (C=S); 173.3 (C=O); 137.2, 132.9, 131.1, 127.6 (ph); 57.8 (CH_2_EtOH); 47.6, 46.3 (CH_2); 45.9 (CH_2_NBu_4); 23.2 (CH_2_ NBu_4); 19.2 (CH_2_ NBu_4); 13.2 (CH_3_EtOH); 13.4, 12.3 (CH_3); 8.9 (CH_3_NBu_4).

UV/Vis (CH_2Cl_2, nm): 232 (ε = 12.5 x 10^3 L $mol^{-1}cm^{-1}$), 283 (ε = 11.5 x 10^3 L $mol^{-1}cm^{-1}$), 368 (ε = 1.8 x 10^3 L $mol^{-1}cm^{-1}$).

$(HNEt_3)_2[\{UO_2(L^1)\}_4(OAc)_2]$

H_2L^1 (39.4 mg, 0.1 mmol) was dissolved in EtOH (3 mL) and added to a stirred solution of $UO_2(CH_3COO)_2 \cdot 2H_2O$ (42.4 mg, 0.1 mmol) in EtOH (3 mL). After 10 min, 3 drops of NEt_3 were added and the reaction mixture was stirred at room temperature for 1 h. The orange-red precipitate was collected by filtration, washed with MeOH and dried in vacuum. Single crystals for X-ray diffraction were obtained after slow evaporation of a CH_2Cl_2/MeOH 1:1 (v/v) solution at room temperature.

Yield: 68 % (52 mg)

Elemental analysis: Calcd. for $C_{90}H_{138}Cl_4N_{18}O_{20}S_8U_4$ ($(HNEt_3)_2[\{UO_2(L^1)\}_4(OAc)_2] \cdot 2\ CH_2Cl_2$): C, 34.40; H, 4.43; N, 8.02; S, 8.16 %. Found: C, 34.42; H, 4.40; N, 8.01; S, 8.27 %.

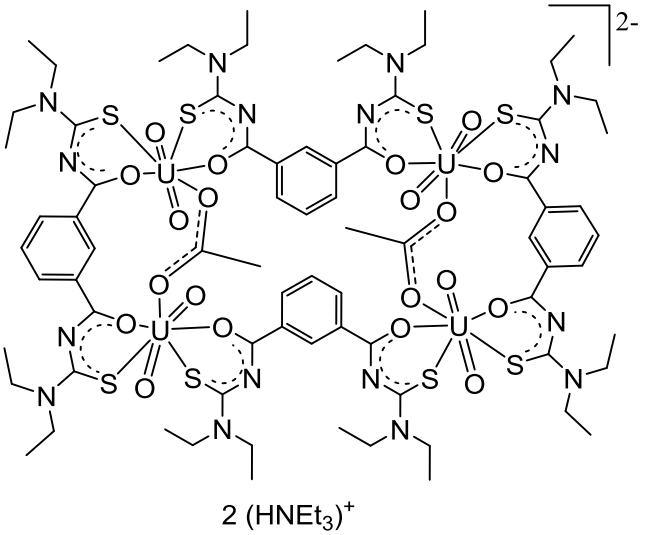

IR (KBr, cm^{-1}): 3062(w), 2976 (w), 2931 (w), 2872 (w), 1680 (w), 1587 (w), 1500 (vs), 1426 (s), 1382 (s), 1311 (w), 1251 (w), 1138 (m), 1078 (m), 1010 (w), 910 (s), 827 (m), 729 (m), 653 (w).

^{1}H NMR ($CDCl_3$, ppm): 10.23 (s, 4H, ph), 8.44 (dd, 8H, J_1 = 8.0 Hz, J_2 = 2.0 Hz, ph), 7.46 (t, 4H, J = 8.0 Hz, ph); 4.35-3.74 (m, 32H, CH_2); 3.00 (s, 6H, CH_3_OAc); 2.26 (m, 6H, CH_2_$HNEt_3$), 1.37-1.08 (m, 48H, CH_3); 0.63 (t, 18H, J = 7.7 Hz, CH_3_$HNEt_3$).

^{13}C NMR ($CDCl_3$, ppm): 184.8 (C=S); 173.1 (C=O_OAc); 170.4 (C=O); 137.2, 132.8, 131.6, 127.8 (ph); 47.7, 46.1 (CH_2); 45.6 (CH_2_$HNEt_3$); 25.6 (CH_3_OAc); 13.6, 12.6 (CH_3); 8.4 (CH_3_$HNEt_3$).

UV/Vis (CH_2Cl_2, nm): 232 ($\varepsilon = 12.5 \times 10^3$ L $mol^{-1}cm^{-1}$), 283 ($\varepsilon = 11.5 \times 10^3$ L $mol^{-1}cm^{-1}$), 368 ($\varepsilon = 1.8 \times 10^3$ L $mol^{-1}cm^{-1}$).

$[UO_2(L^{2a*})(H_2O)]_n$

H_2L^{2a} (39.5 mg, 0.1 mmol) was dissolved in MeOH (3 mL) and added to a stirred solution of $(NBu_4)_2[UO_2Cl_4]$ (90 mg, 0.1 mmol) or $UO_2(CH_3COO)_2 \cdot 2H_2O$ (42.4 mg, 0.1 mmol) or $UO_2(NO_3)_2 \cdot 6H_2O$ (50.2 mg, 0.1 mmol) in MeOH (3 mL) and the reaction mixture was stirred for 1 h. Single crystals for X-ray diffraction were obtained after slow evaporation of the mother solution at room temperature.

Yield: 60 % (27 mg)

IR (KBr, cm^{-1}): 3267(s), 3070(w), 2972(m), 2934(m), 2874(w), 1628(vs), 1522(vs), 1470(vs), 1445(vs), 1417(vs), 1377(m), 1343(w), 1274(m), 1225(s), 1169(m), 1130(m), 1101(m), 998(m), 943(m), 922(s), 862(s), 764(s), 682(m).

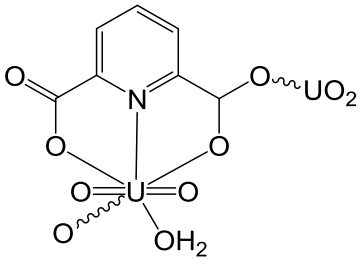

UV/Vis (CH_2Cl_2, nm): 230 (ε = 3.2 x 10^3 L $mol^{-1}cm^{-1}$), 260 (ε = 4.4 x 10^3 L $mol^{-1}cm^{-1}$), 368 (ε = 0.4 x 10^3 L $mol^{-1}cm^{-1}$).

[$UO_2(L^{2a})(MeOH)$]

H_2L^{2a} (39.5 mg, 0.1 mmol) was dissolved in MeOH (3 mL) and added to a stirred solution of $(NBu_4)_2[UO_2Cl_4]$ (90 mg, 0.1 mmol) or $UO_2(CH_3COOH)_2 \cdot 2H_2O$ (42.4 mg, 0.1 mmol) in MeOH (3 mL). After 10 min, 2 drops of NEt_3 were added and the reaction mixture was stirred for 1 h. Single crystals for X-ray diffraction were obtained after slow evaporation of the mother solution at room temperature.

Yield: 70 % (48 mg)

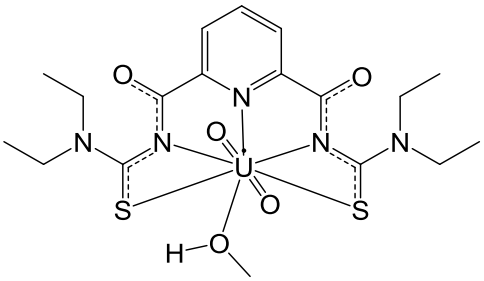

Elemental analysis: Calcd. for $C_{18}H_{27}N_5O_5S_2U$: C, 31.08; H, 3.91; N, 10.07; S, 9.22 %. Found: C, 31.09; H, 3.90; N, 10.05; S, 9.21 %.

IR (KBr, cm^{-1}): 3211(w), 2972(w), 2935(w), 2873(w), 1654(vs), 1591(s), 1523(s), 1429(s), 1396(s), 1348(m), 1313(w), 1263(m), 1205(w), 1151(m), 1078(m), 1016(m), 945(m), 912 (vs), 850(m), 763(m), 680(w).

^{1}H NMR ($(CD_3)_2SO$, ppm): 8.51 (d, 2H, *J* = 8.4 Hz, py); 8.43 (t, 1H, *J* = 8.4 Hz, py); 3.97–3.91 (m, 4H, CH_2); 3.55–3.50 (m, 4H, CH_2); 1.24 (t, 6H, *J* = 7.0 Hz, CH_3); 1.01 (t, 6H, *J* = 7.0 Hz, CH_3).

^{13}C NMR ($(CD_3)_2SO$, ppm): 191.3 (C=S); 174.8 (C=O); 142.4, 139.6, 125.9 (py); 45.1, 46.1 (CH_2); 12.3, 13.5 (CH_3).

+ESI MS (m/z): 1365.3036 (calcd. 1365.3036) $[\{2M–MeOH\}+K]^+$; 702.1331 (calcd. 702.1336) $[\{M–MeOH\}+K]^+$.

UV/Vis (CH_2Cl_2, nm) : 232 (ε = 4.1 x 10^3 L $mol^{-1}cm^{-1}$), 281 (ε = 3.3 x 10^3 L $mol^{-1}cm^{-1}$), 397 (ε = 0.4 x 10^3 L $mol^{-1}cm^{-1}$).

[$UO_2(L^{2a})(DMF)$]

Yellow needles of the compound were synthesized by dissolving [$UO_2(L^{2a})(MeOH)$] (35 mg, 0.05 mmol) in DMF (1 mL) and slow evaporation of the solvent at room temperature.

Yield: 90 % (36 mg)

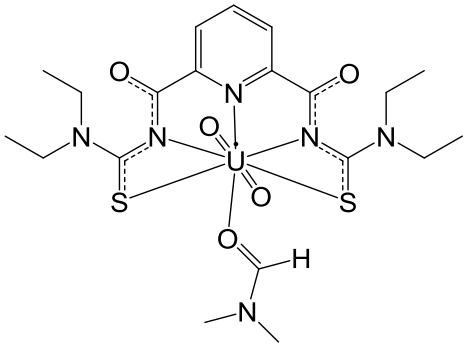

Elemental analysis: Calcd. for $C_{23}H_{37}N_7O_6S_2U$ ($[UO_2(L^{2a})(DMF)] \cdot DMF$): C, 34.12 H, 4.61; N, 12.11; S, 7.92 %. Found: C, 34.11; H, 4.61; N, 12.10; S, 7.89 %.

IR (KBr, cm^{-1}): 3429(w), 2972(w), 2933(w), 2872(w), 1668(w), 1629(vs), 1593(w), 1517(m), 1429(m), 1373(s), 1317(w), 1286(w), 1259(m), 1205(w), 1149(m), 1091(m), 1014(m), 948(m), 904(vs), 842(m), 761(m), 677(w), 653(w), 638(w).

^1H NMR (DMSO, ppm): 8.48 (d, 2H, *J* = 8.0 Hz, py); 8.40 (t, 1H, *J* = 8.0 Hz, py); 7.86 (s, 2H, CH_DMF); 3.97–3.91 (m, 4H, CH_2); 3.55–3.49 (m, 4H, CH_2); 2.83 (s, 12H, CH_3_DMF); 1.23 (t, 6H, *J* = 7.0 Hz, CH_3); 1.00 (t, 6H, *J* = 7.0 Hz, CH_3).

^{13}C NMR (DMSO, ppm): 191.4 (C=S); 163.2 (C=O_DMF); 158.4 (C=O); 121.5, 125.9, 142.4 (py); 45.1, 46.1, (CH_2); 31.3, 36.3 (CH_3_DMF); 12.2, 13.4 (CH_3).

+ESI MS (m/z): 2012.4997 (calcd. 2012.4996) [3{M–DMF}+Na]; 1349.3322 (calcd. 1349.3296) [2{M–DMF}+Na]; 686.1625 (calcd. 686.1597) [{M–DMF}+Na].

$[UO_2(L^{2b})(OH_2)]$

H_2L^{2b} (42.3 mg, 0.1 mmol) was dissolved in MeOH (3 mL) and added to a stirred solution of $(NBu_4)_2[UO_2Cl_4]$ (90 mg, 0.1 mmol) or $UO_2(CH_3COOH)_2 \cdot 2H_2O$ (42.4 mg, 0.1 mmol) in MeOH (3 mL). After 10 min, 2 drops of NEt_3 were added and the reaction mixture was stirred for 1 h. The light yellow precipitate was collected by filtration, washed with MeOH and dried in vacuum. Single crystals for X-ray diffraction were obtained after slow evaporation of a CH_2Cl_2/MeOH 1:1 (v/v) solution at room temperature.

Yield: 60 % (42 mg)

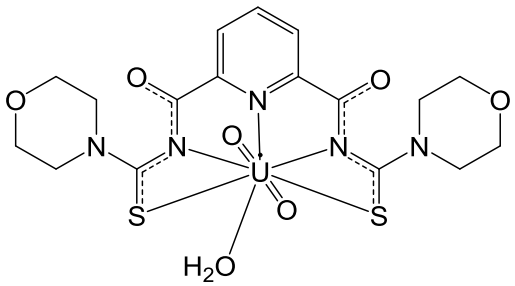

Elemental analysis: Calcd. for $C_{17}H_{21}N_5O_7S_2U$: C, 28.78; H, 2.98; N, 9.87; S, 9.04 %. Found: C, 28.78 H, 2.98; N, 9.89; S, 9.04 %.

IR (KBr, cm^{-1}): 3229(m), 2972(w), 2920(w), 2854(w), 1606(vs), 1516(s),1429(m), 1386(s), 1298(m), 1236(w), 1105(m), 1024(m), 912 (vs), 846(m), 766(w), 698(w), 551(w).

^{1}H NMR ((CD$_3$)$_2$SO, ppm): 8.50 (d, 2H, *J* = 6.8 Hz, py); 8.44 (t, 1H, *J* = 6.8 Hz, py); 3.81–3.51 (m, 16H, CH$_2$).

^{13}C NMR ((CD$_3$)$_2$SO, ppm): 192.1 (C=S); 162.8 (C=O); 158.2, 142.4, 126.1 (py); 66.4 (CH$_2$-O); 46.2 (CH$_2$-N).

+ESI MS (m/z): 2096.3828 (calcd. 2096.3751) [3{M–H$_2$O}+Na]$^+$; 1405.2538 (calcd. 1405.2467) [2{M–H$_2$O}+Na]$^+$; 730.0963 (calcd. 730.0922) [{M–H$_2$O}+K]$^+$; 714.1232 (calcd. 714.1182) [{M–H$_2$O}+Na]$^+$.

UV/Vis (CH$_2$Cl$_2$, nm): 230 (ε = 3.4 x 10^3 L mol^{-1}cm^{-1}), 269 (ε = 2.6 x 10^3 L mol^{-1}cm^{-1}), 370 (ε = 0.4 x 10^3 L mol^{-1}cm^{-1}).

[UO$_2$(L^{2b})(DMF)]

The compound was synthesized from [UO$_2$(L^{2b})(OH$_2$)] and DMF following the procedure given for [UO$_2$(L^{2a})(MeOH)].

Yield: 92 % (35 mg)

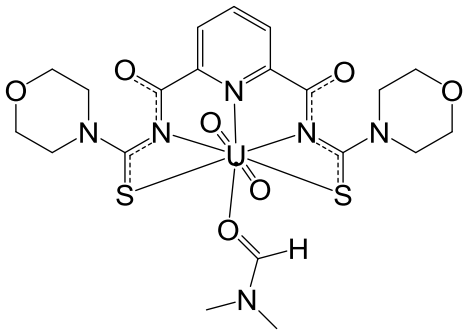

Elemental analysis: Calcd. for C$_{20}$H$_{26}$N$_6$O$_7$S$_2$U: C, 31.42; H, 3.43; N, 10.99; S, 8.39 %. Found: C, 31.40; H, 3.44; N, 10.99; S, 8.37 %.

IR (KBr, cm^{-1}): 3446(w), 2960(w), 2924(w), 2856(w), 1631(s), 1595(w), 1500(vs),1423(m), 1371(s), 1298(m), 1232(w), 1111(m), 1066(w), 1033(m), 908 (vs), 844(m), 759(w), 677(w), 634(w), 607(w), 553(w), 505(w).

^{1}H NMR ((CD$_3$)$_2$SO, ppm): 8.50 (d, *J* = 7.0 Hz, 2H, py), 8.45 (t, *J* = 7.0 Hz, 1H, py), 7.86 (s, 1H, CH_DMF), 3.88–3.55 (m, 16H, CH$_2$), 2.86 (s, 6H, CH$_3$_DMF).

^{13}C NMR ((CD$_3$)$_2$SO, ppm): 192.1 (C=S), 164.5 (C=O_DMF), 159.7 (C=O), 148.6, 133.2, 126.1 (py), 66.7 (CH$_{2–O}$), 46.2 (CH$_{2–N}$), 36.3, 31.5 (CH$_3$_DMF).

+ESI MS (m/z): 1405.2505 (calcd. 1405.2467) [2{M–DMF}+Na]$^+$; 730.1010 (calcd. 730.0922) [{M–DMF+K]$^+$; 714.1219 (calcd. 714.1182) [{M–DMF}+Na]$^+$; 692.1401 (calcd. 692.1363) [{M–DMF+H]$^+$.

[UO$_2$(L^3)]

H$_2$L^3 (42.3 mg, 0.1 mmol) was dissolved in MeOH (3 mL) and added to a stirred solution of (NBu$_4$)$_2$[UO$_2$Cl$_4$] (90 mg, 0.1 mmol) or UO$_2$(CH$_3$COOH)$_2$·2 H$_2$O (42.4 mg, 0.1 mmol) in

MeOH (3 mL). After 10 min, 2 drops of NEt_3 were added and the reaction mixture was stirred for 1 h. The light-yellow precipitate was collected by filtration, washed with MeOH and dried under vacuum. Single crystals for X-ray diffraction were obtained after slow evaporation of a CH_2Cl_2/MeOH 1:1 (v/v) solution at room temperature.

Yield: 90 % (67 mg)

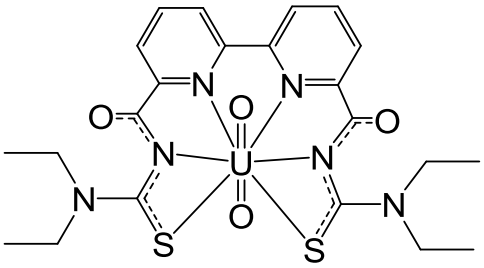

Elemental analysis: Calcd. for $C_{22}H_{26}N_6O_4S_2U$: C, 35.68; H, 3.54; N, 11.35 S, 8.66 %. Found: C, 35.67; H, 3.61; N, 11.36; S, 8.63 %.

IR (KBr, cm^{-1}): 2972(w), 2937(w), 2873(w), 1637(vs), 1598(m), 1517(vs), 1458(m), 1409(m), 1371(s), 1330(w), 1284(w), 1244(m), 1149(m), 1087(m), 1014(m), 908(vs), 819(m), 761(m), 671(w).

^1H NMR ($(CD_3)_2SO$, ppm): 9.13 (d, 2H, *J* = 8.0 Hz, bipy), 8.68 (t, 1H, *J* = 8.0 Hz, bipy), 8.61 (d, 2H, *J* = 8.0 Hz, bipy), 4.13–4.08 (m, 4H, CH_2), 3.84–3.79 (m, 4H, CH_2), 1.40–1.36 (t, 6H, *J* = 7.3 Hz, CH_3), 1.23–1.19 (t, 6H, *J* = 7.3 Hz, CH_3).

^{13}C NMR ($(CD_3)_2SO$, ppm): 182.0 (C=S), 161.6 (C=O), 156.8, 155.9, 143.2, 127.3, 127.0 (bipy), 47.1, 46.1, (CH_2), 12.9, 12.8 (CH_3).

+ESI MS (m/z): 779.1550 (calcd. 779.1602) $[M+K]^+$; 763.1816 (calcd. 763.1862) $[M+Na]^+$; 741.1991 (calcd. 741.2043) $[M+H]^+$.

UV/Vis (CH_2Cl_2, nm): 230 (ε = 2.4 x 10^3 L $mol^{-1}cm^{-1}$), 260 (ε = 2.2 x 10^3 L $mol^{-1}cm^{-1}$), 305 (ε = 1.7 x 10^3 L $mol^{-1}cm^{-1}$).

$(HNEt_3)_2[\{UO_2(L^{2a})(\mu^2\text{-OMe})\}_2]$

H_2L^{2a} (19.8 mg, 0.05 mmol) was dissolved in MeOH (3 mL) at room temperature and added to a stirred solution of $(NBu_4)_2[UO_2Cl_4]$ (90 mg, 0.1 mmol) or $UO_2(CH_3COOH)_2 \cdot 2H_2O$ (42.4 mg, 0.1 mmol) in MeOH (3 mL). After 10 min, 2 drops of NEt_3 were added and the reaction mixture was stirred for 1 h. The obtained precipitate was filtered off, washed with MeOH and dried under vacuum. Single crystals for X-ray diffraction were obtained after slow evaporation of a CH_2Cl_2/MeOH 1:2 (v/v) solution at room temperature.

Yield: 74 % (59 mg)

Elemental analysis: Calcd. for $C_{48}H_{84}N_{12}O_{10}S_4U_2$: C, 35.76; H, 5.17; N, 10.65; S, 8.12 %. Found: C, 35.55; H, 5.27; N, 10.41; S, 8.10 %.

IR (KBr, cm^{-1}): 3429(m), 3070(w), 2974(m), 2933(w), 2874(w), 2681(w), 1589 (vs), 1497(m), 1462(w), 1425(m), 1382(s), 1309(m), 1278(m), 1247(s), 1201(w), 1145(m), 1120(m), 1070(m), 1016(m), 950(w), 912 (vs), 868(w), 766(s), 678(w), 638(m).

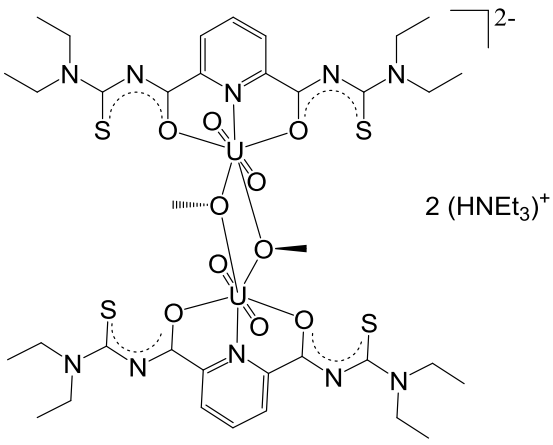

UV/Vis (CH_2Cl_2, nm): 230 (ε = 8.3 x 10^3 L $mol^{-1}cm^{-1}$), 265 (ε = 7.8 x 10^3 L $mol^{-1}cm^{-1}$), 304 (ε = 4.9 x 10^3 L $mol^{-1}cm^{-1}$), 368 (ε = 1.2 x 10^3 L $mol^{-1}cm^{-1}$).

$(EtPPh_3)_2[\{UO_2(L^{2a})(\mu^2\text{-}OMe)\}_2]$

A solution of $(EtPPh_3)Cl$ (32.6 mg, 0.1 mmol) in MeOH (2 mL) was added dropwise to a solution of the complex $(HNEt_3)_2[\{UO_2(L^{2a})(\mu_2\text{-}OMe)\}_2]$ (159.3 mg, 0.1 mmol) in CH_2Cl_2 (2 mL). The reaction mixture was evaporated slowly at room temperature. The obtained yellow crystals were collected, washed with MeOH and dried under vacuum.

Yield: 12 % (24 mg)

Elemental analysis: Calcd. for $C_{76}H_{92}N_{10}O_{10}P_2S_4U_2$: C, 46.29; H, 4.70; N, 7.10; S, 6.50 %. Found: C, 45.85; H, 4.87; N, 7.08; S, 6.46 %.

IR (KBr, cm^{-1}): 3425(m), 3057(w), 2974(m), 2929(m), 2855(w), 2810(w), 2601(w), 1591(vs), 1492(s), 1433(s), 1377(s), 1311(m), 1280(m), 1248(s), 1146(w), 1113(s), 1001(m), 949(w), 905(vs), 843(w), 758(m), 691(m), 631(w), 530(m).

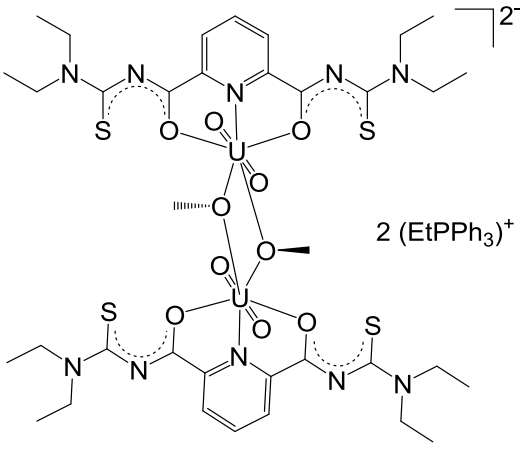

UV/Vis (CH_2Cl_2, nm): 232 (ε = 6.3 x 10^3 L $mol^{-1}cm^{-1}$), 264 (ε = 5.3 x 10^3 L $mol^{-1}cm^{-1}$), 304 (ε = 3.8 x 10^3 L $mol^{-1}cm^{-1}$), 358 (ε = 0.9 x 10^3 L $mol^{-1}cm^{-1}$).

$(HNEt_3)_2[\{UO_2(L^{2b})(\mu^2\text{-}OMe)\}_2]$

H_2L^{2b} (84.6 mg, 0.2 mmol) was dissolved in MeOH (3 mL) and added to a stirred solution of $(NBu_4)_2[UO_2Cl_4]$ (90 mg, 0.1 mmol) or $UO_2(CH_3COOH)_2{\cdot}2H_2O$ (42.4 mg, 0.1 mmol) in MeOH

(3 mL). After 10 min, 2 drops of NEt_3 were added and the reaction mixture was stirred for 1 h. The obtained precipitate was filtered off, washed with MeOH and dried under vacuum. Single crystals for X-ray diffraction were obtained after slow evaporation of a CH_2Cl_2/MeOH 1:1 (v/v) solution at room temperature.

Yield: 77 % (76 mg)

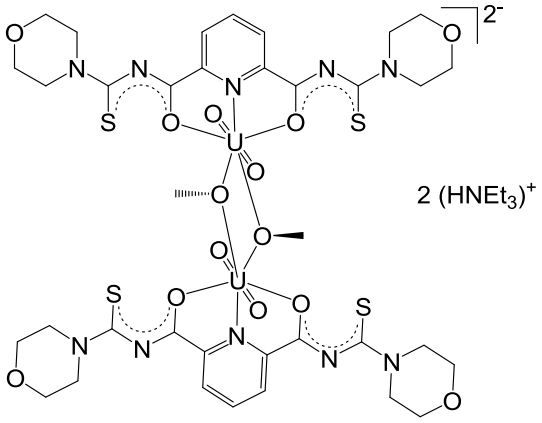

Elemental analysis: Calcd. for $C_{48}H_{76}N_{12}O_{14}S_4U_2$: C, 34.95; H, 4.64; N, 10.19; S, 7.77 %. Found: C, 35.17; H, 5.09; N, 9.53; S, 7.62 %.

IR (KBr, cm^{-1}): 3428(w), 2976(w), 2922(w), 2855(w), 2683(w), 1587(vs), 1475(m), 1427(s), 1381(m), 1280(s), 1229(m), 1111(m), 1064(w), 1026(m), 951(m), 901 (s), 841(m), 777(m), 760(m), 702(w), 629(m).

UV/Vis (CH_2Cl_2, nm): 230 (ε = 3.4 x 10^3 L $mol^{-1}cm^{-1}$), 269 (ε = 2.6 x 10^3 L $mol^{-1}cm^{-1}$), 370 (ε = 0.4 x 10^3 L $mol^{-1}cm^{-1}$).

$(EtPPh_3)_2[\{UO_2(L^{2b})(\mu^2\text{-OMe})\}_2]$

A solution of $(EtPPh_3)Cl$ (32.6 mg, 0.1 mmol) in MeOH was added dropwise to a solution of the complex $(HNEt_3)_2[\{UO_2(L^{2b})(\mu^2\text{-OMe})\}_2]$ (159.3 mg, 0.1 mmol) in CH_2Cl_2. The mixture was evaporated slowly at room temperature and the obtained yellow crystals were collected, washed with MeOH and dried under vacuum.

Yield: 70 % (142 mg)

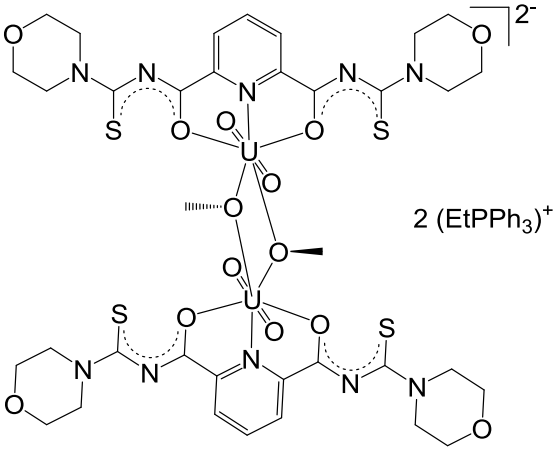

Elemental analysis: Calcd. for $C_{78}H_{94}N_{10}O_{17}P_2S_4U_2$ $((EtPPh_3)_2[\{UO_2(L^{2b})(\mu^2\text{-OMe})\}_2] \cdot 2\ MeOH \cdot H_2O)$: C, 44.40; H, 4.49; N, 6.64; S, 6.08 %. Found: C, 45.01; H, 4.59; N, 6.63; S, 6.02 %.

IR (KBr, cm^{-1}): 3425(w), 3074(w), 2983(w), 2958(w), 2906(w), 2875(w), 2603(w), 1620(m), 1585(s), 1483(s), 1435(s), 1382(m), 1346(m), 1313(w), 1280(m), 1232(w), 1190(m), 1111(s), 1029(m), 995(m), 943(w), 906 (s), 846(m), 754(s), 690(s), 530(m).

UV/Vis (CH_2Cl_2, nm): 230 (ε = 3.4 x 10^3 L $mol^{-1}cm^{-1}$), 269 (ε = 2.6 x 10^3 L $mol^{-1}cm^{-1}$), 370 (ε = 0.4 x 10^3 L $mol^{-1}cm^{-1}$).

$(HNEt_3)[(UO_2)_3(L^{2a**})_2(\mu_2–OH)(\mu_3-O)]$

H_2L^{2a} (79 mg, 0.2 mmol) was added to a stirred solution of $(NBu_4)_2[UO_2Cl_4]$ (90 mg, 0.1 mmol) in H_2O (3 mL). After 10 min, 5 drops of NEt_3 were added and the reaction mixture was stirred at 50°C for 1 h. The obtained precipitate was filtered off, washed with diethyl ether and dried in vacuum. Yellow needles suitable for X-ray diffraction were obtained after slow evaporation of a CH_2Cl_2/EtOH 1:1 (v/v) solution at room temperature.

Yield: 68 % (116 mg)

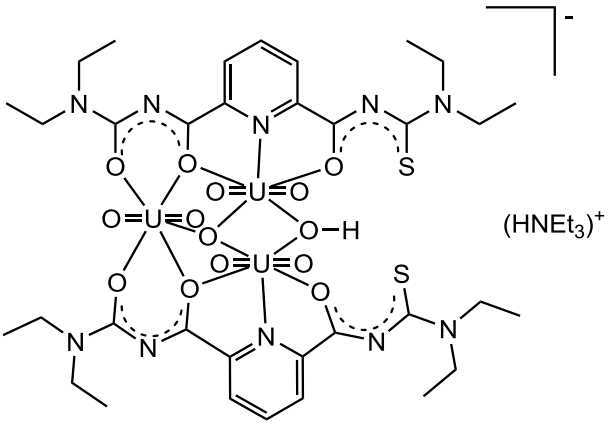

IR (KBr, cm^{-1}): 3456(m), 3143(w), 3074(w), 2972(w), 2978(m), 2931(m), 1597(vs), 1492(s), 1425(s), 1373(vs), 1311(m), 1278(m), 1246(s), 1147(w), 1126(m), 1066(m), 1018(m), 902(vs), 769(m), 638(w).

^{1}H NMR ($(CD_3)_2SO$, ppm): 8.51 (d, 4H, *J* = 8.0 Hz, py); 8.41 (t, 2H, *J* = 8.0 Hz, py); 3.95 (q, 8H, *J* = 7.2 Hz, CH_2); 3.53 (q, 8H, *J* = 7.2 Hz, CH_2); 2.37 (q, 6H, *J* = 7.2 Hz, CH_2_$HNEt_3$); 1.25 (t, 12H, *J* = 7.2 Hz, CH_3); 1.02 (t, 12H, *J* = 7.2 Hz, CH_3); 0.87 (t, 9H, *J* = 7.2 Hz, CH_3_$HNEt_3$).

^{13}C NMR ($(CD_3)_2SO$, ppm): 191.6 (C=S); 162.4 (C=O); 158.6, 142.2, 125.8 (py); 67.4 (CH_2_$HNEt_3$); 46.0, 45.0, (CH_2); 25.5 (CH_3_$HNEt_3$); 13.6, 12.4 (CH_3).

-ESI MS (m/z): 1597.4242 (calcd. 1597.4238) $[M]^-$.

UV/Vis (CH_2Cl_2, nm): 232 (ε = 6.8 x 10^3 L $mol^{-1}cm^{-1}$), 264 (ε = 2.0 x 10^3 L $mol^{-1}cm^{-1}$), 270 (ε = 2.7 x 10^3 L $mol^{-1}cm^{-1}$), 277 (ε = 1.8 x 10^3 L $mol^{-1}cm^{-1}$), 306 (ε = 1.0 x 10^3 L $mol^{-1}cm^{-1}$), 368 (ε = 0.2 x 10^3 L $mol^{-1}cm^{-1}$).

$(EtPPh_3)[(UO_2)_3(L^{2a**})_2(\mu_2–OMe)(\mu_3-O)]$

A solution of $(EtPPh_3)Cl$ (32.6 mg, 0.1 mmol) in MeOH (2 mL) was added dropwise to a solution of the complex $(HNEt_3)_2[\{UO_2(L^{2a})(\mu^2\text{-}OMe)\}_2]$ (159.3 mg, 0.1 mmol) in CH_2Cl_2. (2 mL). The reaction mixture was evaporated slowly at room temperature. The resulting yellow crystals were collected, washed with MeOH and dried under vacuum.

Yield: 60 % (114 mg)

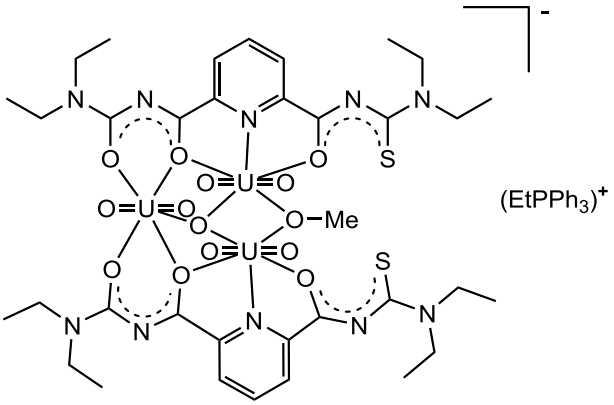

IR (KBr, cm^{-1}): 3433(m), 3055(w), 2968(w), 2926(m), 1593(vs), 1492(s), 1427(s), 1371(vs), 1246(s), 1111(m), 1008(m), 902(vs), 754(m), 688(m), 630(w).

^{1}H NMR ($(CD_3)_2SO$, ppm): 8.51 (d, 2H, *J* = 7.7 Hz, py); 8.43 (t, 1H, *J* = 7.7 Hz, py); 7.89–7.83 (m, 15H, Ph); 4.17–4.13 (m, 8H, CH_2); 3.97 (q, 4H, *J* = 7.2 Hz, CH_2_EtPPh$_3$); 3.62–3.52 (m, 8H, CH_2); 3.12 (s, 3H, OMe); 1.25 (t, 3H, *J* = 7.4 Hz, CH_3_EtPPh$_3$); 1.09–0.90 (m, 24H, *J* = 7.5 Hz, CH_3).

^{13}C NMR ($(CD_3)_2SO$, ppm): 191.5 (C=S); 162.3 (C=O); 158.6, 142.3, 125.6 (py); 135.2, 133.9, 130.6, 119.1, 118.3 (Ph); 48.9 (OMe); 45.8, 45.1 (CH_2); 15.0 (CH_2_EtPPh$_3$); 13.6, 12.4 (CH_3); 6.7 (CH_3_EtPPh$_3$).

^{31}P NMR ($(CD_3)_2SO$, ppm): 25.7.

-ESI MS (m/z): 1611.4395 (calcd. 1611.4395) $[M]^-$.

$(HNEt_3)[(UO_2)_3(L^{2a**})_2(\mu_2–OEt)(\mu_3-O)]$

A solution of NEt_4Cl (32.6 mg, 0.1 mmol) in EtOH (2 mL) was added dropwise to a solution of the complex $(HNEt_3)_2[\{UO_2(L^{2a})_2(\mu^2\text{-}OMe)\}_2]$ (159.3 mg, 0.1 mmol) in CH_2Cl_2 (2 mL). The reaction mixture was evaporated slowly at room temperature. The obtained yellow crystals were collected, washed with EtOH and dried under vacuum.

Yield: 72 % (126 mg)

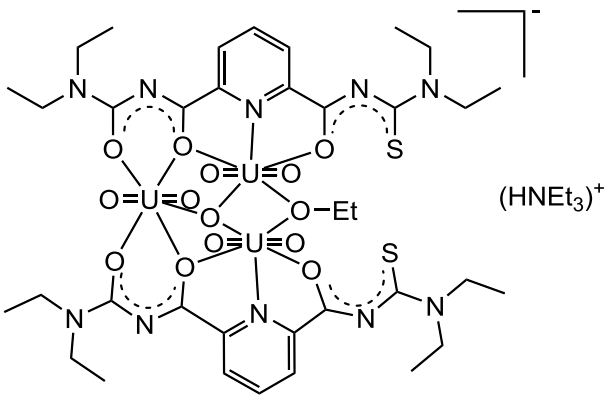

IR (KBr, cm^{-1}): 3442(w), 3078(w), 2978(w), 2934(w), 2874(w), 1597(vs), 1566(w), 1493(s), 1423(m), 1377(s), 1313(w), 1280(m), 1251(m), 1203(w), 1146(m), 1101(w), 995(m), 960(m), 904 (vs), 766(m), 696(w), 635(m).

^{1}H NMR ($(CD_3)_2SO$, ppm): 8.52 (d, 4H, *J* = 8.0 Hz, py); 8.37 (t, 2H, *J* = 8.0 Hz, py); 4.03–3.94 (m, 8H, CH_2); 3.57–3.52 (m, 8H, CH_2); 3.42–3.39 (m, 2H, *J* = 6.8 Hz, CH_2_OEt); 3.15 (q, 8H, *J* = 7.6 Hz, CH_2_HNEt$_3$); 1.26 (t, 3H, *J*= 6.8 Hz, CH_3_OEt); 1.13–1.07 (m, 24H, CH_3); 1.03 (t, 12H, *J* = 6.8 Hz, CH_3_HNEt$_3$).

^{13}C NMR ($(CD_3)_2SO$, ppm): 191.3 (C=S); 162.4 (C=O); 158.6, 143.5, 125.7 (py); 56.4 (CH_2_EtO); 51.8 (CH_2_$HNEt_3$); 45.9, 45.0, (CH_2); 16.7 (CH_3_EtO); 13.6, 12.4 (CH_3); 7.5 (CH_3_ $HNEt_3$).

-ESI MS (m/z): 1625.4546 (calcd. 1625.4551) $[M]^-$.

$(HNEt_3)_2[\{(UO_2)_2(L^{2a})(\mu_2\text{–}OAc)(\mu_3\text{-}O)\}_2]$

A solution of $Ni(CH_3COO)_2{\cdot}4\ H_2O$ (24.8 mg, 0.2 mmol) in MeOH (2 mL) was added dropwise to a solution of the complex $(HNEt_3)_2[\{UO_2(L^{2a})_2(\mu_2\text{-}OMe)\}_2]$ (159.3 mg, 0.1 mmol) in CH_2Cl_2 (2 mL). The mixture was evaporated slowly at room temperature. The obtained yellow crystals were collected, washed with EtOH and dried under vacuum.

Yield: 60 % (133 mg)

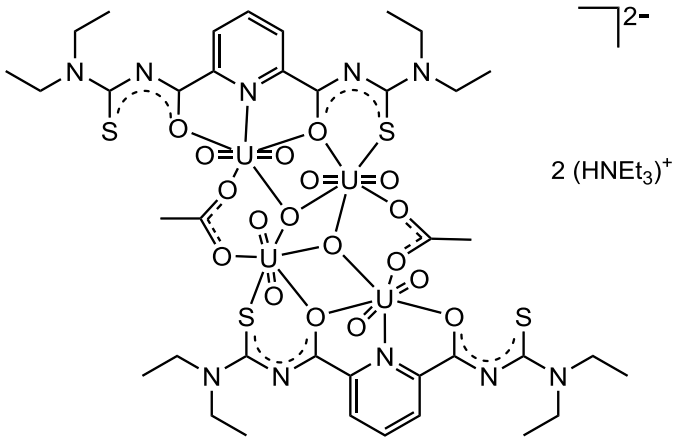

Elemental analysis: Calcd. for $C_{50}H_{84}N_{12}O_{18}S_4U_4$: C, 27.03 H, 3.81; N, 7.57; S, 5.77 %. Found: C, 25.72; H, 3.75; N, 7.13; S, 5.28 %.

IR (KBr, cm^{-1}): 3445(m), 3032(w), 2976(m), 2933(w), 2873(w), 2812(w), 2742(w), 1593(vs), 1552(vs), 1525(w), 1429(s), 1385(vs), 1355(w), 1307(w), 1280(m), 1250(s), 1151(m), 1120(m), 1072(m), 1016(m), 954(w), 907 (vs), 872(m), 843(w), 791(w), 759(m), 654(m), 503(m).

Insoluble => no further analysis.

3.4.3 Mixed-metal complexes of uranium with transition and post-transition metals

3.4.3.1 $[\{UO_2(L^{2a})(\mu_2\text{-}OMe)\}\{Au(PPh_3\}_2]$

A solution of $[Au(PPh_3)Cl]$ (0.1 mmol, 49.7 mg) in CH_2Cl_2 (2 mL) was added dropwise to a solution of the complex $(HNEt_3)_2[\{UO_2(L^{2a})(\mu_2\text{-}OMe)\}_2]$ (79.7 mg, 0.05 mmol) in CH_2Cl_2 (2 mL). The reaction mixture was stirred for 1 h at room temperature, MeOH (2 mL) was added and the mixture was evaporated slowly at room temperature. The obtained yellow crystals were collected, washed with MeOH and dried under vacuum.

Yield: 85 % (96 mg)

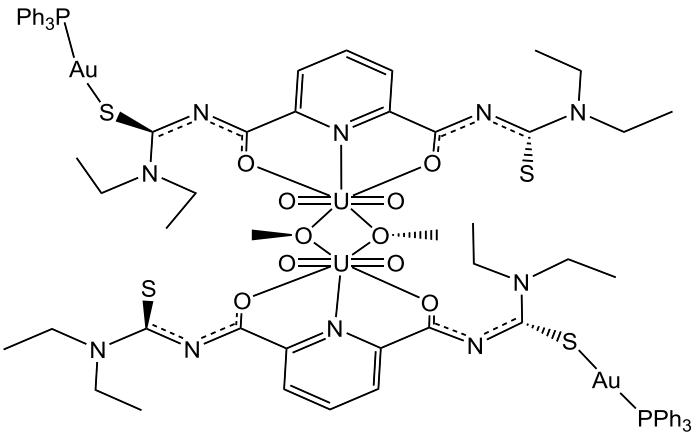

Elemental analysis: Calcd. for $C_{72}H_{82}Au_2N_{10}O_{10}P_2S_4U_2$: C, 37.47; H, 3.58; N, 6.07; S, 5.56 %. Found: C, 36.85; H, 3.51; N, 5.94; S, 5.53 %.

IR (KBr, cm^{-1}): 3445(m), 3051(w), 2974(m), 2932(m), 2872(w), 1587(vs), 1562(vs), 1431(vs), 1393(vs), 1358(w), 1310(m), 1281(m), 1248(s), 1202(m), 1146(m), 1121(m), 1099(s), 1072(w), 1020(m), 949(w), 914(vs), 845 (m), 756(vs), 692(vs), 635(m), 538(vs), 505(vs).

^{1}H NMR ($(CD_3)_2SO$, ppm): 8.23 (d, 4H, *J* = 7.6 Hz, py); 7.64 (t, 2H, *J* = 7.6 Hz, py); 7.41-7.07 (m, 30H, ph); 4.21–3.72 (m, 16H, CH_2); 3.09 (s, 3H, MeO); 1.67–1.21 (m, 24H, *J* = 7.5 Hz, CH_3).

^{13}C NMR ($(CD_3)_2SO$, ppm): 187.6 (C=S); 167.5 (C=O); 157.5, 139.8, 128.3 (py); 133.7, 131.9, 129.2, 118.3 (ph); 51.6 (OMe); 47.9, 45.8 (CH_2); 13.7, 12.1 (CH_3).

^{31}P NMR ($(CD_3)_2SO$, ppm): 36.1.

UV/Vis (CH_2Cl_2, nm): 230 (ε = 5.3 x 10^3 L $mol^{-1}cm^{-1}$), 251 (ε = 4.2 x 10^3 L $mol^{-1}cm^{-1}$), 266 (ε = 3.6 x 10^3 L $mol^{-1}cm^{-1}$), 305 (ε = 1.8 x 10^3 L $mol^{-1}cm^{-1}$), 366 (ε = 0.5 x 10^3 L $mol^{-1}cm^{-1}$).

3.4.3.2 $[Pb_2(UO_2)_3(L^{2a})_4(MeOH)_2(\mu_2\text{-}OMe)_2]$

A solution of $Pb(CH_3COO)_2{\cdot}2H_2O$ (32.6 mg, 0.1 mmol) in MeOH (1 mL) was added to a stirring solution of $UO_2(CH_3COO)_2{\cdot}2H_2O$ (42.4 mg, 0.1 mmol) in MeOH (2 mL). H_2L^{2a} (39.5 mg, 0.1 mmol) was added to the reaction mixture and the solution was stirred at room temperature for 1 h. The formed precipitate was filtered off, washed with MeOH and Et_2O and dried in vacuum. Single crystals for X-ray diffraction were obtained after slow evaporation of a CH_2Cl_2/MeOH 1:1 (v/v) solution at room temperature.

Yield: 70 % (56 mg)

Elemental analysis: Calcd. for: $C_{75}H_{118}N_{20}O_{21}S_8U_3Pb_2$ ($[Pb_2(UO_2)_3(L^{2a})_4$-$(MeOH)_2(\mu_2$-$OMe)_2] \cdot 3\,MeOH$): C, 29.15; H, 3.55; N, 9.31; S, 8.53 %. Found: C, 28.23; H, 3.67; N, 9.36; S, 8.52 %.

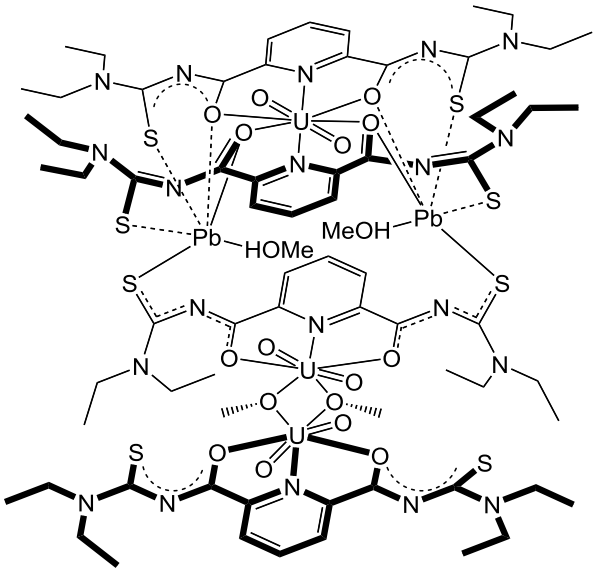

IR (KBr, cm^{-1}): 3443(m), 3084(w), 2974(m), 2934(m), 2874(w), 1597(vs), 1566(vs), 1514(vs), 1429(vs), 1385(vs), 1362(w), 1310(m), 1285(m), 1252(s), 1206(m), 1148(m), 1099(m), 1074(m), 1015(m), 955(w), 916(vs), 845 (m), 758 (s), 696(m), 638(w).

^1H NMR (CD_2Cl_2, ppm): 8.91–7.88 (m, 12H, py); 4.25–4.15 (m, 8H, CH_2); 3.40–3.53 (m, 32H, CH_2); 3.47 (m, 12H, MeOH); 1.59–0.93 (m, 48H, CH_3).

^{13}C NMR (CD_2Cl_2, ppm): 183.6, 181.2 (C=S); 162.6, 161.2 (C=O); 156.1, 154.2, 146.9, 141.1, 128.1, 127.2, 125.3 (py); 49.9, 49.7 (MeOH); 48.1, 47.9, 46.9, 46.2 (CH_2); 13.7, 13.5, 12.4, 12.2 (CH_3).

UV/Vis (CH_2Cl_2, nm): 231 ($\varepsilon = 7.6 \times 10^3$ L $mol^{-1}cm^{-1}$), 258 ($\varepsilon = 7.6 \times 10^3$ L $mol^{-1}cm^{-1}$), 296 ($\varepsilon = 5.5 \times 10^3$ L $mol^{-1}cm^{-1}$), 369 ($\varepsilon = 1.1 \times 10^3$ L $mol^{-1}cm^{-1}$).

3.4.3.3 $[M\{UO_2(L^2)(OAc)\}_2]$ (M = Cd, Zn, Ni, Co, Fe and Mn)

General procedure: A solution of $M(CH_3COO)_2 \cdot nH_2O$ (0.05 mmol) in MeOH (1 mL) was added to a stirred solution of $UO_2(CH_3COO)_2 \cdot 2H_2O$ (42.4 mg, 0.1 mmol) in MeOH (2 mL). H_2L^{2a} (39.5 mg, 0.1 mmol) or H_2L^{2b} (42.4 mg, 0.1 mmol) was added to the reaction mixture. The solution was stirred at room temperature for 1 h. The formed precipitate was filtered off, washed with MeOH and Et_2O and dried in vacuum. Single crystals for X-ray diffraction were obtained after slow evaporation of a CH_2Cl_2/MeOH 1:1 (v/v) solution at room temperature.

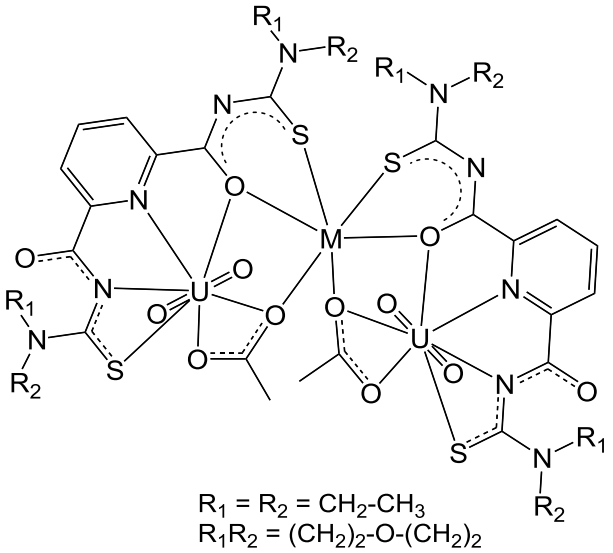

[Cd{$UO_2(L^{2a})(OAc)\}_2$]

Yield: 70 % (54 mg)

Elemental analysis: Calcd. for: $C_{40}H_{60}N_{10}O_{16}S_4U_2Cd$ ([Cd{$UO_2(L^{2a})(OAc)\}_2$] · 2 MeOH): C, 29.63; H, 3.73; N, 8.64; S, 7.91 %. Found: C, 29.99; H, 3.74; N, 8.76; S, 7.90 %.

IR (KBr, cm^{-1}): 3446(m), 3078(w), 2974(m), 2933(m), 2874(w), 1649(s), 1599(vs), 1566(vs), 1518(vs), 1431(vs), 1396(vs), 1360(w), 1310(m), 1287(m), 1254(s), 1204(m), 1149(m), 1123(m), 1076(m), 1013(m), 962(w), 916(vs), 847 (m), 758(s), 679(m), 654(w).

^{1}H NMR (CD_2Cl_2, ppm): 8.67 (d, 4H, *J* = 7.6 Hz, py); 8.41 (t, 2H, *J* = 7.6 Hz, py); 4.25–4.15 (m, 8H, CH_2); 3.98–3.88 (m, 8H, CH_2); 2.29 (s, 6H, CH_3_OAc); 1.30 (t, 12H, *J* = 7.4 Hz, CH_3), 1.09 (t, *J* = 7.4 Hz, 12H, CH_3).

^{13}C NMR (CD_2Cl_2, ppm): 189.3 (C=S); 182.7, 181.04 (C=O); 167.5, 162.6, (C=O); 156.2, 141.3, 127.7 (py); 47.5, 46.7 (CH_2); 25.9(CH_3_OAc); 13.6, 12.1 (CH_3).

+ESI MS (m/z): 1581.2603 (calcd. 1581.2596) $[M+Na]^+$, 1559.2914 (calcd. 1559.2776) $[M+H]^+$.

UV/Vis (CH_2Cl_2, nm): 231 (ε = 13.1 x 10^3 L $mol^{-1}cm^{-1}$), 305 (ε = 9.5 x 10^3 L $mol^{-1}cm^{-1}$), 369 (ε = 1.5 x 10^3 L $mol^{-1}cm^{-1}$).

[Zn{$UO_2(L^{2a})(OAc)\}_2$]

Yield: 72 % (54 mg)

Elemental analysis: Calcd. for: $C_{39}H_{54}Cl_2N_{10}O_{12}S_4U_2Zn$ ($[Zn\{UO_2(L^{2a})(OAc)\}_2] \cdot (CH_2Cl_2)$: C, 29.36; H, 3.41; N, 8.78; S, 8.04 %. Found: C, 29.39; H, 3.49; N, 8.79; S, 8.05 %.
IR (KBr, cm^{-1}): 3445(m), 3080(w), 2976(m), 2936(m), 2874(w), 1647(s), 1597(vs), 1562(vs), 1516(vs), 1431(vs), 1395(vs), 1358(w), 1312(m), 1287(m), 1256(s), 1204(m), 1149(m), 1123(m), 1078(m), 1013(m), 962(w), 916(vs), 847 (m), 758(s), 680(m), 659(w).
UV/Vis (CH_2Cl_2, nm): 234 ($\varepsilon = 11.1 \times 10^3$ L $mol^{-1}cm^{-1}$), 309 ($\varepsilon = 9.1 \times 10^3$ L $mol^{-1}cm^{-1}$), 369 ($\varepsilon = 1.6 \times 10^3$ L $mol^{-1}cm^{-1}$).

$[Ni\{UO_2(L^{2a})(OAc)\}_2]$

Yield: 70 % (53 mg)

Elemental analysis: Calcd. for: $C_{40}H_{58}Cl_2N_{11}O_{12}S_4U_2Ni$ ($[Ni\{UO_2(L^{2a})(OAc)\}_2] \cdot 2\ CH_2Cl_2 \cdot H_2O$): C, 28.70; H, 3.37; N, 8.37; S, 7.66 %. Found: C, 28.74; H, 3.37; N, 7.31; S, 7.65 %.
IR (KBr, cm^{-1}): 3445(m), 3084(w), 2976(m), 2936(m), 2874(w), 1653(s), 1597(vs), 1558(vs), 1518(vs), 1427(vs), 1385(vs), 1348(s), 1314(m), 1290(m), 1256(s), 1206(m), 1149(m), 1082(m), 1013(m), 955(m), 922(vs), 868 (m), 843(m), 762(s), 685(m), 662(w).
UV/Vis (CH_2Cl_2, nm): 229 ($\varepsilon = 13.1 \times 10^3$ L $mol^{-1}cm^{-1}$), 289 ($\varepsilon = 10.4 \times 10^3$ L $mol^{-1}cm^{-1}$), 369 ($\varepsilon = 1.9 \times 10^3$ L $mol^{-1}cm^{-1}$).

$[Mn\{UO_2(L^{2a})(OAc)\}_2]$

Yield: 87 % (62 mg)

Elemental analysis: Calcd. for: $C_{40}H_{56}Cl_2N_{10}O_{12}S_4U_2Mn$ ($[Mn\{UO_2(L^{2a})(OAc)\}_2] \cdot 2\ CH_2Cl_2$): C, 28.70; H, 3.37; N, 8.37; S, 7.66 %. Found: C, 28.69; H, 3.37; N, 8.34; S, 7.62 %.
IR (KBr, cm^{-1}): 3445(w), 3075(w), 2974(m), 2936(m), 2874(w), 1649(s), 1600(vs), 1558(vs), 1518(vs), 1423(vs), 1387(vs), 1348(s), 1314(w), 1292(m), 1258(s), 1206(m), 1149(m), 1082(m), 1016(m), 956(m), 924(vs), 868 (m), 843(m), 760(s), 685(m), 662(w).
UV/Vis (CH_2Cl_2, nm): 231 ($\varepsilon = 10.3 \times 10^3$ L $mol^{-1}cm^{-1}$), 289 ($\varepsilon = 8.5 \times 10^3$ L $mol^{-1}cm^{-1}$), 369 ($\varepsilon = 1.7 \times 10^3$ L $mol^{-1}cm^{-1}$).

$[Fe\{UO_2(L^{2a})(OAc)\}_2]$

Yield 56 % (42 mg)

Elemental analysis: Calcd. for: $C_{38}H_{58}N_{10}O_{15}S_4U_2Fe$ ($[Fe\{UO_2(L^{2a})(OAc)\}_2] \cdot 3\ H_2O$): C, 29.35; H, 3.76; N, 9.01; S, 8.25 %. Found: C, 29.69; H, 3.47; N, 8.91; S, 7.98 %.

IR (KBr, cm^{-1}): 3429(m), 3076(w), 2976(m), 2936(m), 2874(w), 1647(s), 1599(vs), 1562(vs), 1518(vs), 1427(vs), 1385(vs), 1348(s), 1314(w), 1290(m), 1258(s), 1206(m), 1149(m), 1086(m), 1016(m), 955(m), 924(vs), 866 (m), 843(m), 762(s), 685(m), 662(w).

^1H NMR (CD_2Cl_2, ppm): 8.64 (m, 4H, py); 8.34 (m, 2H, py); 4.19-4.07 (m, 8H, CH_2); 3.97-3.85 (m, 8H, CH_2); 2.54 (s, 6H, CH_3_OAc); 1.40–1.32 (t, 12H, CH_3), 1.26–1.22 (m, 12H, CH_3).

^{13}C NMR (CD_2Cl_2, ppm): 189.7 (C=S); 183.7, 174.5 (C=O); 168.6, 164.9 (C=O); 150.4, 140.6, 128.2 (py); 47.7, 46.9 (CH_2); 29.4 (CH_3_OAc); 13.8, 12.6 (CH_3).

UV/Vis (CH_2Cl_2, nm): 229 ($\varepsilon = 11.2 \times 10^3$ L $mol^{-1}cm^{-1}$), 288 ($\varepsilon = 8.9 \times 10^3$ L $mol^{-1}cm^{-1}$), 370 ($\varepsilon = 1.8 \times 10^3$ L $mol^{-1}cm^{-1}$).

$[Co\{UO_2(L^{2a})(OAc)\}_2]$

Yield: 78 % (59 mg)

Elemental analysis: Calcd. for: $C_{40}H_{56}Cl_4N_{10}O_{12}S_4U_2Co$ ($[Co\{UO_2(L^{2a})(OAc)\}_2] \cdot 2\ CH_2Cl_2$): C, 28.70; H, 3.37; N, 8.37; S, 7.60 %. Found: C, 28.85; H, 3.53; N, 8.21; S, 7.53 %.

IR (KBr, cm^{-1}): 3443(m), 3078(w), 2978(m), 2936(m), 2874(w), 1651(s), 1595(vs), 1560(vs), 1516(vs), 1427(vs), 1387(vs), 1346(s), 1314(w), 1290(m), 1258(s), 1206(m), 1149(m), 1086(m), 1015(m), 955(m), 922(vs), 866 (m), 843(m), 760(s), 685(m), 662(w).

UV/Vis (CH_2Cl_2, nm): 230 ($\varepsilon = 12.3 \times 10^3$ L $mol^{-1}cm^{-1}$), 292 ($\varepsilon = 10.5 \times 10^3$ L $mol^{-1}cm^{-1}$), 369 ($\varepsilon = 1.9 \times 10^3$ L $mol^{-1}cm^{-1}$).

$[Cd\{UO_2(L^{2b})(OAc)\}_2]$

Yield: 72 % (58 mg)

Elemental analysis: Calcd. for $C_{40}H_{48}Cl_2N_{10}O_{16}S_4U_2Cd$ ($[Cd\{UO_2(L^{2b})(OAc)\}_2] \cdot 2\ CH_2Cl_2$): C, 29.29; H, 2.75; N, 8.68; S, 7.95 %. Found: C, 29.33; H, 2.80; N, 8.66; S, 8.00 %.

IR (KBr, cm^{-1}): 3441(s), 2964(w), 2922(w), 2857(w), 1647(s), 1595(s), 1562(vs), 1506(vs), 1429(s), 1394(vs), 1342(m), 1292(m), 1233(m), 1113(m), 1069(w), 1030(m), 951(m), 920(vs), 843 (m), 762(m), 685(m), 606(w).

^1H NMR (CD_2Cl_2, ppm): 8.82 (d, J = 7,6 Hz, 4H, py); 8.46 (t, J = 7.6 Hz, 2H, py); 4.40–3.50 (m, 32H, CH_2); 2.32 (s, 6H, CH_3_OAc).

^{13}C NMR (CD_2Cl_2, ppm): 189.5 (*C*=S); 182.3, 169.1, 164.1, (*C*=O); 156.9, 142.0, 128.5 (py); 67.2 (*C*H_2); 52.7 (*C*H_2); 26.4 (*C*H_3_OAc).

+ESI MS (m/z): 1653.1428 (calcd. 1653.1500) $[M+K]^+$; 1637.1689 (calcd. 1637.1761) $[M+Na]^+$

UV/Vis (CH_2Cl_2, nm): 230 ($\varepsilon = 12.4 \times 10^3$ L mol^{-1}cm^{-1}), 300 ($\varepsilon = 10.1 \times 10^3$ L mol^{-1}cm^{-1}), 369 ($\varepsilon = 2.2 \times 10^3$ L mol^{-1}cm^{-1}).

[Zn{UO_2(L^{2b})(OAc)}$_2$]

Yield: 74 % (58 mg)

Elemental analysis: Calcd. for $C_{39}H_{46}Cl_2N_{10}O_{16}S_4U_2Zn$ ([Zn{UO_2(L^{2b})(OAc)}$_2$] · CH_2Cl_2): C, 29.60; H, 3.03; N, 8.42; S, 7.71 %. Found: C, 29.65; H, 3.05; N, 8.42; S, 7.73 %.

IR (KBr, cm^{-1}): 3443(s), 2967(w), 2924(w), 2858(w), 1647(s), 1597(s), 1560(vs), 1506(vs), 1429(s), 1394(vs), 1344(m), 1292(m), 1234(m), 1115(m), 1069(w), 1032(m), 953(m), 922(vs), 843 (m), 764(m), 687(m), 607(w).

+ESI MS (m/z) = 1603.1741 (calcd. 1603.1758) $[M+K]^+$; 1587.2003 (calcd. 1587.2019) $[M+Na]^+$.

UV/Vis (CH_2Cl_2, nm): 230 ($\varepsilon = 12.8 \times 10^3$ L mol^{-1}cm^{-1}), 301 ($\varepsilon = 11.5 \times 10^3$ L mol^{-1}cm^{-1}), 369 ($\varepsilon = 2.5 \times 10^3$ L mol^{-1}cm^{-1}).

[Ni{UO_2(L^{2b})(OAc)}$_2$]

Yield: 60 % (47 mg)

Elemental analysis: Calcd. for $C_{39}H_{46}Cl_2N_{10}O_{16}S_4U_2Ni$ ([Ni{UO_2(L^{2b})(OAc)}$_2$] · CH_2Cl_2): C, 28.96; H, 3.01; N, 8.04; S, 7.36 %. Found: C, 28.99; H, 2.99; N, 8.03; S, 7.35 %.

IR (KBr, cm^{-1}): 3445(s), 2963(w), 2922(w), 2856(w), 1647(s), 1601(s), 1560(s), 1504(vs), 1429(s), 1387(vs), 1341(m), 1290(m), 1269(w), 1232(m), 1113(m), 1032(m), 955(m), 924(vs), 845 (m), 764(m), 687(w), 607(m).

UV/Vis (CH_2Cl_2, nm): 231 ($\varepsilon = 12.8 \times 10^3$ L mol^{-1}cm^{-1}), 298 ($\varepsilon = 11.7 \times 10^3$ L mol^{-1}cm^{-1}), 369 ($\varepsilon = 2.6 \times 10^3$ L mol^{-1}cm^{-1}), 398 ($\varepsilon = 1.9 \times 10^3$ L mol^{-1}cm^{-1}).

[Mn{UO_2(L^{2b})(OAc)}$_2$]

Yield: 80 % (62 mg)

Elemental analysis: Calcd. for $C_{40}H_{48}N_{10}O_{18}S_4U_2Mn$ ([Mn{UO_2(L^{2b})(OAc)}$_2$] · 2 CH_3OH): C, 30.91; H, 3.46; N, 8.58; S, 7.86 %. Found: C, 30.92; H, 3.45; N, 8.56; S, 7.82 %.

IR (KBr, cm^{-1}): IR (KBr, cm^{-1}): 3429(m), 2965(w), 2922(w), 2857(w), 1647(s), 1598(s), 1564(vs), 1506(s), 1429(s), 1391(vs), 1344(m), 1288(m), 1234(m), 1115(m), 1069(w), 1032(m), 953(m), 922(vs), 843 (m), 764(m), 685(m), 607(w).

UV/Vis (CH_2Cl_2, nm): 233 (ε = 12.1 x 10^3 L $mol^{-1}cm^{-1}$), 293 (ε = 11.4 x 10^3 L $mol^{-1}cm^{-1}$), 369 (ε = 2.3 x 10^3 L $mol^{-1}cm^{-1}$), 399 (ε = 1.4 x 10^3 L $mol^{-1}cm^{-1}$).

[Fe{UO_2(L^{2b})(OAc)}$_2$]

Yield: 53 % (42 mg)

Elemental analysis: Calcd. for $C_{38}H_{44}N_{10}O_{16}S_4U_2Fe$: C, 29.31; H, 2.85; N, 9.00; S, 8.24 %. Found: C, 29.25; H, 2.90; N, 9.04; S, 8.24 %.

IR (KBr, cm^{-1}): 3433(vs), 2959(w), 2920(w), 2855(w), 1639(s), 1589(s), 1555(vs), 1506(s), 1431(vs), 1391(vs), 1346(m), 1285(m), 1227(m), 1111(s), 1067(w), 1026(m), 951(m), 916(vs), 841 (m), 758(m), 675(m), 637(w).

^{1}H NMR (CD_2Cl_2, ppm): 8.72 (m, 4H, py); 8.38 (m, 2H, py); 4.35–3.70 (32H, CH_2); 2.59 (s, 6H, CH_3_OAc);

^{13}C NMR (CD_2Cl_2, ppm): 189.0 (*C*=S); 182.9, 168.4, 163.3 (*C*=O); 156.1, 141.5, 128.1 (py); 66.5 (*C*H_2); 49.7 (*C*H_2); 26.6 (*C*H_3_OAc).

UV/Vis (CH_2Cl_2, nm): 231 (ε = 12.2 x 10^3 L $mol^{-1}cm^{-1}$), 284 (ε = 10.8 x 10^3 L $mol^{-1}cm^{-1}$), 368 (ε = 2.2 x 10^3 L $mol^{-1}cm^{-1}$).

[Co{UO_2(L^{2b})(OAc)}$_2$]

Yield: 76 % (59 mg)

Elemental analysis: Calcd. for $C_{40}H_{50}Cl_2N_{10}O_{17}S_4U_2Co$ ([Co{UO_2(L^{2b})(OAc)}$_2$] · CH_2Cl_2 · CH_3OH): C, 29.87; H, 3.22; N, 8.29; S, 7.29 %. Found: C, 29.86; H, 3.20; N, 8.29; S, 7.28 %.

IR (KBr, cm^{-1}): 3427(vs), 2966(w), 2922(w), 2858(w), 1647(s), 1600(s), 1562(s), 1504(vs), 1431(s), 1388(vs), 1342(m), 1292(m), 1232(m), 1113(m), 1032(m), 953(m), 924(vs), 844 (m), 764(m), 683(w), 607(m).

UV/Vis (CH_2Cl_2, nm): 235 (ε = 12.2 x 10^3 L $mol^{-1}cm^{-1}$), 298 (ε = 12.3 x 10^3 L $mol^{-1}cm^{-1}$), 369 (ε = 2.5 x 10^3 L $mol^{-1}cm^{-1}$), 399 (ε = 1.5 x 10^3 L $mol^{-1}cm^{-1}$).

3.4.4 Complexes with Uranium(IV) and Thorium (IV)

3.4.4.1 $[Au_2\{U(L^{2a})_3\}]$

The reaction was performed in an MBraun MB 200B glove box under an argon atmosphere at room temperature. H_2L^{2a} (39.5 mg, 0.1 mmol) was added to a stirred solution of $[U_2I_6(1,4\text{-dioxane})_3]$ (75.2 mg, 0.05 mmol) and [Au(tht)Cl] (32 mg, 0.1 mmol) in THF (3 mL) was added. After 20 min, 3 drops of NEt_3 were added and the reaction mixture was stirred for 1 h. The color of the solution turned brown and a brownish precipitate was formed. The solid was filtered off and washed with THF. Filtrates were collected and overlayered with diethyl ether. Single crystals for X-ray diffraction were obtained from the THF/Et_2O solution.

Yield: 40 % (36 mg)

Elemental analysis: Calcd. for $C_{51}H_{69}N_{15}O_6S_6U \cdot (C_4H_8O)$: C, 35.05; H, 4.12; N, 11.15; S, 10.21 %. Found: C, 34.96; H, 4.22; N, 11.19; S, 10.22 %.

IR (KBr, cm^{-1}): 2970(s), 2935(s), 2872(w), 2764(m), 2681(m), 2479(w), 1582(vs), 1560(vs), 1466(s), 1427(s), 1398(s), 1309(w), 1249(m), 1165(m), 1074(m), 1034(m), 916(s), 847 (w), 758(m).

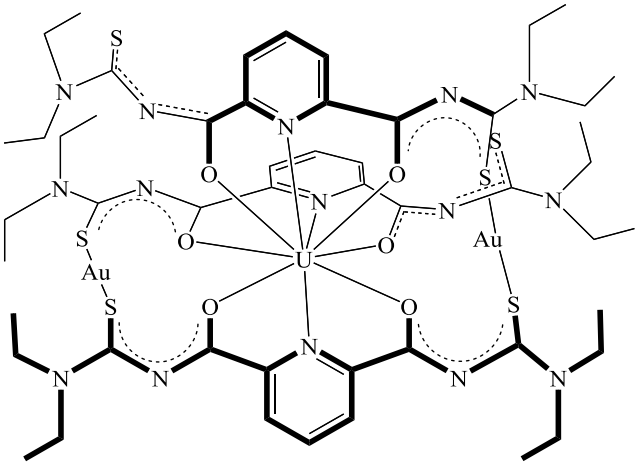

3.4.4.2 $[Th(L^{2a*})_2(H_2O)_4]$

H_2L^{2a} (39.5 mg, 0.1 mmol) was dissolved in MeOH (3 mL) and added to a stirred solution of $Th(NO_3)_2 \cdot 4\ H_2O$ (50.2 mg, 0.1 mmol) in MeOH (3 mL). The reaction mixture was stirred for 1 h. The obtained colorless precipitate was filtered off, washed with MeOH and dried under vacuum. Single crystals for X-ray diffraction were obtained after slow evaporation of a CH_2Cl_2/MeOH 1:1 (v/v) solution at room temperature.

Yield: 30 % (19 mg)

Elemental analysis: Calcd. for $C_{14}H_{14}N_2O_{12}Th$: C, 26.51; H, 2.22; N, 4.42 %. Found: C, 25.86; H, 2.36; N, 4.27 %.

IR (KBr, cm^{-1}): 3449(s), 3093(w), 2974(m), 2926(w), 2872(w), 1635(vs), 1589(vs), 1477(w), 1427(s), 1377(vs), 1271(m), 1186(m), 1078 (s), 1018(m), 921(m), 860(m), 773(s), 729(s), 690(s), 586 (m).

UV/Vis (CH_2Cl_2, nm): 231 (ε = 4.2 x 10^3 $M^{-1}cm^{-1}$), 283 (ε = 1.8 x 10^3 $M^{-1}cm^{-1}$), 335 (ε = 0.3 x 10^3 $M^{-1}cm^{-1}$), 365 (ε = 0.1 x 10^3 $M^{-1}cm^{-1}$).

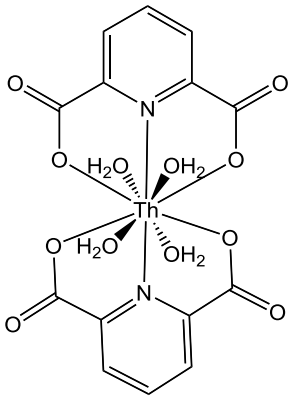

3.4.4.3 $(NH_4)_2[\{Th(L^{2a})\}_3]$

The reaction was performed in an MBraun MB 200B glove box under an argon atmosphere at room temperature. H_2L^{2a} (39.5 mg, 0.1 mmol) was added to a stirred solution of $[ThCl_4(DME)_2]$ (20.3 mg, 0.05 mmol) in dry MeOH (3 mL). After 20 min, 3 drops of NEt_3 were added and the reaction mixture was stirred for 1 h. $NH_4(PF_6)$ (8 mg, 0.05 mmol) was added to the reaction mixture. The color of the solution turned to yellow-green. After 1 h, the mixture was filtered and overlayered with Et_2O. Single crystals for X-ray diffraction were obtained from the THF/Et_2O solution.

Yield: 60 % (44.7 mg)

IR (KBr, cm^{-1}): 3206(w), 2975(m), 2928(m), 2607(m), 2491(w), 1590(vs), 1568(vs), 1496(s), 1483(s), 1423(m), 1369(vs), 1306(s), 1280(m), 1241(s), 1067(m), 1011(m), 946(m), 915 (s), 835(vs), 764(s), 699(m).

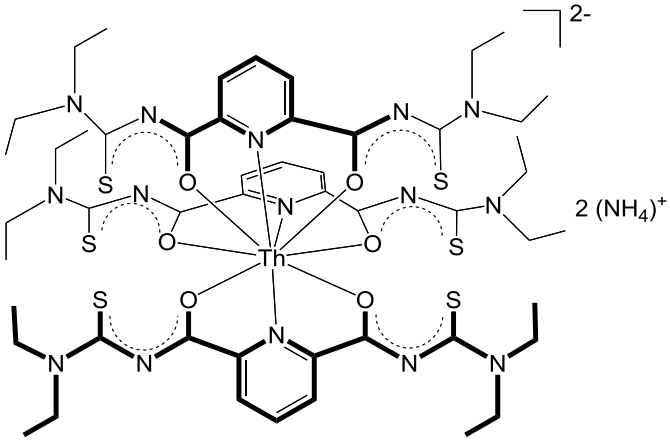

3.4.4.4 $[Ni\{Th(L^3)_2(OAc)_2(MeOH)\}]$

H_2L^{2a} (39.5 mg, 0.1 mmol) was added to a stirred solution of $Th(NO_3)_4 \cdot 6\,H_2O$ (25 mg, 0.05 mmol) in MeOH (2 mL). After 15 min, 3 drops of NEt_3 were added and the reaction mixture was stirred at room temperature for 1 h. Then, a solution of $Ni(CH_3COO)_2 \cdot 4\,H_2O$ (25 mg, 0.1 mmol) in MeOH (1 mL) was added. Within a few minutes, a brownish precipitate was formed. It was filtered off, washed with MeOH and dried in vacuum. Single crystals for X-

ray diffraction were obtained by slow evaporation of a CH_2Cl_2/MeOH 1:1 (v/v) solution at room temperature.

Yield: 38 % (53.2 mg)

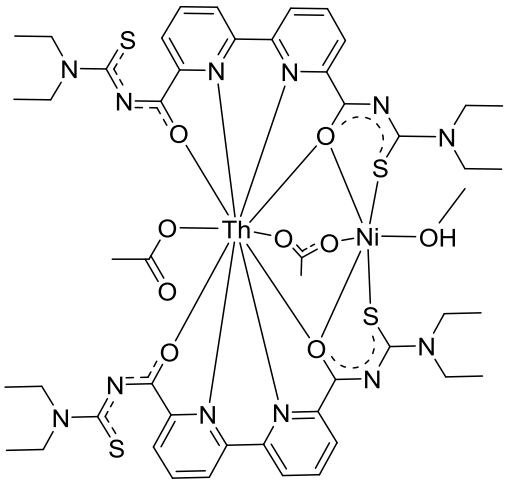

Elemental analysis: Calcd. for $C_{50}H_{68}Cl_2N_{12}O_{11}S_4ThNi$ ($[Ni\{Th(L^3)_2(OAc)_2\text{-}(MeOH)\}] \cdot CH_2Cl_2 \cdot 2\ H_2O$): C, 42.61; H, 4.45; N, 12.17; S, 9.29 %. Found: C, 42.31; H, 4.43; N, 12.09; S, 9.18 %.

IR (KBr, cm^{-1}): 3443(s), 3075(w), 2970(m), 2932(m), 2872(w), 1591(vs), 1568(vs), 1516(m), 1460(m), 1422(s), 1383(vs), 1315(m), 1278(m), 1248(m), 1204(w), 1090(m), 1010(w), 893(m), 847 (s), 818(s), 760(m), 641(m), 509(w).

UV/Vis (CH_2Cl_2, nm): 232 ($\varepsilon = 17.2 \times 10^3$ L $mol^{-1}cm^{-1}$), 258 ($\varepsilon = 15.2 \times 10^3$ L $mol^{-1}cm^{-1}$), 319 ($\varepsilon = 9.3 \times 10^3$ L $mol^{-1}cm^{-1}$), 369 ($\varepsilon = 2.7 \times 10^3$ L $mol^{-1}cm^{-1}$).

3.5 Stability and hydrolysis studies

Stability tests: The complexes $[UO_2(L^{2b})(H_2O)]$, $[UO_2(L^{2a})(MeOH)]$, $[UO_2(L^3)]$, and $(HNEt_3)_2[\{UO_2(L^1)\}_4(OAc)_2]$ were used for the two-phase extraction experiments. They were performed at room temperature in micro centrifuge tubes (5 mL) with a phase ratio $V_{(org)}$:$V_{(aq)}$ of 2 mL : 2 mL. The pH of the aqueous phase was adjusted with nitric acid and a constant ionic strength was maintained by the addition of $(NEt_4)NO_3$ (0.5 mM). The organic phase (0.4 mM) was prepared by dissolving the complexes in CH_2Cl_2. The samples were shaken for 30 min. The aqueous phase was separated from the organic one and the depletion of the uranyl ions was monitored in suitable aliquots (usually 200 μL), measuring the concentration of the uranyl ions radiometrically using a liquid scintillation counter. The remaining organic phase was analyzed using UV/Vis spectroscopy.

Hydrolysis study: A solution of H_2L^{2a} in CH_2Cl_2 (1 mL, 0.01M) was added to an equivalent amounts of water at pH 1-14. The mixtures were shaken for 120 s at room temperature and the solutions were left for 24 h. Then, the organic phases were separated from the aqueous ones and the hydrolysis of H_2L^{2a} was monitored using UV/Vis spectroscopy.

4 Summary

This thesis describes the synthesis and structural characterization of uranium and thorium compounds derived from aroylbis(*N*,*N*-dialkylthioureas). Four bifunctional aroylbis(*N*,*N*-dialkylthioureas), (H_2L^1, H_2L^{2a}, H_2L^{2b} and H_2L^3) were synthesized and fully characterized. They were selected with the expectation that substitution on the "spacers" or the "side chains" will influence the coordination modes of the ligand and, thus, lead to different actinide complexes.

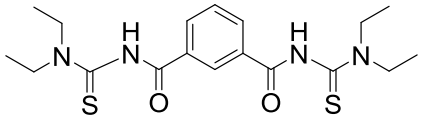

H_2L^1

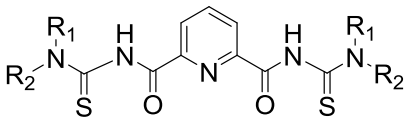

H_2L^{2a}: $R_1 = R_2 = CH_2\text{-}CH_3$
H_2L^{2b}: $R_1R_2 = (CH_2)_2\text{-}O\text{-}(CH_2)_2$

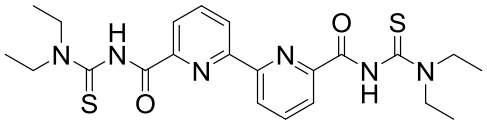

H_2L^3

Reactions of H_2L^1 with uranyl ions formed tetrameric compounds with the composition $(NBu_4)_2[\{UO_2(L^1)\}_4(OAc)_2]$ or $(NBu_4)_2[\{UO_2(L^1)\}_4(OEt)_2(HOEt)_2]$. The deprotonated ligand $\{L^1\}^{2-}$ coordinates bidentate with *S* and *O* and the framework of the complex is stabilized in the solid state by weak interactions such as π-π and cation-π interactions.

Reactions of uranyl ions with H_2L^{2a} and H_2L^{2b} show a strong pH dependence. This is reflected by the structures of the obtained complexes. Neutral complexes of the type $[UO_2(L^2)(solv)]$ are obtained after the addition of two drops of NEt_3 to the reaction mixtures containing uranyl salts and H_2L^2. The ligands coordinate pentadentate via the donor atoms *S*,*N*,*N*,*N*,*S*. The hexagonal-bipyramidal coordination environment of the uranium atom is completed by a solvent molecule, which can readily be exchanged by others. The uranyl complexes with H_2L^2 in aqueous or alcoholic solutions undergo hydrolysis with increasing pH. The selective isolation of the oligomeric uranyl complexes $[\{UO_2(L^2)(\mu_2\text{-}OMe)\}_2]^{2-}$, $[(UO_2)_3(L^{2a**})_2(\mu_2\text{-}X)(\mu_3\text{-}O)]^-$, (X = OH, OMe, OEt)) or $[\{(UO_2)_2(L^{2a})(\mu_2\text{-}OAc)(\mu_3\text{-}O)\}_2]^{2-}$, from such reaction mixtures succeeds by the addition of defined amount of a supporting base (Scheme 4.1). Another factor for the isolation of defined products from such complex solutions, which contain various compounds

in complicated equilibria, is the solubility of the individual compounds. This can partially be controlled for the ionic products by the addition of suitable counter ions.

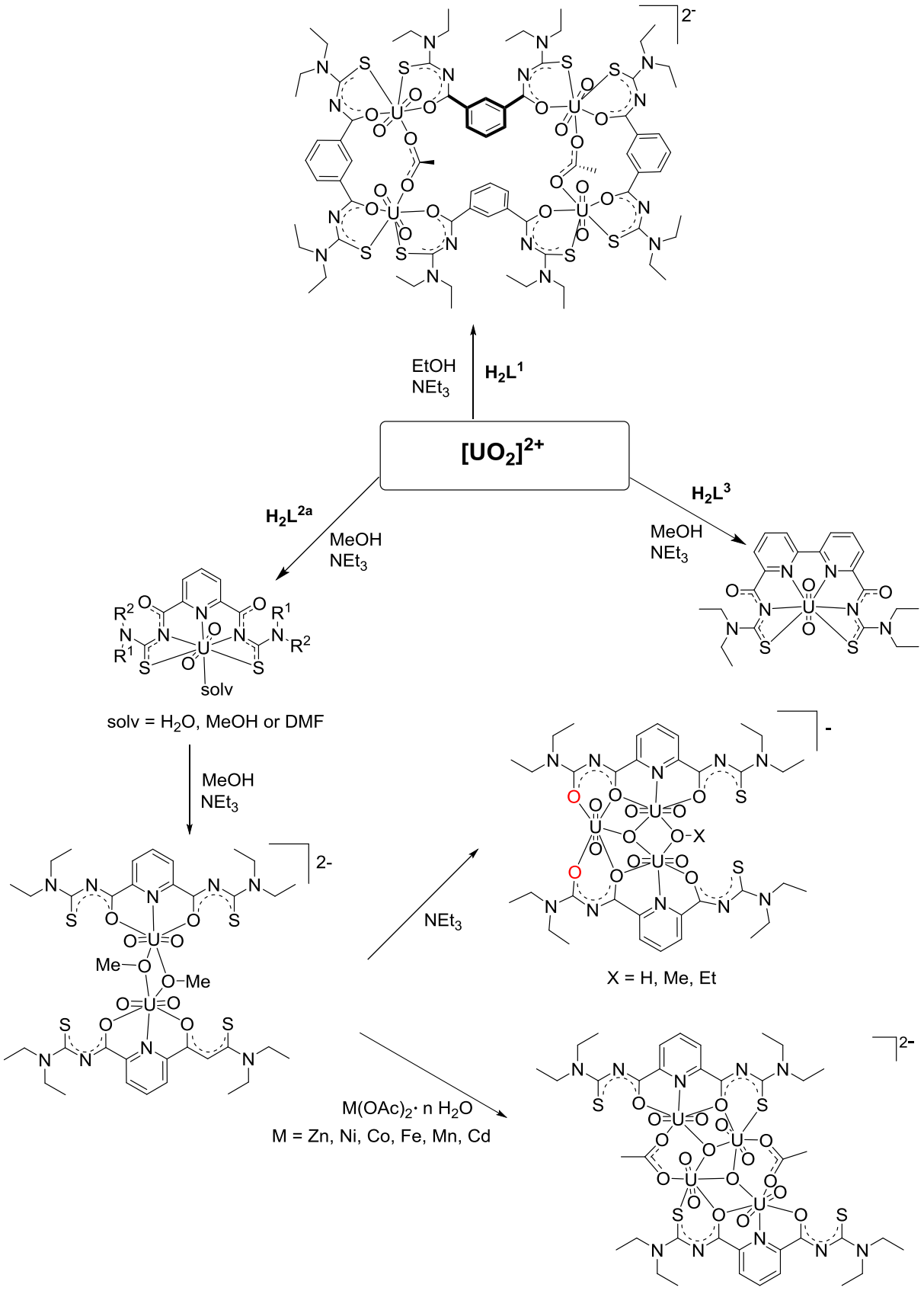

Scheme 4.1: Syntheses of the uranyl complexes derived from H_2L^1, H_2L^{2a} and H_2L^3.

The novel ligand H_2L^3 forms a stable, neutral complex, $[UO_2(L^3)]$, with a hexadentate coordination of the ligand via a *S,N,N,N,N,S* donor set. Stability tests in nitric acid demonstrate, that $[UO_2(L^3)]$ is the most stable complex under such conditions.

In the dimeric complexes of Scheme 4.1, the metal ions are coordinated by the "hard" donor atoms *O,N,O* of the central ligand unit. Thus, the lateral sulfur donor atoms do not participate in the coordination of the uranium atoms. For this reason, the four sulfur atoms can adopt different orientations in the complexes and offer the opportunity for the coordination of additional guest metal ions. Since sulfur is a "soft" donor atom, thiophilic metal ions such as Au(I) and Pb(II) and soft transition metal ions were considered for the design of bimetallic complexes with uranium. Various oligometallic complexes with uranyl units were prepared. (Scheme 4.2).

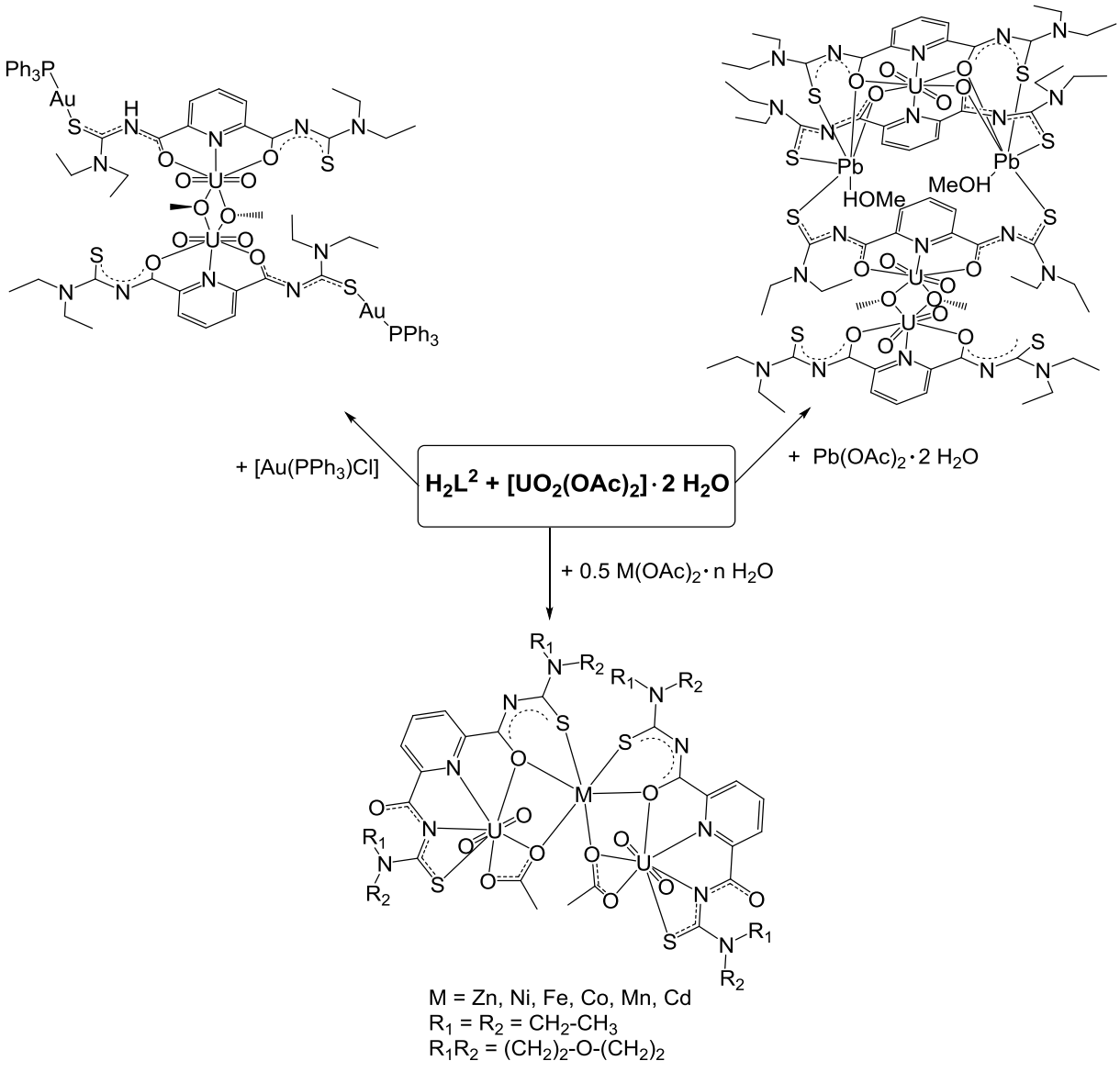

Scheme 4.2: Syntheses of the bimetallic complexes of uranium.

A thorium complex with H_2L^{2a} was obtained from a reaction with $[ThCl_4(DME)_2]$ under absolutely dry conditions. The ammonium counter ions interact via hydrogen bonds with the side chains of the ligands. A similar complex was obtained from the reaction of $[U_2I_6(1,4\text{-dioxane})_3]$ with H_2L^{2a} and [AuCl(tht)]. The heterometallic complex $[Au_2\{U(L^{2a})_3\}]$ was obtained after the oxidation of U^{3+} to U^{4+}. A heterometallic complex of the composition $[Ni\{Th(L^3)_2(OAc)_2(MeOH)\}]$ was obtained from the reaction of $Th(NO_3)_2 \cdot 4\,H_2O$ with $Ni(OAc)_2 \cdot 4\,H_2O$ and H_2L^3. A summary of the reactions and products is given in Scheme 4.3.

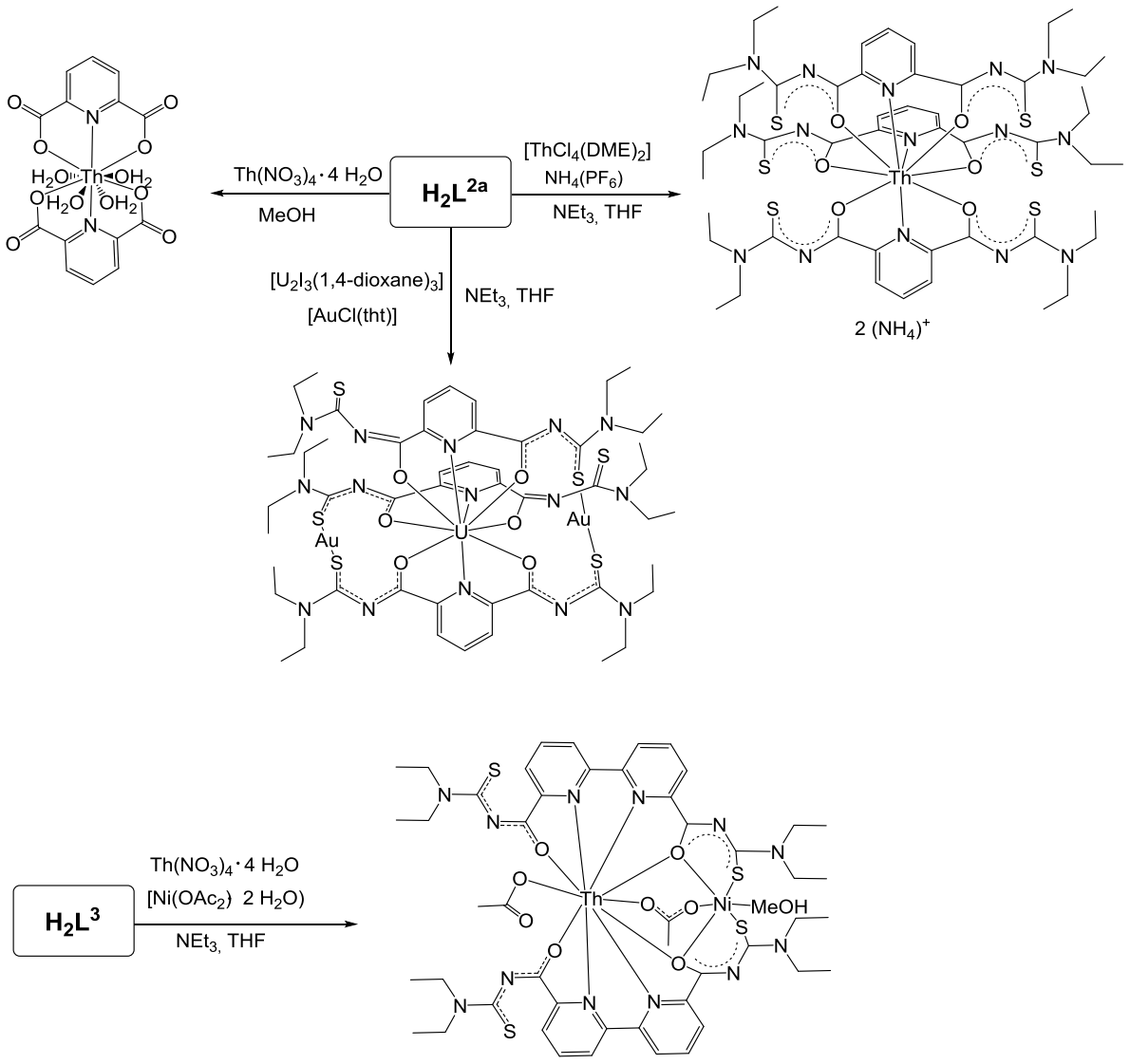

Scheme 4.3: Complexes of Th^{4+} and U^{4+} derived from H_2L^{2a} and H_2L^3.

.

5 Zusammenfassung

Diese Dissertationsarbeit beschreibt die Synthese und strukturelle Charakterisierung von Uran- und Thoriumverbindungen mit Aroylbis(*N*,*N*-dialkylthioharnstoffen). Vier bifunktionelle Aroylbis(*N*,*N*-dialkylthioharnstoffe) wurden synthetisiert und vollständig charakterisiert. Die Liganden wurden mit der Erwartung ausgewählt, dass die Substitution an den "Spacern" oder den "Seitenketten" die Koordinationsmodi des Liganden beeinflussen und somit zur Bildung von verschiedenen Actinoidkomplexen führt.

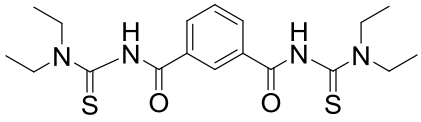

H_2L^1

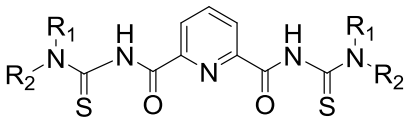

H_2L^{2a}: $R_1 = R_2 = CH_2\text{-}CH_3$
H_2L^{2b}: $R_1R_2 = (CH_2)_2\text{-}O\text{-}(CH_2)_2$

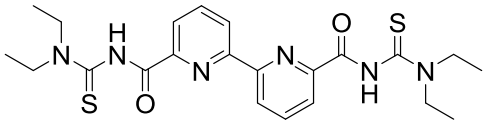

H_2L^3

Reaktionen von H_2L^1 mit Uranylionen führen zur Bildung von vierkernigen Komplexen mit den molekularen Zusammensetzungen $(NBu_4)_2[\{UO_2(L^1)\}_4(OAc)_2]$ oder $(NBu_4)_2[\{UO_2(L^1)\}_4(OEt)_2(HOEt)_2]$. Der deprotonierte Ligand $\{L^1\}^{2-}$ koordiniert zweizähnig mit den *S*- und *O*-Donoratomen und die Festkörperstruktur ist durch schwache Wechselwirkungen wie π-π- und Kation-π-Wechselwirkungen stabilisiert.

Reaktionen von Uranylionen mit H_2L^{2a} oder H_2L^{2b} zeigen eine starke pH-Abhängigkeit. Das spiegelt sich in den Strukturen der erhaltenen Komplexe wider. Neutrale Komplexe der Art $[UO_2(L^2)(solv)]$ werden nach der Zugabe von zwei Tropfen NEt_3 zu den Reaktionsgemischen aus Uranylsalzen und H_2L^2 gewonnen. Die Liganden koordinieren fünfzähnig mit den Donoratomen *S,N,N,N,S.* Die hexagonal-bipyramidale Koordinationssphäre des Uranatoms wird durch die Koordination eines Lösungsmittelmoleküls komplettiert. Letzteres kann leicht durch andere koordinierende Lösungsmittel ausgetauscht werden. Die neutralen Uranylkomplexe mit H_2L^2 aggregieren in wässrigen oder alkoholischen Lösungen mit steigendem pH-Wert. Die selektive Kristallisation der mehrkernigen Uranylkomplexe $[\{UO_2(L^2)(\mu_2\text{-}OMe)\}_2]^{2-}$, $[(UO_2)_3(L^{2a**})_2(\mu_2\text{-}X)(\mu_3\text{-}O)]^-$, (X = OH, OMe, OEt)) oder

$[\{(UO_2)_2(L^{2a})(\mu_2\text{-OAc})(\mu_3\text{-O})\}_2]^{2-}$ gelingt aus solchen Reaktionsgemischen, durch die Zugabe definierter Menge einer Hilfsbase (Scheme 5.1).

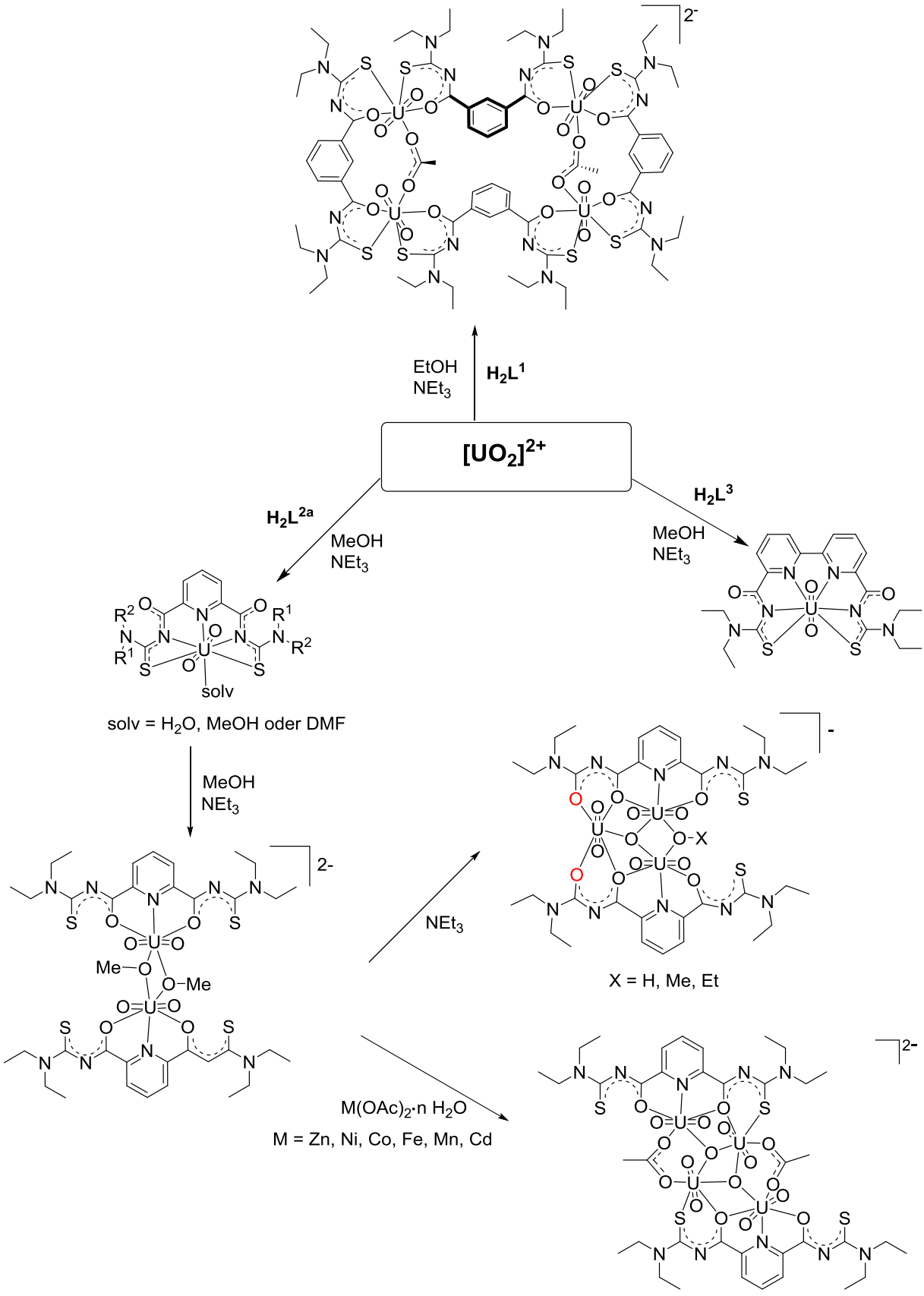

Scheme 5.1: Synthesen von Uranylkomplexen mit H_2L^1, H_2L^{2a} und H_2L^3.

Ein anderer Faktor für die Isolierung definierter Produkte aus solchen Komplexlösungen, die verschiedene Verbindungen in komplizierten Gleichgewichten enthalten, ist die Löslichkeit der einzelnen Verbindungen. Dies kann teilweise für die ionischen Produkte durch die Zugabe von geeigneten Gegenionen kontrolliert werden. Der neue Ligand H_2L^3 bildet einen stabilen, neutralen Komplex, $[UO_2(L^3)]$ mit einer sechszähnigen Koordination des Liganden mit dem *S,N,N,N,N,S* Donorsatz. Stabilitätsstudien in HNO_3 zeigen, dass $[UO_2(L^3)]$ unter solchen Bedingungen der stabilste Komplex ist.

In den mehrkernigen Uranylkomplexen in Schema 5.1 sind die Metallionen durch die "harten" Donoratome *O,N,O* der zentralen Ligandeinheit koordiniert. Somit sind die lateralen Schwefel-Donoratome nicht an der Koordination der Uranatome beteiligt. Aus diesem Grund können die vier Schwefelatome unterschiedliche Orientierungen in den Komplexstrukturen annehmen und bieten die Möglichkeit zur Koordination zusätzlicher Gast-Metallionen. Da Schwefel ein "weiches" Donoratom ist, wurden thiophile Metallionen wie Au(I) und Pb(II) und weiche Übergangsmetallionen für die Herstellung solcher heterometallischen Uranylkomplexen in Betracht gezogen. Verschiedene oligometallische Komplexe mit Uranyleinheiten wurden hergestellt (Scheme 5.2).

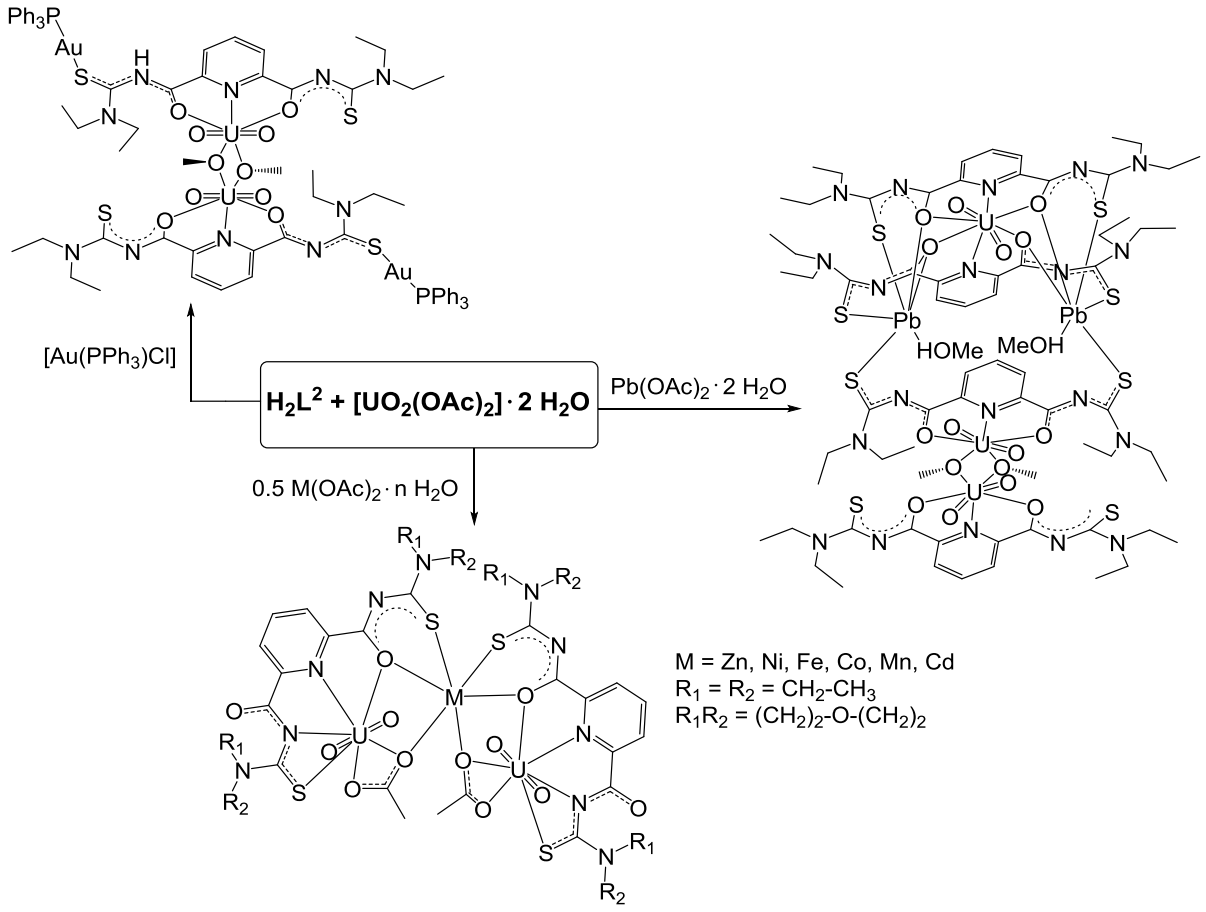

Scheme 5.2: Synthesen von heterometallischen Uraniumkomplexen.

Ein Thoriumkomplex mit H_2L^{2a} wurde aus einer Reaktion mit $[ThCl_4(DME)_2]$ und $NH_4(PF_6)$ unter absolut trockenen Bedingungen erhalten. Die Ammonium-Ionen bilden Wasserstoffbrückenbindungen mit den Schwefelatomen der Liganden aus. Ein ähnlicher Komplex wurde aus der Reaktion von $[U_2I_6(1,4\text{-dioxan})_3]$ mit H_2L^{2a} und [AuCl(tht)] synthetisiert. Der heterometallischer Komplex $[Au_2\{U(L^{2a})_3\}]$ wurde nach der Oxidation von U^{3+} zu U^{4+}. Ein heterometallischer Komplex mit der Zusammensetzung $[Ni\{Th(L^3)_2(OAc)_2\text{-}(MeOH)\}]$ konnte aus der Reaktion von $Th(NO_3)_2{\cdot}4\ H_2O$ mit $Ni(OAc)_2{\cdot}4\ H_2O$ und H_2L^3 erhalten werden. Eine Zusammenfassung der Reaktionen und ihrer Produkten ist in Scheme 5.3 angegeben.

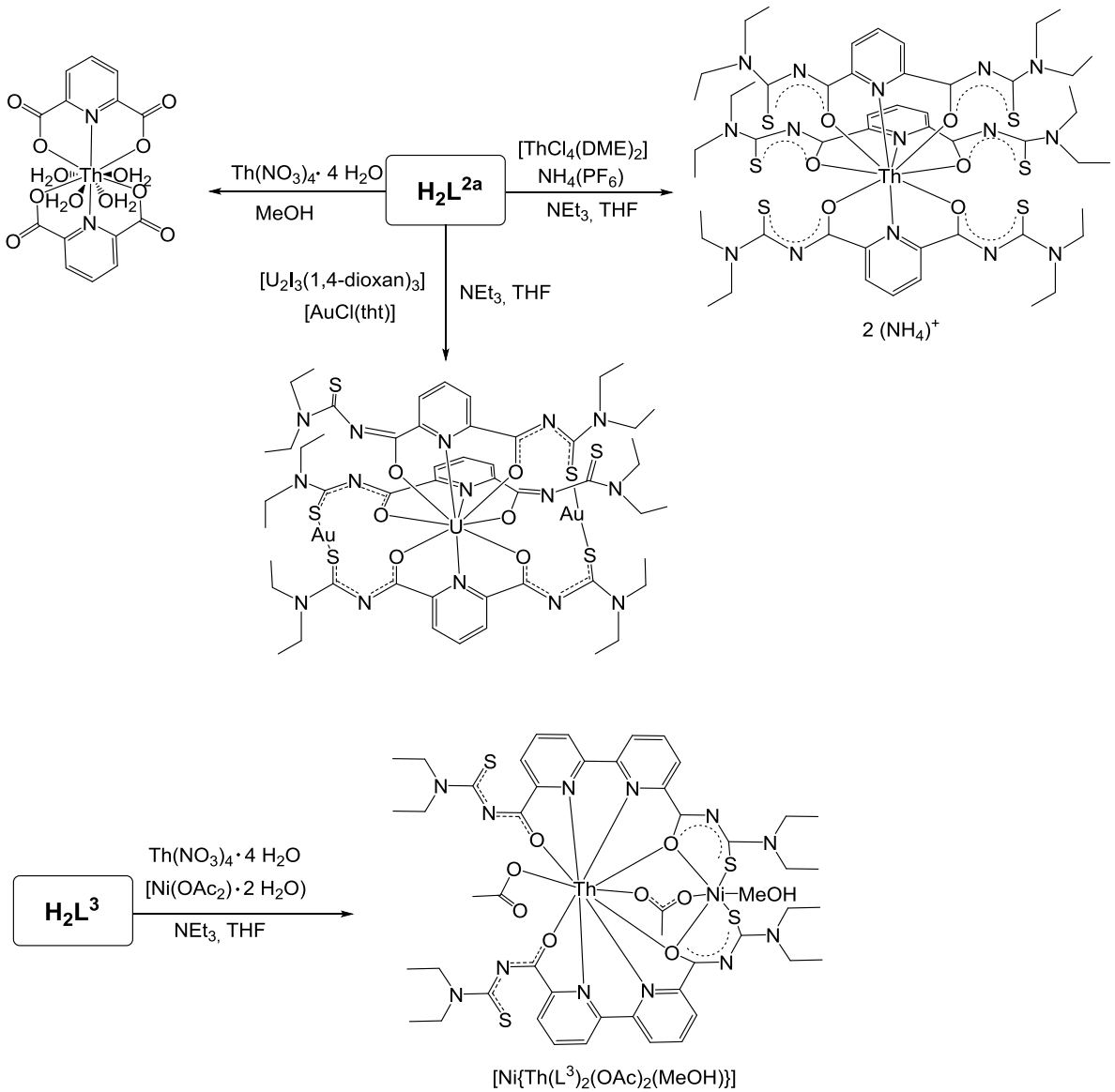

Scheme 5.3: Th^{4+} und U^{4+} Komplexe mit H_2L^{2a} und H_2L^3.

6 References

[1] O. Hahn, F. Strassmann, *Naturwissenschaften* **1939**, *27*, 89.

[2] L. Meitner, O. R. Frisch, *Nature* **1939**, *147*, 471.

[3] R. G. Pearson, *J. Am. Chem. Soc.* **1963**, *85*, 3533.

[4] E. H. P. Cordfunke, *The chemistry of uranium: including its applications in nuclear technology*, Elsevier Publishing Company, Amsterdam/ London/ New York **1969**.

[5] S. Ahrland, *The chemistry of the actinides*, Pergamon Press, Oxford **1975**.

[6] P. C. Burns, R. C. Ewing, F. C. Hawthorne, *Can. Mineral.* **1997**, *35*, 1551.

[7] M. Ephritikhine, *Coord. Chem. Rev.* **2016**, *319*, 35.

[8] K. Abu-Dari, K. N. Raymond, *Inorg. Chem.* **1982**, *21*, 1676.

[9] G. D. Jarvinen, R. R. Ryan, B. F. Smith, J. M. Ritchey, *Inorg. Chim. Acta* **1987**, *129*, 139.

[10] I. G. Santos, U. Abram, *Inorg. Chem. Commun*. **2004**, *7*, 440.

[11] U. Abram, E. S. Lang, E. Bonfada, *Z. Anorg. Allg. Chem.* **2002**, *628*, 1873.

[12] J. Akhtar, M. Akhtar, M. A. Malik, P. O'Brien, J. Raftery, *J. Am. Chem. Soc.* **2012**, *134*, 2485.

[13] M. Nencki, *Ber. Dtsch. Chem. Ges.* **1873**, *6*, 598.

[14] W. H. Pike, *Ber. Dtsch. Chem. Ges.* **1873**, *6*, 755.

[15] K. R. Koch, *Coord. Chem. Rev.* **2001**, *473*, 216.

[16] A. Saeed, U. Flörke, M. F. Erben, *J. Sulfur Chem.* **2013**, *35*, 318.

[17] W. Bensch, M. Schuster, *Z. Anorg. Allg. Chem.* **1992**, *611*, 99.

[18] U. Braun, R. Richter, J. Sieler, A. I. Yanovsky, Y. T. Struchkov, *Z. Anorg. Allg. Chem.* **1985**, *529*, 201.

[19] K. R. Koch, Y. Wang, A. Coetzee, *J. Chem. Soc., Dalton Trans.* **1999**, *6*, 1013.

[20] V. Cîrcu, M. Ilie, M. Iliş, F. Dumitraşcu, I. Neagoe, S. Păsculescu, *Polyhedron* **2009**, *28*, 3739.

[21] H. Pérez, Y. Mascarenhas, A. M. Plutín, R. de Souza Corrêa, J. Duque, *Acta Crystallogr., Sect. E:* **2008**, *64*, m503.

[22] N. Selvakumaran, S. W. Ng, E. R. Tiekink, R. Karvembu, *Inorg. Chim. Acta* **2011**, *376*, 278.

[23] G. Fitzl, L. Beyer, J. Sieler, R. Richter, J. Kaiser, E. Hoyer, *Z. Anorg. Allg. Chem.* **1977**, *433*, 237.

[24] R. Richter, L. Beyer, J. Kaiser, *Z. Anorg. Allg. Chem.* **1980**, *461*, 67.

[25] H. Arslan, U. Flörke, N. Külcü, M. F. Emen, *J. Coord. Chem.* **2006**, *59*, *223*.

[26] H. Arslan, N. Külcü, U. Flörke, *Transition Met. Chem.* **2003**, *28*, 816.

[27] J. Sieler, R. Richter, E. Hoyer, L. Beyer, O. Lindqvist, L. Andersen, *Z. Anorg. Allg. Chem.* **1990**, *580*, 167.

[28] W. Bensch, M. Schuster, *Z. Kristallogr.* **1995**, *210*, 68.

[29] N. H. Huy, U. Abram, *Z. Anorg. Allg. Chem.* **2008**, *634*, 1560.

[30] N. H. Huy, U. Abram, *Inorg. Chem.* **2007**, *46*, 5310.

[31] J. Duque, O. Estévez-Hernández, E. Reguera, J. Ellena, R. S. Corréa, *J. Coord. Chem.* **2009**, *62*, 2804.

[32] O. Estévez-Hernández, J. Duque, E. Reguera, *J. Sulfur Chem.* **2011**, *32*, 213.

[33] E. Otazo-Sánchez, P. Ortiz-del-Toro, O. Estévez-Hernández, L. Pérez-Marín, I. Goicoechea, A. Cerón Beltran, J. Villagómez-Ibarra, *Spectrochim. Acta, Part A:* **2002**, *58*, 2281.

[34] R. C. Luckay, F. Mebrahtu, C. Esterhuysen, K. R. Koch, *Inorg. Chem. Commun.* **2010**, *13*, 468.

[35] A. N. Mautjana, J. D. S. Miller, A. Gie, S. A. Bourne, K. R. Koch, *Dalton Trans.* **2003**, *21*, 1952.

[36] F. M. Emen, N. Külcü, *J. Therm. Anal. Calorim.* **2012**, *109*, 1321.

[37] S. Saeed, N. Rashid, P. G. Jones, M. Ali, R. Hussain, *Eur. J. Med. Chem.* **2010**, *45*, 1323.

[38] Z. Weiqun, Y. Wen, Q. Lihua, Z. Yong, Y. Zhengfeng, *J. Mol. Struct.* **2005**, *749*, 89.

[39] A. Saeed, H. Rafique, A. Hameed, S. Rasheed, *Pharm. Chem. J.* **2008**, *42*, 191.

[40] A. Mishra, K. Srivastava, R. Tripathi, S. K. Puri, S. Batra, *Eur. J. Med. Chem.* **2009**, *44*, 4404.

[41] M. Merdivan, M. Dùz, C. Hamamci, *Talanta* **2001**, *55*, 639.

[42] Y. Zhao, C. Liu, M. Feng, Z. Chen, S. Li, G. Tian, L. Wang, J. Huang, S. Li, *J. Hazard. Mat.* **2010**, *176*, 119.

[43] K. R. Koch, S. A. Bourne, A. Coetzee, J. Miller, *J. Chem. Soc., Dalton Trans.* **1999**, 3157.

[44] V. D. Schwade, L. Kirsten, A. Hagenbach, E. S. Lang, U. Abram, *Polyhedron* **2013**, *55*, 155.

[45] A. Rodenstein, J. A. Odendal, R. Kirmse, K. R. Koch, *Inorg. Chem. Commun.* **2011**, *14*, 99.

[46] A. N. Westra, S. A. Bourne, K. R. Koch, *Dalton Trans.* **2005**, *17*, 2916.

[47] J. J. Jegathesh, *Doctoral thesis*, Freie Universität Berlin, Berlin, **2013**.

[48] C. T. Pham, *Doctoral thesis*, Freie Universität Berlin, Berlin, **2016**.

[49] H. H. Nguyen, J. J. Jegathesh, A. Takiden, D. Hauenstein, C. T. Pham, C. D. Le, U. Abram, *Dalton Trans.* **2016**, *45*, 10771.

[50] T. A. Wioppiold, J. Ackermann, E. Schulz Lang, U. Abram, *Polyhedron* **2015**, *87*, 202.

[51] I. B. Douglass, F. B. Dains, *J. Am. Chem. Soc.* **1934**, *56*, 1408.

[52] A. Rodenstein, R. Richter, R. Kirmse, *Z. Anorg. Allg. Chem.* **2007**, *633*, 1713.

[53] U. Schröder, L. Beyer, J. Sieler, *Inorg. Chem. Commun.* **2000**, *3*, 630.

[54] M. Yokoyama, T. Ikuma, N. Obara, H. Togo, *J. Chem. Soc., Perkin Trans. 1:* **1990**, *12*, 3243.

[55] K. Brandenburg, *Diamond*, Crystal impact GbR, Bonn **2017**.

[56] K. R. Koch, O. Hallale, S. A. Bourne, J. Miller, J. Bacsa, *J. Mol. Struct.* **2001**, *561*, 185.

[57] H. H. Nguyen, P. C. Thang, A. Rodenstein, R. Kirmse, U. Abram, *Inorg. Chem.* **2011**, *50*, 590.

[58] Gaussview 5.0, Gaussian Inc.: Wallingford, CT, **2000-2008**.

[59] S. A. Bourne, O. Hallale, K. R. Koch, *Crystal Growth Res.* **2005**, *5*, 307.

[60] J. P. Gallivan, D. A. Dougherty, *J. Am. Chem. Soc.* **2000**, *122*, 870.

[61] C. T. Pham, H. H. Nguyen, A. Hagenbach, U. Abram, *Inorg Chem* **2017**, *56*, 11406.

[62] H.H. Nguyen, *Doctoral thesis*, Freie Universität Berlin, Berlin, **2009**.

[63] J. Ackermann, *Doctoral thesis*, Freie Universität Berlin, Berlin, **2016**.

[64] A. Immirzi, G. Bombieri, S. Degetto, G. Marangoni, *Acta Crystallogr., Sect. B:* **1975**, *31*, 1023.

[65] C. C. Gatto, *Doctoral thesis*, USFM Santa Maria, Brazil, **2006**.

[66] R. S. Herbst, P. Baron and M. Nilson, *Standard and advanced separation: PUREX processes for nuclear fuel reprocessing*, Woodhead Publishing, Philadelphia, PA, USA **2011**.

[67] M. Nilsson, K. L. Nash, *Solv. Extr. Ion Exch.* **2007**, *25*, 665.

[68] A. Geist, U. Müllich, D. Magnusson, P. Kaden, G. Modolo, A. Wilden, T. Zevaco, *Solv. Extr. Ion Exch.* **2012**, *30*, 433.

[69] D. Magnusson, B. Christiansen, M. R. S. Foreman, A. Geist, J. Glatz, R. Malmbeck, G. Modolo, D. Serrano-Purroy, C. Sorel, *Solv. Extr. Ion Exch.* **2009**, *27*, 97.

[70] A. Wilden, G. Modolo, C. Schreinemachers, F. Sadowski, S. Lange, M. Sypula, D. Magnusson, A. Geist, F. W. Lewis, L. M. Harwood, M. J. Hudson, *Solv. Extr. Ion Exch.* **2013**, *31*, 519.

[71] C. E. Rowland, C. L. Cahill, *Inorg. Chem.* **2010**, *49*, 8668.

[72] R. Guillaumont, T. Fanghänel, V. Neck, J. Fuger, D. A. Palmer, I. Grenthe, M. H. Rand, *Update on the chemical thermodynamics of Uranium, Neptunium, Plutonium, Americium and Technetium: 5th. Chemical Thermodynamics*, Palaiseau, France **2003**.

[73] M. Altmaier, X. Gaona, T. Fanghänel, *Chem. Rev.* **2013**, *113*, 901.

[74] T. Yoshimura, M. Nakaguchi, K. Morimoto, *Inorg. Chem.* **2017**, *56*, 4057.

[75] G. R. Choppin, M. P. Jensen, *Actinides in solution: complexation and kinetics:* Springer, Dordrecht **2010**.

[76] N. P. Martin, C. Falaise, C. Volkringer, N. Henry, P. Farger, C. Falk, E. Delahaye, P. Rabu, T. Loiseau, *Inorg. Chem.* **2016**, *55*, 8697.

[77] C. de Stefano, A. Gianguzza, T. Leggio, S. Sammartano, *J. Chem. Eng. Data* **2002**, *47*, 533.

[78] P. Zanonato, P. Di Bernardo, A. Bismondo, G. Liu, X. Chen, L. Rao, *J. Am. Chem. Soc.* **2004**, *126*, 5515.

[79] P. L. Zanonato, P. Di Bernardo, I. Grenthe, *Dalton Trans.* **2014**, *43*, 2378.

[80] T. A. Maxcy, G. Willhite, D. W. Green, K. Bowman-James, *J. Pet. Sci. Eng.* **1998**, *19*, 253.

[81] J. D Melton, B. H. Bielski, *J. Rad. Phys. Chem.* **1990**, *36*, 725.

[82] D. P. Fairlie, W. A. Wickramasinghe, K. A. Byriel, H. Taube, *Inorg. Chem.* **1997**, *36*, 2242.

[83] E. V. Kudrik, A. Theodoridis, R. van Eldik, S. V. Makarov, *Dalton Trans.* **2005**, *6*, 1117.

[84] S. Sahu, P. Rani Sahoo, S. Patel, B. K. Mishra, *J. Sulfur Chem.* **2011**, *32*, 171.

[85] J. A. García-Valenzuela, *Comments Inorg. Chem.* **2016**, *37*, 99.

[86] S. A. Ansari, P. Pathak, P. K. Mohapatra, V. K. Manchanda, *Chem. Rev.* **2012**, *112*, 1751.

[87] T. E. Müller, J. C. Green, D. P. Mingos, C. McPartlin, C. Whittingham, D. J. Williams, T. M. Woodroffe, *J. Organomet. Chem.* **1998**, *551*, 313.

[88] R. E. M. Brooner, T. J. Brown, R. A. Widenhoefer, *Chem. Eur. J.* **2013**, *19*, 8276.

[89] E. Delgado, E. Hernández, M. A. Maestro, A. Nievas, M. Villa, *J. Organomet. Chem.* **2006**, *691*, 3596.

[90] D. L. Reger, M. F. Huff, A. L. Rheingold, B. S. Haggerty, *J. Am. Chem. Soc.* **1992**, *114*, 579.

[91] D. L. Reger, T. D. Wright, C. A. Little, J. J. S. Lamba, M. D. Smith, *Inorg. Chem.* **2001**, *40*, 3810.

[92] R. D. Shannon, *Acta Cryst., Sect. A*: **1976**, *32*, 751.

[93] S. Degetto, L. Baracco, R. Graziani, E. Celon, *Transition Met. Chem.* **1978**, *3*, 351.

[94] M. J. Monreal, R. K. Thomson, T. Cantat, N. E. Travia, B. L. Scott, J. L. Kiplinger, *Organometallics* **2011**, *30*, 2031.

[95] C. R. Graves, B. L. Scott, D. E. Morris, J. L. Kiplinger, *J. Am. Chem. Soc.* **2007**, *129*, 11914.

[96] L. S. Natrajan, A. N. Swinburne, M. B. Andrews, S. Randall, S. L. Heath, *Coord. Chem. Rev.* **2014**, *171*, 266.

[97] J. Korzekwa, A. Scheurer, F. W. Heinemann, K. Meyer, *Dalton Trans.* **2017**, *46*, 13811.

[98] L. E. Sutton, M. R. Truter, *Molecular structure by diffraction methods: Volume 5*, Royal Society of Chemistry, Cambridge **1977**.

[99] M. E. Garner, S. Hohloch, L. Maron, J. Arnold, *Organometallics* **2016**, *35*, 2915.

[100] P. Yang, E. Zhou, B. Fang, G. Hou, G. Zi, M. D. Walter, *Organometallics* **2016**, *35*, 2129.

[101] E. Mora, L. Maria, B. Biswas, C. Camp, I. C. Santos, J. Pécaut, A. Cruz, J. M. Carretas, J. Marçalo, M. Mazzanti, *Organometallics* **2013**, *32*, 1409.

[102] W. Ren, H. Song, G. Zi, M. D. Walter, *Dalton Trans.* **2012**, *41*, 5965.

[103] W. Ren, G. Zi, M. D. Walter, *Organometallics* **2012**, *31*, 672.

[104] J.-C. Berthet, P. Thuéry, M. Ephritikhine, *C. R. Chimie* **2014**, *17*, 526.

[105] H. Aghabozorg, R. C. Palenik, G. J. Palenik, *Inorg. Chim. Acta* **1983**, *76*, L259.

[106] N. E. Dean, R. D. Hancock, C. L. Cahill, M. Frisch, *Inorg. Chem.* **2008**, *47*, 2000.

[107] C.-L. Xiao, C.-Z. Wang, L.-Y. Yuan, B. Li, H. He, S. Wang, Y.-L. Zhao, Z.-F. Chai, W.-Q. Shi, *Inorg. Chem.* **2014**, *53*, 1712.

[108] R. T. Gephart, N. J. Williams, J. H. Reibenspies, A. S. de Sousa, R. D. Hancock, *Inorg. Chem.* **2009**, *48*, 8201.

[109] A. Ruiz-Martínez, S. Alvarez, *Chem. Eur. J.* **2009**, *15*, 7470.

[110] M. Gál, P. L. Goggin, J. Mink, *Spectrochim. Acta, Part A:* **1992**, *48*, 121.

[111] T. Cantat, B. L. Scott, J. L. Kiplinger, *Chem. Commun.* **2010**, *46*, 919.

[112] M. I. Bruce, B. K. Nicholson, O. B. Shawkataly, J. R. Shapley, T. Henly, *Inorg. Synth.***1989**, *26*, 325.

[113] R. Uson, A. Laguna, M. Laguna, D. A. Briggs, H. H. Murray, J. P. Fackler Jr., *Inorg. Synth.* **1989**, *26*, 86.

[114] SOROBAN, Freie Universität Berlin, https://www.zedat.fu-berlin.de/HPC.

[115] Gaussian 09, Revision A.02, M. J. Frisch, G. W. Trucks, H. B. Schlegel, G. E. Scuseria, M. A. Robb, J. R. Cheeseman, G. Scalmani, V. Barone, G. A. Petersson, H. Nakatsuji, X. Li, M. Caricato, A. Marenich, J. Bloino, B. G. Janesko, R. Gomperts, B. Mennucci, H. P. Hratchian, J. V. Ortiz, A. F. Izmaylov, J. L. Sonnenberg, D. Williams-Young, F. Ding, F. Lipparini, F. Egidi, J. Goings, B. Peng, A. Petrone, T. Henderson, D. Ranasinghe, V. G. Zakrzewski, J. Gao, N. Rega, G. Zheng, W. Liang, M. Hada, M. Ehara, K. Toyota, R. Fukuda, J. Hasegawa, M. Ishida, T. Nakajima, Y. Honda, O. Kitao, H. Nakai, T. Vreven, K. Throssell, J. A. Montgomery, Jr., J. E. Peralta, F. Ogliaro, M. Bearpark, J. J. Heyd, E. Brothers, K. N. Kudin, V. N. Staroverov, T. Keith, R. Kobayashi, J. Normand, K. Raghavachari, A. Rendell, J. C. Burant, S. S. Iyengar, J. Tomasi, M. Cossi, J. M. Millam, M. Klene, C. Adamo, R. Cammi, J. W. Ochterski, R. L. Martin, K. Morokuma, O. Farkas, J. B. Foresman, and D. J. Fox, Gaussian, Inc., Wallingford CT, **2016**.

[116] Gaussian 16, Revision A.03, M. J. Frisch, G. W. Trucks, H. B. Schlegel, G. E. Scuseria, M. A. Robb, J. R. Cheeseman, G. Scalmani, V. Barone, G. A. Petersson, H. Nakatsuji, X. Li, M. Caricato, A. V. Marenich, J. Bloino, B. G. Janesko, R. Gomperts, B. Mennucci, H. P. Hratchian, J. V. Ortiz, A. F. Izmaylov, J. L. Sonnenberg, D. Williams-Young, F. Ding, F. Lipparini, F. Egidi, J. Goings, B. Peng, A. Petrone, T. Henderson, D. Ranasinghe, V. G. Zakrzewski, J. Gao, N. Rega, G. Zheng, W. Liang, M. Hada, M. Ehara, K. Toyota, R. Fukuda, J. Hasegawa, M. Ishida, T. Nakajima, Y. Honda, O. Kitao, H. Nakai, T. Vreven, K. Throssell, J. A. Montgomery, Jr., J. E. Peralta, F. Ogliaro, M. J. Bearpark, J. J. Heyd, E. N. Brothers, K. N. Kudin, V. N. Staroverov, T. A. Keith, R. Kobayashi, J. Normand, K. Raghavachari, A. P. Rendell, J. C. Burant, S. S. Iyengar, J. Tomasi, M. Cossi, J. M. Millam, M. Klene, C. Adamo, R. Cammi, J. W. Ochterski, R. L. Martin, K. Morokuma, O. Farkas, J. B. Foresman, and D. J. Fox, Gaussian, Inc., Wallingford CT, **2016**.

[117] S. H. Vosko, L. Wilk, M. Nusair, *Can. J. Phys.* **1980**, *58*, 1200.

[118] A. D. Becke, *J. Chem. Phys.* **1993**, *98*, 5648.

[119] C. Lee, W. Yang, R. G. Parr, *Phys. Rev. B:* **1988**, *37*, 785.

[120] D. Feller, *J. Comput. Chem.* **1996**, *17*, 1571.

[121] K. L. Schuchardt, B. T. Didier, T. Elsethagen, L. Sun, V. Gurumoorthi, J. Chase, J. Li, T. L. Windus, *J. Chem. Inf. Mod.* **2007**, *47*, 1045.

[122] M. Kretschmar, CHECK-HKL, Universität Tübingen, Germany, **1998**.

[123] G. M. Sheldrick, SADABS, Universität of Göttingen, Germany, **2014**.

[124] X-RED32, STOE & Cie GmbH: Darmstadt, Germany **2002**.

[125] A. L. Spek, PLATON: A Multipurpose Crystallographic Tool, Utrecht University, Utrecht, Netherlands **1980**-**2014**.

[126] G. M. Sheldrick, SHELXS 86, 97, 2014, Universität Göttingen, Germany **1986, 1997, 2014**.

[127] G. M. Sheldrick, SHELXL 2014, Universität Göttingen, Germany **2014**.

[128] C. Cason, Persistance of Vision Raytacer (tm) for Windows Version 3.6,: Persistance of Vision Raytacer Pty. Ltd. **1996**-**2003**.

[129] Ł. Skórka, M. Filapek, L. Zur, J. G. Małecki, W. Pisarski, M. Olejnik, W. Danikiewicz, S. Krompiec, *J. Phys. Chem. C* **2016**, *120*, 7284.

[130] W. Sharmoukh, N. K. Allam, *ACS Appl. Mat. Interfaces* **2012**, *4*, 4413.

Appendix

Crystallographic data

H_2L^3

Table A.1: Crystal data and structure refinement for H_2L^3.

Empirical formula	$C_{22}H_{28}N_6O_2S_2$	
Formula weight	472.62	
Temperature	100(2) K	
Wavelength	1.54178 Å	
Crystal system	Triclinic	
Space group	$P\overline{1}$	
Unit cell dimensions	a = 6.355(4) Å	α= 78.99(2)°
	b = 7.056(5) Å	β= 85.23(2)°
	c = 14.591(9) Å	γ = 64.99(2)°
Volume	582.01(7) $Å^3$	
Z	1	
Density (calculated)	1.348 g/cm^3	
Absorption coefficient	2.334 mm^{-1}	
F(000)	250	
Crystal size	0.3 x 0.06 x 0.03 mm^3	
Theta range for data collection	3.085 to 74.798°	
Index ranges	-7<=h<=7, -8<=k<=8, -18<=l<=18	
Reflections collected	23327	
Independent reflections	2357 [R(int) = 0.0416]	
Completeness to theta = 67.679°	99.8 %	
Absorption correction	Semi-empirical from equivalents	
Max. and min. transmission	0.7538 and 0.5403	
Refinement method	Full-matrix least-squares on F^2	
Data / restraints / parameters	2357 / 0 / 149	
Goodness-of-fit on F^2	1.119	
Final R indices [I>2sigma(I)]	R1 = 0.0395, wR2 = 0.1033	
R indices (all data)	R1 = 0.0412, wR2 = 0.1043	
Largest diff. peak and hole	0.272 and -0.451 e/$Å^3$	
Diffractometer	Bruker, D8 Venture	

Table A.2: Atomic coordinates (x 10^4) and equivalent isotropic displacement parameters ($Å^2$ x 10^3) for H_2L^3.

	x	y	z	U(eq)
S(1)	6059(1)	2740(1)	8413(1)	34(1)
O(5)	5125(2)	8153(2)	6334(1)	22(1)
N(26)	1642(2)	5828(2)	5659(1)	16(1)
N(6)	4935(2)	6855(2)	8399(1)	19(1)
N(3)	3498(3)	6016(3)	7183(1)	21(1)
C(21)	2759(3)	7105(3)	5532(1)	16(1)
C(22)	2902(3)	8328(3)	4685(1)	18(1)
C(25)	603(3)	5725(2)	4918(1)	16(1)
C(4)	3929(3)	7176(3)	6374(1)	18(1)
C(23)	1817(3)	8211(3)	3922(1)	21(1)
C(2)	4818(3)	5349(3)	8004(1)	20(1)
C(24)	661(3)	6896(3)	4038(1)	20(1)
C(7)	3385(3)	9129(3)	8154(1)	26(1)
C(9)	6723(3)	6265(3)	9107(1)	26(1)
C(8)	2216(4)	10069(4)	9019(2)	35(1)
C(10)	8800(3)	6591(4)	8673(2)	39(1)

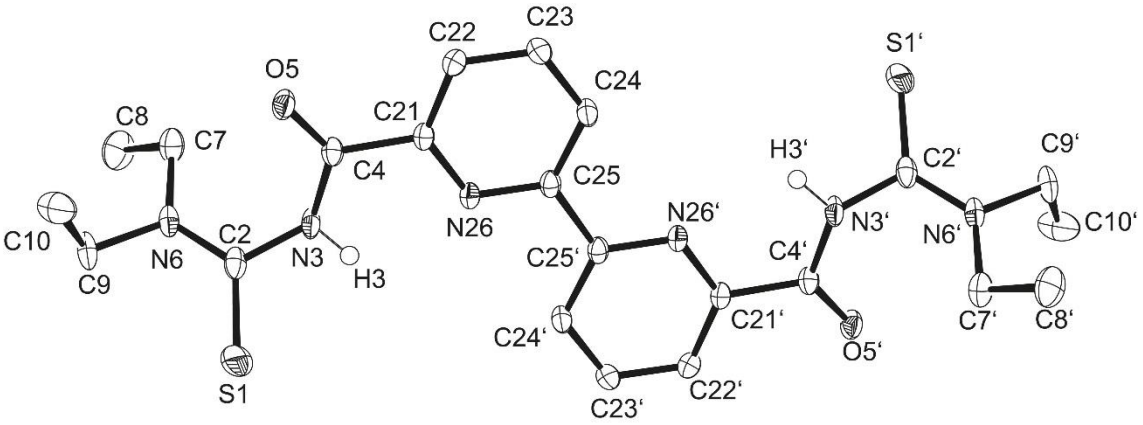

Figure A.1: Ellipsoid plot of H_2L^3. Hydrogen atoms attached to carbon atoms have been omitted for clarity. Thermal ellipsoids are at 50 % probability.

$(HNEt_3)_2[\{UO_2(L^1)\}_4(OAc)_2]$

Table A.3: Crystal data and structure refinement for $(HNEt_3)_2[\{UO_2(L^1)\}_4(OAc)_2] \cdot CH_2Cl_2$.

Empirical formula	$C_{89}H_{136}Cl_2N_{18}O_{20}S_8U_4$	
Formula weight	3057.65	
Temperature	293(2) K	
Wavelength	0.71073 Å	
Crystal system	Triclinic	
Space group	$P\overline{1}$	
Unit cell dimensions	a = 9.396(1) Å	α= 108.55(1)
	b = 17.226(2) Å	β= 93.09(1)
	c = 21.239(2) Å	γ = 96.07(1)
Volume	3226.8(6) $Å^3$	
Z	1	
Density (calculated)	1.573 g/cm^3	
Absorption coefficient	5.235 mm^{-1}	
F(000)	1486	
Crystal size	0.21 x 0.13 x 0.09 mm^3	
Theta range for data collection	2.379 to 26.000°.	
Index ranges	-11<=h<=10, -21<=k<=21, -25<=l<=26	
Reflections collected	26992	
Independent reflections	12628 [R(int) = 0.1247]	
Completeness to theta = 25.242°	99.5 %	
Absorption correction	Integration	
Max. and min. transmission	0.668 and 0.172	
Refinement method	Full-matrix least-squares on F^2	
Data / restraints / parameters	12628 / 88 / 645	
Goodness-of-fit on F^2	1.024	
Final R indices [I>2sigma(I)]	R1 = 0.0707, wR2 = 0.1795	
R indices (all data)	R1 = 0.1081, wR2 = 0.2017	
Largest diff. peak and hole	1.871 and -2.773 e/$Å^3$	
Diffractometer	IPDS, STOE	

Table A.4: Atomic coordinates (x 10^4) and equivalent isotropic displacement parameters ($Å^2$ x 10^3) for $(HNEt_3)_2[\{UO_2(L^1)\}_4(OAc)_2] \cdot CH_2Cl_2$.

	x	y	z	U(eq)
U(2)	7746(1)	5894(1)	2398(1)	55(1)
U(1)	3347(1)	2267(1)	1848(1)	49(1)
O(1)	1992(10)	2842(6)	1689(5)	71(3)
O(2)	4706(11)	1698(6)	2031(5)	67(2)
O(12)	9356(11)	5462(6)	2435(5)	74(3)
O(11)	6128(11)	6344(6)	2394(5)	74(3)
S(11)	8885(5)	6745(3)	1548(2)	85(1)
S(1)	2173(6)	892(3)	724(2)	101(2)
C(2)	2931(17)	887(10)	12(6)	73(4)
N(3)	3568(16)	1558(8)	-137(5)	78(4)
C(4)	4213(14)	2234(8)	317(6)	58(3)
O(5)	4430(10)	2373(6)	941(4)	70(3)
N(6)	2760(20)	188(8)	-498(7)	108(5)
C(7)	3630(30)	115(15)	-1117(10)	143(8)
C(8)	2590(30)	140(20)	-1643(13)	192(12)
C(9)	2030(20)	-580(11)	-450(10)	110(6)
C(10)	3030(30)	-1013(14)	-173(14)	140(8)
C(12)	8530(20)	6217(10)	711(7)	82(5)
N(13)	7648(13)	5501(7)	413(5)	66(3)
C(14)	7062(15)	5000(8)	704(6)	58(3)
O(15)	7172(12)	5078(6)	1312(4)	76(3)
N(16)	9013(19)	6575(9)	279(6)	101(5)
C(17A)	10230(30)	7259(15)	487(11)	138(9)
C(18A)	9650(40)	8041(19)	587(17)	138(9)
C(17B)	10230(30)	7259(15)	487(11)	138(9)
C(18B)	11340(80)	7530(40)	670(30)	138(9)
C(19)	8530(18)	6199(11)	-465(7)	84(5)
C(20)	9410(20)	5543(12)	-775(9)	99(6)
S(21)	1194(4)	1234(3)	2202(2)	74(1)
C(22)	2206(17)	1166(9)	2872(7)	68(4)
N(23)	2622(15)	1792(7)	3456(6)	71(3)
C(24)	7124(18)	7459(9)	6530(7)	69(4)
O(25)	3113(12)	2807(6)	2991(4)	69(3)
N(26)	2638(17)	422(8)	2878(6)	85(4)

C(27)	3470(30)	362(13)	3457(10)	116(6)
C(28)	5060(30)	662(16)	3487(14)	148(9)
C(29A)	2150(30)	-322(11)	2300(10)	122(8)
C(30A)	1050(50)	-780(20)	2460(30)	143(14)
C(29B)	2150(30)	-322(11)	2300(10)	122(8)
C(30B)	3180(50)	-600(30)	1880(30)	143(14)
S(31)	9236(5)	7465(2)	3167(2)	77(1)
C(32)	7860(20)	7763(10)	3655(7)	85(4)
N(33)	7439(17)	7446(8)	4128(6)	85(4)
C(34)	7427(16)	6653(8)	4057(6)	62(3)
O(35)	7542(12)	6091(6)	3528(4)	71(3)
N(36)	7220(30)	8418(12)	3633(9)	137(7)
C(39)	5770(40)	8589(19)	3953(15)	168(9)
C(40)	6280(50)	9160(20)	4636(16)	203(13)
C(41)	4786(14)	2890(8)	45(6)	59(3)
C(42)	4610(20)	2787(10)	-615(7)	77(4)
C(43)	5150(20)	3394(10)	-859(7)	86(5)
C(44)	5940(19)	4101(9)	-443(7)	75(4)
C(45)	6192(14)	4234(8)	250(6)	57(3)
C(46)	5583(13)	3615(8)	475(5)	54(3)
C(51)	7024(15)	6816(9)	5850(6)	59(3)
C(52)	6772(19)	5970(9)	5795(7)	76(4)
C(53)	6755(19)	5387(9)	5172(7)	74(4)
C(54)	6948(19)	5609(9)	4619(7)	74(4)
C(55)	7197(16)	6421(8)	4657(6)	62(3)
C(56)	7207(18)	7025(9)	5291(6)	71(4)
C(60)	8290(20)	2700(11)	2065(8)	91(5)
C(61)	8567(19)	3067(12)	1532(8)	95(5)
C(62A)	7560(20)	2930(20)	3168(11)	140(11)
C(63A)	8410(50)	2350(30)	3320(20)	139(13)
C(62B)	7560(20)	2930(20)	3168(11)	140(11)
C(63B)	6650(70)	3120(40)	3660(30)	139(13)
C(64A)	9500(50)	3870(17)	3017(14)	181(11)
C(65A)	9700(60)	4540(20)	3599(18)	181(11)
C(64B)	9500(50)	3870(17)	3017(14)	181(11)
C(65B)	9970(150)	3720(60)	3440(40)	181(11)
O(71)	5101(9)	3472(5)	2278(4)	57(2)
O(72)	6527(9)	4635(5)	2492(4)	58(2)
C(73)	5263(16)	4242(8)	2340(6)	59(3)

N(10)	8183(18)	3322(11)	2714(7)	97(5)
C(74)	4050(20)	4646(11)	2228(13)	114(8)
C(80A)	2700(60)	6800(70)	4730(40)	178(5)
Cl(8A)	3520(17)	6319(13)	4029(10)	178(5)
Cl(9A)	945(17)	6315(13)	4609(10)	178(5)
C(80B)	1770(60)	6520(80)	3960(50)	178(5)
Cl(8B)	3520(17)	6319(13)	4029(10)	178(5)
Cl(9B)	945(17)	6315(13)	4609(10)	178(5)
C(37)	7550(40)	8869(16)	3166(12)	162(9)
C(38)	6670(60)	8460(20)	2515(17)	280(20)

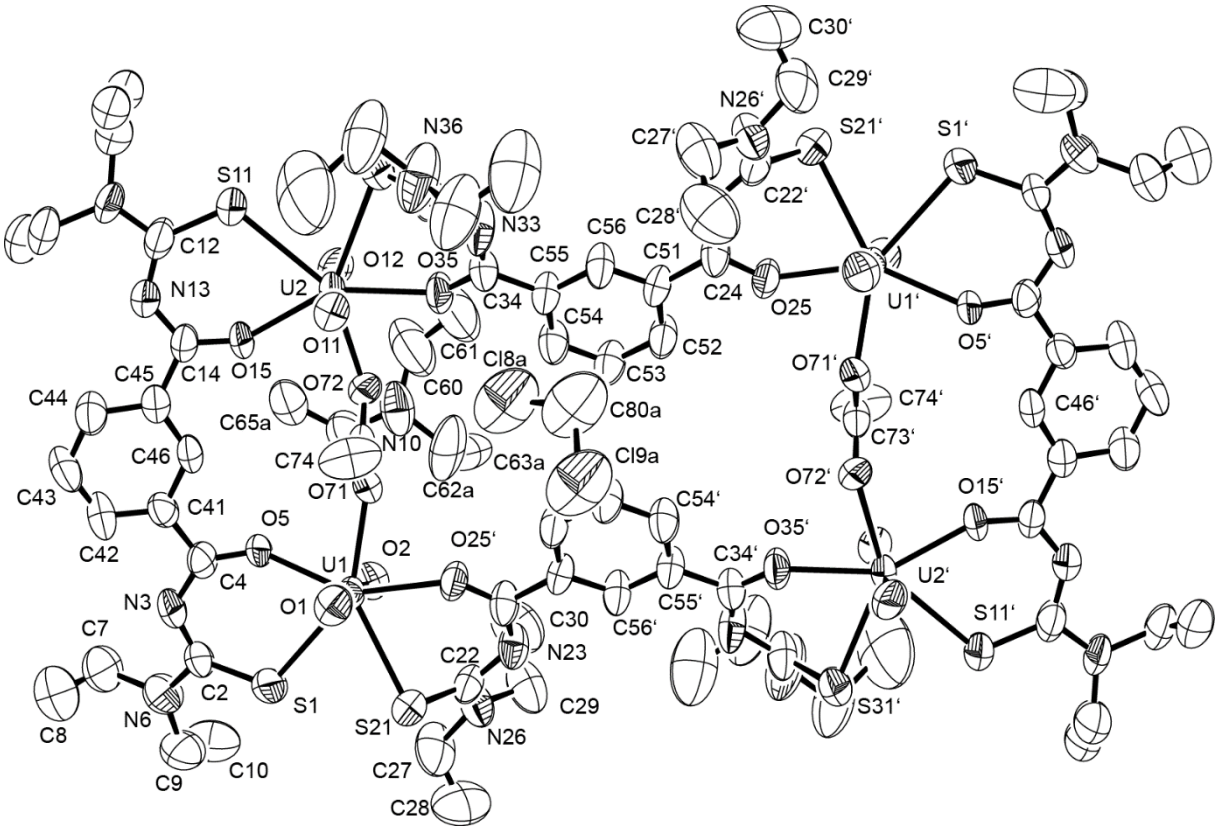

Figure A.2: Ellipsoid plot of $(HNEt_3)_2[\{UO_2(L^1)\}_4(OAc)_2] \cdot CH_2Cl_2$. Hydrogen atoms have been omitted for clarity. Thermal ellipsoids are at 50 % probability.

$[UO_2(L^{2a})(MeOH)]$

Table A.5: Crystal data and structure refinement for $[UO_2(L^{2a})(MeOH)]$.

Empirical formula	$C_{18}H_{27}N_5O_5S_2U$	
Formula weight	695.59	
Temperature	144(2) K	
Wavelength	0.71073 Å	
Crystal system	Monoclinic	
Space group	P 2_1/c	
Unit cell dimensions	a = 17.006(3) Å	α = 90°
	b = 10.108(3) Å	β = 91.470(8)°
	c = 13.661(3) Å	γ = 90°
Volume	2347.5(9) $Å^3$	
Z	4	
Density (calculated)	1.968 g/cm^3	
Absorption coefficient	7.131 mm^{-1}	
F(000)	1336	
Crystal size	0.350 x 0.290 x 0.180 mm^3	
Theta range for data collection	2.344 to 27.129°.	
Index ranges	-21<=h<=20, -12<=k<=11, -17<=l<=17	
Reflections collected	27433	
Independent reflections	5189 [R(int) = 0.0520]	
Completeness to theta = 25.242°	99.8 %	
Absorption correction	Semi-empirical from equivalents	
Max. and min. transmission	0.7455 and 0.3851	
Refinement method	Full-matrix least-squares on F^2	
Data / restraints / parameters	5189 / 0 / 289	
Goodness-of-fit on F^2	1.120	
Final R indices [I>2sigma(I)]	R1 = 0.0225, wR2 = 0.0534	
R indices (all data)	R1 = 0.0262, wR2 = 0.0548	
Largest diff. peak and hole	0.625 and -1.777 e/$Å^3$	
Diffractometer	Bruker, D8 Venture	

Table A.6: Atomic coordinates (x 10^4) and equivalent isotropic displacement parameters ($Å^2$ x 10^3) for $[UO_2(L^{2a})(MeOH)]$.

	x	y	z	U(eq)
U(001)	2342(1)	5264(1)	4246(1)	5(1)
S(1)	3749(1)	3586(1)	3906(1)	10(1)
S(11)	1651(1)	7495(1)	3103(1)	11(1)
O(5)	2757(1)	1833(2)	6415(2)	12(1)
O(3)	2802(1)	5349(2)	2531(2)	10(1)
O(1)	1686(1)	4071(2)	3730(2)	11(1)
O(15)	115(1)	7099(2)	5545(2)	13(1)
O(2)	3022(1)	6451(2)	4731(2)	11(1)
N(16)	1386(2)	9080(3)	4651(2)	8(1)
N(26)	1565(2)	4607(3)	5786(2)	8(1)
N(3)	2948(2)	3705(3)	5478(2)	8(1)
N(13)	1329(2)	6748(3)	4839(2)	8(1)
C(25)	1749(2)	3482(3)	6266(2)	8(1)
C(4)	2542(2)	2912(3)	6066(2)	8(1)
N(6)	4310(2)	3326(3)	5755(2)	10(1)
C(19)	1569(2)	10232(3)	4031(3)	12(1)
C(12)	1403(2)	7869(3)	4284(2)	8(1)
C(23)	502(2)	3447(3)	7039(2)	11(1)
C(24)	1236(2)	2881(3)	6905(2)	9(1)
C(17)	1368(2)	9338(3)	5714(2)	11(1)
C(20)	2451(2)	10483(4)	3985(3)	21(1)
C(21)	866(2)	5171(3)	5945(2)	7(1)
C(31)	3350(2)	6211(4)	2072(3)	22(1)
C(9)	5112(2)	3175(3)	5379(2)	13(1)
C(2)	3697(2)	3462(3)	5147(2)	9(1)
C(7)	4253(2)	3426(4)	6831(2)	16(1)
C(22)	311(2)	4610(3)	6551(2)	10(1)
C(18)	616(2)	9988(4)	6039(3)	16(1)
C(14)	720(2)	6468(3)	5431(2)	8(1)
C(8)	4234(3)	4848(4)	7165(3)	29(1)
C(10)	5309(2)	1731(4)	5222(3)	24(1)

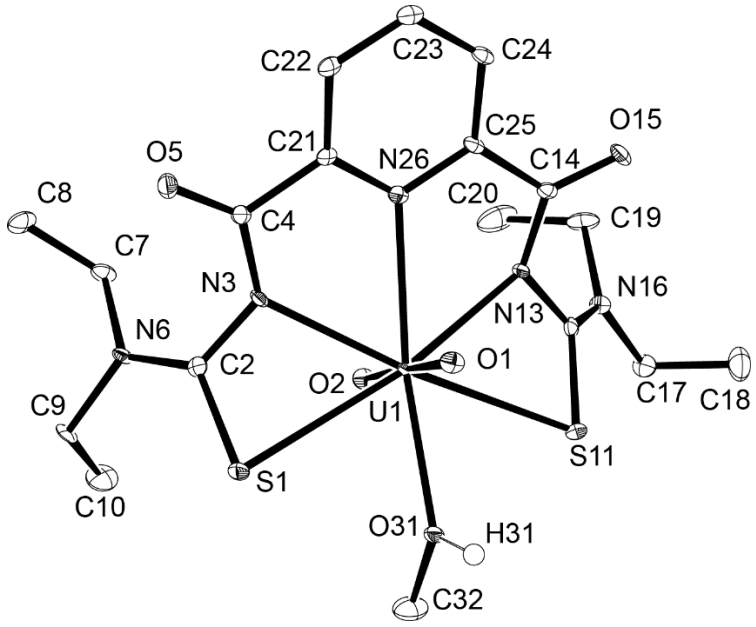

Figure A.3: Ellipsoid plot of $[UO_2(L^{2a})(MeOH)]$. Hydrogen atoms attached to carbon atoms have been omitted for clarity. Thermal ellipsoids are at 50 % probability.

$[UO_2(L^{2a})(DMF)]$

Table A.7: Crystal data and structure refinement for $[UO_2(L^{2a})(DMF)] \cdot DMF$.

Empirical formula	$C_{23}H_{37}N_7O_6S_2U$	
Formula weight	809.74	
Temperature	200(2) K	
Wavelength	0.71073 Å	
Crystal system	Monoclinic	
Space group	P 2_1/n	
Unit cell dimensions	a = 14.253(1) Å	α= 90°
	b = 8.769(1) Å	β= 93.65(1)°
	c = 24.239(2) Å	γ = 90°
Volume	3023.4(5) $Å^3$	
Z	4	
Density (calculated)	1.779 g/cm^3	
Absorption coefficient	5.555 mm^{-1}	
F(000)	1584	
Crystal size	0.6 x 0.04 x 0.01 mm^3	
Theta range for data collection	2.471 to 29.316°	
Index ranges	-19<=h<=19, -11<=k<=12, -33<=l<=23	
Reflections collected	33954	
Independent reflections	8094 [R(int) = 0.1139]	
Completeness to theta = 25.242°	99.4 %	
Absorption correction	Integration	
Max. and min. transmission	0.5909 and 0.2592	
Refinement method	Full-matrix least-squares on F^2	
Data / restraints / parameters	8094 / 0 / 353	
Goodness-of-fit on F^2	0.931	
Final R indices [I>2sigma(I)]	R1 = 0.0613, wR2 = 0.1397	
R indices (all data)	R1 = 0.1056, wR2 = 0.1605	
Largest diff. peak and hole	2.216 and -1.908 e/$Å^3$	
Diffractometer	STOE IPDS	

Table A.8: Atomic coordinates (x 10^4) and equivalent isotropic displacement parameters ($Å^2$ x 10^3) for $[UO_2(L^{2a})(DMF)] \cdot DMF$.

	x	y	z	U(eq)
U(1)	2805(1)	2228(1)	199(1)	38(1)
O(1)	1848(4)	3453(8)	70(3)	49(2)
O(2)	3744(4)	954(7)	338(3)	47(1)
S(1)	2203(2)	433(3)	-785(1)	49(1)
C(2)	3136(6)	1360(9)	-1055(4)	41(2)
N(3)	3422(5)	2564(7)	-742(3)	41(2)
C(4)	3578(6)	3945(10)	-973(4)	41(2)
O(5)	3516(5)	4292(7)	-1460(3)	52(2)
N(6)	3541(5)	873(8)	-1494(3)	43(2)
C(7)	4457(6)	1438(10)	-1653(4)	46(2)
C(8)	5185(7)	237(12)	-1652(5)	60(3)
C(9)	3071(7)	-244(13)	-1869(5)	58(3)
C(10)	2446(9)	527(18)	-2308(6)	85(4)
S(11)	2301(2)	1959(3)	1341(1)	49(1)
C(12)	3266(6)	3111(9)	1469(4)	41(2)
N(13)	3511(5)	3786(8)	991(3)	41(2)
C(14)	3695(6)	5319(10)	958(4)	42(2)
O(15)	3694(5)	6259(7)	1332(3)	48(2)
N(16)	3725(5)	3215(9)	1953(3)	41(2)
C(17)	4660(6)	3934(11)	2048(4)	46(2)
C(18)	4667(8)	5181(12)	2479(5)	58(3)
C(19)	3383(7)	2365(11)	2435(4)	52(2)
C(20)	2610(8)	3162(14)	2704(5)	65(3)
C(21)	3782(6)	5164(10)	-538(4)	42(2)
C(22)	4026(6)	6644(10)	-687(4)	44(2)
C(23)	4180(6)	7701(10)	-279(4)	43(2)
C(24)	4101(6)	7289(10)	259(4)	44(2)
C(25)	3852(5)	5801(9)	386(4)	37(2)
N(26)	3712(4)	4743(8)	-15(3)	40(2)
O(31)	1688(4)	195(7)	365(3)	49(2)
C(32)	1788(6)	-1124(11)	570(5)	57(3)
N(33)	1117(5)	-2039(9)	679(4)	55(2)
C(34)	166(9)	-1590(20)	614(12)	168(13)
C(35)	1270(8)	-3543(13)	915(7)	76(4)

O(41)	9395(7)	6358(16)	1969(6)	113(4)
C(42)	8997(9)	5776(17)	1555(7)	80(4)
N(43)	9191(7)	4363(12)	1367(5)	71(3)
C(44)	9869(14)	3420(30)	1646(9)	135(8)
C(45)	8688(13)	3840(20)	862(9)	120(7)

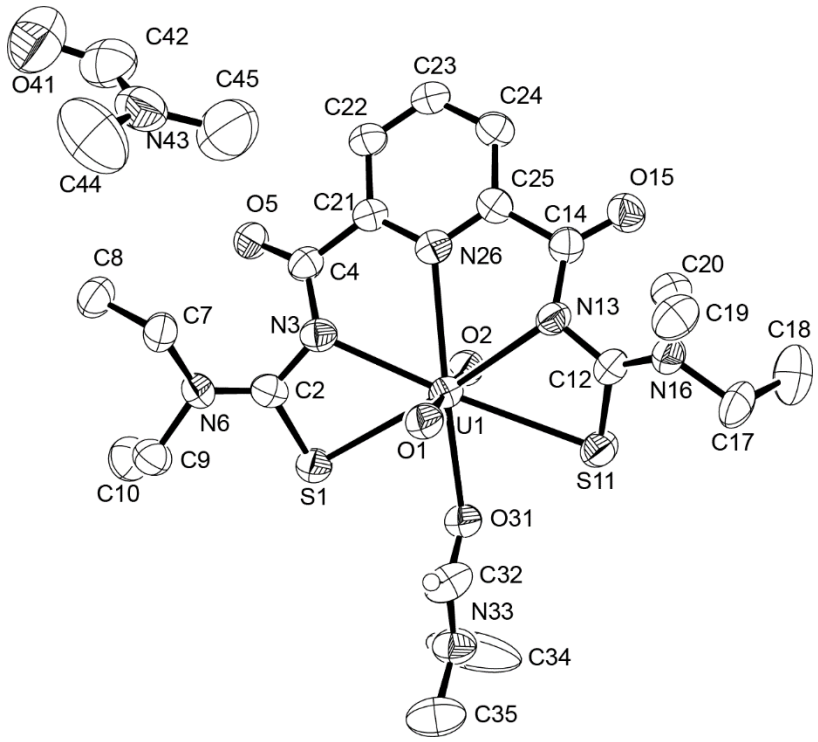

Figure A.4: Ellipsoid plot of $[UO_2(L^{2a})(DMF)] \cdot DMF$. Hydrogen atoms except for the coordinated solvent molecule have been omitted for clarity Thermal ellipsoids are at 50 % probability.

$[UO_2(L^{2b})(H_2O)]$

Table A.9: Crystal data and structure refinement for $[UO_2(L^{2b})(H_2O)]$.

Empirical formula	$C_{17}H_{21}N_5O_7S_2U$	
Formula weight	709.54	
Temperature	100(2) K	
Wavelength	0.71073 Å	
Crystal system	Orthorhombic	
Space group	Pbca	
Unit cell dimensions	a = 15.146(9) Å	α= 90°
	b = 16.277(9) Å	β= 90°
	c = 17.941(2) Å	γ = 90°
Volume	4423.0(5) $Å^3$	
Z	8	
Density (calculated)	2.131 g/cm^3	
Absorption coefficient	7.578 mm^{-1}	
F(000)	2704	
Crystal size	0.23 x 0.12 x 0.04 mm^3	
Theta range for data collection	2.159 to 27.168°.	
Index ranges	-19<=h<=19, -20<=k<=20, -23<=l<=22	
Reflections collected	33776	
Independent reflections	4905 [R(int) = 0.0500]	
Completeness to theta = 25.242°	100.0 %	
Absorption correction	Semi-empirical from equivalents	
Max. and min. transmission	0.7455 and 0.4076	
Refinement method	Full-matrix least-squares on F^2	
Data / restraints / parameters	4905 / 0 / 298	
Goodness-of-fit on F^2	0.948	
Final R indices [I>2sigma(I)]	R1 = 0.0248, wR2 = 0.0466	
R indices (all data)	R1 = 0.0412, wR2 = 0.0523	
Largest diff. peak and hole	1.710 and -0.970 e/$Å^3$	
Diffractometer	Bruker D8 Venture	

Table A.10: Atomic coordinates (x 10^4) and equivalent isotropic displacement parameters ($Å^2$ x 10^3) for $[UO_2(L^{2b})(H_2O)]$.

	x	y	z	U(eq)
U(1)	6271(1)	2572(1)	5752(1)	8(1)
O(1)	6210(2)	2159(2)	6664(2)	13(1)
O(2)	6338(2)	2990(2)	4837(2)	11(1)
S(1)	5012(1)	1361(1)	5257(1)	13(1)
C(2)	4275(3)	1971(2)	5723(3)	10(1)
N(3)	4627(2)	2734(2)	5864(2)	9(1)
C(4)	4167(3)	3443(2)	5811(2)	10(1)
O(5)	3370(2)	3542(2)	5701(2)	15(1)
N(6)	3499(2)	1717(2)	5955(2)	12(1)
C(7)	2973(3)	2098(3)	6552(3)	14(1)
C(8)	2863(3)	1485(3)	7184(3)	21(1)
C(10)	3039(3)	361(3)	6386(3)	19(1)
C(9)	3130(3)	918(3)	5715(3)	15(1)
O(10)	2478(2)	736(2)	6928(2)	24(1)
S(11)	8201(1)	2477(1)	5855(1)	12(1)
C(12)	8088(3)	3352(2)	6362(3)	11(1)
N(13)	7257(2)	3683(2)	6292(2)	10(1)
C(14)	7126(3)	4470(3)	6121(2)	11(1)
O(15)	7696(2)	5008(2)	6014(2)	15(1)
N(16)	8696(2)	3648(2)	6814(2)	12(1)
C(17)	8573(3)	4352(3)	7318(3)	13(1)
C(18)	9302(3)	4969(3)	7183(3)	16(1)
C(20)	10281(3)	3928(3)	6823(3)	19(1)
C(19)	9580(3)	3274(3)	6896(3)	15(1)
O(20)	10143(2)	4595(2)	7325(2)	19(1)
N(26)	5618(2)	4027(2)	5989(2)	10(1)
C(21)	6166(3)	4674(2)	6050(2)	11(1)
C(22)	5872(3)	5478(3)	6036(2)	12(1)
C(23)	4976(3)	5633(3)	5957(2)	12(1)
C(24)	4409(3)	4970(3)	5884(2)	12(1)
C(25)	4752(3)	4178(3)	5904(2)	10(1)
O(31)	6920(2)	1313(2)	5185(2)	13(1)

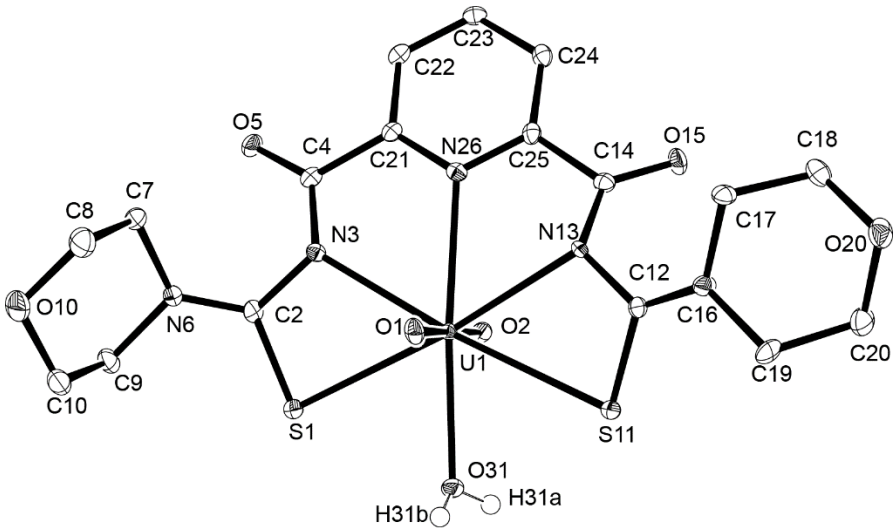

Figure A.5: Ellipsoid plot of $[UO_2(L^{2b})(H_2O)]$. Hydrogen atoms attached to carbon atoms have been omitted for clarity. Thermal ellipsoids are at 50 % probability.

$[UO_2(L^{2b})(DMF)]$

Table A.11: Crystal data and structure refinement for $[UO_2(L^{2b})(DMF)]$.

Empirical formula	$C_{20}H_{26}N_6O_7S_2U$	
Formula weight	764.62	
Temperature	100(2) K	
Wavelength	0.71073 Å	
Crystal system	Monoclinic	
Space group	P 2_1/c	
Unit cell dimensions	a = 8.686(5) Å	α= 90°
	b = 14.382(8) Å	β= 101.96(3)
	c = 20.092(1) Å	γ = 90°
Volume	2455.4(2) $Å^3$	
Z	4	
Density (calculated)	2.068 g/cm^3	
Absorption coefficient	6.835 mm^{-1}	
F(000)	1472	
Crystal size	0.17 x 0.09 x 0.05 mm^3	
Theta range for data collection	2.397 to 26.406°.	
Index ranges	-10<=h<=10, -17<=k<=16, -25<=l<=25	
Reflections collected	27203	
Independent reflections	5015 [R(int) = 0.0719]	
Completeness to theta = 25.242°	100.0 %	
Absorption correction	Semi-empirical from equivalents	
Max. and min. transmission	0.7454 and 0.6467	
Refinement method	Full-matrix least-squares on F^2	
Data / restraints / parameters	5015 / 18 / 321	
Goodness-of-fit on F^2	1.218	
Final R indices [I>2sigma(I)]	R1 = 0.0439, wR2 = 0.0727	
R indices (all data)	R1 = 0.0636, wR2 = 0.0773	
Largest diff. peak and hole	1.331 and -1.229 e/$Å^3$	
Diffractometer	Bruker D8 Venture	

Table A.12: Atomic coordinates (x 10^4) and equivalent isotropic displacement parameters ($Å^2$ x 10^3) for $[UO_2(L^{2b})(DMF)]$.

	x	y	z	U(eq)
U(1)	2599(1)	2830(1)	4611(1)	19(1)
O(1)	3749(5)	3771(3)	4425(3)	27(1)
O(2)	1460(5)	1889(3)	4792(3)	25(1)
S(1)	2324(3)	2239(2)	3199(1)	40(1)
C(2)	1002(9)	3129(5)	3055(3)	25(2)
N(3)	523(6)	3395(4)	3631(3)	19(1)
C(4)	-1005(8)	3505(5)	3659(4)	21(2)
S(11)	4956(2)	2369(1)	5835(1)	32(1)
C(12)	4121(10)	3276(5)	6184(4)	37(2)
O(5)	-2163(6)	3414(4)	3198(3)	33(1)
O(10)	-1020(7)	4156(4)	1153(3)	39(2)
O(31)	4511(7)	1671(4)	4427(3)	46(2)
N(13)	2765(7)	3570(4)	5769(3)	25(1)
C(21)	-1169(8)	3749(4)	4364(4)	17(1)
C(25)	61(8)	3965(4)	5478(3)	20(2)
N(6)	566(8)	3562(4)	2459(3)	30(2)
N(26)	162(6)	3729(3)	4849(3)	15(1)
N(33)	6621(7)	819(4)	4391(3)	26(1)
C(7)	1095(10)	3262(6)	1840(4)	35(2)
C(8)	-274(10)	3273(6)	1256(4)	38(2)
C(9)	-288(9)	4457(5)	2354(4)	32(2)
C(10)	-1579(10)	4406(6)	1745(4)	36(2)
C(19B)	5019(16)	4765(8)	6776(6)	22(1)
C(17B)	6600(13)	3380(9)	7063(7)	22(1)
C(18B)	7307(15)	3790(9)	7466(7)	22(1)
C(20B)	5751(16)	5122(9)	7213(6)	22(1)
O(20B)	6618(12)	4583(7)	7890(5)	22(1)
N(16B)	4576(12)	3610(7)	6846(6)	22(1)
C(17A)	5838(17)	3146(9)	7347(6)	22(1)
C(20A)	5091(14)	4912(10)	7484(7)	22(1)
C(19A)	4240(15)	4542(9)	7082(7)	22(1)
C(18A)	6634(17)	3576(8)	7769(7)	22(1)
O(20A)	6931(12)	4674(7)	7683(6)	22(1)
N(16A)	5161(14)	3767(8)	6642(6)	22(1)

C(14)	1499(11)	3869(5)	6020(4)	33(2)
O(15)	1413(9)	3992(4)	6620(3)	59(2)
C(22)	-2623(8)	3970(5)	4504(4)	26(2)
C(24)	-1350(10)	4239(5)	5645(4)	32(2)
C(23)	-2698(9)	4237(5)	5155(4)	31(2)
C(32)	5912(11)	1592(6)	4455(5)	39(2)
C(34)	5833(15)	-49(7)	4269(6)	78(4)
C(35)	8303(11)	770(10)	4445(5)	83(4)

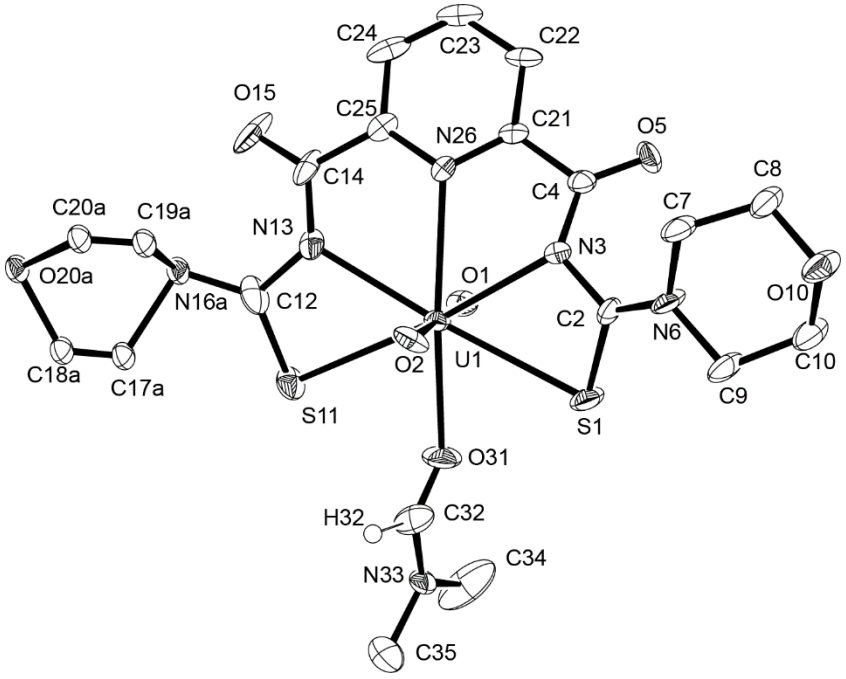

Figure A.6: Ellipsoid plot of $[UO_2(L^{2b})(DMF)]$. Hydrogen atoms except for the coordinated solvent molecule have been omitted for clarity Thermal ellipsoids are at 50 % probability.

anti,anti-$(HNEt_3)_2[\{UO_2(L^{2a})(\mu_2\text{-}OMe)\}_2]$

Table A.13: Crystal data and structure refinement for *anti,anti*-$(HNEt_3)_2[\{UO_2(L^{2a})(\mu_2\text{-}OMe)\}_2]$.

Empirical formula	$C_{48}H_{84}N_{12}O_{10}S_4U_2$	
Formula weight	1593.57	
Temperature	200(2) K	
Wavelength	0.71073 Å	
Crystal system	Triclinic	
Space group	$P\overline{1}$	
Unit cell dimensions	a = 15.705(1) Å	α= 68.70(1)°
	b = 16.060(1) Å	β= 79.47(1)°
	c = 16.014(1) Å	γ = 60.73(1)°
Volume	3282.7(5) $Å^3$	
Z	2	
Density (calculated)	1.612 g/cm^3	
Absorption coefficient	5.111 mm^{-1}	
F(000)	1568	
Crystal size	0.200 x 0.167 x 0.100 mm^3	
Theta range for data collection	4.666 to 25.499°	
Index ranges	-19<=h<=19, -19<=k<=17, -19<=l<=19	
Reflections collected	26504	
Independent reflections	12120 [R(int) = 0.0848]	
Completeness to theta = 25.242°	99.1 %	
Absorption correction	Integration	
Max. and min. transmission	0.7697 and 0.3055	
Refinement method	Full-matrix least-squares on F^2	
Data / restraints / parameters	12120 / 114 / 743	
Goodness-of-fit on F^2	1.044	
Final R indices [I>2sigma(I)]	R1 = 0.0601, wR2 = 0.1487	
R indices (all data)	R1 = 0.0764, wR2 = 0.1601	
Extinction coefficient	0.0023(3)	
Largest diff. peak and hole	2.477 and -3.984 e/$Å^3$	
Diffractometer	IPDS, STOE	

Table A.14: Atomic coordinates (x 10^4) and equivalent isotropic displacement parameters ($Å^2$ x 10^3) for *anti,anti*-$(HNEt_3)_2[\{UO_2(L^{2a})(\mu_2\text{-}OMe)\}_2]$.

	x	y	z	U(eq)
U(1)	9397(1)	6177(1)	7379(1)	42(1)
U(2)	7865(1)	4975(1)	7337(1)	44(1)
O(1)	8104(4)	4459(5)	8506(4)	50(1)
O(2)	7614(5)	5479(5)	6167(4)	57(2)
O(3)	9492(4)	5470(5)	8528(4)	51(1)
O(4)	9315(5)	6904(5)	6233(4)	56(2)
C(60)	7054(7)	7431(7)	6864(8)	65(3)
O(61)	7773(3)	6468(4)	7345(4)	43(1)
C(62)	9959(8)	4581(11)	6269(8)	86(4)
O(63)	9430(4)	4859(5)	7036(4)	48(1)
S(1)	6976(2)	9054(3)	9239(2)	83(1)
C(2)	7456(7)	9436(8)	8232(7)	61(3)
N(3)	8460(5)	9008(6)	8101(5)	53(2)
C(4)	8919(6)	8189(7)	7897(6)	53(2)
O(5)	8557(4)	7665(5)	7774(4)	56(2)
N(6)	6929(6)	10216(7)	7538(7)	70(2)
C(7)	7405(11)	10528(9)	6685(8)	88(4)
C(8)	7521(14)	9962(11)	6032(9)	123(7)
C(9)	5866(9)	10798(10)	7606(12)	105(5)
C(10)	5345(10)	10286(12)	7405(14)	125(6)
S(11)	13418(2)	2918(2)	8038(2)	61(1)
C(12)	13061(6)	4000(7)	7158(6)	50(2)
N(13)	12716(5)	4899(6)	7298(5)	48(2)
C(14)	11774(5)	5466(7)	7339(5)	46(2)
O(15)	11114(4)	5254(5)	7221(5)	54(2)
N(16)	13183(5)	4010(6)	6305(5)	55(2)
C(17)	12834(8)	4939(9)	5544(7)	71(3)
C(18)	13636(12)	5215(12)	5119(10)	106(5)
C(19)	13649(8)	3087(8)	6060(8)	70(3)
C(20)	12942(10)	2735(10)	6008(9)	84(3)
S(21)	3800(2)	7477(3)	8523(2)	81(1)
C(22)	4164(6)	7199(8)	7563(7)	61(2)
N(23)	4564(5)	6212(6)	7563(6)	56(2)
C(24)	5497(6)	5649(7)	7582(6)	50(2)

O(25)	6165(4)	5904(5)	7589(5)	55(2)
N(26)	4032(6)	7890(7)	6748(7)	69(2)
C(27)	3505(9)	8980(9)	6615(10)	87(4)
C(28)	4173(13)	9411(11)	6613(16)	151(9)
C(29)	4411(9)	7608(10)	5945(9)	82(3)
C(30)	3751(12)	7370(12)	5595(10)	99(4)
S(31)	10557(2)	501(2)	7782(2)	65(1)
C(32)	9727(6)	1407(7)	6984(6)	51(2)
N(33)	8755(5)	1850(6)	7199(5)	54(2)
C(34)	8322(6)	2723(7)	7313(5)	47(2)
O(35)	8696(4)	3308(5)	7268(4)	56(2)
N(36)	9964(5)	1700(6)	6112(5)	54(2)
C(37)	10975(7)	1176(9)	5793(7)	68(3)
C(38)	11557(8)	1707(10)	5808(8)	79(3)
C(39)	9256(8)	2477(9)	5427(7)	71(3)
C(40)	8814(11)	2091(13)	4999(9)	104(5)
C(41)	10014(6)	7748(7)	7784(6)	49(2)
C(42)	10536(7)	8219(8)	7865(7)	61(2)
C(43)	11533(7)	7724(8)	7779(7)	64(3)
C(44)	11993(7)	6828(8)	7619(6)	54(2)
C(45)	11414(6)	6412(7)	7526(5)	48(2)
N(46)	10432(5)	6923(5)	7607(5)	45(2)
C(51)	5855(6)	4604(7)	7570(6)	50(2)
C(52)	5259(6)	4170(7)	7588(6)	48(2)
C(53)	5695(8)	3233(10)	7564(9)	81(3)
C(54)	6705(7)	2651(8)	7553(8)	66(3)
C(55)	7242(6)	3177(7)	7473(6)	49(2)
N(56)	6821(5)	4095(5)	7508(5)	46(2)
N(70)	3420(7)	3479(9)	9894(7)	86(3)
C(71)	4147(11)	2557(11)	10561(9)	91(4)
C(75)	2422(9)	3863(12)	10290(9)	92(4)
C(73)	3757(10)	4266(12)	9440(8)	91(4)
C(74)	3761(12)	4822(12)	10022(9)	96(4)
C(76)	1717(12)	4632(17)	9650(10)	144(9)
C(72)	5025(13)	1932(14)	10176(13)	133(7)
N(80)	10740(40)	2290(30)	8880(40)	214(17)
C(81)	10683(19)	3029(15)	9167(14)	72(6)
C(82)	10260(30)	3300(20)	9980(19)	120(12)
C(83)	11565(19)	1730(20)	8480(20)	103(9)

C(84)	12360(20)	690(30)	8660(30)	143(17)
C(85)	10514(19)	1500(16)	9276(19)	78(8)
C(86)	9520(30)	1780(30)	9650(30)	190(30)
N(80A)	10530(20)	1560(30)	9760(40)	214(17)
C(81A)	11050(20)	540(30)	10090(20)	128(14)
C(82A)	11950(20)	-230(30)	9810(30)	160(20)
C(83A)	11201(17)	1900(20)	9316(18)	84(8)
C(84A)	10920(40)	2490(60)	8370(30)	290(50)
C(85A)	9550(20)	2140(20)	9580(20)	84(8)
C(86A)	8880(30)	1690(30)	9830(20)	131(15)

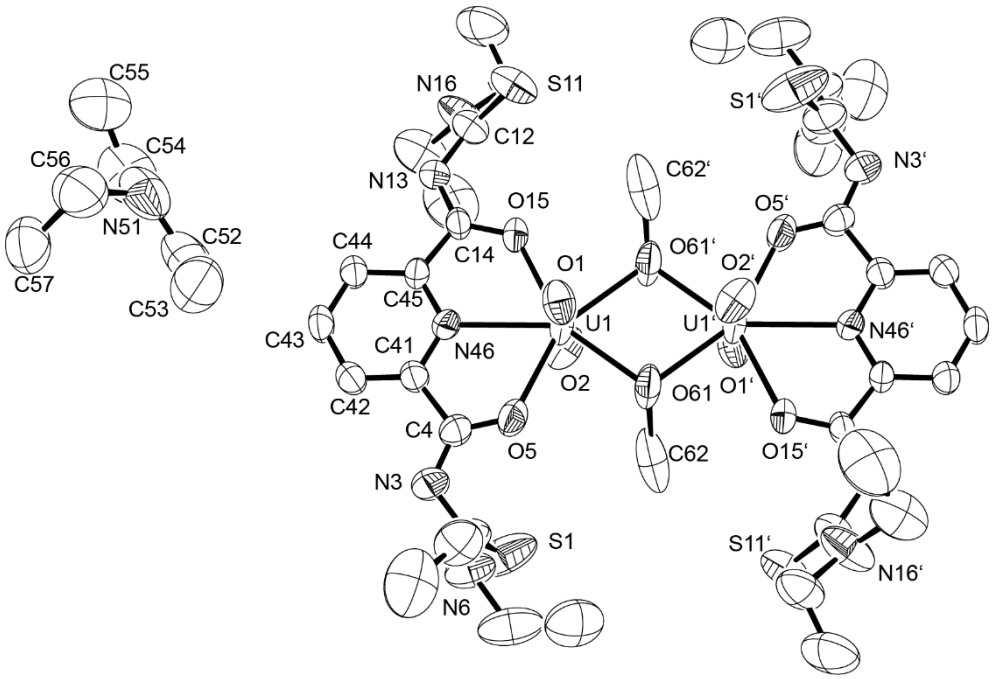

Figure A.7: Ellipsoid plot of *anti*,*anti*-$(HNEt_3)_2[\{UO_2(L^{2a})(\mu_2\text{-}OMe)\}_2]$. Hydrogen atoms have been omitted for clarity. Thermal ellipsoids are at 50 % probability.

syn,syn-$(HNEt_3)_2[\{UO_2(L^{2a})(\mu_2\text{-}OMe)\}_2]$

Table A.15: Crystal data and structure refinement for *syn,syn*-$(HNEt_3)_2[\{UO_2(L^{2a})(\mu_2\text{-}OMe)\}_2]$.

Empirical formula	$C_{48}H_{84}N_{12}O_{10}S_4U_2$	
Formula weight	1593.57	
Temperature	200(2) K	
Wavelength	0.71073 Å	
Crystal system	Monoclinic	
Space group	C 2/c	
Unit cell dimensions	a = 33.452(2) Å	α= 90°
	b = 9.702(2) Å	β= 119.96(2)°
	c = 22.278(2) Å	γ = 90°
Volume	6264(2) $Å^3$	
Z	4	
Density (calculated)	1.690 g/cm^3	
Absorption coefficient	5.357 mm^{-1}	
F(000)	3136	
Crystal size	0.22 x 0.22 x 0.04 mm^3	
Theta range for data collection	4.703 to 29.253°	
Index ranges	-45<=h<=45, -13<=k<=12, -30<=l<=28	
Reflections collected	35378	
Independent reflections	8398 [R(int) = 0.0879]	
Completeness to theta = 25.242°	99.3 %	
Absorption correction	Integration	
Max. and min. transmission	0.6468 and 0.2357	
Refinement method	Full-matrix least-squares on F^2	
Data / restraints / parameters	8398 / 1 / 365	
Goodness-of-fit on F^2	0.902	
Final R indices [I>2sigma(I)]	R1 = 0.0449, wR2 = 0.0861	
R indices (all data)	R1 = 0.1033, wR2 = 0.1006	
Largest diff. peak and hole	1.061 and -1.572 e/$Å^3$	
Diffractometer	IPDS, STOE	

Table A.16: Atomic coordinates (x 10^4) and equivalent isotropic displacement parameters ($Å^2$ x 10^3) for *syn,syn*-$(HNEt_3)_2[\{UO_2(L^{2a})(\mu_2\text{-}OMe)\}_2]$.

	x	y	z	U(eq)
U(1)	2360(1)	8519(1)	596(1)	48(1)
O(2)	2308(2)	6941(5)	957(3)	67(1)
O(1)	2409(2)	10086(5)	231(3)	75(2)
S(1)	4023(1)	8456(3)	2985(1)	82(1)
C(2)	3792(3)	10010(8)	2871(4)	64(2)
N(3)	3338(2)	10244(7)	2735(3)	59(2)
C(4)	2984(2)	9836(7)	2163(3)	48(2)
O(5)	2994(2)	9219(5)	1658(2)	57(1)
N(6)	4023(3)	11172(8)	2946(5)	99(3)
C(7)	3807(4)	12569(12)	2894(7)	120(4)
C(8)	3589(6)	13063(15)	2180(9)	162(6)
S(11)	764(1)	10972(4)	-1083(1)	134(2)
C(12)	702(3)	10009(10)	-517(4)	77(2)
N(13)	989(2)	10171(7)	201(3)	68(2)
C(14)	1406(3)	9729(8)	479(3)	55(2)
O(15)	1577(2)	8953(5)	197(2)	65(1)
N(16)	357(3)	9114(8)	-703(4)	86(2)
C(19)	30(5)	8794(17)	-1441(6)	125(5)
C(20)	-338(7)	9688(19)	-1713(10)	128(6)
C(19A)	30(5)	8794(17)	-1441(6)	125(5)
C(20A)	145(15)	7990(40)	-1840(20)	128(6)
C(41)	2519(2)	10172(7)	2048(3)	47(2)
C(42)	2427(2)	10901(8)	2504(3)	56(2)
C(43)	1982(3)	11243(8)	2299(4)	64(2)
C(44)	1622(3)	10881(8)	1641(4)	63(2)
C(45)	1734(2)	10140(7)	1213(3)	51(2)
N(46)	2177(2)	9808(5)	1417(2)	46(1)
C(56)	1314(5)	5322(15)	4151(8)	123(4)
C(57)	1010(6)	4079(18)	3952(6)	147(6)
C(54)	1436(5)	5078(14)	5387(6)	122(4)
C(55)	1062(5)	6064(12)	5295(6)	117(4)
C(52)	1909(5)	6768(12)	5156(8)	131(5)
C(53)	2299(5)	6678(11)	5890(7)	123(4)
C(9A)	4549(10)	11170(30)	3324(15)	90(6)

C(10A)	4717(8)	11050(30)	2808(13)	124(7)
C(9B)	4444(10)	11130(30)	2862(14)	90(6)
C(10B)	4817(9)	11200(30)	3584(15)	124(7)
C(17A)	398(14)	7960(50)	-260(20)	94(6)
C(18A)	-14(18)	7940(40)	-200(20)	153(9)
C(18B)	457(11)	7080(30)	-16(13)	153(9)
C(17B)	260(8)	8540(30)	-170(12)	94(6)
N(51)	1641(4)	5359(10)	4940(5)	114(3)
O(7)	2032(2)	7478(7)	-498(3)	77(2)
C(1)	1627(4)	8518(11)	-1262(7)	119(4)

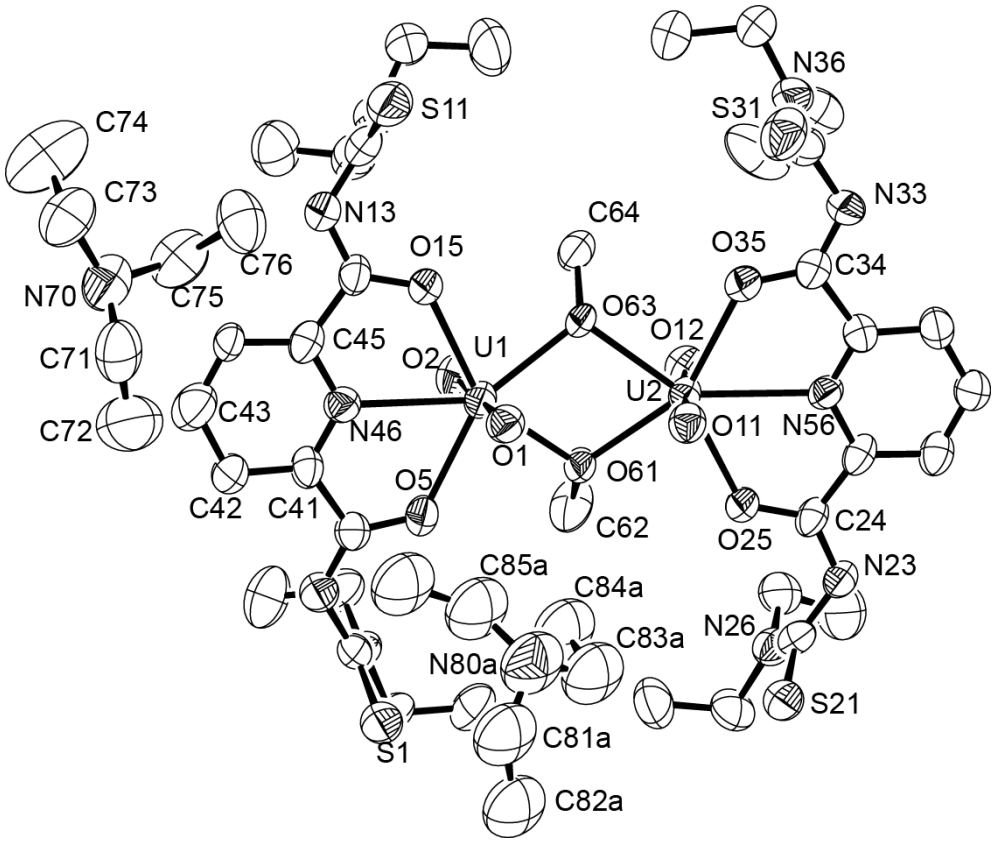

Figure A.8: Ellipsoid plot of *syn,syn*-$(HNEt_3)_2[\{UO_2(L^{2a})(\mu_2\text{-}OMe)\}_2]$. Hydrogen atoms have been omitted for clarity. Thermal ellipsoids are at 50 % probability.

anti,syn-$(EtPPh_3)_2[\{UO_2(L^{2a})(\mu_2\text{-}OMe)\}_2]$

Table A.17: Crystal data and structure refinement for *anti,syn*-$(EtPPh_3)_2[\{UO_2(L^{2a})(\mu_2\text{-}OMe)\}_2]$.

Empirical formula	$C_{76}H_{92}N_{10}O_{10}P_2S_4U_2$	
Formula weight	1971.83	
Temperature	100(2) K	
Wavelength	0.71073 Å	
Crystal system	Monoclinic	
Space group	P $2_1/n$	
Unit cell dimensions	a = 14.277(1) Å	α= 90°
	b = 25.632(1) Å	β= 97.39(2)°
	c = 22.738(1) Å	γ = 90°
Volume	8251.8(8) $Å^3$	
Z	4	
Density (calculated)	1.587 g/cm^3	
Absorption coefficient	4.120 mm^{-1}	
F(000)	3904	
Crystal size	0.42 x 0.11 x 0.08 mm^3	
Theta range for data collection	2.253 to 26.446°	
Index ranges	-17<=h<=17, -32<=k<=32, -28<=l<=28	
Reflections collected	187388	
Independent reflections	16919 [R(int) = 0.0543]	
Completeness to theta = 25.242°	99.9 %	
Absorption correction	Semi-empirical from equivalents	
Max. and min. transmission	0.7454 and 0.5066	
Refinement method	Full-matrix least-squares on F^2	
Data / restraints / parameters	16919 / 0 / 919	
Goodness-of-fit on F^2	1.088	
Final R indices [I>2sigma(I)]	R1 = 0.0314, wR2 = 0.0656	
R indices (all data)	R1 = 0.0447, wR2 = 0.0739	
Largest diff. peak and hole	1.705 and -1.386 e/$Å^3$	
Diffractometer	Bruker D8 Venture	

Table A.18: Atomic coordinates (x 10^4) and equivalent isotropic displacement parameters ($Å^2$ x 10^3) for *anti,syn*-$(EtPPh_3)_2[\{UO_2(L^{2a})(\mu_2\text{-}OMe)\}_2]$.

	x	y	z	U(eq)
U(1)	3794(1)	6376(1)	6119(1)	15(1)
U(2)	6161(1)	6594(1)	5618(1)	16(1)
P(2)	5462(1)	8555(1)	6709(1)	16(1)
P(1)	6085(1)	6039(1)	8211(1)	19(1)
S(21)	6102(1)	8831(1)	4865(1)	29(1)
S(11)	4309(1)	4648(1)	7770(1)	24(1)
S(1)	1565(1)	7928(1)	5093(1)	27(1)
S(31)	8989(1)	4990(1)	6786(1)	28(1)
O(61)	4614(2)	6924(1)	5545(1)	16(1)
O(62)	5210(2)	5954(1)	5977(1)	19(1)
O(1)	3195(2)	6106(1)	5452(1)	23(1)
O(25)	6328(2)	7427(1)	5206(1)	22(1)
O(5)	2745(2)	7090(1)	6059(1)	22(1)
O(12)	6414(2)	6885(1)	6337(1)	25(1)
O(2)	4387(2)	6642(1)	6792(1)	19(1)
O(35)	7363(2)	5968(1)	5870(1)	23(1)
O(15)	3626(2)	5578(1)	6615(1)	18(1)
O(11)	5921(2)	6326(1)	4888(1)	22(1)
N(46)	2261(3)	6241(1)	6553(2)	18(1)
N(13)	2784(3)	4952(1)	7057(2)	17(1)
N(56)	7784(3)	6825(1)	5363(2)	19(1)
N(3)	1292(3)	7478(1)	6124(2)	20(1)
N(23)	7030(3)	7983(2)	4597(2)	24(1)
N(33)	8871(3)	5631(2)	5846(2)	21(1)
N(6)	1502(3)	8360(1)	6156(2)	21(1)
C(73)	5018(3)	8182(2)	6064(2)	18(1)
N(16)	3612(3)	4264(2)	6711(2)	23(1)
C(4)	1900(3)	7100(2)	6195(2)	18(1)
N(36)	8323(3)	4792(2)	5658(2)	26(1)
N(26)	5547(3)	8104(2)	4052(2)	30(1)
C(64)	5203(4)	5434(2)	5740(2)	30(1)
C(63)	4145(3)	7101(2)	4983(2)	23(1)
C(14)	2885(3)	5408(2)	6825(2)	16(1)
C(45)	2073(3)	5780(2)	6787(2)	16(1)

C(74)	3945(3)	8219(2)	5914(2)	26(1)
C(34)	8230(3)	5988(2)	5765(2)	20(1)
C(42)	709(3)	6541(2)	6673(2)	18(1)
C(96)	4936(3)	6091(2)	8452(2)	20(1)
C(55)	7917(3)	7275(2)	5079(2)	21(1)
C(125)	4799(3)	7750(2)	7347(2)	22(1)
C(136)	6723(3)	8603(2)	6746(2)	19(1)
C(2)	1479(3)	7927(2)	5826(2)	21(1)
C(41)	1575(3)	6614(2)	6500(2)	18(1)
C(43)	515(3)	6061(2)	6908(2)	21(1)
C(71)	5980(4)	5716(2)	7502(2)	25(1)
C(22)	6204(4)	8271(2)	4488(2)	22(1)
C(44)	1197(3)	5674(2)	6966(2)	19(1)
C(126)	5129(3)	8264(2)	7370(2)	19(1)
C(12)	3554(3)	4620(2)	7134(2)	19(1)
C(32)	8680(3)	5141(2)	6061(2)	22(1)
C(24)	7031(3)	7586(2)	4952(2)	20(1)
C(91)	4121(3)	6067(2)	8050(2)	24(1)
C(111)	5286(4)	9526(2)	6194(2)	25(1)
C(135)	7212(3)	8267(2)	6406(2)	27(1)
C(54)	8790(3)	7408(2)	4922(2)	24(1)
C(121)	5198(3)	8543(2)	7900(2)	22(1)
C(51)	8503(3)	6489(2)	5492(2)	18(1)
C(17)	2971(4)	4276(2)	6142(2)	27(1)
C(116)	4962(3)	9198(2)	6617(2)	18(1)
C(53)	9548(3)	7066(2)	5060(2)	26(1)
C(131)	7218(3)	8971(2)	7121(2)	25(1)
C(52)	9396(3)	6593(2)	5336(2)	24(1)
C(114)	3705(3)	9802(2)	6726(2)	25(1)
C(92)	3247(3)	6098(2)	8245(2)	29(1)
C(106)	6616(3)	6672(2)	8159(2)	23(1)
C(86)	6793(3)	5659(2)	8767(2)	21(1)
C(20)	5169(4)	4001(2)	6474(2)	39(1)
C(124)	4510(4)	7523(2)	7850(2)	28(1)
C(72)	6904(4)	5485(2)	7338(2)	33(1)
C(19)	4321(4)	3849(2)	6764(2)	31(1)
C(38)	7303(4)	4124(2)	6025(3)	43(2)
C(115)	4176(3)	9342(2)	6884(2)	24(1)
C(93)	3176(4)	6154(2)	8842(2)	31(1)

C(9)	1618(4)	8882(2)	5907(2)	28(1)
C(95)	4875(4)	6157(2)	9056(2)	31(1)
C(84)	8015(4)	5571(2)	9599(2)	31(1)
C(7)	1403(4)	8338(2)	6789(2)	25(1)
C(133)	8676(4)	8678(2)	6808(2)	32(1)
C(122)	4915(4)	8310(2)	8399(2)	27(1)
C(134)	8188(4)	8308(2)	6438(2)	34(1)
C(132)	8189(4)	9006(2)	7146(2)	29(1)
C(85)	7530(3)	5877(2)	9152(2)	25(1)
C(37)	8230(4)	4236(2)	5805(3)	35(1)
C(112)	4821(4)	9987(2)	6041(2)	31(1)
C(83)	7773(4)	5053(2)	9654(2)	36(1)
C(123)	4566(4)	7799(2)	8371(2)	31(1)
C(8)	2343(4)	8246(2)	7172(2)	34(1)
C(105)	7016(4)	6813(2)	7660(2)	37(1)
C(29)	4637(4)	8375(2)	3889(2)	39(1)
C(94)	3991(4)	6189(2)	9244(2)	37(1)
C(101)	6621(4)	7022(2)	8625(2)	35(1)
C(81)	6555(4)	5133(2)	8827(2)	33(1)
C(113)	4032(4)	10124(2)	6303(2)	32(1)
C(104)	7432(5)	7302(2)	7629(3)	50(2)
C(82)	7061(4)	4833(2)	9270(3)	40(1)
C(10)	669(4)	9135(2)	5696(2)	37(1)
C(102)	7052(4)	7511(2)	8598(3)	41(1)
C(27)	5681(4)	7621(2)	3722(2)	35(1)
C(28)	6370(5)	7698(2)	3275(3)	47(2)
C(103)	7451(5)	7647(2)	8100(3)	42(2)
C(18)	2082(4)	3962(2)	6177(3)	44(2)
C(30)	4557(4)	8624(2)	3285(3)	45(1)
C(39)	8005(3)	4929(2)	5032(2)	26(1)
C(40)	8774(4)	4854(3)	4644(3)	48(2)

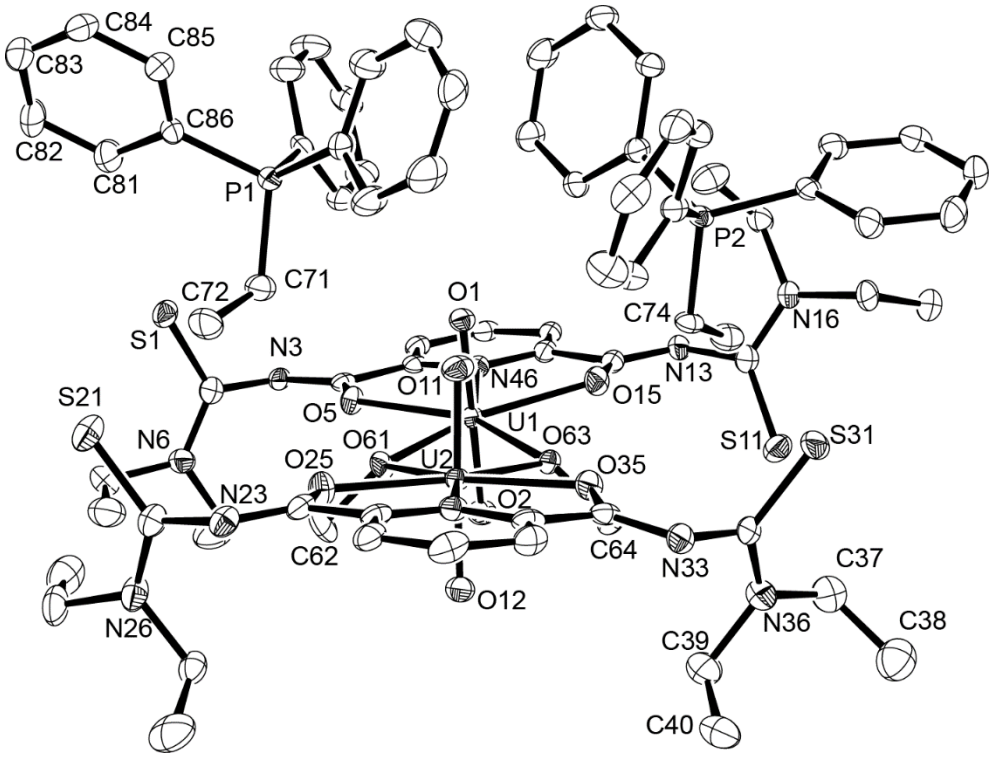

Figure A.9: Ellipsoid plot of *anti*,*syn*-$(EtPPh_3)_2[\{UO_2(L^{2a})(\mu_2\text{-}OMe)\}_2]$. Hydrogen atoms have been omitted for clarity. Thermal ellipsoids are at 50 % probability.

anti,anti-$(EtPPh_3)_2[\{UO_2(L^{2b})(\mu_2\text{-}OMe)\}_2]$

Table A.19: Crystal data and structure refinement for *anti,anti*-$(EtPPh_3)_2[\{UO_2(L^{2b})(\mu_2\text{-}OMe)\}_2] \cdot 1.5\ H_2O \cdot 1.5\ CH_3OH$.

Empirical formula	$C_{78}H_{90}N_{10}O_{17}P_2S_4U_2$	
Formula weight	2105.33	
Temperature	174(2) K	
Wavelength	0.71073 Å	
Crystal system	Triclinic	
Space group	$P\overline{1}$	
Unit cell dimensions	a = 12.009(6) Å	α= 91.38(2)°
	b = 14.640(9) Å	β= 90.96(2)°
	c = 25.11(2) Å	γ = 94.32(1)°
Volume	4400(5) $Å^3$	
Z	2	
Density (calculated)	1.589 g/cm^3	
Absorption coefficient	3.875 mm^{-1}	
F(000)	2083	
Crystal size	0.230 x 0.190 x 0.130 mm^3	
Theta range for data collection	2.167 to 27.095°	
Index ranges	-14<=h<=15, -18<=k<=18, -32<=l<=32	
Reflections collected	98355	
Independent reflections	19332 [R(int) = 0.0325]	
Completeness to theta = 25.242°	99.7 %	
Absorption correction	Semi-empirical from equivalents	
Max. and min. transmission	0.7455 and 0.5734	
Refinement method	Full-matrix least-squares on F^2	
Data / restraints / parameters	19332 / 0 / 1058	
Goodness-of-fit on F^2	1.086	
Final R indices [I>2sigma(I)]	R1 = 0.0283, wR2 = 0.0687	
R indices (all data)	R1 = 0.0310, wR2 = 0.0700	
Extinction coefficient	0.00239(8)	
Largest diff. peak and hole	1.831 and -0.852 e/$Å^3$	
Diffractometer	Bruker D8 Venture	

Table A.20: Atomic coordinates (x 10^4) and equivalent isotropic displacement parameters ($Å^2$ x 10^3) for *ant,anti*-$(EtPPh_3)_2[\{UO_2(L^{2b})(\mu_2\text{-}OMe)\}_2] \cdot 2\ H_2O \cdot 1.5\ CH_3OH$.

	x	y	z	U(eq)
U(1)	6118(1)	9933(1)	5545(1)	15(1)
U(2)	3491(1)	5119(1)	9768(1)	14(1)
O(1)	5055(2)	9845(2)	6035(1)	21(1)
O(2)	7180(2)	10043(2)	5052(1)	22(1)
O(11)	3927(2)	5012(2)	9095(1)	20(1)
O(12)	3064(2)	5229(2)	10446(1)	21(1)
S(1)	8134(1)	13653(1)	6138(1)	29(1)
C(2)	7418(3)	12920(3)	6523(2)	32(1)
N(3)	7886(3)	12101(2)	6666(1)	25(1)
C(4)	7590(3)	11364(2)	6384(1)	20(1)
O(5)	6895(2)	11293(2)	5986(1)	23(1)
S(11)	5528(1)	6248(1)	6219(1)	51(1)
C(12)	6737(4)	6592(3)	5943(2)	38(1)
N(13)	7421(3)	7316(2)	6183(1)	30(1)
C(14)	7223(3)	8150(2)	6082(1)	21(1)
O(15)	6531(2)	8419(2)	5729(1)	24(1)
N(16)	7164(4)	6166(2)	5520(2)	51(1)
C(17)	6616(6)	5340(3)	5265(2)	66(2)
C(18)	6419(6)	5527(3)	4677(2)	61(2)
C(19)	8190(5)	6487(4)	5247(2)	64(2)
C(20)	7921(6)	6600(4)	4660(2)	66(2)
O(20)	7390(4)	5801(3)	4413(2)	72(1)
S(21)	1039(1)	1542(1)	9900(1)	40(1)
C(22)	1182(4)	2152(3)	9345(2)	32(1)
N(23)	666(3)	2985(2)	9313(1)	28(1)
C(24)	1262(3)	3725(2)	9454(1)	19(1)
O(25)	2281(2)	3788(2)	9638(1)	21(1)
N(26)	1698(4)	1874(3)	8906(2)	48(1)
C(27)	1809(5)	2398(3)	8417(2)	51(1)
C(28)	3006(5)	2592(3)	8290(2)	54(1)
C(29)	2273(5)	1029(3)	8867(2)	52(1)
C(30)	3479(5)	1256(3)	8721(2)	52(1)
O(30)	3559(4)	1752(2)	8235(1)	54(1)
S(31)	3582(1)	8870(1)	9021(1)	46(1)

C(32)	2762(3)	8447(2)	9505(2)	29(1)
N(33)	1900(2)	7771(2)	9390(1)	23(1)
C(34)	2108(3)	6928(2)	9474(1)	18(1)
O(35)	3049(2)	6647(2)	9632(1)	21(1)
N(36)	2839(4)	8733(3)	10014(2)	47(1)
C(37)	3760(5)	9389(4)	10214(3)	70(2)
C(38)	3331(6)	10099(5)	10550(3)	78(2)
C(39)	2108(5)	8380(4)	10442(2)	56(1)
C(40)	1752(6)	9169(6)	10745(3)	84(2)
O(40)	2699(5)	9714(5)	10980(2)	113(2)
C(41)	8058(3)	10483(2)	6548(1)	18(1)
C(42)	8867(3)	10406(2)	6942(1)	24(1)
C(43)	9163(3)	9534(3)	7068(1)	26(1)
C(44)	8645(3)	8771(2)	6803(1)	23(1)
C(45)	7858(3)	8902(2)	6405(1)	20(1)
N(46)	7583(2)	9744(2)	6278(1)	17(1)
C(51)	756(3)	4623(2)	9382(1)	15(1)
C(52)	-359(3)	4724(2)	9260(1)	20(1)
C(53)	-701(3)	5604(3)	9211(1)	23(1)
C(54)	69(3)	6359(2)	9280(1)	21(1)
C(55)	1178(3)	6198(2)	9389(1)	16(1)
N(56)	1503(2)	5349(2)	9450(1)	15(1)
O(61)	4989(2)	10925(2)	5105(1)	16(1)
C(62)	4450(3)	11579(2)	5429(1)	24(1)
O(62)	4806(2)	4064(2)	9984(1)	15(1)
C(64)	4823(3)	3246(2)	9653(1)	22(1)
P(1)	2069(1)	7886(1)	5945(1)	18(1)
P(2)	5388(1)	6802(1)	8216(1)	26(1)
C(71)	3446(3)	7793(2)	5680(1)	21(1)
C(72)	3565(3)	7098(3)	5224(2)	29(1)
C(73)	5578(3)	6996(3)	8923(1)	24(1)
C(74)	6783(3)	7270(3)	9121(2)	29(1)
C(81)	2074(3)	8464(3)	7013(2)	31(1)
C(82)	2254(4)	9128(3)	7424(2)	40(1)
C(83)	2571(4)	10027(3)	7305(2)	43(1)
C(84)	2694(4)	10283(3)	6779(2)	39(1)
C(85)	2519(3)	9632(3)	6366(2)	28(1)
C(86)	2208(3)	8722(3)	6485(1)	23(1)
C(91)	277(3)	8837(3)	5612(2)	30(1)

C(92)	-528(3)	9065(3)	5249(2)	41(1)
C(93)	-520(4)	8734(4)	4728(2)	44(1)
C(94)	295(4)	8164(4)	4567(2)	40(1)
C(95)	1088(3)	7912(3)	4935(2)	30(1)
C(96)	1087(3)	8248(2)	5457(1)	22(1)
C(101)	379(4)	6615(4)	6202(2)	47(1)
C(102)	-49(5)	5773(4)	6376(2)	66(2)
C(103)	668(5)	5123(4)	6544(2)	57(2)
C(105)	2247(4)	6156(3)	6354(2)	33(1)
C(104)	1793(5)	5315(3)	6534(2)	45(1)
C(106)	1533(3)	6801(3)	6185(1)	25(1)
C(121)	3832(6)	5383(3)	7871(2)	64(2)
C(122)	2773(8)	4994(4)	7791(3)	88(3)
C(123)	1875(7)	5480(5)	7903(2)	76(2)
C(124)	2021(5)	6375(4)	8104(2)	56(2)
C(125)	3098(4)	6776(3)	8190(2)	37(1)
C(126)	4009(4)	6280(3)	8074(1)	34(1)
C(131)	6004(6)	8654(3)	8107(2)	59(2)
C(132)	6080(6)	9470(4)	7826(2)	63(2)
C(133)	5667(4)	9485(3)	7316(2)	39(1)
C(134)	5185(4)	8695(4)	7076(2)	49(1)
C(135)	5106(4)	7880(3)	7351(2)	41(1)
C(136)	5536(3)	7862(3)	7869(1)	27(1)
O(34)	1177(6)	3265(4)	7268(2)	51(2)
C(142)	1310(7)	2669(6)	6823(4)	39(2)
C(80A)	6563(5)	6137(4)	7984(3)	39(1)
C(75A)	7203(5)	6399(4)	7549(2)	39(1)
C(76A)	8042(5)	5863(4)	7378(2)	39(1)
C(77A)	8241(5)	5066(4)	7641(2)	39(1)
C(78A)	7601(6)	4803(4)	8076(2)	39(1)
C(79A)	6762(5)	5339(5)	8247(2)	39(1)
C(80B)	6212(5)	5917(4)	8001(2)	39(1)
C(75B)	6657(5)	5916(3)	7494(2)	39(1)
C(76B)	7326(5)	5227(4)	7336(2)	39(1)
C(77B)	7550(4)	4540(3)	7686(2)	39(1)
C(78B)	7105(5)	4541(3)	8193(2)	39(1)
C(79B)	6436(5)	5229(4)	8351(2)	39(1)
N(6A)	6289(7)	12963(6)	6603(4)	25(2)
C(9A)	5626(8)	12240(6)	6874(4)	31(2)

C(10A)	4803(12)	12643(10)	7246(6)	44(3)
O(10A)	4220(20)	13150(17)	6986(11)	86(8)
C(8A)	4769(18)	13982(13)	6780(8)	45(4)
C(7A)	5631(8)	13684(6)	6383(4)	36(3)
N(6B)	6576(6)	13158(5)	6854(3)	29(2)
C(8B)	4844(12)	13768(10)	6613(5)	35(3)
C(7B)	6016(7)	14009(5)	6779(3)	35(2)
C(10B)	4828(10)	12348(8)	7053(5)	41(2)
C(9B)	6002(7)	12551(5)	7238(3)	34(2)
O(10B)	4182(13)	13233(9)	6986(7)	39(4)
O(31)	9103(5)	2616(4)	7596(2)	40(2)
C(141)	8690(9)	2275(7)	8051(4)	50(3)
O(36)	-525(4)	7927(4)	8212(2)	28(1)
O(37)	628(5)	8579(4)	8571(2)	34(1)
O(32)	9996(5)	7729(4)	7673(3)	43(2)
O(33)	135(7)	10927(6)	11220(4)	68(2)
C(144)	158(9)	10114(8)	11533(4)	53(2)
C(143)	9109(11)	7121(9)	7792(5)	63(3)

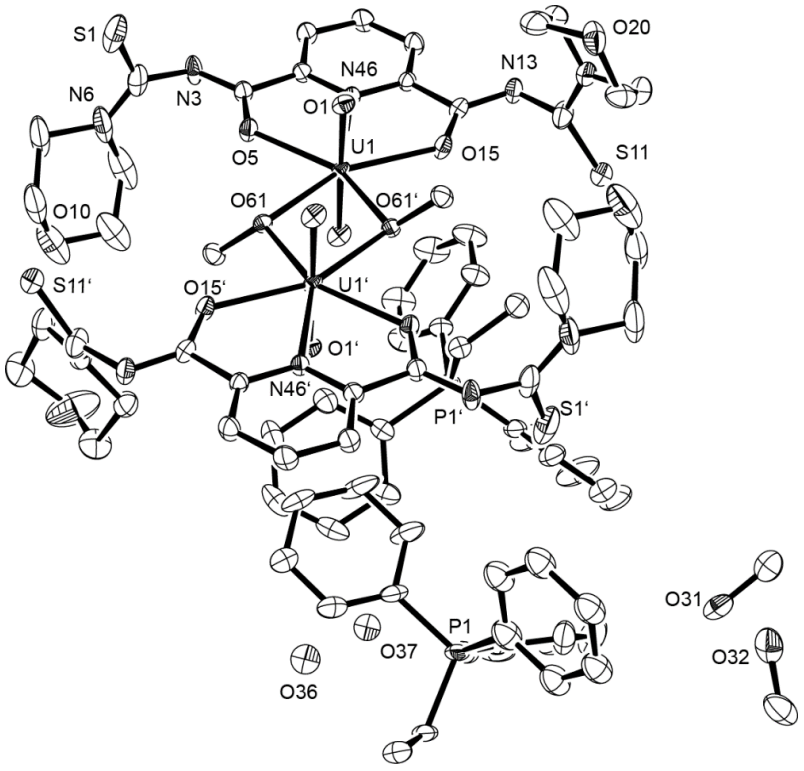

Figure A.10: Ellipsoid plot of *anti,anti*-$(EtPPh_3)_2[\{UO_2(L^{2b})(\mu_2\text{-}OMe)\}_2] \cdot 2\ H_2O \cdot 1.5\ CH_3OH$. Hydrogen atoms have been omitted for clarity. Thermal ellipsoids are at 50 % probability.

anti,anti-(EtPPh$_3$)$_2$[{UO$_2$(L^{2b})(μ$_2$-OMe)}$_2$] (SQUEEZE)

Table A.21: Crystal data and structure refinement for *anti,anti*-(EtPPh$_3$)$_2$[{UO$_2$(L^{2b})(μ$_2$-OMe)}$_2$] **(SQUEEZE)**.

Empirical formula	$C_{76}H_{84}N_{10}O_{14}P_2S_4U_2$	
Formula weight	2027.77	
Temperature	174(2) K	
Wavelength	0.71073 Å	
Crystal system	Triclinic	
Space group	$P\overline{1}$	
Unit cell dimensions	a = 12.009(6) Å	α= 91.38(2)°
	b = 14.640(9) Å	β= 90.96(2)°
	c = 25.11(2) Å	γ = 94.32(1)°
Volume	4400(5) Å^3	
Z	2	
Density (calculated)	1.530 g/cm^3	
Absorption coefficient	3.869 mm^{-1}	
F(000)	2000	
Crystal size	0.230 x 0.190 x 0.130 mm^3	
Theta range for data collection	2.167 to 27.095°.	
Index ranges	-14<=h<=15, -18<=k<=18, -32<=l<=32	
Reflections collected	98424	
Independent reflections	19345 [R(int) = 0.0324]	
Completeness to theta = 25.242°	99.8 %	
Absorption correction	Semi-empirical from equivalents	
Max. and min. transmission	0.7455 and 0.5734	
Refinement method	Full-matrix least-squares on F^2	
Data / restraints / parameters	19345 / 3 / 930	
Goodness-of-fit on F^2	1.095	
Final R indices [I>2sigma(I)]	R1 = 0.0242, wR2 = 0.0526	
R indices (all data)	R1 = 0.0266, wR2 = 0.0535	
Extinction coefficient	0.00233(6)	
Largest diff. peak and hole	1.142 and -0.798 e/Å^3	
Diffractometer	Bruker D8 Venture	

Table A.22: Atomic coordinates (x 10^4) and equivalent isotropic displacement parameters ($Å^2$ x 10^3) for $(EtPPh_3)_2[\{UO_2(L^{2b})(\mu_2\text{-}OMe)\}_2]$ **(SQUEEZE)**.

	x	y	z	U(eq)
U(1)	6118(1)	9933(1)	5545(1)	15(1)
U(2)	3491(1)	5119(1)	9768(1)	14(1)
O(1)	5057(2)	9846(1)	6035(1)	21(1)
O(2)	7179(2)	10044(1)	5052(1)	22(1)
O(3)	3926(2)	5011(1)	9094(1)	20(1)
O(4)	3064(2)	5228(1)	10446(1)	21(1)
S(1)	8134(1)	13653(1)	6138(1)	29(1)
C(2)	7420(3)	12920(2)	6523(1)	31(1)
N(3)	7887(2)	12102(2)	6666(1)	25(1)
C(4)	7589(2)	11364(2)	6384(1)	19(1)
O(5)	6893(2)	11292(1)	5986(1)	22(1)
S(11)	5528(1)	6248(1)	6219(1)	51(1)
C(12)	6743(3)	6594(2)	5943(1)	39(1)
N(13)	7423(2)	7315(2)	6182(1)	30(1)
C(14)	7224(2)	8151(2)	6082(1)	21(1)
O(15)	6532(2)	8419(1)	5728(1)	23(1)
N(16)	7169(3)	6167(2)	5519(1)	50(1)
C(17)	6618(5)	5338(3)	5263(2)	66(2)
C(18)	6417(5)	5527(3)	4676(2)	61(1)
C(19)	8189(4)	6487(3)	5246(2)	63(1)
C(20)	7917(4)	6603(3)	4658(2)	67(1)
O(20)	7386(3)	5801(3)	4413(1)	75(1)
S(21)	1039(1)	1542(1)	9899(1)	40(1)
C(22)	1181(3)	2153(2)	9346(1)	32(1)
N(23)	667(2)	2984(2)	9313(1)	28(1)
C(24)	1263(2)	3724(2)	9455(1)	19(1)
O(25)	2280(2)	3788(1)	9638(1)	21(1)
N(26)	1696(3)	1876(2)	8906(1)	48(1)
C(27)	1805(4)	2401(3)	8416(1)	52(1)
C(28)	3008(4)	2590(3)	8290(2)	55(1)
C(29)	2275(4)	1028(3)	8867(2)	53(1)
C(30)	3483(4)	1256(3)	8720(2)	52(1)
O(30)	3561(3)	1752(2)	8236(1)	54(1)
S(31)	3581(1)	8870(1)	9021(1)	46(1)

C(32)	2762(3)	8445(2)	9506(1)	29(1)
N(33)	1901(2)	7771(2)	9390(1)	23(1)
C(34)	2109(2)	6929(2)	9473(1)	18(1)
O(35)	3050(2)	6646(1)	9632(1)	21(1)
N(36A)	2840(3)	8733(3)	10013(1)	56(1)
C(37A)	3787(5)	9367(4)	10207(2)	56(1)
C(38A)	3329(5)	10110(4)	10553(2)	56(1)
C(39A)	2142(7)	8355(6)	10441(4)	56(1)
C(40A)	1747(5)	9186(4)	10745(2)	56(1)
O(40A)	2671(3)	9764(3)	10967(2)	56(1)
N(36B)	2840(3)	8733(3)	10013(1)	56(1)
C(37B)	3340(20)	9708(16)	10213(9)	56(1)
C(38B)	3881(18)	9387(15)	10668(8)	56(1)
C(39B)	1950(30)	8480(20)	10440(14)	56(1)
C(40B)	2311(18)	8435(15)	10870(8)	56(1)
O(40B)	3090(12)	9161(10)	11086(6)	56(1)
C(41)	8059(2)	10482(2)	6548(1)	18(1)
C(42)	8868(2)	10405(2)	6942(1)	24(1)
C(43)	9163(3)	9534(2)	7067(1)	26(1)
C(44)	8645(2)	8772(2)	6803(1)	24(1)
C(45)	7860(2)	8902(2)	6406(1)	19(1)
N(46)	7583(2)	9744(2)	6277(1)	16(1)
C(51)	755(2)	4623(2)	9383(1)	16(1)
C(52)	-359(2)	4726(2)	9260(1)	19(1)
C(53)	-702(2)	5603(2)	9212(1)	23(1)
C(54)	69(2)	6358(2)	9279(1)	21(1)
C(55)	1177(2)	6197(2)	9389(1)	16(1)
N(56)	1503(2)	5349(2)	9451(1)	15(1)
O(61)	4989(2)	10924(1)	5105(1)	16(1)
C(62)	4452(2)	11580(2)	5430(1)	24(1)
O(62)	4805(1)	4064(1)	9984(1)	15(1)
C(64)	4822(2)	3247(2)	9653(1)	22(1)
P(1)	2069(1)	7886(1)	5944(1)	18(1)
P(2)	5388(1)	6802(1)	8216(1)	26(1)
C(71)	3444(2)	7794(2)	5680(1)	21(1)
C(72)	3562(3)	7096(2)	5223(1)	29(1)
C(73)	5576(3)	6996(2)	8923(1)	24(1)
C(74)	6782(3)	7269(2)	9122(1)	30(1)
C(81)	2073(3)	8465(2)	7013(1)	31(1)

C(82)	2253(3)	9130(3)	7424(1)	40(1)
C(83)	2567(3)	10026(3)	7305(2)	43(1)
C(84)	2693(3)	10283(2)	6779(2)	39(1)
C(85)	2519(2)	9632(2)	6367(1)	28(1)
C(86)	2208(2)	8722(2)	6485(1)	23(1)
C(91)	277(2)	8834(2)	5612(1)	30(1)
C(92)	-527(3)	9063(3)	5250(2)	41(1)
C(93)	-520(3)	8730(3)	4729(1)	43(1)
C(94)	294(3)	8165(3)	4568(1)	40(1)
C(95)	1086(3)	7910(2)	4935(1)	30(1)
C(96)	1087(2)	8248(2)	5457(1)	22(1)
C(101)	381(3)	6612(3)	6201(2)	47(1)
C(102)	-45(4)	5768(4)	6376(2)	68(2)
C(103)	659(4)	5129(3)	6545(2)	57(1)
C(105)	2248(3)	6156(2)	6353(1)	33(1)
C(104)	1789(4)	5318(3)	6533(1)	45(1)
C(106)	1532(3)	6801(2)	6184(1)	24(1)
C(121)	3831(5)	5383(3)	7872(2)	64(2)
C(122)	2772(6)	4993(3)	7791(2)	86(2)
C(123)	1880(5)	5479(4)	7903(2)	76(2)
C(124)	2023(4)	6375(3)	8103(1)	55(1)
C(125)	3099(3)	6775(3)	8190(1)	37(1)
C(126)	4008(3)	6281(2)	8074(1)	34(1)
C(131)	6010(5)	8653(3)	8106(2)	60(1)
C(132)	6083(5)	9468(3)	7826(2)	63(1)
C(133)	5669(3)	9483(3)	7314(1)	39(1)
C(134)	5189(3)	8693(3)	7076(2)	49(1)
C(135)	5109(3)	7882(3)	7352(1)	41(1)
C(136)	5536(3)	7861(2)	7869(1)	27(1)
C(80A)	6563(4)	6135(3)	7985(2)	39(1)
C(75A)	7204(4)	6400(3)	7551(2)	39(1)
C(76A)	8045(4)	5866(3)	7380(2)	39(1)
C(77A)	8244(4)	5068(3)	7642(2)	39(1)
C(78A)	7603(4)	4803(3)	8076(2)	39(1)
C(79A)	6763(4)	5337(4)	8247(2)	39(1)
C(80B)	6213(4)	5917(3)	8001(2)	39(1)
C(75B)	6660(4)	5917(3)	7494(2)	39(1)
C(76B)	7331(4)	5230(3)	7337(1)	39(1)
C(77B)	7554(4)	4542(3)	7686(2)	39(1)

C(78B)	7107(4)	4541(3)	8193(2)	39(1)
C(79B)	6437(4)	5229(3)	8351(1)	39(1)
N(6A)	6295(6)	12960(5)	6605(3)	38(1)
C(9A)	5626(7)	12237(5)	6876(3)	38(1)
C(10A)	4803(7)	12653(6)	7237(4)	38(1)
O(10A)	4208(7)	13070(4)	6963(4)	38(1)
C(8A)	4789(8)	14002(6)	6767(4)	38(1)
C(7A)	5633(7)	13681(5)	6379(3)	36(2)
N(6B)	6577(5)	13162(4)	6852(3)	38(1)
C(8B)	4826(6)	13747(5)	6612(3)	38(1)
C(7B)	6022(5)	14005(4)	6780(3)	35(1)
C(10B)	4812(6)	12332(5)	7059(3)	38(1)
C(9B)	6005(5)	12555(4)	7240(3)	38(1)
O(10B)	4185(6)	13308(3)	7007(3)	38(1)

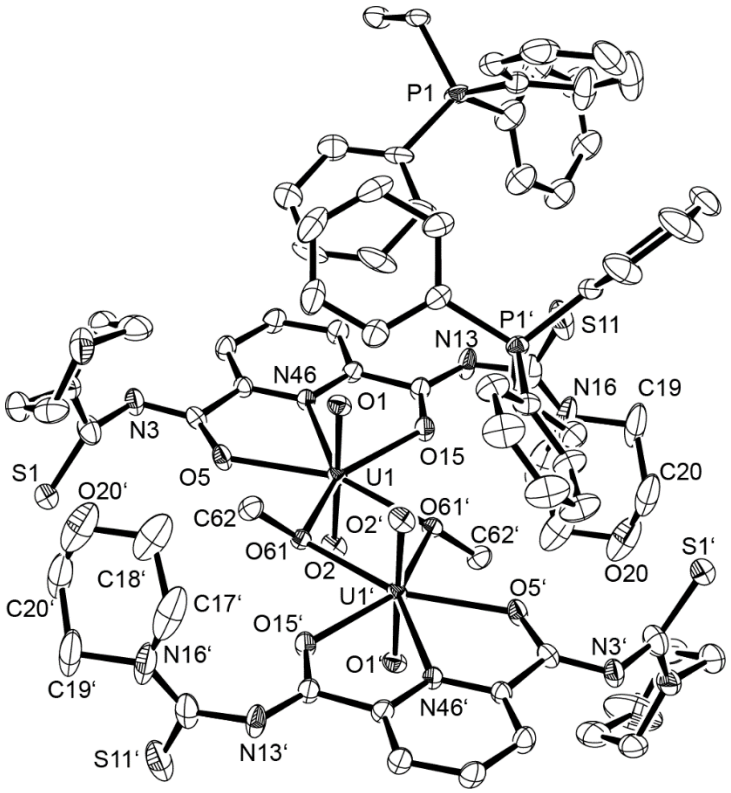

Figure A.11: Ellipsoid plot of *anti,anti*-$(EtPPh_3)_2[\{UO_2(L^{2b})(\mu_2\text{-}OMe)\}_2]$ **(SQUEEZE).** Hydrogen atoms have been omitted for clarity. Thermal ellipsoids are at 50 % probability.

$(HNEt_3)[(UO_2)_3(L^{2a**})_2(\mu_2–OH)(\mu_3\text{-}O)]$

Table A.23: Crystal data and structure refinement for $(HNEt_3)[(UO_2)_3(L^{2a**})_2(\mu_2\text{-}OH)(\mu_3\text{-}O)] \cdot H_2O$.

Empirical formula	$C_{40}H_{65}N_{11}O_{15}S_2U_3$	
Formula weight	1718.24	
Temperature	200(2) K	
Wavelength	0.71073 Å	
Crystal system	Monoclinic	
Space group	C 2/c	
Unit cell dimensions	a = 38.356(2) Å	α= 90°
	b = 9.525(1) Å	β= 110.67(2)°
	c = 34.782(2) Å	γ = 90°
Volume	11889(2) $Å^3$	
Z	8	
Density (calculated)	1.920 g/cm^3	
Absorption coefficient	8.288 mm^{-1}	
F(000)	6480	
Crystal size	0.18 x 0.04 x 0.04 mm^3	
Theta range for data collection	4.589 to 25.000°.	
Index ranges	-44<=h<=45, -11<=k<=11, -41<=l<=41	
Reflections collected	43654	
Independent reflections	10410 [R(int) = 0.0933]	
Completeness to theta = 25.000°	99.3 %	
Absorption correction	Integration	
Max. and min. transmission	0.7866 and 0.4448	
Refinement method	Full-matrix least-squares on F^2	
Data / restraints / parameters	10410 / 45 / 643	
Goodness-of-fit on F^2	0.861	
Final R indices [I>2sigma(I)]	R1 = 0.0475, wR2 = 0.0850	
R indices (all data)	R1 = 0.0965, wR2 = 0.0967	
Largest diff. peak and hole	0.905 and -1.405 e/$Å^3$	
Diffractometer	IPDS, STOE	

Table A.24: Atomic coordinates (x 10^4) and equivalent isotropic displacement parameters ($Å^2$ x 10^3) for $(HNEt_3)[(UO_2)_3(L^{2a**})_2(\mu_2\text{-}OH)(\mu_3\text{-}O)] \cdot H_2O$.

	x	y	z	U(eq)
U(1)	1082(1)	-882(1)	935(1)	38(1)
U(2)	2028(1)	-1758(1)	926(1)	37(1)
U(3)	1335(1)	277(1)	-2(1)	37(1)
S(11)	526(2)	-3753(5)	1961(1)	94(2)
S(31)	3101(1)	-5712(4)	2077(1)	68(1)
O(1)	814(2)	1474(9)	-442(3)	52(2)
O(61)	1469(2)	-805(9)	592(3)	52(2)
O(12)	846(2)	-2364(8)	657(3)	46(2)
O(11)	1288(2)	645(8)	1215(3)	50(2)
O(5)	823(2)	510(8)	293(2)	42(2)
O(32)	1896(2)	-3367(8)	655(2)	44(2)
O(31)	2190(2)	-187(8)	1200(3)	49(2)
O(42)	1151(2)	-1309(8)	-264(3)	49(2)
O(41)	1503(2)	1887(8)	235(3)	51(2)
O(62)	1613(2)	-2304(8)	1281(2)	42(2)
O(15)	797(2)	-1300(9)	1421(3)	51(2)
O(21)	1633(2)	611(10)	-465(3)	59(3)
O(25)	1989(2)	-638(8)	264(2)	38(2)
O(35)	2539(2)	-2893(9)	1385(3)	49(2)
N(3)	351(2)	1912(10)	-158(3)	39(2)
N(6)	347(2)	2953(10)	-750(3)	42(2)
N(13)	309(3)	-1186(12)	1661(3)	53(3)
N(16)	628(4)	-1312(17)	2358(4)	87(4)
N(23)	2268(2)	7(10)	-218(3)	42(2)
N(26)	1992(2)	1133(10)	-830(3)	40(2)
N(33)	3164(3)	-3410(11)	1675(3)	49(3)
N(36)	3127(3)	-3042(13)	2328(3)	64(3)
N(46)	442(2)	199(9)	778(3)	33(2)
N(56)	2611(2)	-1749(10)	744(3)	36(2)
C(2)	524(3)	2085(12)	-444(4)	41(3)
C(4)	509(3)	1157(12)	169(4)	35(2)
C(7)	-10(3)	3652(13)	-787(4)	51(3)
C(8)	58(4)	5005(17)	-545(6)	94(6)
C(9)	498(4)	3232(16)	-1075(4)	61(4)

C(10)	780(7)	4390(30)	-965(7)	152(10)
C(12)	504(4)	-2005(16)	2008(4)	60(4)
C(14)	468(3)	-920(14)	1398(4)	47(3)
C(17)	835(5)	-2010(30)	2748(5)	127(8)
C(18)	568(6)	-2400(30)	2961(7)	157(10)
C(19)	550(6)	250(20)	2376(6)	122(7)
C(20)	860(6)	1010(30)	2321(9)	179(12)
C(22)	1946(3)	606(13)	-491(4)	40(3)
C(24)	2260(3)	-567(11)	119(3)	35(3)
C(27)	2361(3)	1154(14)	-878(4)	50(3)
C(28)	2603(4)	2333(17)	-651(5)	80(5)
C(29)	1676(3)	1762(14)	-1152(4)	53(3)
C(30)	1702(5)	3314(19)	-1199(7)	128(8)
C(32)	3122(3)	-3955(15)	2031(4)	52(3)
C(34)	2872(3)	-2928(12)	1384(3)	38(3)
C(37)	3098(5)	-1510(20)	2266(5)	96(6)
C(38)	3466(6)	-900(30)	2359(8)	145(9)
C(39)	3123(5)	-3524(18)	2724(4)	85(5)
C(40)	2730(6)	-3730(20)	2722(6)	121(7)
C(41)	282(2)	1003(11)	443(3)	31(2)
C(42)	-72(3)	1568(12)	350(4)	36(3)
C(43)	-250(3)	1355(12)	632(4)	46(3)
C(44)	-88(3)	551(12)	978(4)	47(3)
C(45)	264(3)	-28(12)	1040(4)	38(3)
C(51)	2617(3)	-1209(12)	396(4)	39(3)
C(52)	2946(3)	-1202(12)	289(4)	41(3)
C(53)	3261(3)	-1845(13)	567(4)	46(3)
C(54)	3255(3)	-2413(12)	931(4)	45(3)
C(55)	2921(3)	-2352(13)	1010(4)	43(3)
N(60)	1315(3)	4827(10)	1035(3)	50(3)
C(61)	1037(4)	4467(16)	592(5)	77(5)
C(62)	1132(4)	4946(17)	250(5)	74(4)
C(63)	1632(4)	3877(16)	1130(5)	77(4)
C(64)	1964(4)	4305(16)	1506(5)	83(5)
C(65)	1110(4)	4915(15)	1325(5)	66(4)
C(66)	917(4)	3601(15)	1383(5)	76(5)
O(2)	1539(4)	-2453(15)	2042(4)	114(4)

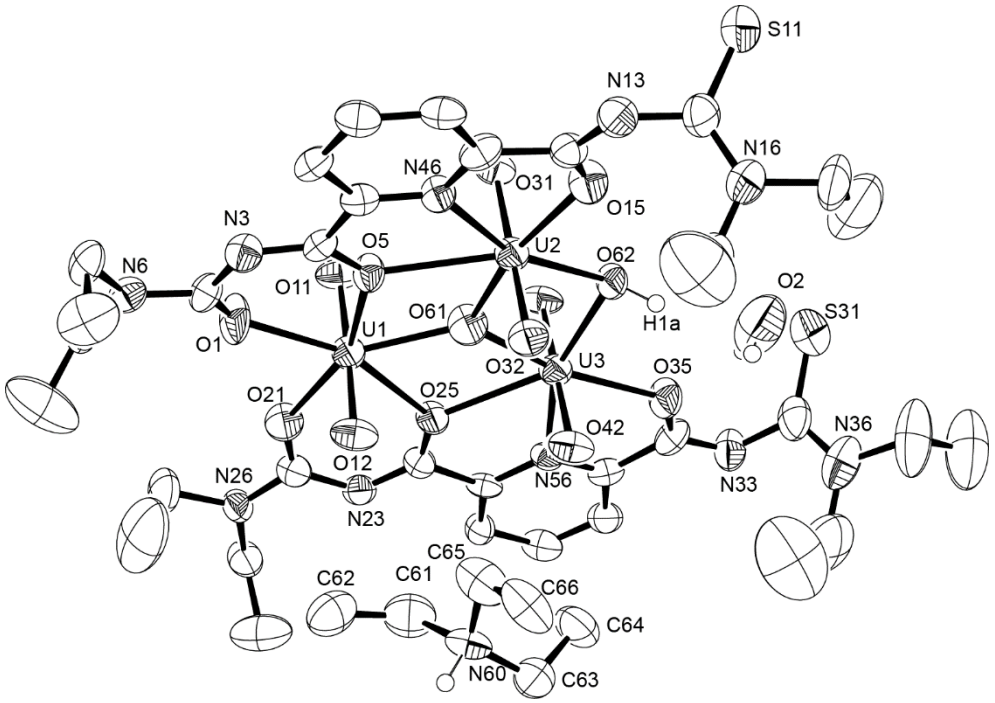

Figure A.12: Ellipsoid plot of $(HNEt_3)[(UO_2)_3(L^{2a**})_2(\mu_2\text{-}OH)(\mu_3\text{-}O)] \cdot H_2O$. Hydrogen atoms have been omitted for clarity. Thermal ellipsoids are at 50 % probability.

$(EtPPh_3)[(UO_2)_3(L^{2a**})_2(\mu_2–OMe)(\mu_3\text{-}O)]$

Table A.25: Crystal data and structure refinement for $(EtPPh_3)[(UO_2)_3(L^{2a**})_2(\mu_2\text{-}OMe)(\mu_3\text{-}O)]$.

Empirical formula	$C_{55}H_{69}N_{10}O_{13.86}PS_{2.14}U_3$	
Formula weight	1905.59	
Temperature	100(2) K	
Wavelength	0.71073 Å	
Crystal system	Monoclinic	
Space group	P $2_1/c$	
Unit cell dimensions	a = 12.666(1) Å	α= 90°
	b = 18.255(2) Å	β= 103.06(1)°
	c = 27.928(3) Å	γ = 90°
Volume	6290.4(11) $Å^3$	
Z	4	
Density (calculated)	2.012 g/cm^3	
Absorption coefficient	7.870 mm^{-1}	
F(000)	3620	
Crystal size	0.48 x 0.10 x 0.05 mm^3	
Theta range for data collection	2.231 to 27.205°	
Index ranges	-16<=h<=16, -23<=k<=23, -35<=l<=35	
Reflections collected	164666	
Independent reflections	13972 [R(int) = 0.0764]	
Completeness to theta = 25.242°	99.9 %	
Absorption correction	Semi-empirical from equivalents	
Max. and min. transmission	0.7455 and 0.4925	
Refinement method	Full-matrix least-squares on F^2	
Data / restraints / parameters	13972 / 18 / 766	
Goodness-of-fit on F^2	1.038	
Final R indices [I>2sigma(I)]	R1 = 0.0341, wR2 = 0.0575	
R indices (all data)	R1 = 0.0522, wR2 = 0.0620	
Largest diff. peak and hole	2.253 and -1.391 e/$Å^3$	
Diffractometer	Bruker D8 Venture	

Table A.26: Atomic coordinates (x 10^4) and equivalent isotropic displacement parameters ($Å^2$ x 10^3) for $(EtPPh_3)[(UO_2)_3(L^{2a**})_2(\mu_2–OMe)(\mu_3\text{-}O)]$.

	x	y	z	U(eq)
U(3)	1616(1)	2626(1)	3261(1)	13(1)
U(2)	2280(1)	3507(1)	2091(1)	12(1)
U(1)	2229(1)	1481(1)	2175(1)	14(1)
O(11)	825(3)	1449(2)	1868(1)	19(1)
O(12)	3631(3)	1480(2)	2476(1)	19(1)
O(31)	897(3)	3538(2)	1755(1)	17(1)
O(32)	3663(3)	3524(2)	2423(1)	18(1)
O(41)	193(3)	2637(2)	3005(1)	20(1)
O(42)	3014(3)	2624(2)	3557(1)	26(1)
O(9)	2479(3)	2433(2)	1641(1)	17(1)
O(10)	1980(3)	2537(2)	2528(1)	18(1)
O(1)	1213(4)	1801(2)	3837(1)	21(1)
S(1)	1900(30)	1673(13)	4035(10)	21(1)
O(21)	1386(4)	3593(2)	3782(2)	19(1)
S(21)	1937(18)	3581(10)	3973(7)	19(1)
C(2)	939(5)	1139(3)	3864(2)	31(2)
N(3)	1055(4)	589(2)	3542(2)	29(1)
C(4)	1419(4)	714(2)	3153(2)	15(1)
O(5)	1695(3)	1330(2)	2983(1)	18(1)
S(11)	2736(1)	-14(1)	599(1)	28(1)
C(12)	3133(4)	-637(3)	1048(2)	22(1)
N(13)	2700(4)	-696(2)	1459(2)	18(1)
C(14)	2469(4)	-155(3)	1716(2)	15(1)
O(15)	2652(3)	536(2)	1682(1)	19(1)
N(16)	3836(4)	-1185(2)	1018(2)	26(1)
C(17)	4171(5)	-1738(3)	1410(2)	32(1)
C(18)	3451(7)	-2392(4)	1354(3)	50(2)
C(19)	4280(5)	-1272(3)	577(2)	33(2)
C(20)	3543(6)	-1719(4)	176(2)	45(2)
C(22)	953(4)	4227(3)	3724(2)	18(1)
N(23)	974(3)	4688(2)	3336(1)	14(1)
C(24)	1372(4)	4478(3)	2969(2)	12(1)
O(25)	1681(3)	3837(2)	2860(1)	15(1)
N(26)	486(4)	4501(2)	4066(2)	19(1)

C(27)	524(5)	4071(3)	4520(2)	28(1)
C(28)	-377(5)	3517(3)	4449(2)	36(2)
C(29)	-12(4)	5227(3)	4029(2)	20(1)
C(30)	795(5)	5801(3)	4283(2)	27(1)
S(31)	3101(1)	5153(1)	386(1)	34(1)
C(32)	3767(5)	5285(3)	971(2)	20(1)
N(33)	3206(4)	5504(2)	1323(2)	17(1)
C(34)	2777(4)	5033(3)	1566(2)	15(1)
O(35)	2798(3)	4328(2)	1540(1)	16(1)
N(36)	4843(4)	5252(3)	1130(2)	25(1)
C(37)	5577(5)	5129(4)	800(2)	37(2)
C(38)	5960(7)	5840(4)	630(3)	58(2)
C(39)	5382(5)	5387(3)	1650(2)	30(1)
C(40)	5574(5)	4683(4)	1943(2)	40(2)
C(41)	1485(4)	61(3)	2838(2)	15(1)
C(42)	1142(4)	-631(3)	2947(2)	19(1)
C(43)	1204(4)	-1197(3)	2622(2)	19(1)
C(44)	1625(4)	-1066(3)	2214(2)	17(1)
C(45)	1976(4)	-362(3)	2137(2)	13(1)
N(46)	1883(3)	190(2)	2439(2)	14(1)
C(50)	1855(4)	2378(3)	1142(2)	24(1)
C(51)	2212(4)	5344(3)	1940(2)	13(1)
C(52)	1938(4)	6077(3)	1961(2)	19(1)
C(53)	1402(4)	6296(3)	2319(2)	21(1)
C(54)	1193(4)	5785(3)	2655(2)	16(1)
C(55)	1509(4)	5069(3)	2616(2)	13(1)
N(56)	1996(3)	4849(2)	2258(1)	12(1)
P(1)	4507(1)	7121(1)	3706(1)	20(1)
C(61)	4855(4)	7569(3)	3190(2)	28(1)
C(62)	3968(5)	7582(4)	2719(2)	39(2)
C(71)	4659(5)	5801(3)	3225(2)	29(1)
C(72)	4484(5)	5059(3)	3156(2)	31(1)
C(73)	3951(5)	4670(3)	3456(2)	32(1)
C(74)	3577(5)	5023(3)	3824(2)	30(1)
C(75)	3729(4)	5766(3)	3886(2)	25(1)
C(76)	4265(4)	6162(3)	3591(2)	23(1)
C(81)	2292(4)	7277(3)	3547(2)	22(1)
C(82)	1332(4)	7557(3)	3633(2)	26(1)
C(83)	1378(5)	8075(3)	3997(2)	29(1)

C(84)	2359(5)	8305(3)	4281(2)	29(1)
C(85)	3317(5)	8021(3)	4196(2)	24(1)
C(86)	3290(4)	7504(3)	3830(2)	20(1)
C(91)	5907(5)	6675(4)	4564(2)	34(1)
C(92)	6642(5)	6798(4)	5005(3)	45(2)
C(93)	7084(5)	7480(5)	5112(2)	47(2)
C(94)	6799(5)	8048(4)	4785(3)	43(2)
C(95)	6043(5)	7941(3)	4347(2)	32(1)
C(96)	5580(4)	7250(3)	4239(2)	24(1)
N(6A)	671(10)	932(5)	4290(4)	38(1)
C(7A)	221(12)	1431(8)	4642(5)	38(1)
C(8A)	-896(11)	1673(7)	4415(5)	38(1)
C(9A)	-229(10)	233(6)	4149(4)	38(1)
C(10A)	584(11)	-291(6)	4452(4)	38(1)
N(6B)	218(10)	945(5)	4131(4)	38(1)
C(7B)	307(11)	1507(8)	4560(5)	38(1)
C(8B)	-850(10)	1572(7)	4604(5)	38(1)
C(9B)	664(10)	137(6)	4422(4)	38(1)
C(10B)	-374(10)	-240(6)	4169(4)	38(1)

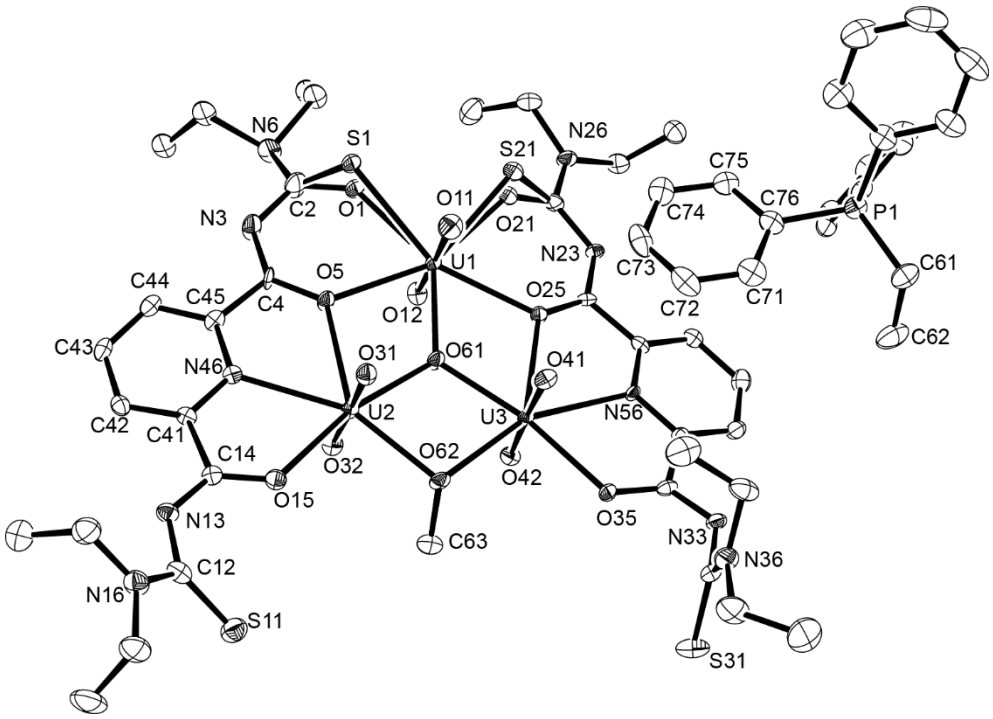

Figure A.13: Ellipsoid plot of $(EtPPh_3)[(UO_2)_3(L^{2a**})_2(\mu_2\text{-}OMe)(\mu_3\text{-}O)]$. Hydrogen atoms have been omitted for clarity. Thermal ellipsoids are at 50 % probability.

$(EtPPh_3)[(UO_2)_3(L^{2a**})_2(\mu_2–OMe)(\mu_3\text{-}O)]$

Table A.27: Crystal data and structure refinement for $(EtPPh_3)[(UO_2)_3(L^{2a**})_2(\mu_2\text{-}OMe)(\mu_3\text{-}O)]$.

Empirical formula	$C_{55}H_{69}N_{10}O_{14}PS_2U_3$	
Formula weight	1903.38	
Temperature	200(2) K	
Wavelength	0.71073 Å	
Crystal system	Monoclinic	
Space group	P $2_1/c$	
Unit cell dimensions	a = 12.752(1) Å	α= 90°
	b = 18.341(1) Å	β= 103.02(3)°
	c = 28.125(2) Å	γ = 90°
Volume	6408.9(8) $Å^3$	
Z	4	
Density (calculated)	1.973 g/cm^3	
Absorption coefficient	7.721 mm^{-1}	
F(000)	3616	
Crystal size	0.68 x 0.04 x 0.04 mm^3	
Theta range for data collection	4.599 to 26.000°	
Index ranges	-15<=h<=15, -19<=k<=22, -34<=l<=34	
Reflections collected	54941	
Independent reflections	12531 [R(int) = 0.0830]	
Completeness to theta = 25.242°	99.3 %	
Absorption correction	Integration	
Max. and min. transmission	0.8485 and 0.3154	
Refinement method	Full-matrix least-squares on F^2	
Data / restraints / parameters	12531 / 42 / 774	
Goodness-of-fit on F^2	0.850	
Final R indices [I>2sigma(I)]	R1 = 0.0396, wR2 = 0.0699	
R indices (all data)	R1 = 0.0805, wR2 = 0.0782	
Largest diff. peak and hole	0.846 and -1.584 e/$Å^3$	
Diffractometer	Bruker D8 Venture	

Table A.28: Atomic coordinates (x 10^4) and equivalent isotropic displacement parameters ($Å^2$ x 10^3) for $(EtPPh_3)[(UO_2)_3(L^{2a**})_2(\mu_2–OMe)(\mu_3\text{-}O)]$.

	x	y	z	U(eq)
U(1)	7219(1)	-1513(1)	-2822(1)	34(1)
U(2)	7267(1)	-3534(1)	-2908(1)	32(1)
U(3)	6556(1)	-2652(1)	-1758(1)	36(1)
S(11)	8067(2)	-5163(2)	-4594(1)	77(1)
S(31)	7771(3)	-6(2)	-4376(1)	74(1)
O(1)	6295(7)	-3602(3)	-1244(2)	68(2)
O(12)	5846(4)	-1485(3)	-3126(2)	43(1)
O(11)	8595(4)	-1507(3)	-2525(2)	46(1)
O(32)	8627(4)	-3556(3)	-2582(2)	42(1)
O(5)	6646(4)	-3863(3)	-2149(2)	36(1)
O(31)	5914(4)	-3567(3)	-3242(2)	41(1)
O(41)	7924(5)	-2675(4)	-1449(2)	57(2)
O(42)	5173(4)	-2643(3)	-2033(2)	52(2)
O(62)	7485(4)	-2466(3)	-3350(2)	39(1)
O(61)	6985(4)	-2570(3)	-2471(2)	43(1)
O(15)	7776(5)	-4351(3)	-3460(2)	40(1)
O(21)	6170(5)	-1839(3)	-1178(2)	52(2)
O(25)	6673(4)	-1365(3)	-2027(2)	38(1)
O(35)	7638(5)	-568(3)	-3312(2)	45(2)
N(3)	5964(5)	-4709(4)	-1676(2)	35(2)
N(6)	5430(7)	-4517(4)	-960(3)	54(2)
N(13)	8188(6)	-5519(4)	-3667(2)	43(2)
N(16)	9827(6)	-5270(5)	-3864(3)	62(2)
N(23)	5990(6)	-633(4)	-1484(3)	51(2)
N(26)	5322(10)	-994(5)	-836(4)	97(3)
N(33)	7699(6)	654(4)	-3525(3)	47(2)
N(36)	8841(7)	1167(5)	-3957(3)	69(2)
N(46)	6995(5)	-4874(3)	-2739(2)	32(2)
N(56)	6878(5)	-224(4)	-2559(2)	36(2)
C(2)	5888(8)	-4246(5)	-1304(3)	45(2)
C(4)	6364(6)	-4501(4)	-2035(3)	30(2)
C(7)	5493(12)	-4075(6)	-488(5)	84(3)
C(8)	4603(14)	-3614(10)	-568(6)	128(6)
C(9)	4990(7)	-5255(5)	-979(3)	47(2)

C(10)	5858(9)	-5789(6)	-716(4)	71(3)
C(12)	8752(8)	-5292(5)	-4019(3)	55(2)
C(14)	7763(6)	-5048(5)	-3429(3)	36(2)
C(17)	10379(9)	-5408(7)	-3356(4)	73(3)
C(18)	10565(9)	-4707(8)	-3077(5)	93(4)
C(19)	10533(10)	-5125(8)	-4207(4)	86(4)
C(20)	10921(16)	-5815(10)	-4370(6)	150(8)
C(22)	5865(8)	-1191(5)	-1166(3)	48(2)
C(24)	6381(7)	-760(5)	-1870(3)	38(2)
C(29)	4743(10)	-203(7)	-854(4)	81(3)
C(30)	5612(10)	123(9)	-552(5)	98(4)
C(32)	8149(8)	625(6)	-3924(4)	58(3)
C(34)	7469(7)	119(5)	-3270(3)	42(2)
C(37)	9185(10)	1701(7)	-3560(4)	78(3)
C(38)	8475(16)	2351(10)	-3617(6)	161(8)
C(39)	9268(10)	1260(8)	-4392(5)	91(4)
C(40)	8533(13)	1692(9)	-4786(5)	115(5)
C(41)	6522(6)	-5091(4)	-2384(3)	32(2)
C(42)	6231(7)	-5800(5)	-2336(3)	42(2)
C(43)	6467(7)	-6316(5)	-2662(3)	48(2)
C(44)	6979(7)	-6090(5)	-3023(3)	45(2)
C(45)	7234(6)	-5366(4)	-3050(3)	34(2)
C(11)	6895(7)	-2393(6)	-3856(3)	61(3)
C(51)	6470(6)	-102(5)	-2162(3)	36(2)
C(52)	6139(6)	590(4)	-2048(3)	38(2)
C(53)	6228(7)	1167(5)	-2366(3)	43(2)
C(54)	6655(7)	1030(5)	-2770(3)	41(2)
C(55)	6981(6)	326(5)	-2852(3)	34(2)
P(1)	483(2)	-2142(1)	-3734(1)	47(1)
C(61)	122(6)	-2596(7)	-3238(3)	67(3)
C(62)	986(8)	-2607(8)	-2757(4)	86(4)
C(71)	2682(7)	-2298(5)	-3559(3)	54(2)
C(72)	3642(6)	-2571(6)	-3642(3)	56(2)
C(73)	3625(8)	-3073(6)	-4005(4)	61(3)
C(74)	2656(8)	-3300(6)	-4293(4)	73(3)
C(75)	1691(7)	-3012(6)	-4213(4)	58(3)
C(76)	1709(6)	-2511(5)	-3846(3)	44(2)
C(81)	-1025(8)	-2963(6)	-4377(4)	67(3)
C(82)	-1797(9)	-3073(9)	-4814(5)	84(4)

C(83)	-2036(9)	-2501(12)	-5138(4)	96(5)
C(84)	-1610(11)	-1824(11)	-5032(5)	104(5)
C(85)	-888(8)	-1703(7)	-4593(4)	77(3)
C(86)	-566(7)	-2273(6)	-4270(4)	53(2)
C(91)	1261(7)	-796(5)	-3895(4)	55(2)
C(92)	1418(8)	-57(6)	-3816(4)	65(3)
C(93)	1028(8)	301(7)	-3458(5)	77(3)
C(94)	496(9)	-102(7)	-3172(5)	75(3)
C(95)	295(7)	-842(6)	-3253(4)	59(3)
C(96)	712(6)	-1199(5)	-3613(3)	45(2)
C(27)	5148(12)	-1523(7)	-461(5)	97(4)
C(28)	4035(14)	-1738(9)	-545(7)	144(6)

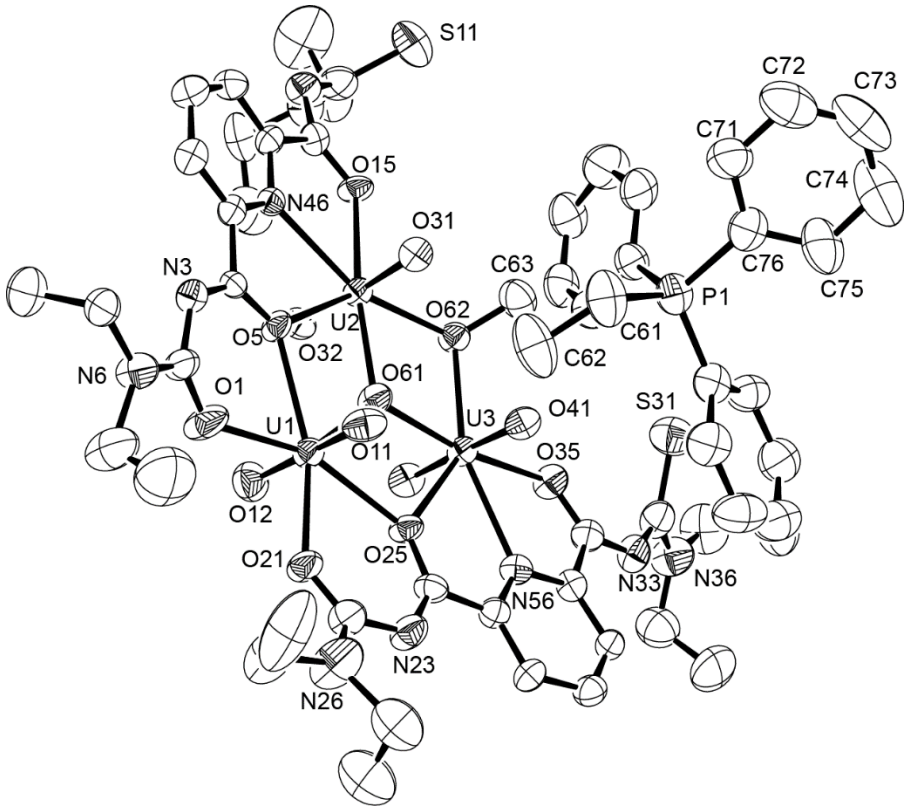

Figure A.14: Ellipsoid plot of $(EtPPh_3)[(UO_2)_3(L^{2a**})_2(\mu_2\text{-}OMe)(\mu_3\text{-}O)] \cdot H_2O$. Hydrogen atoms have been omitted for clarity. Thermal ellipsoids are at 50 % probability.

$(HNEt_3)[(UO_2)_3(L^{2a**})_2(\mu_2\text{–}OEt)(\mu_3\text{-}O)]$

Table A.29. Crystal data and structure refinement for $(HNEt_3)[(UO_2)_3(L^{2a**})_2(\mu_2\text{-}OEt)(\mu_3\text{-}O)] \cdot 2\ H_2O$.

Empirical formula	$C_{43}H_{51}N_{12}O_{14}S_2U_3$	
Formula weight	1738.16	
Temperature	100(2) K	
Wavelength	0.71073 Å	
Crystal system	Orthorhombic	
Space group	Pnma	
Unit cell dimensions	a = 23.754(5) Å	α= 90°
	b = 19.292(4) Å	β= 90°
	c = 13.997(3) Å	γ = 90°
Volume	6414(2) $Å^3$	
Z	4	
Density (calculated)	1.800 g/cm^3	
Absorption coefficient	7.682 mm^{-1}	
F(000)	3252	
Crystal size	0.4 x 0.08 x 0.04 mm^3	
Theta range for data collection	2.484 to 26.319°	
Index ranges	-29<=h<=29, -22<=k<=23, -17<=l<=17	
Reflections collected	50325	
Independent reflections	6641 [R(int) = 0.0960]	
Completeness to theta = 25.242°	99.1 %	
Absorption correction	Semi-empirical from equivalents	
Max. and min. transmission	0.7455 and 0.4903	
Refinement method	Full-matrix least-squares on F^2	
Data / restraints / parameters	6641 / 69 / 364	
Goodness-of-fit on F^2	1.171	
Final R indices [I>2sigma(I)]	R1 = 0.0840, wR2 = 0.1721	
R indices (all data)	R1 = 0.1147, wR2 = 0.1868	
Largest diff. peak and hole	3.532 and -3.078 e/$Å^3$	
Diffractometer	Bruker D8 Venture	

Table A.30: Atomic coordinates (x 10^4) and equivalent isotropic displacement parameters ($Å^2$ x 10^3) for $(HNEt_3)[(UO_2)_3(L^{2a**})_2(\mu_2–OEt)(\mu_3\text{-}O)] \cdot 2\ H_2O$.

	x	y	z	U(eq)
U(2)	3864(1)	3469(1)	6144(1)	27(1)
U(1)	4414(1)	2500	3867(1)	28(1)
S(11)	3511(2)	5188(4)	9655(4)	68(2)
O(5)	4256(4)	3711(5)	4514(7)	28(2)
O(61)	4007(7)	2500	5279(12)	37(4)
O(22)	3171(5)	3545(5)	5675(8)	36(3)
O(23)	4579(4)	3454(5)	6599(8)	31(2)
O(2)	3728(8)	2500	3270(13)	47(5)
O(62)	3630(7)	2500	7103(11)	35(4)
O(15)	3620(4)	4291(5)	7293(8)	32(2)
O(3)	5099(7)	2500	4410(11)	32(4)
O(1)	4739(6)	3352(6)	2794(8)	50(3)
N(46)	4027(5)	4736(6)	5684(9)	26(3)
N(2)	4551(6)	4487(7)	3287(9)	37(3)
C(4)	4360(6)	4308(7)	4144(11)	25(3)
C(41)	3899(6)	5236(8)	6307(11)	27(3)
N(13)	3402(6)	5404(7)	7775(11)	42(4)
C(45)	4258(6)	4909(8)	4835(11)	28(3)
C(44)	4372(6)	5589(7)	4590(13)	32(4)
C(2)	4685(7)	3994(8)	2636(12)	39(4)
N(6)	4743(8)	4219(8)	1765(11)	56(4)
C(14)	3621(6)	4955(8)	7227(12)	33(4)
C(43)	4250(8)	6103(8)	5262(15)	47(5)
C(42)	3994(6)	5916(9)	6108(14)	40(4)
C(64)	3328(16)	2500	8587(19)	105(16)
C(12)	3143(8)	5181(10)	8616(15)	52(5)
N(16)	2592(7)	5008(11)	8592(13)	69(6)
C(9)	4895(12)	3774(12)	963(15)	75(7)
C(10)	4385(11)	3490(14)	453(18)	76(7)
C(8)	5093(9)	5366(13)	1630(16)	71(7)
C(7)	4590(9)	4957(10)	1457(15)	57(5)
C(63)	3813(14)	2500	8134(19)	59(7)
C(17)	2304(11)	4804(17)	9480(20)	100(9)
C(19)	2282(12)	4950(20)	7700(20)	128(15)

C(18)	2373(14)	4065(19)	9770(30)	135(14)
C(20)	2040(30)	5610(30)	7550(40)	230(30)
N(71)	1785(11)	2500	4820(20)	74(6)
C(76)	2374(15)	2500	4270(30)	82(8)
C(77)	2360(30)	3180(30)	3810(50)	120(20)
C(72)	1320(20)	2200(20)	4100(40)	80(9)
C(73)	1260(20)	2500	3120(40)	114(13)
C(74)	1806(19)	1920(20)	5520(40)	72(8)
C(75)	2150(20)	2240(20)	6490(40)	94(14)
O(81)	5550(20)	2500	7010(40)	94(16)
O(80)	6240(30)	2500	6470(50)	110(20)

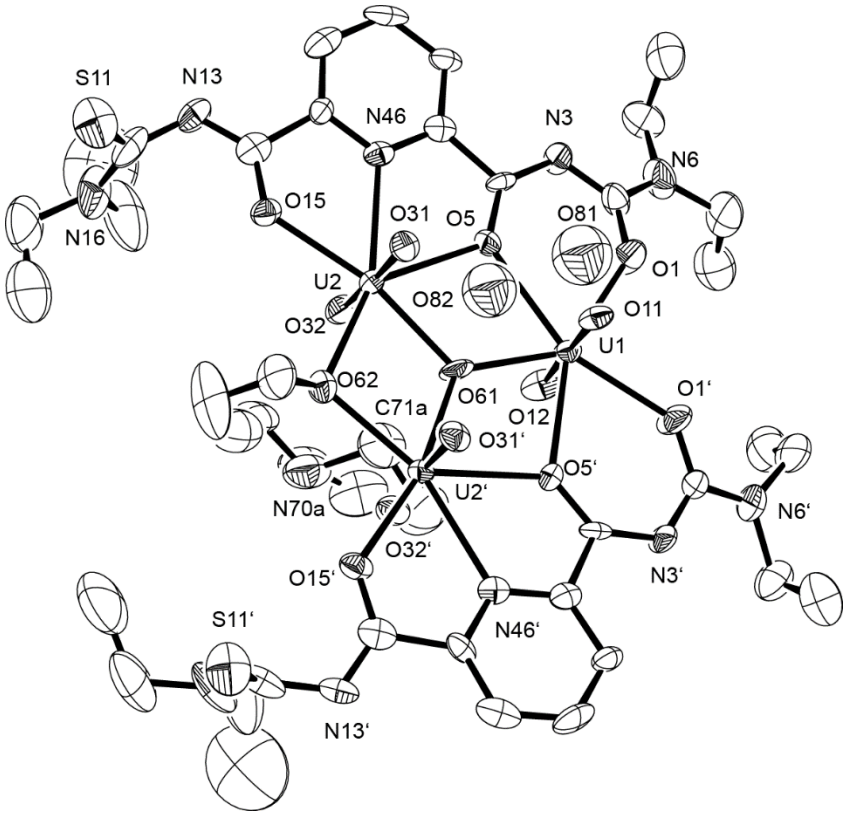

Figure A.15: Ellipsoid plot of $(HNEt_3)[(UO_2)_3(L^{2a**})_2(\mu_2\text{-}OEt)(\mu_3\text{-}O)] \cdot 2\ H_2O$. Hydrogen atoms have been omitted for clarity. Thermal ellipsoids are at 50 % probability.

$(HNEt_3)_2[\{(UO_2)_2(L^{2a})(\mu_2\text{–}OAc)(\mu_3\text{-}O)\}_2]$

Table A.31: Crystal data and structure refinement for $(HNEt_3)_2[\{(UO_2)_2(L^{2a})(\mu_2\text{-}OAc)(\mu_3\text{-}O)\}_2]$.

Empirical formula	$C_{49}H_{82}N_{12}O_{18.25}S_{3.75}U_4$	
Formula weight	2203.65	
Temperature	200(2) K	
Wavelength	0.71073 Å	
Crystal system	Triclinic	
Space group	$P\overline{1}$	
Unit cell dimensions	a = 11.651(1) Å	α= 112.57(1)°
	b = 11.736(1) Å	β= 100.57(1)°
	c = 13.889(1) Å	γ = 92.68(1)°
Volume	1709.5(3) $Å^3$	
Z	1	
Density (calculated)	2.141 g/cm^3	
Absorption coefficient	9.631 mm^{-1}	
F(000)	1034	
Crystal size	0.21 x 0.13 x 0.08 mm^3	
Theta range for data collection	3.287 to 26.000°	
Index ranges	-14<=h<=14, -14<=k<=14, -17<=l<=17	
Reflections collected	14795	
Independent reflections	6659 [R(int) = 0.0890]	
Completeness to theta = 25.242°	99.1 %	
Absorption correction	Integration	
Max. and min. transmission	0.1366 and 0.0298	
Refinement method	Full-matrix least-squares on F^2	
Data / restraints / parameters	6659 / 45 / 401	
Goodness-of-fit on F^2	1.044	
Final R indices [I>2sigma(I)]	R1 = 0.0446, wR2 = 0.1087	
R indices (all data)	R1 = 0.0556, wR2 = 0.1137	
Largest diff. peak and hole	2.190 and -2.430 e/$Å^3$	
Diffractometer	Bruker D8 Venture	

Table A.32: Atomic coordinates (x 10^4) and equivalent isotropic displacement parameters ($Å^2$ x 10^3) for $(HNEt_3)_2[\{(UO_2)_2(L^{2a})(\mu_2\text{–}OAc)(\mu_3\text{-}O)\}_2]$.

	x	y	z	U(eq)
U(1)	8345(1)	9560(1)	1760(1)	28(1)
U(2)	10481(1)	11569(1)	1031(1)	27(1)
O(2)	9665(6)	9378(7)	2516(6)	50(2)
O(3)	6992(6)	9791(6)	1075(5)	42(2)
S(1)	5133(3)	6885(3)	3250(3)	52(1)
S(11)	11130(4)	14003(3)	2793(3)	42(1)
O(11)	10660(80)	13660(70)	2360(70)	42(1)
O(12)	11579(6)	11014(5)	1777(5)	37(1)
O(13)	9446(6)	12253(5)	385(5)	38(1)
O(15)	9146(6)	11782(5)	2299(5)	35(1)
O(31)	9270(5)	9798(5)	558(4)	27(1)
O(5)	7329(6)	8800(5)	2780(5)	39(2)
O(32)	7879(9)	7378(6)	763(6)	64(2)
O(33)	12133(6)	12626(7)	811(6)	50(2)
N(26)	7826(7)	11169(6)	3423(6)	34(2)
N(3)	6556(8)	9053(7)	4272(7)	42(2)
N(13)	8991(8)	13888(7)	3225(7)	44(2)
N(16)	9350(10)	15236(9)	2460(9)	63(3)
N(6)	7098(8)	7473(7)	4767(7)	48(2)
C(21)	7202(8)	10796(8)	3990(8)	35(2)
C(22)	6817(10)	11618(9)	4832(8)	48(2)
C(23)	7142(10)	12897(9)	5146(9)	51(3)
C(24)	7795(11)	13284(9)	4577(9)	52(3)
C(25)	8135(9)	12398(8)	3714(8)	38(2)
C(4)	7009(8)	9423(8)	3634(8)	38(2)
C(2)	6342(9)	7812(9)	4106(8)	41(2)
C(14)	8839(8)	12732(7)	3028(8)	35(2)
C(12)	9741(10)	14385(9)	2790(8)	47(2)
C(10)	6226(13)	6388(12)	5703(11)	69(4)
C(9)	6908(12)	6297(10)	4867(9)	56(3)
C(7)	8188(11)	8318(11)	5469(10)	60(3)
C(8)	9195(11)	8143(14)	4915(11)	77(4)
C(33)	7554(9)	6904(8)	-248(8)	39(2)
C(34)	6813(15)	5692(12)	-724(13)	88(5)

C(43)	4442(11)	7932(12)	751(10)	63(3)
C(42)	3516(13)	8805(16)	765(13)	28(3)
C(44)	4687(12)	10750(13)	2233(12)	75(3)
C(45)	4687(13)	11550(18)	1634(15)	100(5)
C(17)	8109(11)	15514(11)	2428(11)	62(3)
C(18)	7251(14)	14534(14)	1567(12)	84(4)
C(19)	10106(16)	16022(19)	2124(18)	113(6)
C(20)	9970(20)	15570(20)	1050(20)	158(9)
N(41)	3622(9)	9829(10)	1825(9)	66(3)
C(46)	3514(14)	9373(18)	2711(12)	92(5)
C(47)	2426(16)	8460(20)	2405(16)	114(7)

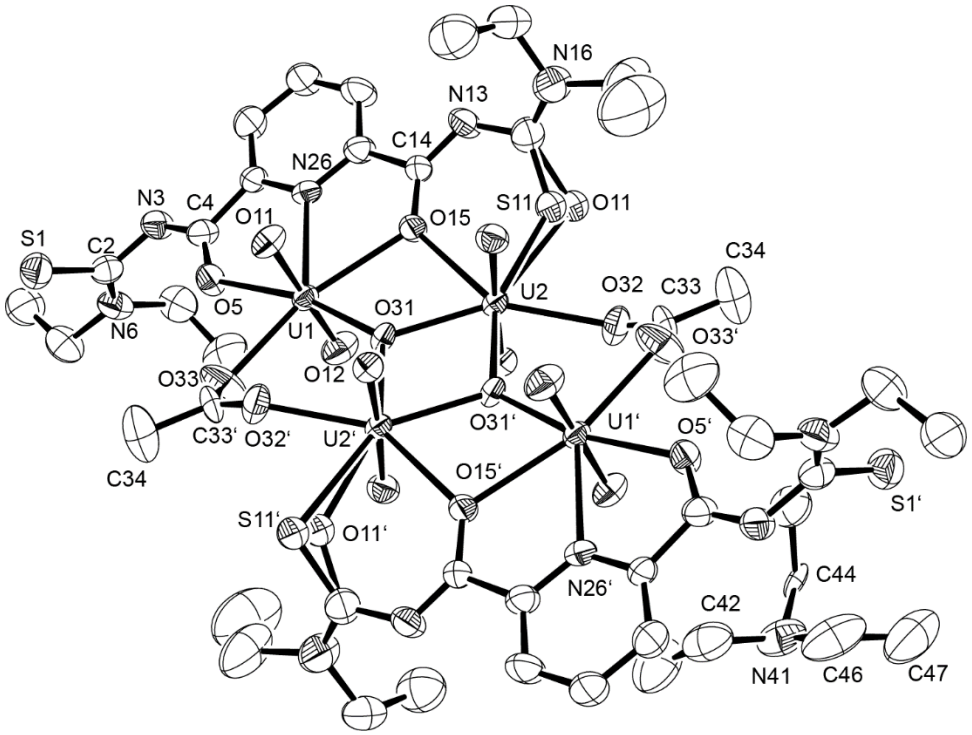

Figure A.16: Ellipsoid plot of $(HNEt_3)_2[\{(UO_2)_2(L^{2a})(\mu_2\text{–}OAc)(\mu_3\text{-}O)\}_2]$. Hydrogen atoms have been omitted for clarity. Thermal ellipsoids are at 50 % probability.

[{$UO_2(L^{2a})(\mu_2$-OMe)}{$Au(PPh_3)$}$_2$]

Table A.33: Crystal data and structure refinement for [{$UO_2(L^{2a})(\mu_2$-OMe)}{$Au(PPh_3)$}$_2$].

Empirical formula	$C_{72}H_{82}Au_2N_{10}O_{10}P_2S_4U_2$	
Formula weight	2307.64	
Temperature	200(2) K	
Wavelength	0.71073 Å	
Crystal system	Triclinic	
Space group	$P\overline{1}$	
Unit cell dimensions	a = 9.9110(8) Å	α= 100.98(7)°
	b = 15.627(2) Å	β= 97.04(6)°
	c = 31.476(2) Å	γ = 96.71(7)°
Volume	4700.2(7) $Å^3$	
Z	2	
Density (calculated)	1.631 g/cm^3	
Absorption coefficient	6.721 mm^{-1}	
F(000)	2200	
Crystal size	0.22 x 0.13 x 0.13 mm^3	
Theta range for data collection	3.175 to 25.000°	
Index ranges	-11<=h<=11, -18<=k<=18, -37<=l<=37	
Reflections collected	36196	
Independent reflections	16463 [R(int) = 0.1645]	
Completeness to theta = 25.000°	99.3 %	
Absorption correction	Integration	
Max. and min. transmission	0.5207 and 0.3293	
Refinement method	Full-matrix least-squares on F^2	
Data / restraints / parameters	16463 / 959 / 823	
Goodness-of-fit on F^2	0.898	
Final R indices [I>2sigma(I)]	R1 = 0.0738, wR2 = 0.1822	
R indices (all data)	R1 = 0.1588, wR2 = 0.2165	
Largest diff. peak and hole	1.372 and -1.685 e/$Å^3$	
Diffractometer	IPDS, STOE	

Table A.34: Atomic coordinates (x 10^4) and equivalent isotropic displacement parameters ($Å^2$ x 10^3) for [{UO_2(L^{2a})(μ_2-OMe)}{Au(PPh_3)}$_2$].

	x	y	z	U(eq)
U(1)	727(1)	6009(1)	4797(1)	55(1)
U(2)	583(1)	4037(1)	223(1)	85(1)
Au(2)	2253(1)	4454(1)	2144(1)	87(1)
Au(1)	2342(1)	5897(1)	3026(1)	72(1)
P(1)	1168(5)	6897(4)	2765(2)	72(1)
P(2)	716(7)	3427(5)	2296(2)	105(2)
O(1)	1980(10)	6358(8)	5273(4)	62(3)
O(2)	-477(10)	5709(8)	4310(4)	62(3)
O(11)	1910(16)	4013(10)	-95(5)	104(4)
O(12)	-761(15)	4043(10)	549(5)	103(4)
S(1)	-1440(7)	8818(4)	5778(2)	98(2)
C(2)	-1769(19)	8721(13)	5235(7)	73(4)
N(3)	-728(14)	8708(9)	4992(5)	65(4)
C(4)	-113(16)	8019(11)	4886(6)	56(4)
O(5)	-344(11)	7284(8)	4994(4)	64(3)
N(6)	-3025(15)	8727(11)	5022(5)	75(4)
C(7)	-3240(20)	8625(16)	4543(7)	96(6)
C(8)	-3180(30)	9513(19)	4402(9)	134(10)
C(9)	-4230(20)	8853(15)	5254(8)	94(6)
C(10)	-4930(20)	8002(18)	5331(9)	120(9)
S(11)	3628(6)	4935(4)	3324(2)	82(2)
C(12)	4405(16)	5611(12)	3797(6)	59(3)
N(13)	4026(14)	6431(10)	3932(5)	67(3)
C(14)	3086(16)	6487(12)	4181(6)	58(4)
O(15)	2544(10)	5910(8)	4359(4)	60(3)
N(16)	5508(15)	5406(11)	4048(5)	75(4)
C(17)	5970(20)	4557(15)	3917(8)	92(6)
C(18)	5160(30)	3852(17)	4054(9)	117(8)
C(19)	6340(20)	6080(17)	4419(8)	103(6)
C(20)	6120(30)	5819(19)	4834(8)	126(9)
S(21)	-1550(20)	906(8)	-1047(6)	336(10)
C(22)	-2100(40)	970(50)	-557(12)	355(12)
N(23)	-1120(50)	1129(19)	-194(8)	282(13)
C(24)	-380(40)	1894(17)	-27(11)	185(14)

O(25)	-440(20)	2608(11)	-159(6)	129(5)
N(26)	-3190(60)	1090(40)	-492(19)	355(12)
C(27)	-3570(60)	1030(40)	-60(20)	355(12)
C(28)	-4010(60)	1920(40)	142(18)	355(12)
C(29)	-4290(70)	1080(40)	-860(20)	355(12)
C(30)	-4770(80)	90(40)	-970(20)	355(12)
S(31)	3883(6)	5490(5)	1986(2)	96(2)
C(32)	4340(20)	4911(17)	1525(7)	89(5)
N(33)	3860(20)	4067(13)	1363(6)	91(4)
C(34)	2870(30)	3869(17)	1042(8)	95(6)
O(35)	2279(15)	4417(10)	865(5)	91(4)
N(36)	5410(20)	5277(17)	1363(8)	131(7)
C(37)	6100(30)	6210(20)	1584(11)	139(8)
C(38)	5370(40)	6880(20)	1438(13)	179(14)
C(39)	6130(30)	4790(20)	1025(10)	156(10)
C(40)	5510(40)	4970(40)	616(12)	250(20)
C(41)	1022(15)	8119(11)	4628(5)	54(4)
C(42)	1418(18)	8851(13)	4453(7)	72(5)
C(43)	2441(17)	8846(13)	4198(6)	70(5)
C(44)	3019(18)	8101(13)	4085(6)	72(5)
C(45)	2562(15)	7386(12)	4270(6)	56(4)
N(46)	1578(12)	7378(9)	4533(4)	52(3)
C(51)	790(40)	1900(20)	313(12)	189(15)
C(52)	1260(50)	1180(20)	501(12)	220(20)
C(53)	2210(50)	1380(20)	858(13)	220(20)
C(54)	2740(40)	2237(19)	1065(10)	142(11)
C(55)	2400(30)	2912(18)	897(9)	114(7)
N(56)	1340(20)	2739(14)	537(7)	118(5)
C(61)	1170(30)	7169(18)	1926(7)	112(7)
C(62)	760(30)	6910(20)	1457(8)	126(9)
C(63)	120(30)	6100(20)	1294(8)	107(7)
C(64)	-260(20)	5549(17)	1530(7)	94(6)
C(65)	50(20)	5860(16)	1988(7)	91(5)
C(66)	740(20)	6687(15)	2192(7)	77(4)
C(71)	3560(20)	8065(18)	2931(10)	117(8)
C(72)	4460(30)	8830(20)	3074(12)	148(12)
C(73)	3800(30)	9570(20)	3164(11)	141(11)
C(74)	2490(30)	9571(19)	3150(10)	123(8)
C(75)	1690(30)	8755(18)	3019(10)	116(8)

C(76)	2173(19)	7958(14)	2921(6)	73(4)
C(81)	-1631(19)	7158(16)	2739(7)	86(6)
C(82)	-2810(20)	7191(17)	2913(7)	98(8)
C(83)	-2840(20)	7143(17)	3354(7)	93(7)
C(84)	-1680(20)	7008(16)	3586(7)	94(7)
C(85)	-500(20)	6939(15)	3426(6)	81(6)
C(86)	-465(19)	7001(14)	2987(6)	72(5)
C(91)	-500(30)	1777(16)	1851(6)	181(5)
C(92)	-1260(30)	1186(12)	1490(8)	181(5)
C(93)	-1590(30)	1459(14)	1100(6)	181(5)
C(94)	-1170(30)	2324(15)	1071(6)	181(5)
C(95)	-420(30)	2915(11)	1431(8)	181(5)
C(96)	-80(30)	2641(14)	1821(6)	181(5)
O(3)	833(11)	4523(8)	4767(4)	63(3)
C(101)	707(15)	2534(14)	2977(6)	128(9)
C(102)	1330(20)	2107(13)	3280(6)	149(11)
C(103)	2710(20)	1997(12)	3284(6)	130(9)
C(104)	3453(15)	2314(13)	2986(6)	130(9)
C(105)	2826(17)	2741(12)	2684(6)	121(9)
C(106)	1453(18)	2851(12)	2679(5)	114(7)
O(13)	-932(13)	4429(8)	-307(4)	76(3)
C(111)	-1940(20)	3855(14)	2245(6)	153(9)
C(112)	-2985(17)	4277(16)	2409(7)	172(11)
C(113)	-2800(20)	4727(13)	2843(8)	158(9)
C(114)	-1560(20)	4755(13)	3112(6)	147(9)
C(115)	-520(17)	4332(14)	2947(7)	138(8)
C(116)	-710(19)	3882(13)	2514(7)	129(7)
C(3)	920(20)	3999(13)	4354(6)	80(5)
C(13)	-2240(20)	3964(15)	-450(8)	96(7)

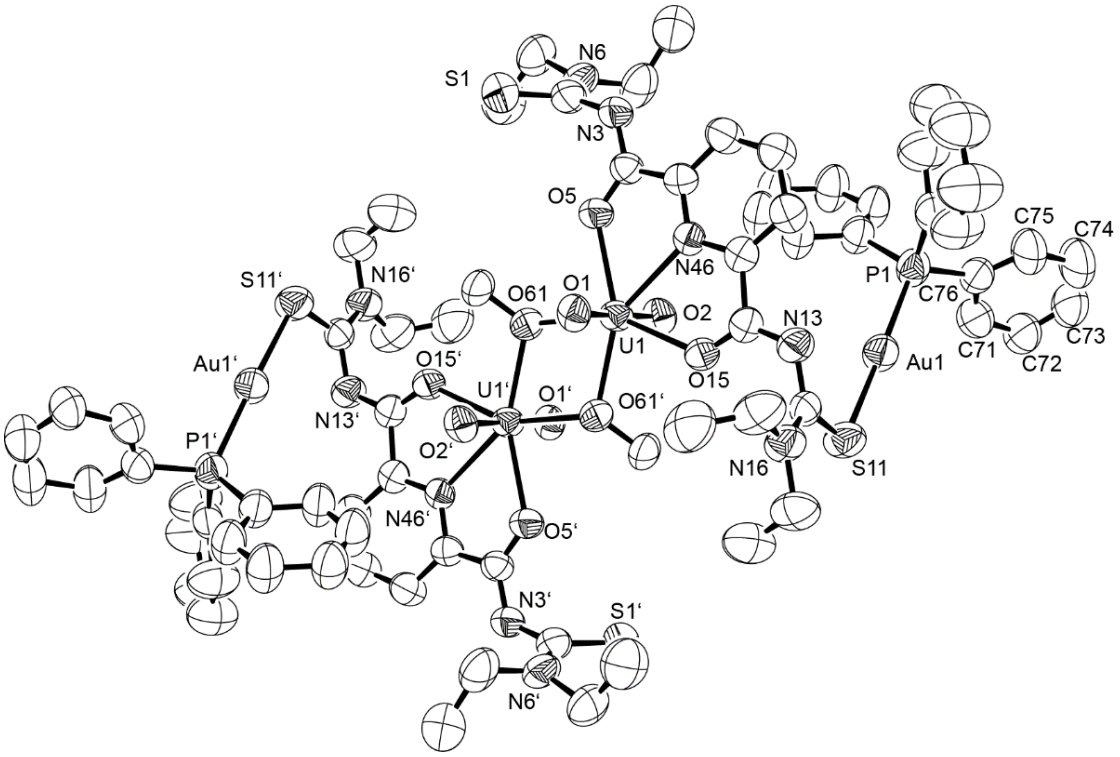

Figure A.17: Ellipsoid plot of [{$UO_2(L^{2a})(\mu_2\text{-}OMe)$}{$Au(PPh_3)$}$_2$]. Hydrogen atoms have been omitted for clarity. Thermal ellipsoids are at 50 % probability.

$[Pb_2(UO_2)_3(L^{2a})_4(MeOH)_2(\mu_2\text{-}OMe)_2]$

Table A.35: Crystal data and structure refinement for $[Pb_2(UO_2)_3(L^{2a})_4(MeOH)_2(\mu_2\text{-}OMe)_2] \cdot 3\ CH_3OH$.

Empirical formula	$C_{75}H_{117}N_{20}O_{22}Pb_2S_8U_3$	
Formula weight	3035.83	
Temperature	100(2) K	
Wavelength	0.71073 Å	
Crystal system	Monoclinic	
Space group	P 2_1/m	
Unit cell dimensions	a = 10.686(2) Å	α= 90(3)°
	b = 29.664(6) Å	β= 100.81(3)°
	c = 17.074(3) Å	γ = 90(3)°
Volume	5316(2) $Å^3$	
Z	2	
Density (calculated)	1.896 g/cm^3	
Absorption coefficient	7.938 mm^{-1}	
F(000)	2902	
Crystal size	0.07 x 0.03 x 0.02 mm^3	
Theta range for data collection	2.377 to 27.202°	
Index ranges	-13<=h<=12, -33<=k<=38, -21<=l<=21	
Reflections collected	46320	
Independent reflections	11835 [R(int) = 0.0227]	
Completeness to theta = 25.242°	99.1 %	
Absorption correction	Semi-empirical from equivalents	
Max. and min. transmission	0.7455 and 0.6372	
Refinement method	Full-matrix least-squares on F^2	
Data / restraints / parameters	11835 / 0 / 626	
Goodness-of-fit on F^2	1.200	
Final R indices [I>2sigma(I)]	R1 = 0.0278, wR2 = 0.0665	
R indices (all data)	R1 = 0.0336, wR2 = 0.0695	
Largest diff. peak and hole	3.186 and -1.660 e/$Å^3$	
Diffractometer	Bruker D8 Venture	

Table A.36: Atomic coordinates (x 10^4) and equivalent isotropic displacement parameters ($Å^2$ x 10^3) for $[Pb_2(UO_2)_3(L^{2a})_4(MeOH)_2(\mu_2\text{-}OMe)_2] \cdot 3\ CH_3OH$.

	x	y	z	U(eq)
U(2)	4829(1)	7500	6368(1)	12(1)
U(3)	1229(1)	7500	3019(1)	11(1)
Pb(1)	2698(1)	6320(1)	3973(1)	14(1)
U(1)	3070(1)	7500	8047(1)	17(1)
S(11)	890(1)	5673(1)	3962(1)	22(1)
S(1)	3572(1)	5741(1)	2831(1)	21(1)
S(21)	1055(2)	5736(1)	8047(1)	39(1)
N(46)	2686(5)	7500	1920(3)	14(1)
N(56)	-254(5)	7500	4102(3)	13(1)
O(2)	4399(5)	7500	8843(3)	25(1)
O(25)	2471(4)	6791(1)	8463(2)	26(1)
O(1)	1716(5)	7500	7260(3)	25(1)
C(51)	-570(4)	7113(2)	4420(3)	13(1)
N(13)	-815(4)	6336(1)	4118(2)	16(1)
N(66)	1689(6)	7500	9097(3)	19(1)
N(6)	1567(4)	5664(1)	1640(3)	21(1)
C(4)	2573(5)	6706(2)	1980(3)	16(1)
N(3)	2720(4)	6322(1)	1652(3)	18(1)
C(14)	-267(4)	6708(2)	3981(3)	13(1)
N(16)	-1600(4)	5702(1)	3437(3)	16(1)
N(23)	1612(5)	6307(2)	9278(3)	24(1)
C(2)	2513(5)	5918(2)	2005(3)	18(1)
C(12)	-579(5)	5927(2)	3803(3)	16(1)
C(41)	3039(5)	7113(2)	1616(3)	15(1)
C(52)	-1124(5)	7098(2)	5091(3)	17(1)
N(26)	3039(5)	5719(2)	9241(3)	31(1)
C(53)	-1390(7)	7500	5445(4)	19(1)
C(43)	4139(7)	7500	724(4)	21(2)
C(63)	286(7)	7500	10287(5)	26(2)
C(42)	3772(5)	7099(2)	1024(3)	20(1)
C(61)	1357(5)	7108(2)	9391(3)	18(1)
C(22)	1987(6)	5931(2)	8890(3)	28(1)
C(17)	-1531(5)	5236(2)	3147(3)	21(1)
C(24)	1844(5)	6704(2)	9014(3)	19(1)

C(62)	630(5)	7095(2)	9992(3)	22(1)
C(9)	615(6)	5846(2)	980(4)	30(1)
C(10)	-419(6)	6095(2)	1298(5)	44(2)
C(7)	1355(6)	5198(2)	1886(4)	29(1)
C(19)	-2881(5)	5906(2)	3320(3)	22(1)
C(18)	-1741(6)	4896(2)	3775(4)	34(1)
C(27)	3817(7)	5875(2)	9998(4)	39(2)
C(20)	-3153(6)	6186(2)	2564(3)	32(1)
C(8)	1952(7)	4863(2)	1393(4)	44(2)
C(29)	3515(8)	5318(2)	8897(4)	45(2)
C(30)	3006(9)	4888(2)	9189(5)	60(2)
C(28)	4899(7)	6164(3)	9847(5)	50(2)
S(31)	3902(1)	5659(1)	5018(1)	19(1)
O(21)	3212(5)	7500	5814(3)	15(1)
O(35)	5158(3)	6790(1)	5822(2)	17(1)
O(11)	2537(4)	7500	3830(3)	16(1)
O(5)	2053(3)	6783(1)	2589(2)	17(1)
O(3)	4205(3)	7037(1)	7301(2)	18(1)
O(15)	467(3)	6776(1)	3471(2)	15(1)
O(12)	-78(5)	7500	2217(3)	18(1)
N(33)	5563(4)	6306(1)	4842(2)	14(1)
N(76)	5454(5)	7500	5002(3)	12(1)
O(22)	6459(5)	7500	6854(3)	20(1)
C(34)	5417(4)	6703(1)	5135(3)	12(1)
C(32)	5324(5)	5929(2)	5285(3)	14(1)
C(71)	5562(4)	7108(1)	4627(3)	13(1)
O(13)	1960(4)	6689(1)	5249(2)	21(1)
N(36)	6202(4)	5774(1)	5867(3)	19(1)
C(73)	5847(8)	7500	3464(4)	21(2)
C(72)	5748(5)	7094(2)	3846(3)	18(1)
C(39)	5984(5)	5367(2)	6320(3)	20(1)
C(13)	1827(6)	6453(2)	5960(3)	27(1)
C(40)	5315(6)	5477(2)	7007(3)	29(1)
C(37)	7433(5)	6002(2)	6135(4)	31(1)
C(3)	4930(7)	6660(2)	7650(4)	34(1)
C(38)	8512(6)	5758(3)	5857(5)	44(2)
O(100)	8749(6)	6421(2)	7980(5)	79(2)
C(100)	9108(9)	6811(3)	7527(6)	66(3)
O(101)	7793(11)	6412(7)	9378(8)	85(5)

C(101)	7467(18)	6873(10)	9399(16)	115(11)

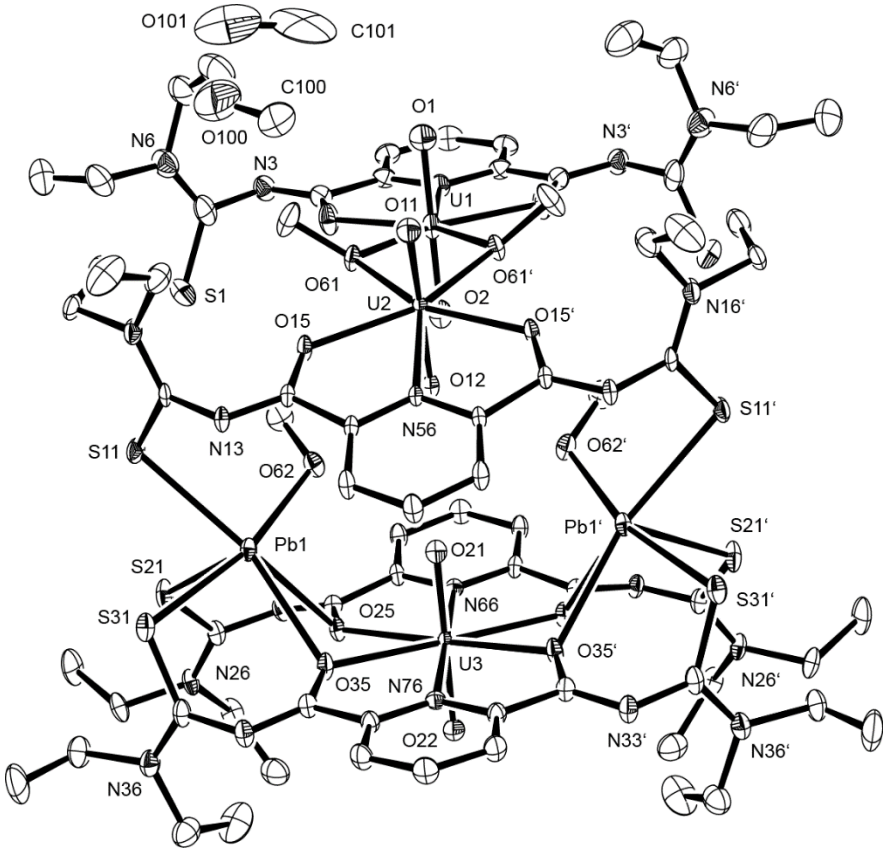

Figure A.18: Ellipsoid plot of $[Pb_2(UO_2)_3(L^{2a})_4(MeOH)_2(\mu_2\text{-}OMe)_2] \cdot 3\,CH_3OH$. Hydrogen atoms have been omitted for clarity. Thermal ellipsoids are at 50 % probability.

$[Pb_2(UO_2)_3(L^{2a})_4(MeOH)_2(\mu_2\text{-}OMe)_2]$ (SQUEEZE)

Table A.37. Crystal data and structure refinement for $[Pb_2(UO_2)_3(L^{2a})_4(MeOH)_2(\mu_2\text{-}OMe)_2]$ **(SQUEEZE).**

Empirical formula	$C_{72}H_{106}N_{20}O_{18}Pb_2S_8U_3$	
Formula weight	2924.71	
Temperature	100(2) K	
Wavelength	0.71073 Å	
Crystal system	Monoclinic	
Space group	P 2_1/m	
Unit cell dimensions	a = 10.686(2) Å	α= 90°
	b = 29.664(6) Å	β= 100.81(3)°
	c = 17.074(3) Å	γ = 90°
Volume	5316(2) $Å^3$	
Z	2	
Density (calculated)	1.827 g/cm^3	
Absorption coefficient	7.931 mm^{-1}	
F(000)	2888	
Crystal size	0.07 x 0.03 x 0.02 mm^3	
Theta range for data collection	2.377 to 27.202°	
Index ranges	-13<=h<=12, -33<=k<=38, -21<=l<=21	
Reflections collected	46320	
Independent reflections	11835 [R(int) = 0.0224]	
Completeness to theta = 25.242°	99.1 %	
Absorption correction	Semi-empirical from equivalents	
Max. and min. transmission	0.7455 and 0.6372	
Refinement method	Full-matrix least-squares on F^2	
Data / restraints / parameters	11835 / 0 / 587	
Goodness-of-fit on F^2	1.119	
Final R indices [I>2sigma(I)]	R1 = 0.0250, wR2 = 0.0544	
R indices (all data)	R1 = 0.0295, wR2 = 0.0563	
Largest diff. peak and hole	1.598 and -1.564 e/$Å^3$	
Diffractometer	Bruker D8 Venture	

Table A.38. Atomic coordinates (x 10^4) and equivalent isotropic displacement parameters ($Å^2$ x 10^3) for $[Pb_2(UO_2)_3(L^{2a})_4(MeOH)_2(\mu_2\text{-}OMe)_2]$ **(SQUEEZE**).

	x	y	z	U(eq)
U(2)	4829(1)	7500	6368(1)	12(1)
U(3)	1229(1)	7500	3019(1)	11(1)
Pb(1)	2698(1)	6320(1)	3973(1)	14(1)
U(1)	3070(1)	7500	8047(1)	17(1)
S(11)	890(1)	5673(1)	3962(1)	22(1)
S(1)	3572(1)	5741(1)	2831(1)	21(1)
S(21)	1056(2)	5736(1)	8047(1)	39(1)
N(46)	2687(5)	7500	1920(3)	14(1)
N(56)	-253(4)	7500	4102(3)	13(1)
O(2)	4398(5)	7500	8843(3)	25(1)
O(25)	2466(3)	6791(1)	8461(2)	26(1)
O(1)	1717(5)	7500	7261(3)	25(1)
C(51)	-570(4)	7114(1)	4420(2)	13(1)
N(13)	-816(3)	6336(1)	4118(2)	16(1)
N(66)	1689(5)	7500	9097(3)	19(1)
N(6)	1566(4)	5664(1)	1641(2)	21(1)
C(4)	2574(4)	6706(1)	1981(2)	16(1)
N(3)	2720(4)	6321(1)	1652(2)	18(1)
C(14)	-266(4)	6708(1)	3981(2)	13(1)
N(16)	-1601(3)	5702(1)	3437(2)	16(1)
N(23)	1609(4)	6308(1)	9277(2)	24(1)
C(2)	2514(4)	5917(1)	2006(2)	18(1)
C(12)	-580(4)	5927(1)	3803(2)	15(1)
C(41)	3038(4)	7113(1)	1617(2)	15(1)
C(52)	-1123(4)	7098(1)	5092(2)	17(1)
N(26)	3039(4)	5718(1)	9241(2)	32(1)
C(53)	-1385(6)	7500	5447(4)	19(1)
C(43)	4146(6)	7500	726(4)	22(1)
C(63)	282(6)	7500	10286(4)	25(1)
C(42)	3774(4)	7099(1)	1026(2)	20(1)
C(61)	1353(4)	7108(1)	9390(2)	19(1)
C(22)	1982(5)	5931(2)	8888(3)	27(1)
C(17)	-1534(4)	5237(1)	3147(3)	21(1)
C(24)	1839(4)	6704(1)	9013(2)	19(1)

C(62)	631(4)	7095(2)	9993(2)	21(1)
C(9)	610(5)	5847(2)	980(3)	30(1)
C(10)	-424(5)	6095(2)	1293(4)	44(1)
C(7)	1353(5)	5198(2)	1887(3)	29(1)
C(19)	-2884(4)	5906(2)	3319(3)	22(1)
C(18)	-1744(5)	4896(2)	3772(3)	34(1)
C(27)	3825(6)	5875(2)	10000(3)	39(1)
C(20)	-3154(5)	6187(2)	2562(3)	31(1)
C(8)	1953(6)	4862(2)	1394(4)	44(1)
C(29)	3518(6)	5317(2)	8896(4)	45(2)
C(30)	3003(8)	4886(2)	9188(4)	61(2)
C(28)	4905(6)	6165(2)	9849(4)	50(2)
S(31)	3902(1)	5659(1)	5017(1)	19(1)
O(21)	3212(4)	7500	5814(2)	16(1)
O(35)	5157(3)	6791(1)	5821(2)	17(1)
O(11)	2535(4)	7500	3830(2)	15(1)
O(5)	2053(3)	6783(1)	2587(2)	17(1)
O(3)	4205(3)	7037(1)	7301(2)	18(1)
O(15)	467(3)	6777(1)	3472(2)	15(1)
O(12)	-77(4)	7500	2216(2)	18(1)
N(33)	5564(3)	6305(1)	4842(2)	14(1)
N(76)	5455(4)	7500	5002(3)	12(1)
O(22)	6457(4)	7500	6854(2)	20(1)
C(34)	5416(4)	6703(1)	5135(2)	12(1)
C(32)	5324(4)	5929(1)	5285(2)	14(1)
C(71)	5561(4)	7108(1)	4626(2)	12(1)
O(13)	1960(3)	6689(1)	5249(2)	21(1)
N(36)	6202(3)	5774(1)	5867(2)	19(1)
C(73)	5845(6)	7500	3463(4)	21(1)
C(72)	5747(4)	7094(1)	3846(2)	17(1)
C(39)	5985(4)	5367(1)	6321(3)	20(1)
C(13)	1829(5)	6453(2)	5962(3)	27(1)
C(40)	5317(5)	5477(2)	7007(3)	30(1)
C(37)	7431(5)	6002(2)	6136(3)	31(1)
C(3)	4932(6)	6660(2)	7650(3)	34(1)
C(38)	8512(5)	5758(2)	5857(4)	43(1)

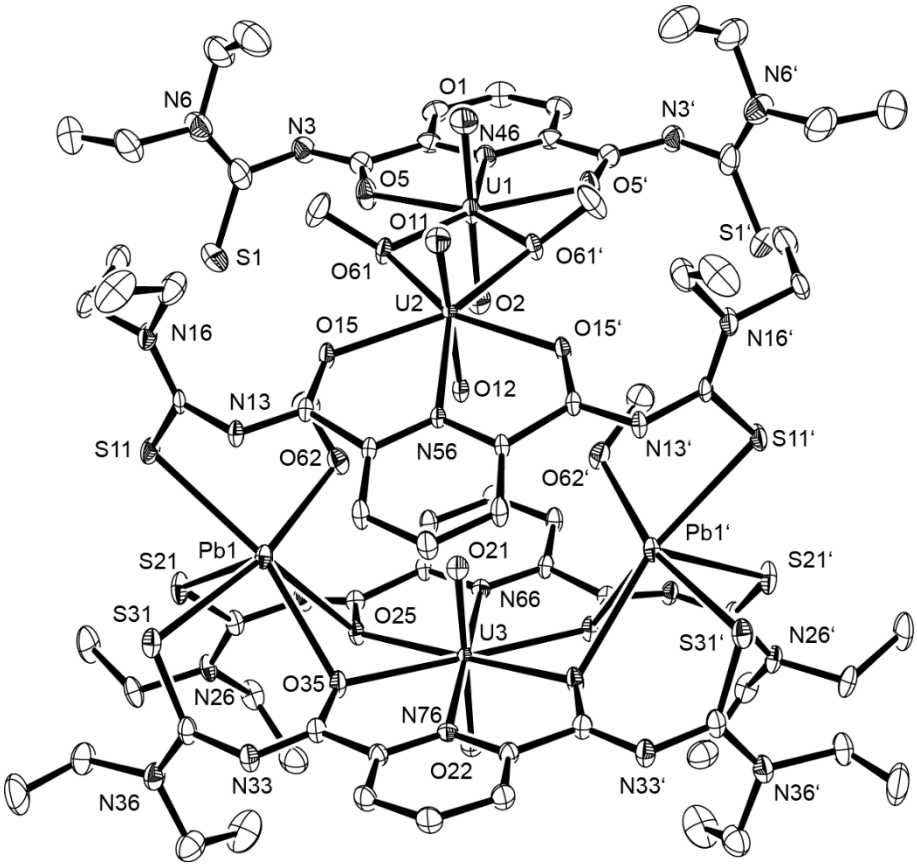

Figure A.19: Ellipsoid plot of $[Pb_2(UO_2)_3(L^{2a})_4(MeOH)_2(\mu_2\text{-}OMe)_2]$ **(SQUEEZE)**. Hydrogen atoms have been omitted for clarity. Thermal ellipsoids are at 50 % probability.

$[Ni\{UO_2(L^{2a})(OAc)\}_2]$

Table A.39: Crystal data and structure refinement for $[Ni\{UO_2(L^{2a})(OAc)\}_2] \cdot 2\ CH_2Cl_2$.

Empirical formula	$C_{40}H_{56}Cl_4N_{10}NiO_{12}S_4U_2$	
Formula weight	1673.75	
Temperature	104(2) K	
Wavelength	0.71073 Å	
Crystal system	Monoclinic	
Space group	C 2/c	
Unit cell dimensions	a = 18.736(5) Å	α= 90°
	b = 10.645(3) Å	β= 92.82(1)°
	c = 28.020(7) Å	γ = 90°
Volume	5582(3) $Å^3$	
Z	4	
Density (calculated)	1.992 g/cm^3	
Absorption coefficient	6.528 mm^{-1}	
F(000)	3224	
Crystal size	0.200 x 0.200 x 0.020 mm^3	
Theta range for data collection	2.201 to 27.244°	
Index ranges	-24<=h<=24, -13<=k<=13, -35<=l<=35	
Reflections collected	101172	
Absorption correction	Semi-empirical from equivalents	
Independent reflections	6213 [R(int) = 0.0349]	
Completeness to theta = 25.242°	100.0 %	
Refinement method	Full-matrix least-squares on F^2	
Data / restraints / parameters	6213 / 6 / 348	
Goodness-of-fit on F^2	1.103	
Final R indices [I>2sigma(I)]	R1 = 0.0219, wR2 = 0.0557	
R indices (all data)	R1 = 0.0251, wR2 = 0.0572	
Largest diff. peak and hole	0.571 and -2.123 e/$Å^3$	
Diffractometer	Bruker D8 Venture	

Table A.40. Atomic coordinates (x 10^4) and equivalent isotropic displacement parameters ($Å^2$ x 10^3) for $[Ni\{UO_2(L^{2a})(OAc)\}_2] \cdot 2\ CH_2Cl_2$.

	x	y	z	U(eq)
U(1)	4942(1)	3597(1)	6389(1)	13(1)
Ni(1)	5000	5479(1)	7500	15(1)
S(1)	5546(1)	1621(1)	5852(1)	18(1)
O(15)	4418(1)	5316(2)	6861(1)	17(1)
O(31)	5516(1)	4032(2)	7174(1)	18(1)
O(1)	5431(1)	4793(2)	6110(1)	21(1)
O(2)	4419(1)	2465(2)	6678(1)	19(1)
O(32)	6142(1)	2842(2)	6729(1)	22(1)
N(26)	3744(1)	4531(3)	6077(1)	16(1)
O(5)	3468(1)	2336(3)	5138(1)	30(1)
N(3)	4482(2)	2985(3)	5579(1)	17(1)
N(6)	5087(2)	2021(3)	4943(1)	18(1)
N(13)	3612(2)	6996(3)	6914(1)	18(1)
C(14)	3850(2)	5962(3)	6737(1)	14(1)
C(21)	3390(2)	4013(3)	5695(1)	18(1)
C(33)	6106(2)	3476(3)	7102(1)	18(1)
C(2)	4987(2)	2208(3)	5403(1)	16(1)
C(25)	3425(2)	5451(3)	6314(1)	15(1)
C(4)	3782(2)	3012(3)	5433(1)	21(1)
C(24)	2747(2)	5893(3)	6175(1)	17(1)
C(9)	5697(2)	1244(4)	4806(1)	28(1)
C(7)	4742(2)	2757(4)	4552(1)	24(1)
C(34)	6722(2)	3593(4)	7460(1)	27(1)
C(8)	4299(2)	1957(4)	4198(1)	32(1)
C(23)	2384(2)	5341(4)	5787(1)	22(1)
C(22)	2706(2)	4374(4)	5546(1)	23(1)
C(10)	6373(2)	2024(6)	4772(2)	48(1)
S(11)	4200(1)	6901(1)	7828(1)	28(1)
N(16)	3842(2)	8860(3)	7283(1)	20(1)
C(12)	3892(2)	7616(3)	7310(1)	18(1)
C(17)	3528(2)	9481(3)	6852(1)	24(1)
C(19)	4082(2)	9678(4)	7682(1)	25(1)
C(18)	4057(2)	9574(4)	6461(1)	31(1)
C(20)	3490(2)	9898(4)	8025(1)	26(1)

Cl(1A)	2507(1)	1863(2)	6353(1)	71(1)
C(35A)	1969(1)	1006(2)	5943(1)	71(1)
Cl(1B)	2507(1)	1863(2)	6353(1)	71(1)
C(35B)	2346(1)	1078(2)	5799(1)	71(1)

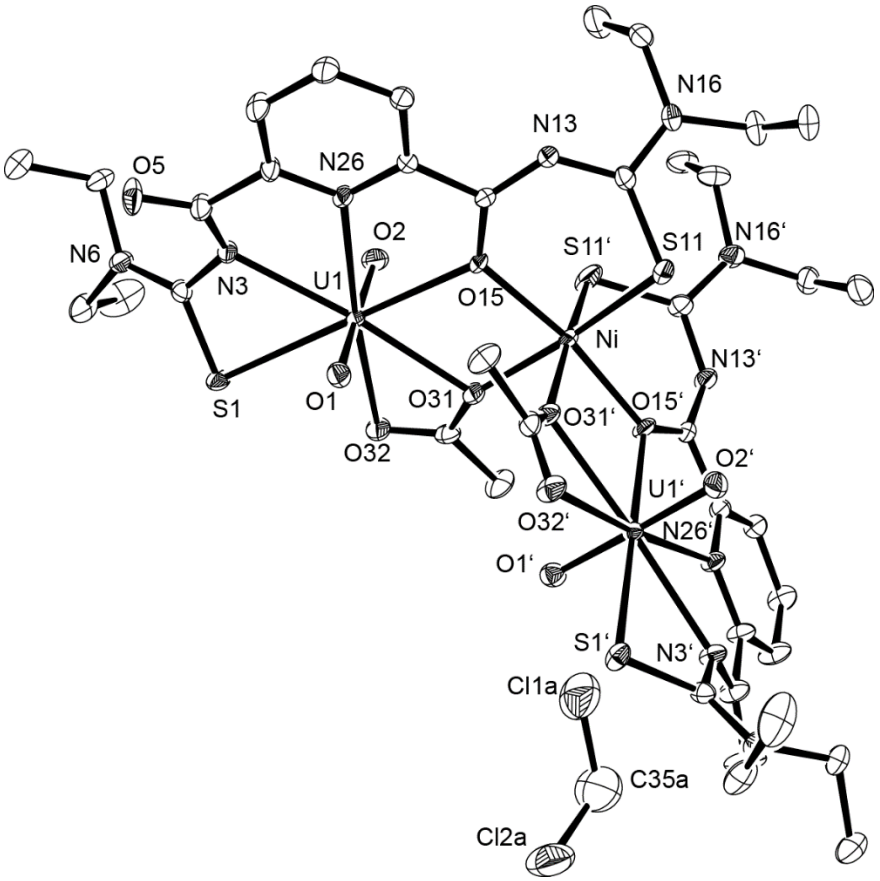

Figure A.20: Ellipsoid plot of [Ni{$UO_2(L^{2a})(OAc)$}$_2$] · 2 CH_2Cl_2. Hydrogen atoms have been omitted for clarity. Thermal ellipsoids are at 50 % probability.

[Mn{$UO_2(L^{2a})(OAc)\}_2$]

Table A.41. Crystal data and structure refinement for [Mn{$UO_2(L^{2a})(OAc)\}_2$] · 2.5 CH_2Cl_2.

Empirical formula	$C_{40.50}H_{57}Cl_5MnN_{10}O_{12}S_4U_2$	
Formula weight	1712.45	
Temperature	100(2) K	
Wavelength	0.71073 Å	
Crystal system	Monoclinic	
Space group	P $2_1/c$	
Unit cell dimensions	a = 9.1432(6) Å	α= 90°
	b = 20.902(1) Å	β= 91.75(2)°
	c = 31.498(2) Å	γ = 90°
Volume	6016.9(6) $Å^3$	
Z	4	
Density (calculated)	1.890 g/cm^3	
Absorption coefficient	5.998 mm^{-1}	
F(000)	3296	
Crystal size	0.22 x 0.12 x 0.04 mm^3	
Theta range for data collection	2.171 to 27.207°	
Index ranges	-11<=h<=11, -26<=k<=26, -40<=l<=40	
Reflections collected	196816	
Independent reflections	13379 [R(int) = 0.0430]	
Completeness to theta = 25.242°	99.9 %	
Absorption correction	Semi-empirical from equivalents	
Max. and min. transmission	0.7455 and 0.4903	
Refinement method	Full-matrix least-squares on F^2	
Data / restraints / parameters	13379 / 0 / 696	
Goodness-of-fit on F^2	1.017	
Final R indices [I>2sigma(I)]	R1 = 0.0325, wR2 = 0.0825	
R indices (all data)	R1 = 0.0360, wR2 = 0.0845	
Largest diff. peak and hole	2.596 and -1.999 e/$Å^3$	
Diffractometer	Bruker D8 Venture	

Table A.42: Atomic coordinates (x 10^4) and equivalent isotropic displacement parameters ($Å^2$ x 10^3) for $[Mn\{UO_2(L^{2a})(OAc)\}_2] \cdot 2.5\ CH_2Cl_2$.

	x	y	z	U(eq)
U(2)	9724(1)	2420(1)	3240(1)	11(1)
U(1)	8139(1)	2853(1)	1220(1)	12(1)
Mn(1)	8893(1)	1611(1)	2136(1)	12(1)
S(11)	9113(2)	3935(1)	743(1)	26(1)
S(1)	7216(1)	689(1)	2318(1)	16(1)
S(21)	10759(1)	1003(1)	1726(1)	19(1)
S(31)	8787(2)	3231(1)	3922(1)	26(1)
O(61)	10631(4)	3234(2)	1462(1)	19(1)
O(62)	9651(4)	2486(2)	1839(1)	17(1)
O(1)	7261(4)	3360(2)	1583(1)	18(1)
O(2)	8988(4)	2325(2)	860(1)	17(1)
O(12)	10506(4)	3074(2)	2966(1)	16(1)
O(11)	8942(4)	1764(2)	3507(1)	19(1)
O(15)	4405(5)	3828(2)	523(2)	32(1)
O(5)	7393(3)	1845(2)	1592(1)	13(1)
O(25)	10481(3)	1625(2)	2686(1)	13(1)
O(35)	13510(5)	3140(2)	4053(1)	29(1)
O(71)	8052(4)	2235(2)	2619(1)	17(1)
O(72)	7283(4)	2936(2)	3071(1)	18(1)
N(13)	6676(5)	3339(2)	631(1)	18(1)
N(16)	7378(6)	3950(3)	37(2)	38(1)
N(3)	5929(4)	930(2)	1548(1)	14(1)
N(6)	7011(4)	-47(2)	1624(1)	16(1)
N(46)	5550(4)	2441(2)	1072(1)	12(1)
N(23)	12109(5)	817(2)	2499(2)	20(1)
N(26)	11668(5)	-73(2)	2105(2)	29(1)
N(56)	12366(4)	2016(2)	3278(1)	14(1)
N(33)	11259(5)	2664(2)	3883(1)	19(1)
N(36)	10641(6)	2962(3)	4580(1)	29(1)
C(63)	10758(5)	2839(2)	1759(2)	15(1)
C(64)	12146(5)	2766(3)	2021(2)	20(1)
C(12)	7584(6)	3763(3)	435(2)	24(1)
C(14)	5200(6)	3391(2)	652(2)	19(1)
C(19)	6250(9)	3662(4)	-250(2)	50(2)

C(20)	6629(14)	3009(6)	-379(3)	90(4)
C(17)	8390(8)	4406(4)	-166(3)	54(2)
C(18)	7778(10)	5057(4)	-160(3)	62(2)
C(2)	6749(5)	515(2)	1797(2)	13(1)
C(4)	6224(5)	1521(2)	1482(1)	12(1)
C(7)	7712(5)	-576(2)	1863(2)	21(1)
C(8)	6569(6)	-992(3)	2073(2)	33(1)
C(9)	6612(6)	-183(3)	1178(2)	21(1)
C(10)	7855(7)	-15(4)	884(2)	38(2)
C(41)	4572(5)	2820(2)	864(2)	15(1)
C(42)	3092(5)	2678(2)	838(2)	16(1)
C(43)	2620(5)	2099(3)	1001(2)	17(1)
C(44)	3631(5)	1693(2)	1198(2)	16(1)
C(45)	5079(5)	1893(2)	1238(1)	13(1)
C(22)	11502(5)	556(2)	2138(2)	19(1)
C(24)	11710(5)	1315(2)	2703(2)	15(1)
C(27)	12187(8)	-463(3)	2474(3)	53(2)
C(28)	10945(11)	-653(4)	2742(3)	72(3)
C(29)	11452(6)	-407(3)	1697(2)	32(1)
C(30)	12861(8)	-387(4)	1453(4)	66(3)
C(51)	13350(6)	2295(2)	3547(2)	18(1)
C(52)	14830(6)	2146(3)	3552(2)	23(1)
C(53)	15295(6)	1666(3)	3285(2)	23(1)
C(54)	14300(5)	1366(3)	3014(2)	21(1)
C(55)	12842(5)	1570(2)	3012(2)	16(1)
C(32)	10371(6)	2954(3)	4163(2)	24(1)
C(34)	12727(6)	2753(3)	3860(2)	22(1)
C(37)	9632(9)	3262(4)	4876(2)	43(2)
C(38)	10207(13)	3894(5)	5037(3)	75(3)
C(39)	11829(7)	2577(3)	4784(2)	35(1)
C(40)	11413(9)	1880(4)	4805(2)	43(2)
C(73)	7079(5)	2640(2)	2731(2)	14(1)
C(74)	5752(5)	2741(3)	2449(2)	20(1)
Cl(1)	4264(3)	4252(1)	1680(1)	87(1)
Cl(2)	2334(5)	5298(1)	1400(1)	103(1)
Cl(5)	1053(4)	532(2)	3659(1)	44(1)
Cl(3)	5591(4)	1449(2)	191(1)	113(1)
Cl(4)	6447(6)	335(2)	-301(1)	62(1)
Cl(6)	3870(5)	380(3)	4087(1)	63(1)

C(75)	2801(9)	4492(4)	1341(3)	53(2)
C(77)	2727(13)	130(5)	3682(4)	28(2)
C(76)	5492(14)	1068(6)	-286(4)	32(3)

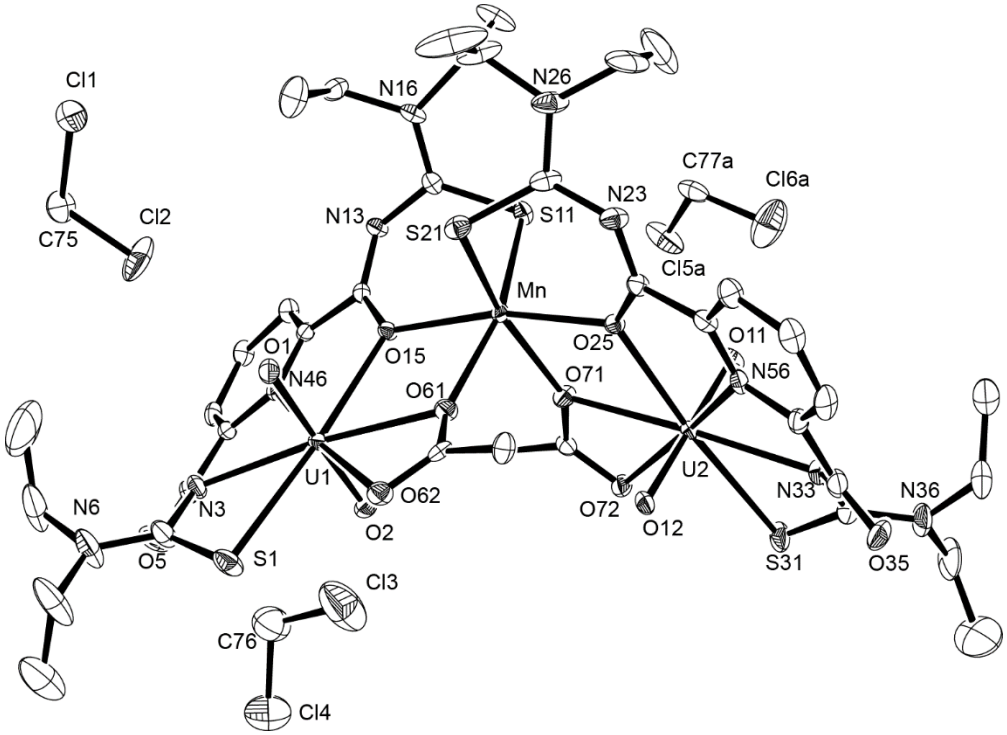

Figure A.21: Ellipsoid plot of $[Mn\{UO_2(L^{2a})(OAc)\}_2] \cdot 2.5\ CH_2Cl_2$. Hydrogen atoms have been omitted for clarity. Thermal ellipsoids are at 50 % probability.

$[Co\{UO_2(L^{2a})(OAc)\}_2]$

Table A.43. Crystal data and structure refinement for $[Co\{UO_2(L^{2a})(OAc)\}_2] \cdot 2\ CH_2Cl_2$.

Empirical formula	$C_{40}H_{56}Cl_4CoN_{10}O_{12}S_4U_2$	
Formula weight	1673.97	
Temperature	100(2) K	
Wavelength	0.71073 Å	
Crystal system	Monoclinic	
Space group	C 2/c	
Unit cell dimensions	a = 18.801(1) Å	α= 90°
	b = 10.699(1) Å	β= 92.77(4)°
	c = 28.381(1) Å	γ = 90°
Volume	5702.2(6) $Å^3$	
Z	4	
Density (calculated)	1.950 g/cm^3	
Absorption coefficient	6.351 mm^{-1}	
F(000)	3220	
Crystal size	0.21 x 0.14 x 0.06 mm^3	
Theta range for data collection	3.517 to 25.999°	
Index ranges	-23<=h<=23, -13<=k<=13, -34<=l<=34	
Reflections collected	22029	
Independent reflections	5559 [R(int) = 0.0379]	
Completeness to theta = 25.242°	99.2 %	
Refinement method	Full-matrix least-squares on F^2	
Data / restraints / parameters	5559 / 0 / 331	
Goodness-of-fit on F^2	1.107	
Final R indices [I>2sigma(I)]	R1 = 0.0294, wR2 = 0.0658	
R indices (all data)	R1 = 0.0386, wR2 = 0.0680	
Largest diff. peak and hole	0.735 and -1.358 e/$Å^3$	
Diffractometer	Bruker D8 Venture	

Table A.44: Atomic coordinates (x 10^4) and equivalent isotropic displacement parameters ($Å^2$ x 10^3) for $[Co\{UO_2(L^{2a})(OAc)\}_2] \cdot 2\ CH_2Cl_2$.

	x	y	z	U(eq)
U(1)	75(1)	1452(1)	8625(1)	26(1)
Co(1)	0	-423(1)	7500	30(1)
S(1)	-528(1)	3400(1)	9165(1)	38(1)
O(50)	-1096(2)	2270(3)	8277(1)	44(1)
N(46)	1260(2)	504(3)	8935(1)	28(1)
C(45)	1613(2)	1006(5)	9311(2)	33(1)
O(1)	-425(2)	268(3)	8886(1)	36(1)
N(16)	1166(2)	-3748(4)	7721(1)	37(1)
O(2)	607(2)	2573(3)	8352(1)	36(1)
N(3)	521(2)	2016(4)	9433(1)	32(1)
O(5)	1529(2)	2642(4)	9873(1)	54(1)
C(41)	1587(2)	-393(4)	8692(2)	28(1)
C(42)	2266(2)	-829(5)	8825(2)	32(1)
C(2)	18(2)	2787(4)	9604(2)	30(1)
C(4)	1216(3)	1988(5)	9577(2)	36(1)
N(6)	-88(2)	2952(4)	10056(1)	35(1)
C(44)	2297(2)	653(5)	9453(2)	39(1)
C(43)	2618(3)	-283(5)	9212(2)	42(1)
C(7)	-695(3)	3716(6)	10198(2)	53(2)
C(8)	-1368(4)	2949(9)	10220(3)	84(2)
O(15)	596(2)	-263(3)	8157(1)	30(1)
N(13)	1405(2)	-1906(4)	8093(1)	34(1)
C(14)	1160(2)	-888(4)	8272(2)	30(1)
S(11)	-850(1)	-1774(1)	7814(1)	49(1)
O(51)	-485(2)	1064(3)	7842(1)	36(1)
Cl(2)	2837(2)	5552(4)	9154(1)	159(1)
C(52)	-1063(3)	1655(4)	7910(2)	37(1)
C(12)	1134(3)	-2512(5)	7698(2)	34(1)
C(17)	1452(3)	-4375(5)	8149(2)	44(1)
C(53)	-1673(3)	1569(6)	7551(2)	51(1)
C(19)	936(3)	-4548(5)	7321(2)	44(1)
C(9)	254(3)	2206(5)	10445(2)	42(1)
C(20)	1529(3)	-4801(6)	6993(2)	55(2)

C(18)	911(4)	-4491(6)	8521(2)	57(2)
C(10)	686(3)	2986(7)	10799(2)	60(2)
Cl(1)	2484(2)	3226(3)	8655(1)	115(1)
C(54)	2885(9)	4109(12)	9102(7)	209(9)

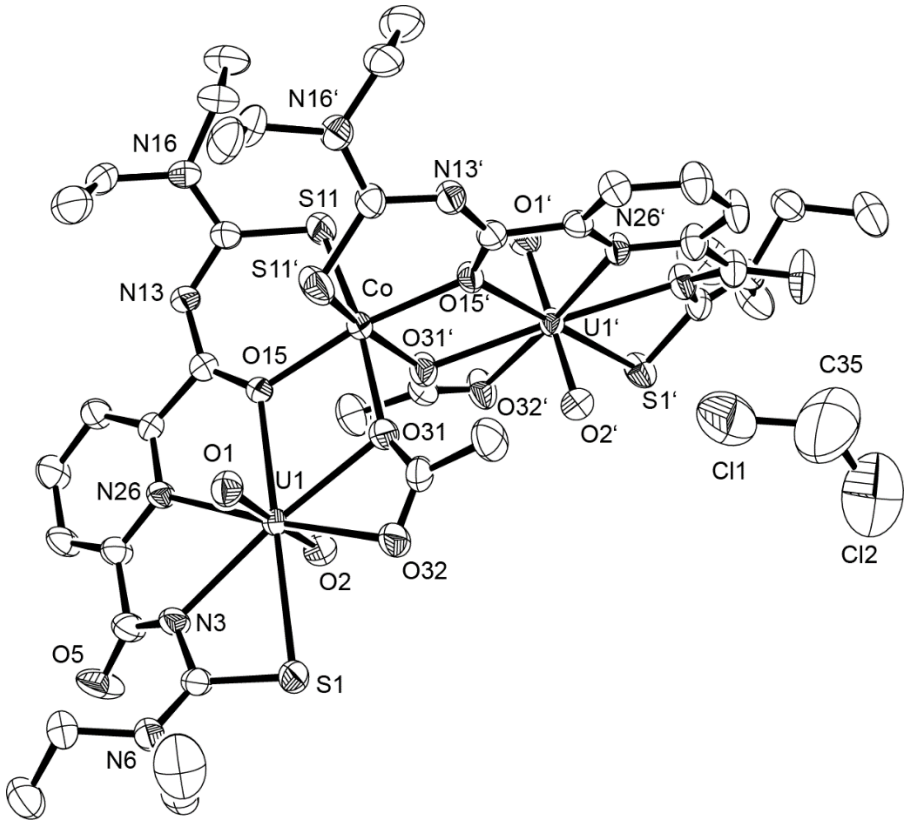

Figure A.22: Ellipsoid plot of $[Co\{UO_2(L^{2a})(OAc)\}_2] \cdot 2\ CH_2Cl_2$. Hydrogen atoms have been omitted for clarity. Thermal ellipsoids are at 50 % probability.

$[Fe\{UO_2(L^{2a})(OAc)\}_2]$

Table A.45: Crystal data and structure refinement for $[Fe\{UO_2(L^{2a})(OAc)\}_2] \cdot 3\ H_2O$.

Empirical formula	$C_{38}H_{52}FeN_{10}O_{15}S_4U_2$	
Formula weight	1549.04	
Temperature	200(2) K	
Wavelength	0.71073 Å	
Crystal system	Monoclinic	
Space group	C 2/c	
Unit cell dimensions	a = 18.774(2) Å	α= 90°
	b = 10.632(1) Å	β= 92.14(1)°
	c = 28.219(3) Å	γ = 90°
Volume	5628(1) $Å^3$	
Z	4	
Density (calculated)	1.828 g/cm^3	
Absorption coefficient	6.209 mm^{-1}	
F(000)	2976	
Crystal size	0.12 x 0.12 x 0.02 mm^3	
Theta range for data collection	3.550 to 25.998°	
Index ranges	-23<=h<=19, -13<=k<=13, -34<=l<=34	
Reflections collected	16292	
Independent reflections	5516 [R(int) = 0.0490]	
Completeness to theta = 25.242°	99.6 %	
Absorption correction	Integration	
Max. and min. transmission	0.7322 and 0.4762	
Refinement method	Full-matrix least-squares on F^2	
Data / restraints / parameters	5516 / 0 / 322	
Goodness-of-fit on F^2	0.952	
Final R indices [I>2sigma(I)]	R1 = 0.0340, wR2 = 0.0692	
R indices (all data)	R1 = 0.0529, wR2 = 0.0734	
Largest diff. peak and hole	1.143 and -0.851 $e/Å^3$	
Diffractometer	IPDS, STOE	

Table A.46: Atomic coordinates (x 10^4) and equivalent isotropic displacement parameters ($Å^2$ x 10^3) for $[Fe\{UO_2(L^{2a})(OAc)\}_2] \cdot 3\ H_2O$.

	x	y	z	U(eq)
U(1)	5061(1)	3648(1)	8615(1)	26(1)
Fe(1)	5000	5619(1)	7500	34(1)
S(1)	4440(1)	1655(1)	9140(1)	37(1)
S(15)	5903(2)	6988(2)	7201(1)	72(1)
O(1)	4569(2)	4814(4)	8900(2)	38(1)
O(2)	5572(2)	2537(4)	8314(2)	35(1)
N(46)	6265(2)	4515(4)	8922(2)	28(1)
O(32)	3863(2)	2908(4)	8279(2)	44(1)
N(3)	5516(2)	2986(4)	9409(2)	29(1)
O(11)	5591(2)	5411(3)	8165(1)	31(1)
O(31)	4480(2)	4117(4)	7838(2)	39(1)
N(6)	4906(3)	2038(5)	10040(2)	34(1)
O(5)	6525(2)	2230(5)	9817(2)	49(1)
C(45)	6618(3)	3958(5)	9288(2)	31(1)
C(12)	6172(3)	6012(5)	8289(2)	30(1)
N(13)	6425(3)	7045(4)	8119(2)	36(1)
C(42)	7273(3)	5872(6)	8835(2)	31(1)
C(41)	6597(3)	5460(5)	8699(2)	28(1)
C(2)	5003(3)	2224(5)	9587(2)	30(1)
C(44)	7304(3)	4275(6)	9429(2)	39(2)
C(7)	4307(4)	1250(7)	10189(2)	47(2)
C(43)	7639(3)	5264(6)	9205(2)	40(2)
C(4)	6216(3)	2953(6)	9540(2)	36(1)
C(14)	6161(4)	7693(6)	7728(2)	39(2)
C(8)	3637(4)	2001(10)	10239(4)	77(3)
N(16)	6194(3)	8923(5)	7761(2)	42(1)
C(31)	3902(3)	3530(6)	7908(2)	37(1)
C(32)	3294(4)	3604(8)	7548(3)	53(2)
C(20)	6565(4)	9993(7)	7034(3)	58(2)
C(17)	6471(5)	9525(6)	8195(3)	56(2)
C(19)	5961(4)	9757(7)	7372(3)	54(2)
C(18)	5912(7)	9610(8)	8551(4)	90(4)
C(9)	5259(4)	2773(6)	10420(2)	41(2)
C(10)	5708(4)	1986(7)	10773(3)	52(2)

O(42)	2118(4)	527(15)	866(4)	197(7)
O(41)	7567(11)	1739(19)	8637(7)	148(8)

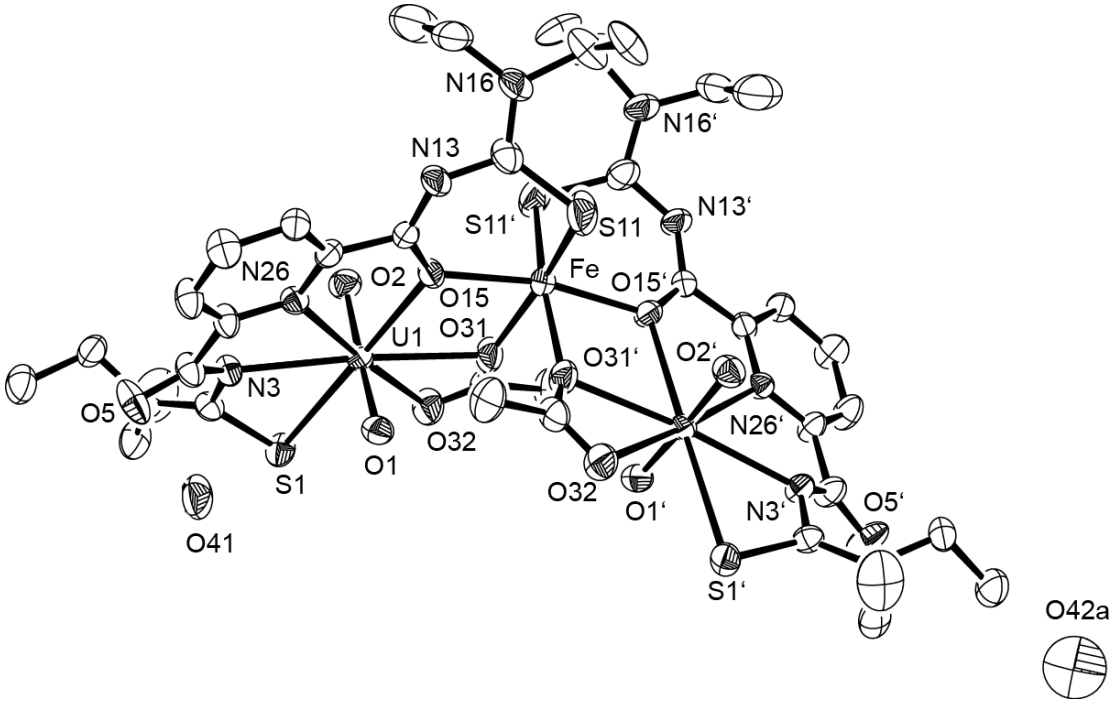

Figure A.23: Ellipsoid plot of $[Fe\{UO_2(L^{2a})(OAc)\}_2] \cdot 3\ H_2O$. Hydrogen atoms have been omitted for clarity. Thermal ellipsoids are at 50 % probability.

$[Fe\{UO_2(L^{2a})(OAc)\}_2]$ (SQUEEZE)

Table A.47: Crystal data and structure refinement for $[Fe\{UO_2(L^{2a})(OAc)\}_2]$ **(SQUEEZE).**

Empirical formula	$C_{38}H_{52}FeN_{10}O_{12}S_4U_2$	
Formula weight	1501.04	
Temperature	200(2) K	
Wavelength	0.71073 Å	
Crystal system	Monoclinic	
Space group	C 2/c	
Unit cell dimensions	a = 18.774(2) Å	α= 90°
	b = 10.632(1) Å	β= 92.14(1)°
	c = 28.219(3) Å	γ = 90°
Volume	5628.7(10) $Å^3$	
Z	4	
Density (calculated)	1.771 g/cm^3	
Absorption coefficient	6.202 mm^{-1}	
F(000)	2880	
Crystal size	0.12 x 0.12 x 0.02 mm^3	
Theta range for data collection	3.550 to 25.998°	
Index ranges	-23<=h<=19, -13<=k<=13, -34<=l<=34	
Reflections collected	16292	
Independent reflections	5516 [R(int) = 0.0474]	
Completeness to theta = 25.242°	99.6 %	
Absorption correction	Integration	
Max. and min. transmission	0.7322 and 0.4762	
Refinement method	Full-matrix least-squares on F^2	
Data / restraints / parameters	5516 / 0 / 304	
Goodness-of-fit on F^2	0.925	
Final R indices [I>2sigma(I)]	R1 = 0.0305, wR2 = 0.0565	
R indices (all data)	R1 = 0.0486, wR2 = 0.0598	
Largest diff. peak and hole	0.689 and -0.898 $e/Å^3$	
Diffractometer	IPDS, STOE	

Table A.48. Atomic coordinates (x 10^4) and equivalent isotropic displacement parameters ($Å^2$ x 10^3) for [Fe{UO_2(L^{2a})(OAc)}$_2$] **(SQUEEZE).**

	x	y	z	U(eq)
U(1)	5061(1)	3648(1)	8615(1)	26(1)
Fe(1)	5000	5619(1)	7500	34(1)
S(1)	4440(1)	1655(1)	9140(1)	36(1)
S(15)	5903(1)	6988(2)	7201(1)	71(1)
O(1)	4569(2)	4814(3)	8901(1)	37(1)
O(2)	5571(2)	2538(3)	8315(1)	35(1)
N(46)	6265(2)	4515(3)	8921(2)	27(1)
O(32)	3861(2)	2910(4)	8279(1)	44(1)
N(3)	5516(2)	2984(4)	9408(2)	29(1)
O(11)	5591(2)	5413(3)	8165(1)	30(1)
O(31)	4480(2)	4116(4)	7839(1)	39(1)
N(6)	4904(2)	2039(4)	10040(2)	33(1)
O(5)	6527(2)	2231(4)	9817(2)	49(1)
C(45)	6618(3)	3954(4)	9288(2)	31(1)
C(12)	6175(3)	6011(4)	8289(2)	29(1)
N(13)	6426(2)	7050(4)	8119(2)	36(1)
C(42)	7273(3)	5879(5)	8836(2)	31(1)
C(41)	6598(3)	5464(4)	8700(2)	28(1)
C(2)	5002(3)	2226(4)	9587(2)	29(1)
C(44)	7304(3)	4278(5)	9431(2)	39(1)
C(7)	4306(3)	1258(6)	10191(2)	47(1)
C(43)	7636(3)	5270(5)	9206(2)	40(1)
C(4)	6216(3)	2953(5)	9540(2)	35(1)
C(14)	6163(3)	7692(5)	7727(2)	39(1)
C(8)	3631(4)	2005(9)	10239(3)	77(2)
N(16)	6193(3)	8923(4)	7762(2)	42(1)
C(31)	3901(3)	3525(5)	7908(2)	36(1)
C(32)	3296(3)	3606(7)	7550(2)	53(2)
C(20)	6564(4)	9995(6)	7033(3)	58(2)
C(17)	6472(4)	9526(5)	8197(2)	56(2)
C(19)	5961(4)	9757(6)	7373(3)	54(2)
C(18)	5917(6)	9619(7)	8555(3)	90(3)
C(9)	5261(3)	2773(5)	10420(2)	40(1)
C(10)	5707(4)	1994(6)	10775(2)	51(2)

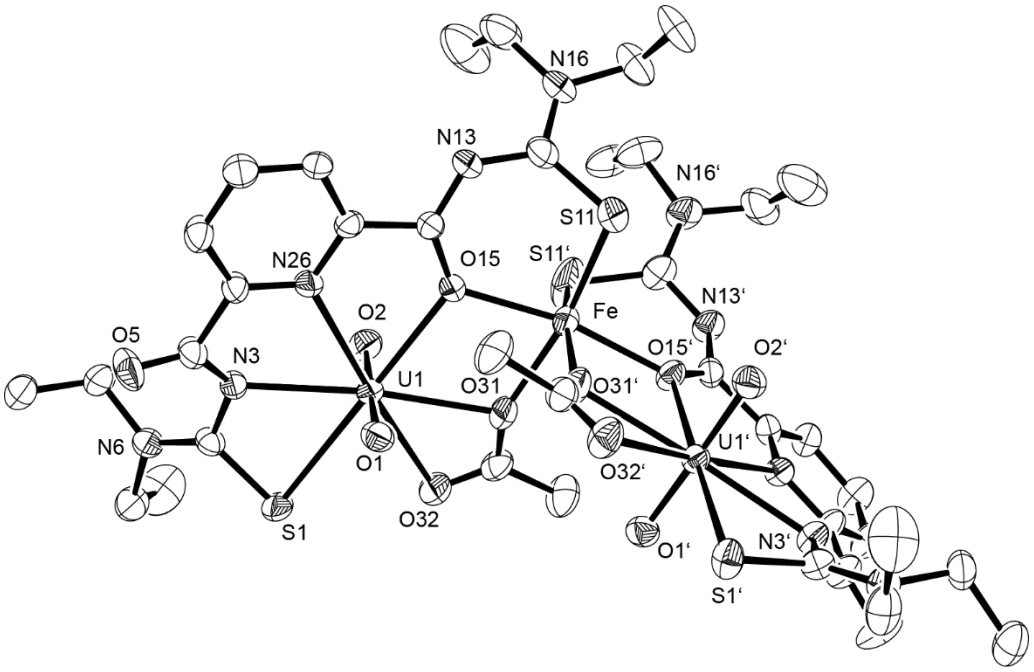

Figure A.24: Ellipsoid plot of [Fe{$UO_2(L^{2a})(OAc)\}_2$] **(SQUEEZE)**. Hydrogen atoms have been omitted for clarity. Thermal ellipsoids are at 50 % probability.

$[Ni\{UO_2(L^{2b})(OAc)\}_2]$

Table A.49: Crystal data and structure refinement for $[Ni\{UO_2(L^{2b})(OAc)\}_2] \cdot 1.5\ CH_2Cl_2$.

Empirical formula	$C_{39.5}H_{47}Cl_3N_{10}NiO_{16}S_4U_2$	
Formula weight	1687.23	
Temperature	100(2) K	
Wavelength	0.71073 Å	
Crystal system	Monoclinic	
Space group	C 2/c	
Unit cell dimensions	a = 44.57(4) Å	α= 90°
	b = 10.733(1) Å	β= 128.85(1)°
	c = 29.030(2) Å	γ = 90°
Volume	10815(2) $Å^3$	
Z	8	
Density (calculated)	2.072 g/cm^3	
Absorption coefficient	6.697 mm^{-1}	
F(000)	6472	
Crystal size	0.19 x 0.17 x 0.03 mm^3	
Theta range for data collection	2.328 to 24.998°.	
Index ranges	-52<=h<=52, -12<=k<=12, -33<=l<=34	
Reflections collected	123253	
Independent reflections	9481 [R(int) = 0.0429]	
Completeness to theta = 24.998°	99.5 %	
Absorption correction	Semi-empirical from equivalents	
Max. and min. transmission	0.7455 and 0.5977	
Refinement method	Full-matrix least-squares on F^2	
Data / restraints / parameters	9481 / 1156 / 782	
Goodness-of-fit on F^2	1.147	
Final R indices [I>2sigma(I)]	R1 = 0.0350, wR2 = 0.0745	
R indices (all data)	R1 = 0.0387, wR2 = 0.0765	
Largest diff. peak and hole	1.255 and -2.298 e/$Å^3$	
Diffractometer	Bruker D8 Venture	

Table A.50: Atomic coordinates (x 10^4) and equivalent isotropic displacement parameters ($Å^2$ x 10^3) for $[Ni\{UO_2(L^{2b})(OAc)\}_2] \cdot 1.5\ CH_2Cl_2$.

	x	y	z	U(eq)
U(1)	6272(1)	3183(1)	7348(1)	13(1)
O(1)	6094(1)	4690(4)	7311(2)	15(1)
O(2)	6463(1)	1689(5)	7396(2)	26(1)
U(2)	6248(1)	3172(1)	5038(1)	15(1)
O(11)	5897(1)	2154(4)	4939(2)	14(1)
O(12)	6588(1)	4225(6)	5135(2)	34(1)
Ni(1)	6353(1)	4736(1)	6290(1)	16(1)
S(1)	5763(1)	2175(2)	7540(1)	31(1)
N(3)	6446(2)	2990(7)	8338(3)	33(2)
C(4)	6810(2)	2754(9)	8835(3)	38(2)
O(5)	6909(2)	2145(7)	9271(2)	53(2)
C(2A)	6116(2)	2686(8)	8244(3)	32(2)
N(6A)	6011(4)	2691(15)	8584(6)	22(2)
C(7A)	5643(4)	2332(16)	8433(6)	22(2)
C(8A)	5853(5)	2072(15)	9134(6)	24(2)
C(9A)	6256(6)	3428(19)	9120(6)	31(4)
C(10A)	6477(5)	3020(20)	9795(7)	32(4)
O(10A)	6113(3)	2767(11)	9675(5)	24(2)
C(2B)	6116(2)	2686(8)	8244(3)	32(2)
N(6B)	6103(4)	3094(15)	8682(6)	22(2)
C(7B)	5751(5)	2773(14)	8602(7)	22(2)
C(8B)	5727(5)	1616(13)	8950(7)	24(2)
C(9B)	6373(5)	3754(16)	9250(6)	21(3)
C(10B)	6338(5)	2673(14)	9623(7)	18(3)
O(10B)	5977(3)	2310(11)	9494(5)	24(2)
C(14)	7055(2)	4445(8)	7571(3)	27(2)
O(15)	6689(1)	4265(5)	7180(2)	21(1)
S(11A)	6895(1)	5988(4)	6552(2)	14(1)
N(13A)	7333(3)	4546(11)	7536(5)	13(2)
C(12A)	7253(3)	4934(12)	7024(5)	12(2)
N(16A)	7503(3)	4549(10)	6949(4)	19(2)
C(17A)	7842(3)	3767(12)	7378(5)	22(2)
C(18A)	7861(4)	2663(13)	7071(5)	29(2)
C(19A)	7488(4)	4925(13)	6445(5)	28(2)

C(20A)	7513(3)	3745(14)	6181(5)	34(2)
O(20A)	7853(2)	3056(10)	6597(4)	35(2)
S(11B)	6764(1)	6418(5)	6449(2)	14(1)
N(13B)	7263(4)	5046(14)	7444(6)	13(2)
C(12B)	7161(4)	5497(16)	6917(6)	12(2)
N(16B)	7415(3)	5256(13)	6822(5)	19(2)
C(17B)	7771(4)	4532(16)	7224(6)	22(2)
C(18B)	7813(5)	3553(16)	6891(7)	29(2)
C(19B)	7384(5)	5794(17)	6326(6)	28(2)
C(20B)	7451(4)	4755(18)	6042(7)	34(2)
O(20B)	7805(3)	4127(13)	6443(5)	35(2)
S(21B)	6028(2)	6251(4)	6361(2)	16(1)
S(21A)	5875(2)	6122(6)	6223(3)	16(1)
C(22)	5840(3)	7078(7)	5718(3)	38(2)
N(23)	5659(2)	6610(5)	5158(3)	26(1)
C(24)	5752(2)	5600(6)	5035(3)	16(1)
O(25)	6042(1)	4857(4)	5384(2)	15(1)
N(26)	5871(3)	8310(6)	5759(3)	47(2)
C(27A)	5979(3)	9004(7)	6274(3)	38(2)
C(28A)	5687(4)	9763(11)	6130(5)	34(2)
C(29A)	5769(2)	9131(6)	5276(3)	23(1)
C(30A)	5468(3)	9885(10)	5159(5)	26(2)
O(30A)	5554(3)	10571(7)	5649(3)	31(2)
C(27B)	5979(3)	9004(7)	6274(3)	38(2)
C(28B)	6306(5)	9549(16)	6487(7)	34(2)
C(29B)	5769(2)	9131(6)	5276(3)	23(1)
C(30B)	6138(4)	9569(15)	5549(6)	26(2)
O(30B)	6277(4)	10294(11)	6060(5)	31(2)
S(31)	6488(1)	1250(2)	4642(1)	27(1)
C(32)	6240(2)	2162(6)	4018(3)	16(1)
N(33)	6005(1)	2989(5)	4010(2)	14(1)
C(34)	5636(2)	3218(6)	3530(2)	12(1)
O(35)	5461(1)	2804(4)	3025(2)	18(1)
N(36)	6292(2)	2127(5)	3618(2)	17(1)
C(37)	6537(2)	1183(8)	3632(3)	28(2)
C(38)	6331(2)	679(7)	3015(3)	25(2)
C(39)	6171(2)	3093(6)	3175(3)	18(1)
C(40)	5973(2)	2494(7)	2575(3)	21(1)
O(40)	6229(1)	1641(4)	2602(2)	22(1)

N(46)	5651(1)	4428(5)	4245(2)	10(1)
C(45)	5496(2)	5260(6)	4390(3)	14(1)
C(44)	5131(2)	5732(6)	3979(3)	19(1)
C(43)	4909(2)	5319(6)	3402(3)	21(1)
C(42)	5065(2)	4469(6)	3245(3)	18(1)
C(41)	5441(2)	4082(6)	3675(3)	12(1)
N(56)	6971(2)	3668(7)	8255(2)	28(1)
C(55)	7217(2)	4176(8)	8194(3)	29(2)
C(54)	7601(2)	4425(8)	8675(3)	36(2)
C(53)	7726(3)	4100(9)	9232(3)	47(2)
C(52)	7480(2)	3519(9)	9299(3)	45(2)
C(51)	7101(2)	3322(8)	8799(3)	33(2)
C(61)	5700(2)	3044(6)	6081(3)	16(1)
C(62)	5394(2)	3244(10)	5427(3)	39(2)
O(63)	5625(1)	2693(5)	6410(2)	21(1)
O(64)	6049(1)	3317(4)	6324(2)	11(1)
C(71)	6757(2)	2298(8)	6247(3)	29(2)
C(72)	6964(2)	1794(10)	6852(3)	47(3)
O(73)	6746(2)	1740(7)	5858(2)	45(2)
O(74)	6585(1)	3349(5)	6104(2)	22(1)
C(101)	4944(4)	8872(10)	6267(7)	30(3)
Cl(1)	5164(1)	10299(4)	6358(2)	34(1)
Cl(2)	5097(1)	7675(3)	6056(2)	26(1)
C(102)	5058(4)	9331(13)	7102(4)	26(3)
Cl(3)	5169(1)	10198(4)	7642(2)	32(1)
Cl(4)	4777(1)	9331(4)	6349(2)	39(1)
C(103)	7484(5)	2890(14)	4713(8)	50(1)
Cl(5)	7121(1)	3858(5)	4585(2)	50(1)
Cl(6)	7610(1)	1654(5)	5187(2)	50(1)

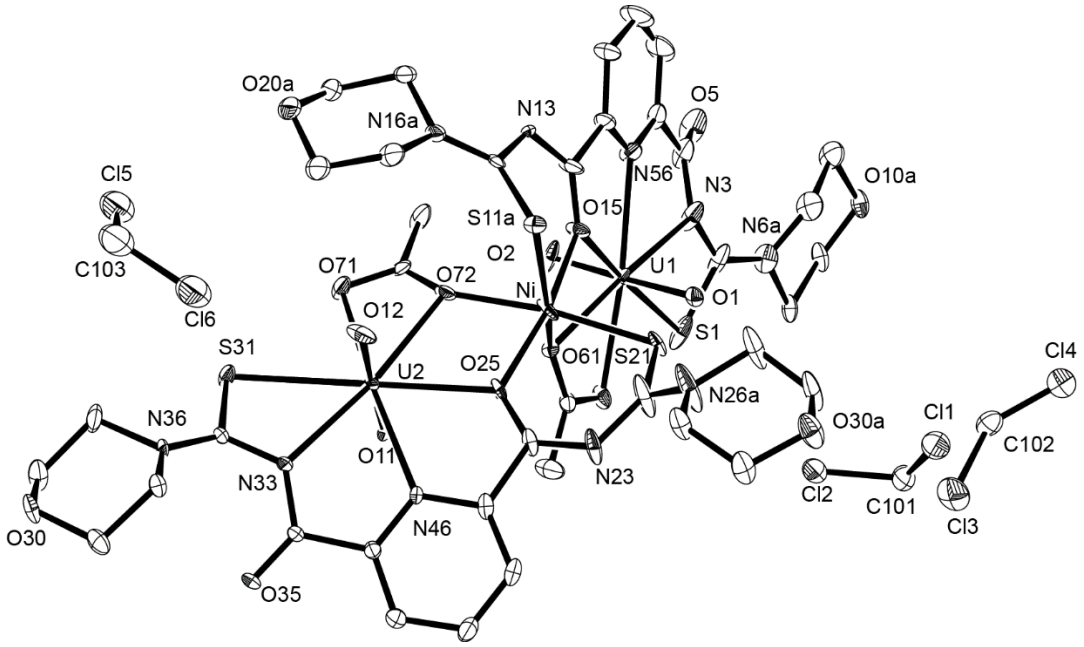

Figure A.25: Ellipsoid plot of $[Ni\{UO_2(L^{2b})(OAc)\}_2] \cdot 1.5\ CH_2Cl_2$. Hydrogen atoms have been omitted for clarity. Thermal ellipsoids are at 50 % probability.

$[Co\{UO_2(L^{2b})(OAc)\}_2]$

Table A.51: Crystal data and structure refinement for $[Co\{UO_2(L^{2b})(OAc)\}_2] \cdot 0.5\ CH_2Cl_2 \cdot CH_3OH \cdot 0.5\ H_2O$.

Empirical formula	$C_{39.5}H_{50}ClCoN_{10}O_{17.5}S_4U_2$	
Formula weight	1643.57	
Temperature	100(2) K	
Wavelength	0.71073 Å	
Crystal system	Monoclinic	
Space group	C 2/c	
Unit cell dimensions	a = 44.055(5) Å	α= 90°
	b = 10.798(1) Å	β= 128.05(2)°
	c = 29.051(3) Å	γ = 90°
Volume	10882.7(19) $Å^3$	
Z	8	
Density (calculated)	2.006 g/cm^3	
Absorption coefficient	6.518 mm^{-1}	
F(000)	6312	
Crystal size	0.16 x 0.07 x 0.05 mm^3	
Theta range for data collection	2.311 to 26.542°	
Index ranges	-55<=h<=54, -13<=k<=13, -33<=l<=36	
Reflections collected	84792	
Independent reflections	11236 [R(int) = 0.0564]	
Completeness to theta = 25.242°	99.9 %	
Absorption correction	Semi-empirical from equivalents	
Max. and min. transmission	0.7454 and 0.5554	
Refinement method	Full-matrix least-squares on F^2	
Data / restraints / parameters	11236 / 13 / 693	
Goodness-of-fit on F^2	1.156	
Final R indices [I>2sigma(I)]	R1 = 0.0400, wR2 = 0.0710	
R indices (all data)	R1 = 0.0499, wR2 = 0.0736	
Largest diff. peak and hole	1.627 and -1.637 e/$Å^3$	
Diffractometer	Bruker D8 Venture	

Table A.52: Atomic coordinates (x 10^4) and equivalent isotropic displacement parameters ($Å^2$ x 10^3) for $[Co\{UO_2(L^{2b})(OAc)\}_2] \cdot 0.5\ CH_2Cl_2 \cdot CH_3OH \cdot 0.5\ H_2O$.

	x	y	z	U(eq)
U(1)	3764(1)	3318(1)	4973(1)	14(1)
U(2)	3730(1)	3093(1)	2617(1)	13(1)
Co(1)	3701(1)	4782(1)	3720(1)	14(1)
S(11)	4193(1)	5968(2)	3806(1)	22(1)
S(31)	3239(1)	6394(2)	3495(1)	23(1)
S(21)	4232(1)	1999(2)	2422(1)	23(1)
O(35)	3341(1)	4320(4)	2811(2)	14(1)
O(64)	3447(1)	3502(4)	3921(2)	16(1)
S(1)	3479(1)	1464(2)	5329(1)	26(1)
O(2)	3436(1)	4423(4)	4887(2)	20(1)
O(15)	4008(1)	4909(4)	4656(2)	15(1)
O(61)	3951(1)	3210(4)	3635(2)	16(1)
O(5)	4521(1)	2856(5)	6955(2)	28(1)
O(10)	3748(1)	1735(4)	7373(2)	26(1)
O(25)	3086(1)	2123(5)	716(2)	29(1)
O(63)	3240(1)	1978(4)	4147(2)	23(1)
N(46)	4370(1)	4489(5)	5774(2)	14(1)
N(56)	3052(1)	3753(5)	1734(2)	15(1)
O(62)	4346(1)	2296(5)	3531(2)	26(1)
N(23)	3563(2)	2914(5)	1639(2)	20(1)
N(33)	2745(1)	5041(5)	2510(2)	17(1)
N(3)	3986(1)	3109(5)	5981(2)	18(1)
N(13)	4432(1)	6539(5)	4893(2)	18(1)
O(1)	4104(1)	2242(4)	5071(2)	20(1)
C(34)	2982(2)	4612(5)	2425(2)	16(1)
C(61)	3246(2)	2513(6)	3772(2)	16(1)
C(45)	4539(2)	5284(6)	5641(2)	16(1)
C(43)	5106(2)	5370(7)	6630(3)	25(2)
N(6)	3686(1)	2265(5)	6363(2)	18(1)
C(42)	4939(2)	4530(7)	6777(3)	23(1)
N(36)	2592(2)	5200(6)	3127(2)	25(1)
C(41)	4564(2)	4144(6)	6333(2)	16(1)
N(16)	4254(2)	8161(5)	4279(2)	25(1)
C(9)	3808(2)	3221(6)	6806(2)	21(1)

C(55)	2813(2)	4326(6)	1803(3)	19(1)
O(20)	3768(2)	10236(5)	3893(2)	50(2)
C(32)	2844(2)	5462(6)	3031(3)	19(1)
C(51)	2916(2)	3382(6)	1196(3)	20(1)
C(62)	3031(2)	2025(6)	3163(3)	21(1)
C(44)	4904(2)	5767(6)	6064(3)	22(1)
C(14)	4307(2)	5610(5)	5007(2)	14(1)
C(24)	3194(2)	2732(6)	1147(3)	22(1)
C(4)	4356(2)	3295(6)	6466(3)	21(1)
C(63)	4281(2)	2719(6)	3866(3)	21(1)
C(7)	3440(2)	1323(6)	6348(3)	24(2)
O(40)	2198(2)	4049(7)	3499(2)	57(2)
C(8)	3652(2)	792(6)	6959(3)	27(2)
C(22)	3889(2)	2518(6)	1725(3)	21(1)
C(2)	3740(2)	2309(6)	5966(2)	19(1)
C(37)	2238(2)	4468(7)	2723(3)	28(2)
C(53)	2296(2)	4240(7)	778(3)	30(2)
C(12)	4285(2)	6948(6)	4350(2)	17(1)
C(64)	4581(2)	2686(8)	4518(3)	30(2)
C(52)	2540(2)	3584(7)	712(3)	26(2)
C(54)	2436(2)	4617(7)	1336(3)	27(2)
C(10)	4002(2)	2608(6)	7398(3)	26(2)
C(19)	4121(2)	8808(7)	3743(3)	32(2)
C(20)	3745(2)	9413(7)	3485(3)	39(2)
C(40)	2551(2)	4680(11)	3902(3)	58(3)
C(17)	4278(2)	9012(7)	4699(3)	31(2)
C(18)	3891(3)	9567(7)	4411(4)	43(2)
C(38)	2194(2)	3488(8)	3052(4)	42(2)
C(39)	2618(2)	5709(9)	3618(3)	42(2)
O(12)	3952(1)	4527(4)	2697(2)	19(1)
N(26)	3954(2)	2631(6)	1336(2)	28(1)
C(27)	4312(2)	2211(8)	1458(3)	38(2)
O(30)	3997(2)	2283(5)	414(2)	42(1)
O(102)	2754(3)	6303(9)	293(4)	121(5)
C(104)	3062(3)	5404(12)	487(5)	73(3)
C(29)	3716(2)	3372(7)	795(3)	33(2)
C(30)	3644(2)	2607(8)	301(3)	41(2)
C(28)	4216(2)	1535(9)	921(4)	44(2)
O(11)	3491(1)	1686(4)	2526(2)	17(1)

Cl(1)	5085(2)	377(7)	1175(4)	99(2)
Cl(2)	5081(2)	-2337(9)	1043(4)	121(3)
C(71)	5002(7)	-780(20)	1266(11)	77(8)
O(72)	5000	-306(18)	2500	350(20)

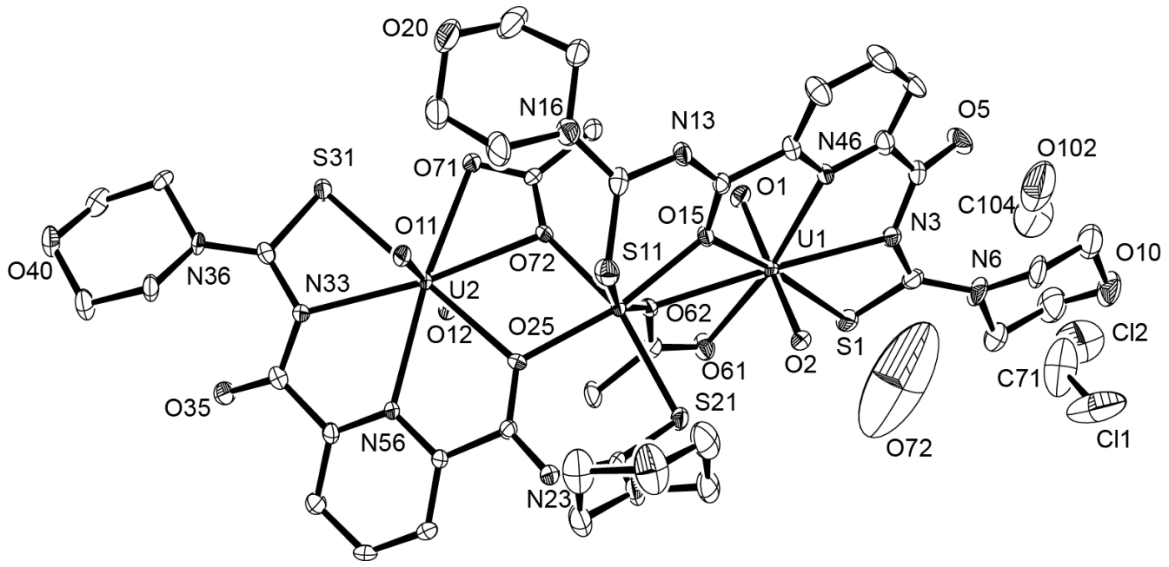

Figure A.26: Ellipsoid plot of $[Co\{UO_2(L^{2b})(OAc)\}_2] \cdot 0.5\,CH_2Cl_2 \cdot CH_3OH \cdot 0.5\,H_2O$. Hydrogen atoms have been omitted for clarity. Thermal ellipsoids are at 50 % probability.

$[Zn\{UO_2(L^{2b})(OAc)\}_2]$

Table A.53: Crystal data and structure refinement for $[Zn\{UO_2(L^{2b})(OAc)\}_2] \cdot 1.5\ CH_2Cl_2$.

Empirical formula	$C_{39.5}H_{47}Cl_3N_{10}ZnO_{16}S_4U_2$	
Formula weight	1693.89	
Temperature	100(2) K	
Wavelength	0.71073 Å	
Crystal system	Monoclinic	
Space group	C 2/c	
Unit cell dimensions	a = 44.414(4) Å	α= 90°
	b = 10.739(1) Å	β= 128.64(1)°
	c = 29.198(2) Å	γ = 90°
Volume	10878(2) $Å^3$	
Z	8	
Density (calculated)	2.069 g/cm^3	
Absorption coefficient	6.753 mm^{-1}	
F(000)	6488	
Crystal size	0.300 x 0.060 x 0.030 mm^3	
Theta range for data collection	2.322 to 24.997°	
Index ranges	-52<=h<=52, -12<=k<=12, -34<=l<=34	
Reflections collected	112872	
Independent reflections	9568 [R(int) = 0.0540]	
Completeness to theta = 24.997°	99.8 %	
Absorption correction	Semi-empirical from equivalents	
Max. and min. transmission	0.7455 and 0.5024	
Refinement method	Full-matrix least-squares on F^2	
Data / restraints / parameters	9568 / 1136 / 707	
Goodness-of-fit on F^2	1.080	
Final R indices [I>2sigma(I)]	R1 = 0.0291, wR2 = 0.0574	
R indices (all data)	R1 = 0.0359, wR2 = 0.0611	
Largest diff. peak and hole	1.427 and -1.436 $e/Å^3$	
Diffractometer	Bruker D8 Venture	

Table A.54: Atomic coordinates (x 10^4) and equivalent isotropic displacement parameters ($Å^2$ x 10^3) for $[Zn\{UO_2(L^{2b})(OAc)\}_2] \cdot 1.5\ CH_2Cl_2$.

	x	y	z	U(eq)
U(1)	3763(1)	3215(1)	4982(1)	19(1)
O(1)	3421(1)	4270(5)	4883(2)	39(1)
O(2)	4114(1)	2198(3)	5083(1)	18(1)
U(2)	3716(1)	3143(1)	2628(1)	15(1)
O(11)	3906(1)	4632(3)	2683(1)	17(1)
Zn(1)	3663(1)	4807(1)	3716(1)	19(1)
S(1)	3516(1)	1293(2)	5372(1)	31(1)
C(2)	3762(1)	2193(5)	5991(2)	19(1)
N(3)	3999(1)	3025(4)	6001(2)	16(1)
C(4)	4367(1)	3242(5)	6481(2)	14(1)
O(5)	4538(1)	2827(3)	6977(1)	18(1)
N(6)	3706(1)	2168(4)	6386(2)	21(1)
C(7)	3462(2)	1223(6)	6376(2)	30(1)
C(8)	3665(2)	726(5)	6985(2)	26(1)
C(9)	3823(2)	3154(5)	6822(2)	19(1)
C(10)	4021(2)	2559(5)	7418(2)	22(1)
O(10)	3767(1)	1693(3)	7395(2)	23(1)
N(13)	4381(2)	6590(4)	4884(2)	28(1)
C(14)	4272(2)	5614(5)	5003(2)	19(1)
O(15)	3977(1)	4899(3)	4657(1)	17(1)
S(11A)	4188(1)	6048(3)	3841(2)	14(1)
C(12A)	4280(3)	7019(9)	4385(4)	14(2)
N(16A)	4250(3)	8249(8)	4326(4)	17(2)
C(17A)	4261(4)	9077(17)	4739(7)	25(1)
C(18A)	3870(3)	9606(9)	4442(4)	25(1)
C(20A)	3740(3)	9520(9)	3535(4)	25(1)
O(20A)	3750(2)	10300(6)	3936(3)	25(1)
C(19A)	4115(3)	8935(11)	3790(5)	25(1)
S(11B)	4029(1)	6184(4)	3688(2)	14(1)
C(12B)	4132(4)	7054(11)	4266(5)	14(2)
N(16B)	4081(3)	8271(10)	4213(5)	17(2)
C(17B)	4211(5)	9107(19)	4706(9)	25(1)
C(18B)	4537(4)	9863(11)	4839(5)	25(1)
C(20B)	4320(3)	9712(10)	3873(5)	25(1)

O(20B)	4446(2)	10535(7)	4346(3)	25(1)
C(19B)	3982(4)	8961(13)	3697(5)	25(1)
S(21)	4226(1)	2140(1)	2433(1)	33(1)
N(23)	3545(1)	2984(5)	1644(2)	35(1)
C(24)	3180(2)	2756(8)	1148(3)	50(1)
O(25)	3081(1)	2151(5)	718(2)	50(1)
C(22A)	3877(2)	2663(6)	1736(3)	33(1)
N(26A)	3977(3)	2673(11)	1399(5)	20(2)
C(27A)	4348(4)	2345(12)	1546(5)	25(1)
C(28A)	4260(4)	1609(11)	1031(5)	25(1)
C(29A)	3659(3)	2584(12)	366(5)	25(1)
C(30A)	3723(4)	3375(11)	848(5)	25(1)
O(30A)	4017(3)	2295(10)	493(4)	28(2)
C(22B)	3877(2)	2663(6)	1736(3)	33(1)
N(26B)	3895(4)	3092(12)	1298(6)	20(2)
C(27B)	4244(4)	2714(13)	1382(6)	25(1)
C(28B)	4142(4)	2045(12)	844(6)	25(1)
C(29B)	3550(4)	3058(13)	239(5)	25(1)
C(30B)	3630(4)	3793(12)	750(5)	25(1)
O(30B)	3893(3)	2756(10)	326(4)	28(2)
N(33)	2694(1)	4827(6)	2485(2)	47(2)
C(34)	2941(2)	4467(7)	2410(2)	35(2)
O(35)	3301(1)	4244(4)	2797(1)	24(1)
S(31A)	3214(1)	6464(3)	3485(1)	15(1)
C(32A)	2828(3)	5477(12)	3043(4)	26(1)
N(36A)	2579(2)	5237(9)	3146(3)	26(1)
C(37A)	2225(3)	4507(11)	2750(4)	26(1)
C(38A)	2185(3)	3537(10)	3086(4)	26(1)
C(39A)	2614(3)	5758(10)	3643(4)	26(1)
C(40A)	2553(2)	4735(10)	3935(4)	26(1)
O(40A)	2197(2)	4109(7)	3535(3)	26(1)
S(31B)	3088(1)	6007(3)	3408(2)	15(1)
C(32B)	2739(3)	4939(14)	2956(5)	26(1)
N(36B)	2491(3)	4536(11)	3036(4)	26(1)
C(37B)	2156(3)	3731(12)	2619(5)	26(1)
C(38B)	2142(3)	2641(12)	2933(5)	26(1)
C(39B)	2517(3)	4899(12)	3546(5)	26(1)
C(40B)	2503(3)	3736(12)	3826(5)	26(1)
O(40B)	2159(2)	3043(9)	3413(3)	26(1)

N(46)	4360(1)	4459(4)	5778(2)	14(1)
C(45)	4524(1)	5275(4)	5641(2)	16(1)
C(44)	4890(2)	5750(5)	6054(2)	21(1)
C(43)	5107(2)	5333(5)	6626(2)	23(1)
C(42)	4944(1)	4497(5)	6775(2)	19(1)
C(41)	4569(1)	4099(4)	6344(2)	13(1)
N(56)	3022(1)	3684(5)	1730(2)	32(1)
C(55)	2773(2)	4201(7)	1788(2)	33(1)
C(54)	2394(2)	4463(6)	1313(2)	37(2)
C(53)	2269(2)	4145(7)	759(3)	45(2)
C(52)	2514(2)	3547(7)	696(2)	43(2)
C(51)	2892(2)	3344(7)	1189(2)	36(1)
C(61)	3258(2)	2365(7)	3784(2)	36(2)
C(62)	3048(2)	1886(9)	3180(2)	56(2)
O(63)	3262(1)	1816(5)	4165(2)	51(1)
O(64)	3436(1)	3400(4)	3926(1)	26(1)
C(71)	4279(1)	2924(5)	3877(2)	19(1)
C(72)	4582(2)	3031(9)	4525(3)	58(2)
O(73)	3937(1)	3262(3)	3642(1)	12(1)
O(74)	4355(1)	2572(4)	3549(2)	26(1)
C(100)	-68(3)	3843(10)	1263(5)	22(2)
Cl(1)	81(1)	2667(2)	1043(1)	18(1)
Cl(2)	164(1)	5278(2)	1364(1)	26(1)
C(101)	69(3)	4353(11)	2130(5)	26(2)
Cl(3)	-161(1)	5165(3)	2360(1)	32(1)
Cl(4)	-214(1)	4312(3)	1355(1)	43(1)
C(102)	2495(4)	7820(16)	9710(6)	52(3)
Cl(5)	2128(1)	8822(4)	9594(2)	45(1)
Cl(6)	2612(1)	6603(4)	10180(2)	52(1)
O(12)	3510(1)	1670(4)	2563(2)	36(1)

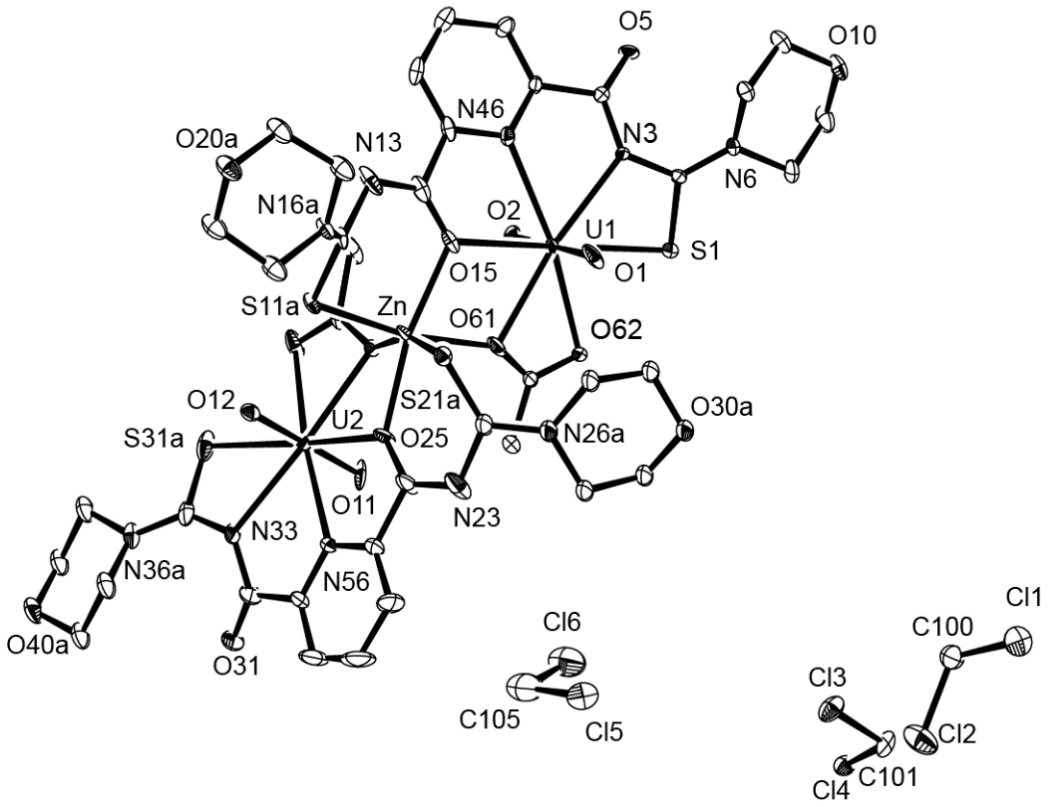

Figure A.27: Ellipsoid plot of $[Zn\{UO_2(L^{2b})(OAc)\}_2] \cdot 1.5\ CH_2Cl_2$. Hydrogen atoms have been omitted for clarity. Thermal ellipsoids are at 50 % probability.

[Ni{Th(L^3)$_2$(OAc)$_2$(MeOH)}]

Table A.55: Crystal data and structure refinement for [Ni{Th(L^3)$_2$(OAc)$_2$(MeOH)}] · CH_2Cl_2 · 2.5 H_2O.

Empirical formula	$C_{50}H_{69}Cl_2N_{12}NiO_{11.5}S_4Th$	
Formula weight	1512.06	
Temperature	100(2) K	
Wavelength	0.71073 Å	
Crystal system	Monoclinic	
Space group	C 2/c	
Unit cell dimensions	a = 29.532(2) Å	α= 90°
	b = 11.069(1) Å	β= 102.67(3)°
	c = 40.252(3) Å	γ = 90°
Volume	12837(2) $Å^3$	
Z	8	
Density (calculated)	1.565 g/cm^3	
Absorption coefficient	2.884 mm^{-1}	
F(000)	6088	
Crystal size	0.500 x 0.220 x 0.020 mm^3	
Theta range for data collection	2.239 to 26.379°	
Index ranges	-36<=h<=36, -13<=k<=13, -50<=l<=50	
Reflections collected	76666	
Independent reflections	13109 [R(int) = 0.0453]	
Completeness to theta = 25.242°	99.9 %	
Absorption correction	Semi-empirical from equivalents	
Max. and min. transmission	0.7454 and 0.5177	
Refinement method	Full-matrix least-squares on F^2	
Data / restraints / parameters	13109 / 61 / 759	
Goodness-of-fit on F^2	1.205	
Final R indices [I>2sigma(I)]	R1 = 0.0583, wR2 = 0.1341	
R indices (all data)	R1 = 0.0687, wR2 = 0.1385	
Largest diff. peak and hole	2.560 and -1.701 e/$Å^3$	
Diffractometer	Bruker D8 Venture	

Table A.56: Atomic coordinates (x 10^4) and equivalent isotropic displacement parameters ($Å^2$ x 10^3) for [Ni{Th(L^3)$_2$(OAc)$_2$(MeOH)}] · CH_2Cl_2 · 2.5 H_2O.

	x	y	z	U(eq)
Th(1)	6805(1)	6640(1)	6289(1)	16(1)
Ni(1)	6774(1)	4343(1)	5630(1)	19(1)
S(1)	6344(1)	2529(2)	5472(1)	27(1)
S(11)	8154(1)	10150(2)	6666(1)	28(1)
S(41)	7285(1)	3869(2)	5280(1)	26(1)
S(51)	5326(1)	7015(3)	6979(1)	48(1)
O(45)	7097(2)	5969(4)	5778(1)	22(1)
O(82)	7231(2)	3512(4)	6020(1)	23(1)
O(55)	6274(2)	7261(5)	6625(1)	22(1)
O(5)	6386(2)	4851(4)	5971(1)	20(1)
N(26)	6437(2)	4891(5)	6623(1)	16(1)
O(15)	7512(2)	7554(4)	6551(1)	17(1)
O(81)	7350(2)	4971(4)	6413(1)	21(1)
N(36)	7133(2)	6275(5)	6962(1)	17(1)
O(86)	6192(2)	7305(5)	5864(1)	29(1)
O(89)	6292(2)	5314(5)	5260(1)	30(1)
N(66)	7137(2)	8277(5)	5896(1)	19(1)
N(76)	6679(2)	9019(5)	6370(1)	19(1)
N(13)	8140(2)	8033(5)	6979(2)	20(1)
N(3)	5813(2)	3379(6)	5892(2)	24(1)
O(85)	5781(2)	7261(6)	5338(2)	44(2)
N(43)	7653(2)	6123(6)	5446(2)	25(1)
C(21)	6089(2)	4227(6)	6440(2)	20(2)
C(44)	7365(3)	6550(7)	5620(2)	22(2)
C(35)	6916(3)	5552(6)	7148(2)	20(2)
C(4)	6094(2)	4148(6)	6070(2)	18(1)
N(16)	8666(2)	8188(6)	6631(2)	28(2)
C(31)	7521(3)	6849(6)	7107(2)	19(2)
C(83)	7428(3)	3952(6)	6299(2)	21(2)
N(56)	6046(3)	7565(7)	7486(2)	40(2)
C(61)	7353(3)	7890(7)	5657(2)	22(2)
N(53)	6010(3)	8601(6)	6985(2)	31(2)
C(65)	7123(3)	9480(7)	5951(2)	22(2)
C(64)	7324(3)	10314(7)	5760(2)	24(2)

C(14)	7739(2)	7535(6)	6864(2)	16(1)
C(71)	6428(3)	9344(6)	6593(2)	20(1)
N(6)	5431(3)	2849(7)	5360(2)	36(2)
C(25)	6515(3)	4882(6)	6966(2)	20(2)
C(42)	7712(3)	4921(7)	5390(2)	25(2)
C(54)	6217(3)	8323(7)	6743(2)	23(2)
C(74)	6844(3)	11093(7)	6294(2)	27(2)
C(33)	7494(3)	6041(8)	7651(2)	29(2)
C(32)	7716(3)	6761(7)	7455(2)	24(2)
C(12)	8328(3)	8719(7)	6751(2)	22(2)
C(52)	5822(3)	7725(8)	7163(2)	33(2)
C(34)	7098(3)	5413(7)	7499(2)	24(2)
C(22)	5781(3)	3581(7)	6587(2)	28(2)
N(46)	8154(2)	4608(6)	5399(2)	32(2)
C(87)	5908(3)	7759(8)	5614(2)	34(2)
C(19)	8924(3)	8864(9)	6419(2)	36(2)
C(24)	6221(3)	4213(7)	7130(2)	28(2)
C(72)	6385(3)	10526(7)	6690(2)	27(2)
C(62)	7555(3)	8666(8)	5463(2)	29(2)
C(75)	6891(2)	9865(6)	6209(2)	16(1)
C(73)	6603(3)	11412(7)	6538(2)	30(2)
C(63)	7543(3)	9877(7)	5515(2)	30(2)
C(23)	5850(3)	3591(7)	6937(2)	30(2)
C(2)	5834(3)	2991(7)	5573(2)	27(2)
C(84)	7794(3)	3186(8)	6524(2)	39(2)
C(17)	8795(3)	6911(8)	6705(2)	36(2)
C(59)	6511(4)	8123(8)	7614(2)	43(2)
C(49)	8534(3)	5500(8)	5453(2)	37(2)
C(18)	8538(4)	6063(9)	6434(3)	55(3)
C(20)	8688(4)	8905(9)	6051(2)	46(2)
C(90)	6313(4)	5489(11)	4918(2)	55(3)
C(60)	6476(5)	9427(9)	7712(3)	59(3)
C(47)	8295(3)	3353(8)	5353(2)	40(2)
C(50)	8623(4)	5948(10)	5116(3)	53(3)
C(57)	5873(4)	6763(10)	7723(3)	55(3)
C(48)	8394(4)	2655(10)	5681(3)	57(3)
C(58)	5869(4)	7394(12)	8058(3)	64(3)
C(9A)	5385(4)	2312(10)	5020(2)	52(3)
C(10A)	5365(8)	1055(17)	5011(5)	61(5)

C(9B)	5385(4)	2312(10)	5020(2)	52(3)
C(10B)	5437(9)	3090(20)	4757(6)	61(5)
Cl(3)	9564(1)	8612(3)	7250(1)	75(1)
O(20)	5102(4)	2270(9)	4084(3)	89(3)
C(92)	10000	9457(17)	7500	68(5)
O(30)	5188(2)	4596(7)	3840(2)	52(2)
O(40)	4735(5)	3684(13)	3849(4)	52(4)
C(88A)	5813(9)	9160(20)	5637(6)	36(6)
C(88B)	5611(12)	8700(30)	5739(8)	61(11)
C(7A)	4998(4)	3232(12)	5447(3)	69(3)
C(8A)	4809(5)	2114(17)	5662(4)	69(3)
C(7B)	4998(4)	3232(12)	5447(3)	69(3)
C(8B)	4949(13)	4680(30)	5310(10)	69(3)
Cl(1)	4942(5)	-1000(13)	3274(3)	146(4)
Cl(2)	5461(6)	538(15)	3799(4)	179(6)
C(91)	4959(13)	210(40)	3526(10)	113(12)

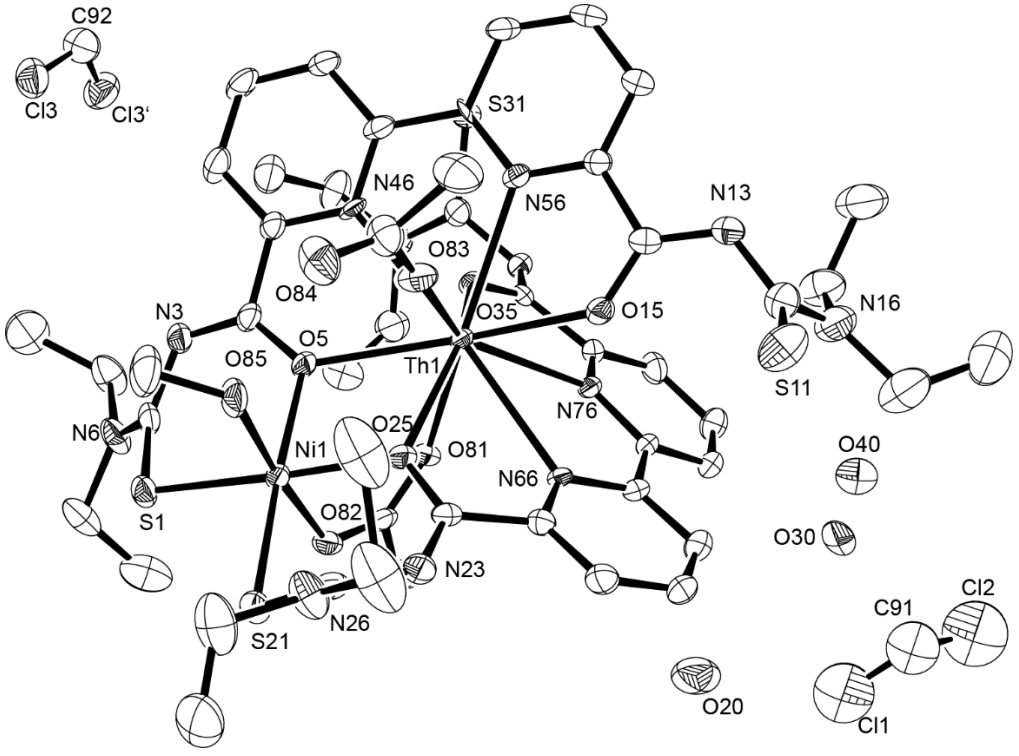

Figure A.28: Ellipsoid plot of $[Ni\{Th(L^3)_2(OAc)_2(MeOH)\}] \cdot CH_2Cl_2 \cdot 2.5\ H_2O$. Hydrogen atoms have been omitted for clarity.Thermal ellipsoids are at 50 % probability.

[Ni{Th(L^3)$_2$(OAc)$_2$(MeOH)}] (SQUEEZE)

Table A.57: Crystal data and structure refinement for [Ni{Th(L^3)$_2$(OAc)$_2$(MeOH)}] **(SQUEEZE).**

Empirical formula	$C_{49}H_{62}N_{12}NiO_9S_4Th$	
Formula weight	1382.09	
Temperature	100(2) K	
Wavelength	0.71073 Å	
Crystal system	Monoclinic	
Space group	C 2/c	
Unit cell dimensions	a = 29.532(2) Å	α= 90°
	b = 11.069(1) Å	β= 102.67(3)°
	c = 40.252(3) Å	γ = 90°
Volume	12837(2) Å^3	
Z	8	
Density (calculated)	1.430 g/cm^3	
Absorption coefficient	2.794 mm^{-1}	
F(000)	5552	
Crystal size	0.500 x 0.220 x 0.020 mm^3	
Theta range for data collection	2.239 to 26.379°.	
Index ranges	-36<=h<=36, -13<=k<=13, -50<=l<=50	
Reflections collected	76646	
Independent reflections	13105 [R(int) = 0.0446]	
Completeness to theta = 25.242°	99.8 %	
Absorption correction	Semi-empirical from equivalents	
Max. and min. transmission	0.7454 and 0.5177	
Refinement method	Full-matrix least-squares on F^2	
Data / restraints / parameters	13105 / 60 / 700	
Goodness-of-fit on F^2	1.158	
Final R indices [I>2sigma(I)]	R1 = 0.0480, wR2 = 0.0936	
R indices (all data)	R1 = 0.0570, wR2 = 0.0961	
Extinction coefficient	0.000086(9)	
Largest diff. peak and hole	2.393 and -1.584 e/Å^3	
Diffractometer	Bruker D8 Venture	

Table A.58. Atomic coordinates (x 10^4) and equivalent isotropic displacement parameters ($Å^2$ x 10^3) for [Ni{Th(L^3)$_2$(OAc)$_2$(MeOH)}] **(SQUEEZE).**

	x	y	z	U(eq)
Th(1)	6805(1)	6640(1)	6289(1)	16(1)
Ni(1)	6774(1)	4343(1)	5630(1)	19(1)
S(1)	6344(1)	2530(1)	5473(1)	27(1)
S(11)	8154(1)	10149(1)	6666(1)	28(1)
S(41)	7285(1)	3869(1)	5280(1)	26(1)
S(51)	5326(1)	7014(2)	6979(1)	49(1)
O(45)	7097(1)	5970(3)	5778(1)	22(1)
O(82)	7230(1)	3510(3)	6020(1)	24(1)
O(55)	6273(1)	7259(3)	6626(1)	22(1)
O(5)	6386(1)	4853(3)	5971(1)	20(1)
N(26)	6438(2)	4892(4)	6623(1)	16(1)
O(15)	7513(1)	7555(3)	6552(1)	17(1)
O(81)	7350(1)	4970(3)	6413(1)	21(1)
N(36)	7131(2)	6274(4)	6962(1)	18(1)
O(86)	6193(2)	7306(4)	5863(1)	29(1)
O(89)	6294(2)	5312(4)	5260(1)	31(1)
N(66)	7138(2)	8277(4)	5896(1)	19(1)
N(76)	6678(2)	9017(4)	6369(1)	18(1)
N(13)	8140(2)	8032(4)	6980(1)	20(1)
N(3)	5811(2)	3375(5)	5892(1)	24(1)
O(85)	5779(2)	7257(5)	5337(1)	45(1)
N(43)	7651(2)	6125(4)	5446(1)	25(1)
C(21)	6089(2)	4228(5)	6440(1)	20(1)
C(44)	7364(2)	6548(5)	5620(1)	22(1)
C(35)	6917(2)	5551(5)	7149(1)	19(1)
C(4)	6093(2)	4150(5)	6069(1)	19(1)
N(16)	8667(2)	8189(5)	6632(1)	28(1)
C(31)	7521(2)	6845(5)	7107(1)	20(1)
C(83)	7429(2)	3949(5)	6300(1)	22(1)
N(56)	6045(2)	7566(5)	7484(2)	41(1)
C(61)	7352(2)	7891(5)	5658(1)	21(1)
N(53)	6008(2)	8599(4)	6984(1)	32(1)
C(65)	7127(2)	9483(5)	5952(1)	22(1)
C(64)	7324(2)	10313(5)	5761(1)	24(1)

C(14)	7740(2)	7536(5)	6863(1)	16(1)
C(71)	6430(2)	9344(5)	6593(1)	20(1)
N(6)	5432(2)	2850(5)	5359(1)	38(1)
C(25)	6514(2)	4876(5)	6966(1)	20(1)
C(42)	7715(2)	4915(5)	5392(1)	26(1)
C(54)	6216(2)	8317(5)	6743(1)	23(1)
C(74)	6845(2)	11098(5)	6294(2)	27(1)
C(33)	7492(2)	6045(6)	7651(1)	29(1)
C(32)	7717(2)	6762(6)	7455(1)	25(1)
C(12)	8330(2)	8718(5)	6751(1)	22(1)
C(52)	5822(2)	7720(6)	7162(2)	34(2)
C(34)	7097(2)	5418(5)	7498(1)	24(1)
C(22)	5783(2)	3580(5)	6589(2)	27(1)
N(46)	8154(2)	4607(5)	5401(1)	32(1)
C(87)	5909(2)	7750(6)	5616(2)	34(1)
C(19)	8927(2)	8862(7)	6420(2)	36(2)
C(24)	6220(2)	4216(5)	7129(2)	29(1)
C(72)	6381(2)	10535(5)	6689(2)	27(1)
C(62)	7555(2)	8665(6)	5465(2)	29(1)
C(75)	6894(2)	9863(5)	6209(1)	16(1)
C(73)	6603(2)	11413(5)	6538(2)	31(1)
C(63)	7542(2)	9880(6)	5515(2)	30(1)
C(23)	5850(2)	3588(5)	6936(2)	30(1)
C(2)	5836(2)	2984(5)	5574(2)	28(1)
C(84)	7795(3)	3193(6)	6524(2)	39(2)
C(17)	8796(2)	6914(6)	6705(2)	37(2)
C(59)	6509(3)	8125(6)	7612(2)	44(2)
C(49)	8534(2)	5499(6)	5453(2)	37(2)
C(18)	8534(3)	6058(7)	6432(2)	57(2)
C(20)	8688(3)	8898(7)	6049(2)	47(2)
C(90)	6316(3)	5495(8)	4919(2)	55(2)
C(60)	6474(4)	9426(7)	7711(2)	62(2)
C(47)	8295(2)	3356(6)	5353(2)	40(2)
C(50)	8620(3)	5957(8)	5116(2)	54(2)
C(57)	5867(3)	6768(8)	7725(2)	60(2)
C(48)	8394(3)	2657(7)	5681(2)	57(2)
C(58)	5865(3)	7400(9)	8056(2)	64(2)
C(9A)	5386(3)	2319(8)	5021(2)	53(2)
C(10A)	5368(6)	1057(14)	5006(4)	62(3)

C(9B)	5386(3)	2319(8)	5021(2)	53(2)
C(10B)	5437(7)	3092(15)	4753(4)	62(3)
C(88A)	5806(5)	9152(12)	5644(4)	46(3)
C(88B)	5596(7)	8675(17)	5746(5)	46(3)
C(7A)	4995(3)	3223(10)	5451(2)	70(2)
C(8A)	4939(11)	4780(40)	5305(9)	70(2)
C(7B)	4995(3)	3223(10)	5451(2)	70(2)
C(8B)	4809(4)	2126(12)	5663(3)	70(2)

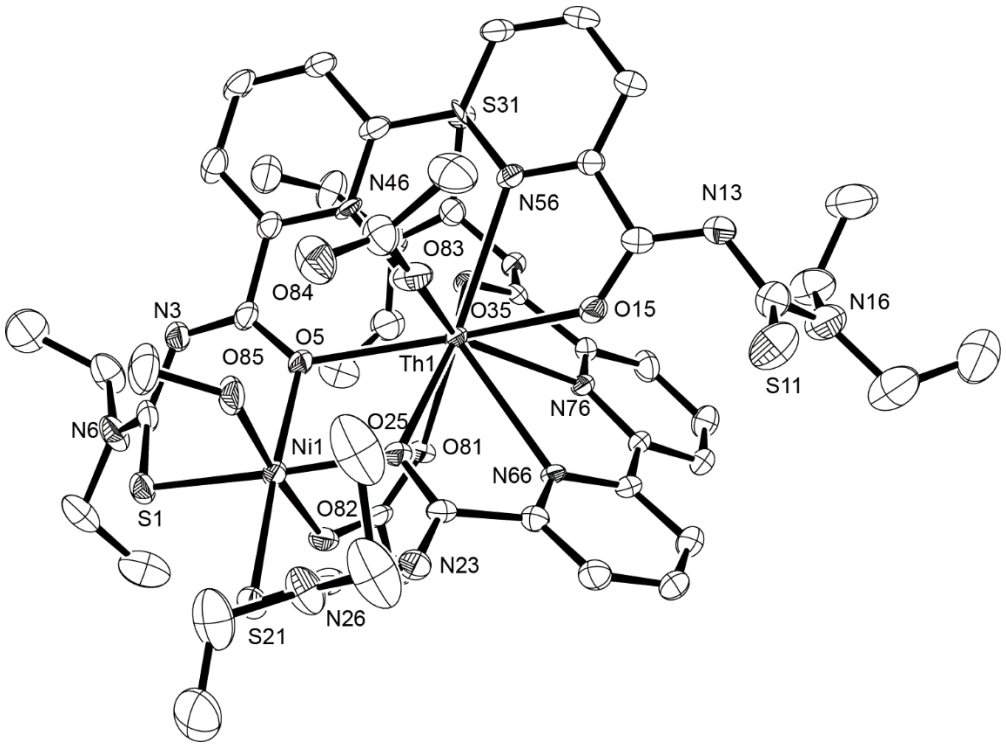

Figure A.29: Ellipsoid plot of [Ni{Th(L^3)$_2$(OAc)$_2$(MeOH)}] **(SQUEEZE)**. Hydrogen atoms have been omitted for clarity. Thermal ellipsoids are at 50 % probability.

$[Au_2\{U(L^{2a})_3\}]$

Table A.59: Crystal data and structure refinement for $[Au_2\{U(L^{2a})_3\}] \cdot THF$.

Empirical formula	$C_{55}H_{77}Au_2N_{15}O_7S_6U$	
Formula weight	1884.63	
Temperature	107(2) K	
Wavelength	0.71073 Å	
Crystal system	Monoclinic	
Space group	P $2_1/c$	
Unit cell dimensions	a = 18.862(1) Å	α= 90°
	b = 14.635(1) Å	β= 94.55(1)°
	c = 24.924(1) Å	γ = 90°
Volume	6858.5(7) $Å^3$	
Z	4	
Density (calculated)	1.825 g/cm^3	
Absorption coefficient	6.864 mm^{-1}	
F(000)	3656	
Crystal size	0.08 x 0.054 x 0.043 mm^3	
Theta range for data collection	2.349 to 24.712°	
Index ranges	-22<=h<=22, -17<=k<=17, -29<=l<=29	
Reflections collected	165608	
Independent reflections	11685 [R(int) = 0.1385]	
Completeness to theta = 24.712°	99.9 %	
Absorption correction	Semi-empirical from equivalents	
Max. and min. transmission	0.7062 and 0.5996	
Refinement method	Full-matrix least-squares on F^2	
Data / restraints / parameters	11685 / 772 / 764	
Goodness-of-fit on F^2	1.085	
Final R indices [I>2sigma(I)]	R1 = 0.0457, wR2 = 0.0660	
R indices (all data)	R1 = 0.0791, wR2 = 0.0724	
Largest diff. peak and hole	1.760 and -1.047 $e/Å^3$	
Diffractometer	Bruker D8 Venture	

Table A.60: Atomic coordinates (x 10^4) and equivalent isotropic displacement parameters ($Å^2$ x 10^3) for $[Au_2\{U(L^{2a})_3\}] \cdot THF$.

	x	y	z	U(eq)
U(1)	7368(1)	6874(1)	4054(1)	8(1)
Au(1)	9337(1)	8047(1)	2916(1)	16(1)
Au(2)	4678(1)	6022(1)	3376(1)	21(1)
S(1)	9822(1)	6615(1)	2939(1)	20(1)
C(2)	9113(4)	5880(5)	2795(3)	14(2)
N(3)	8482(3)	6175(4)	2564(2)	14(1)
C(4)	8011(4)	6399(5)	2895(3)	13(2)
O(5)	8095(3)	6319(3)	3410(2)	13(1)
N(6)	9209(3)	4986(4)	2893(2)	13(1)
C(7)	9880(4)	4609(5)	3145(3)	19(2)
C(8)	9870(5)	4616(6)	3755(3)	25(2)
C(9)	8629(4)	4317(5)	2808(3)	18(2)
C(10)	8668(5)	3785(6)	2289(3)	27(2)
S(11)	4307(1)	7161(2)	3913(1)	25(1)
C(12)	4860(4)	8062(6)	3771(3)	16(2)
N(13)	5259(3)	7976(4)	3338(2)	14(1)
C(14)	5922(4)	7748(5)	3412(3)	11(2)
O(15)	6289(3)	7700(3)	3867(2)	15(1)
N(16)	4864(4)	8804(5)	4064(3)	29(2)
C(17)	5315(6)	9590(7)	3958(4)	48(3)
C(18)	4888(6)	10320(7)	3641(4)	56(3)
C(19)	4444(6)	8881(7)	4542(4)	46(3)
C(20)	4854(7)	8473(8)	5045(4)	70(4)
S(21)	8942(1)	9530(1)	2909(1)	21(1)
C(22)	8854(4)	9784(5)	3579(3)	12(2)
N(23)	9017(3)	9159(4)	3968(2)	14(1)
C(24)	8652(4)	8421(5)	4050(3)	10(2)
O(25)	8016(3)	8240(3)	3859(2)	12(1)
N(26)	8694(4)	10619(4)	3734(3)	20(1)
C(27)	8667(5)	11400(5)	3371(3)	20(1)
C(28)	9362(5)	11916(6)	3413(4)	32(2)
C(29)	8580(5)	10791(5)	4300(3)	25(2)
C(30)	7828(5)	10524(6)	4422(4)	32(2)
S(31)	8226(1)	3287(1)	4353(1)	20(1)

C(32)	8306(4)	3901(5)	4923(3)	18(2)
N(33)	8708(3)	4696(4)	4955(2)	14(1)
C(34)	8462(4)	5431(5)	4733(3)	11(2)
O(35)	7827(3)	5569(3)	4506(2)	12(1)
C(37)	8239(7)	4183(7)	5920(5)	70(3)
C(38)	7651(8)	4789(10)	5906(6)	104(5)
N(36)	8059(5)	3641(5)	5380(3)	47(2)
C(39)	7700(6)	2766(6)	5442(4)	47(2)
C(40)	8176(7)	2040(7)	5682(4)	71(4)
S(41)	5077(1)	4849(2)	2877(1)	26(1)
C(42)	5713(4)	4342(5)	3322(3)	18(2)
N(43)	5761(3)	4556(4)	3860(3)	19(2)
C(44)	6180(4)	5212(5)	4029(3)	13(2)
O(45)	6588(3)	5682(3)	3739(2)	13(1)
N(46)	6109(4)	3684(5)	3156(3)	28(2)
C(47)	6651(5)	3243(7)	3533(4)	39(2)
C(48)	6313(6)	2541(7)	3883(5)	56(3)
C(49)	6065(5)	3372(7)	2591(4)	38(2)
C(50)	6605(6)	3864(10)	2282(4)	73(4)
S(51)	7114(2)	9628(2)	5816(1)	37(1)
C(52)	7499(5)	8603(6)	5833(3)	22(2)
N(53)	7076(4)	7823(4)	5749(2)	17(2)
C(54)	7016(4)	7438(5)	5284(3)	13(2)
O(55)	7335(3)	7667(3)	4862(2)	11(1)
N(56)	8191(4)	8454(5)	5970(3)	23(2)
C(57)	8669(5)	9198(6)	6168(3)	31(2)
C(58)	9112(6)	9565(7)	5724(4)	46(3)
C(59)	8517(5)	7541(6)	5969(4)	28(2)
C(60)	8450(5)	7036(6)	6492(3)	33(2)
C(61)	7329(4)	6783(5)	2675(3)	10(2)
C(62)	7062(4)	6751(5)	2142(3)	14(2)
C(63)	6378(4)	7091(5)	2006(3)	16(2)
C(64)	5989(4)	7443(5)	2403(3)	17(2)
C(65)	6287(4)	7458(5)	2933(3)	9(2)
N(66)	6942(3)	7137(4)	3058(2)	9(1)
C(71)	9031(4)	7722(5)	4398(3)	11(2)
C(72)	9721(4)	7803(5)	4627(3)	15(2)
C(73)	10029(4)	7084(5)	4906(3)	17(2)
C(74)	9646(4)	6281(5)	4942(3)	12(2)

C(75)	8961(4)	6246(5)	4728(3)	9(2)
N(76)	8649(3)	6958(4)	4453(2)	9(1)
C(81)	6557(4)	6611(5)	5218(3)	12(2)
C(82)	6208(4)	6196(6)	5621(3)	20(2)
C(83)	5859(5)	5378(6)	5509(3)	28(2)
C(84)	5846(4)	5005(6)	4991(3)	22(2)
C(85)	6175(4)	5485(5)	4606(3)	13(2)
N(86)	6528(3)	6258(4)	4721(2)	8(1)
O(91)	7121(5)	1371(7)	2725(4)	91(3)
C(92)	7204(6)	893(10)	2282(5)	66(3)
C(94)	6814(7)	-226(10)	2870(5)	78(4)
C(95)	6630(8)	677(10)	3005(6)	97(5)
C(93)	7033(6)	-157(10)	2286(5)	72(3)

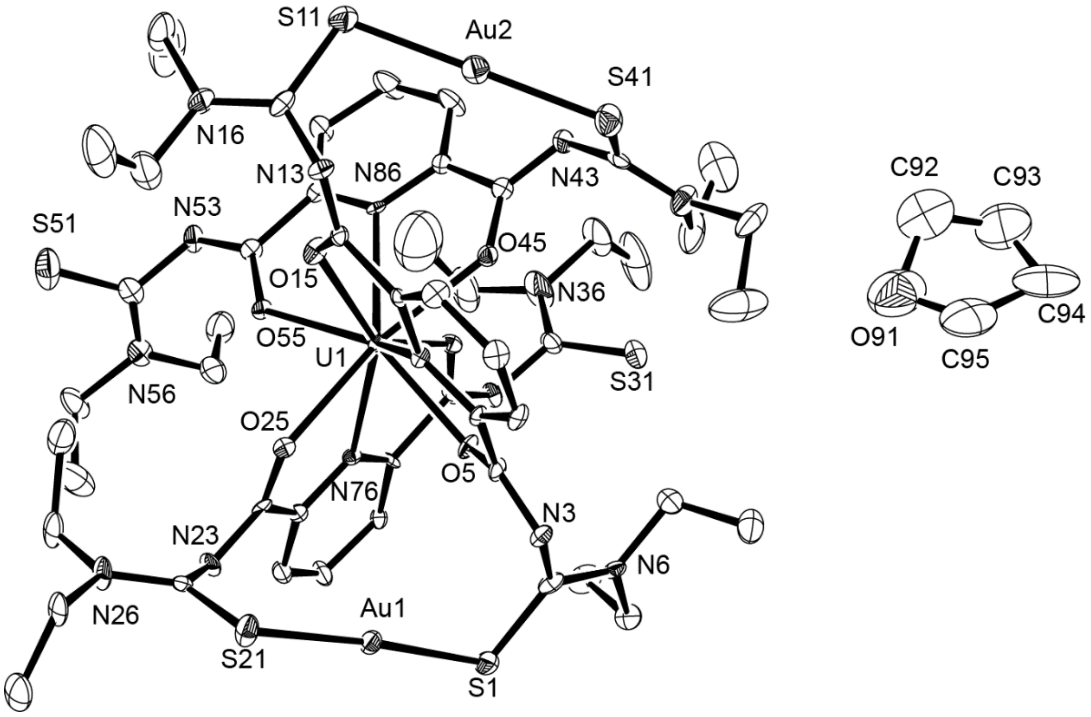

Figure A.30: Ellipsoid plot of $[Au_2\{U(L^{2a})_3\}] \cdot THF$. Hydrogen atoms have been omitted for clarity.Thermal ellipsoids are at 50 % probability.

$(NH_4)_2[\{Th(L^{2a})\}_3]$

Table A.61: Crystal data and structure refinement for $(NH_4)_2[\{Th(L^{2a})\}_3] \cdot (CH_3OH)$.

Empirical formula	$C_{52}H_{81}N_{17}O_7S_6Th$	
Formula weight	1480.73	
Temperature	107(2) K	
Wavelength	0.71073 Å	
Crystal system	Monoclinic	
Space group	P 2_1/c	
Unit cell dimensions	a = 13.351(1) Å	α= 90°
	b = 24.531(1) Å	β= 100.64(1)°
	c = 20.663(1) Å	γ = 90°
Volume	6651.1(7) $Å^3$	
Z	4	
Density (calculated)	1.479 g/cm^3	
Absorption coefficient	2.490 mm^{-1}	
F(000)	3016	
Crystal size	0.3 x 0.08 x 0.06 mm^3	
Theta range for data collection	2.273 to 30.034°	
Index ranges	-18<=h<=18, -34<=k<=34, -29<=l<=29	
Reflections collected	264039	
Independent reflections	19406 [R(int) = 0.0293]	
Completeness to theta = 25.242°	99.6 %	
Absorption correction	Semi-empirical from equivalents	
Max. and min. transmission	0.7461 and 0.6289	
Refinement method	Full-matrix least-squares on F^2	
Data / restraints / parameters	19406 / 9 / 785	
Goodness-of-fit on F^2	1.067	
Final R indices [I>2sigma(I)]	R1 = 0.0193, wR2 = 0.0472	
R indices (all data)	R1 = 0.0209, wR2 = 0.0480	
Largest diff. peak and hole	2.547 and -1.113 e/$Å^3$	
Diffractometer	Bruker D8 Venture	

Table A.62: Atomic coordinates (x 10^4) and equivalent isotropic displacement parameters ($Å^2$ x 10^3) for $(NH_4)_2[\{Th(L^{2a})\}_3] \cdot (CH_3OH)$.

	x	y	z	U(eq)
Th(1)	2484(1)	6201(1)	7347(1)	8(1)
S(1)	5480(1)	6764(1)	5695(1)	27(1)
C(2)	4803(1)	6179(1)	5563(1)	18(1)
C(4)	4334(1)	5829(1)	6518(1)	13(1)
N(3)	4868(1)	5789(1)	6057(1)	17(1)
O(5)	3637(1)	6188(1)	6567(1)	14(1)
N(6)	4268(1)	6045(1)	4974(1)	22(1)
C(7)	3705(2)	5528(1)	4859(1)	29(1)
C(8)	2600(2)	5603(1)	4928(1)	43(1)
C(9)	4154(2)	6421(1)	4406(1)	28(1)
C(10)	4922(2)	6308(1)	3975(1)	35(1)
S(11)	1722(1)	4293(1)	9235(1)	22(1)
C(12)	2510(1)	4846(1)	9309(1)	15(1)
N(13)	3253(1)	4845(1)	8919(1)	14(1)
C(14)	3191(1)	5160(1)	8411(1)	12(1)
O(15)	2525(1)	5545(1)	8231(1)	12(1)
N(16)	2500(1)	5237(1)	9750(1)	18(1)
C(17)	1811(1)	5222(1)	10231(1)	24(1)
C(18)	879(2)	5577(1)	10021(1)	37(1)
C(19)	3174(1)	5722(1)	9797(1)	20(1)
C(20)	4137(1)	5642(1)	10301(1)	26(1)
S(21)	-124(1)	4228(1)	6603(1)	21(1)
C(22)	887(1)	4441(1)	6283(1)	13(1)
N(23)	783(1)	4926(1)	5929(1)	14(1)
C(24)	1124(1)	5368(1)	6228(1)	11(1)
O(25)	1672(1)	5403(1)	6816(1)	12(1)
N(26)	1730(1)	4148(1)	6304(1)	17(1)
C(27)	2600(1)	4347(1)	6023(1)	25(1)
C(28)	2553(2)	4141(1)	5320(1)	36(1)
C(29)	1861(2)	3613(1)	6630(1)	24(1)
C(30)	2347(2)	3662(1)	7353(1)	35(1)
C(32)	1943(1)	8222(1)	6480(1)	14(1)
C(34)	1663(1)	7278(1)	6372(1)	11(1)
S(31)	3086(1)	8429(1)	6326(1)	21(1)

N(33)	1467(1)	7769(1)	6163(1)	15(1)
O(35)	2265(1)	7122(1)	6907(1)	12(1)
N(36)	1401(1)	8511(1)	6838(1)	19(1)
C(37)	393(1)	8324(1)	6945(1)	29(1)
C(38)	454(2)	7936(1)	7517(1)	38(1)
C(39)	1784(1)	9026(1)	7153(1)	24(1)
C(40)	2434(2)	8944(1)	7831(1)	29(1)
S(41)	6097(1)	7601(1)	8141(1)	27(1)
C(42)	5794(1)	7131(1)	8681(1)	16(1)
N(43)	4843(1)	7125(1)	8859(1)	16(1)
C(44)	4040(1)	6919(1)	8505(1)	12(1)
O(45)	3961(1)	6659(1)	7949(1)	13(1)
N(46)	6475(1)	6790(1)	9005(1)	18(1)
C(47)	6188(1)	6357(1)	9427(1)	25(1)
C(48)	5879(2)	5841(1)	9031(1)	36(1)
C(49)	7558(1)	6808(1)	8949(1)	26(1)
C(50)	8162(2)	7169(1)	9481(1)	41(1)
S(51)	-1378(1)	5505(1)	8242(1)	23(1)
C(52)	-1155(1)	6128(1)	7933(1)	15(1)
N(53)	-373(1)	6446(1)	8278(1)	16(1)
C(54)	520(1)	6454(1)	8122(1)	12(1)
O(55)	796(1)	6228(1)	7614(1)	13(1)
N(56)	-1775(1)	6343(1)	7419(1)	17(1)
C(57)	-2654(1)	6038(1)	7058(1)	24(1)
C(58)	-2352(2)	5634(1)	6566(1)	33(1)
C(59)	-1654(2)	6904(1)	7198(1)	25(1)
C(60)	-1321(2)	6929(1)	6536(1)	35(1)
C(61)	4517(1)	5406(1)	7052(1)	13(1)
C(62)	5250(1)	4998(1)	7097(1)	18(1)
C(63)	5311(1)	4616(1)	7599(1)	21(1)
C(64)	4644(1)	4648(1)	8042(1)	17(1)
C(65)	3952(1)	5076(1)	7972(1)	12(1)
N(66)	3886(1)	5444(1)	7485(1)	11(1)
C(71)	1120(1)	6832(1)	5952(1)	12(1)
C(72)	478(1)	6915(1)	5350(1)	17(1)
C(73)	39(1)	6464(1)	5003(1)	22(1)
C(74)	237(1)	5944(1)	5266(1)	19(1)
C(75)	867(1)	5897(1)	5877(1)	12(1)
N(76)	1303(1)	6332(1)	6210(1)	11(1)

C(81)	3076(1)	6963(1)	8776(1)	13(1)
C(82)	3027(1)	7178(1)	9392(1)	17(1)
C(83)	2094(1)	7175(1)	9600(1)	20(1)
C(84)	1241(1)	6958(1)	9192(1)	18(1)
C(85)	1351(1)	6743(1)	8586(1)	13(1)
N(86)	2253(1)	6747(1)	8386(1)	11(1)
O(91)	3809(1)	3604(1)	8873(1)	40(1)
C(92)	3397(3)	3083(1)	8934(1)	51(1)
N(1)	641(1)	4974(1)	7914(1)	21(1)
N(2)	4435(1)	7346(1)	6833(1)	20(1)

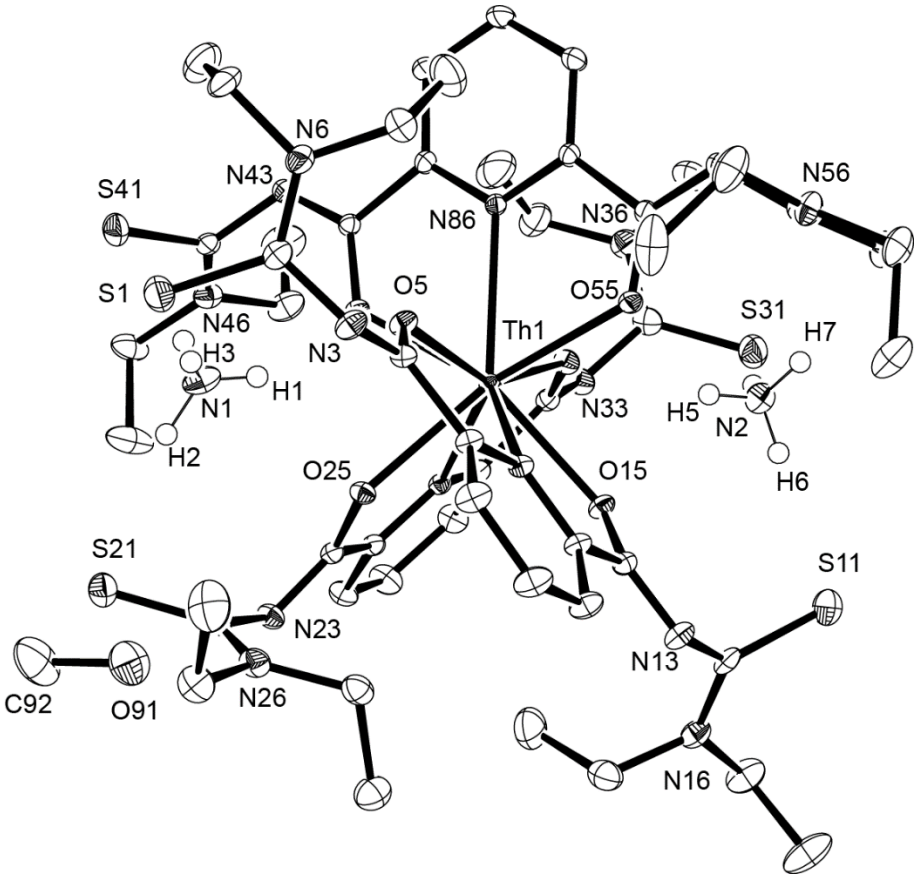

Figure A.31: Ellipsoid plot of $(NH_4)_2[\{Th(L^{2a})\}_3] \cdot (CH_3OH)$. Hydrogen atoms have been omitted for clarity. Thermal ellipsoids are at 50 % probability.

Cartesian coordinates of the calculated molecules

Table A. 63: Coordinates of H_2L^1, conformation A

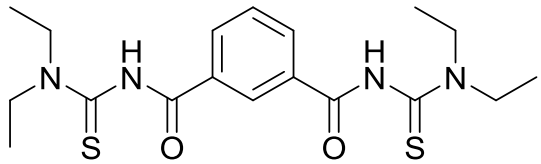

C	16.83835	3.33148	3.52449
C	15.06244	2.29466	4.66772
C	13.13974	0.00254	6.77284
C	14.75291	1.13919	5.59739
S	15.94180	4.34088	2.99554
N	18.08070	3.31681	3.09301
O	14.14031	3.00594	4.27429
C	14.09284	-0.88594	7.28685
C	15.74921	0.31595	6.07571
C	18.98611	2.14917	3.18410
C	18.66232	4.40289	2.30016
H	13.84190	-1.57748	7.85651
C	15.41724	-0.70714	6.92435
H	16.63470	0.45144	5.82598
H	18.53052	1.40849	3.61396
H	19.76703	2.37481	3.71171
C	19.40305	1.75646	1.78981
H	19.44229	4.75847	2.75345
H	18.01662	5.11927	2.20120
C	19.05707	3.87219	0.93855
H	16.07477	-1.27632	7.25392
H	20.11447	0.95890	1.84160
H	18.54474	1.43355	1.23851
H	18.19103	3.48956	0.44009
H	19.48289	4.66315	0.35720
N	16.36912	2.36532	4.36247
H	16.90813	2.35829	5.20474
H	19.84590	2.59816	1.29958
H	19.77633	3.08874	1.05591
C	13.46361	0.97848	5.92704
H	12.71103	1.62057	5.51931
C	11.65591	-0.11798	7.16695
O	10.80872	0.68611	6.69867
N	11.2277	-1.17596	8.09335
C	9.93845	-1.28640	8.43261
S	8.75036	-0.56877	7.48612
N	9.55998	-2.03828	9.63775
C	8.92450	-3.30456	9.24584
H	7.89093	-3.13274	9.02879
H	9.41160	-3.69396	8.37635
C	8.61585	-1.24251	10.43541
H	8.53299	-1.66420	11.41531
H	8.97122	-0.23595	10.50916
C	7.23454	-1.25064	9.75458
H	6.49660	-1.59411	10.44911
H	6.98897	-0.25969	9.43423
H	7.25832	-1.90375	8.90737
C	9.04527	-4.31801	10.39907
H	8.13188	-4.33491	10.95616
H	9.23739	-5.29182	9.99947
H	9.85045	-4.03144	11.04287
H	11.90017	-1.81311	8.46994

Table A.64: Coordinates of H_2L^1, conformation B

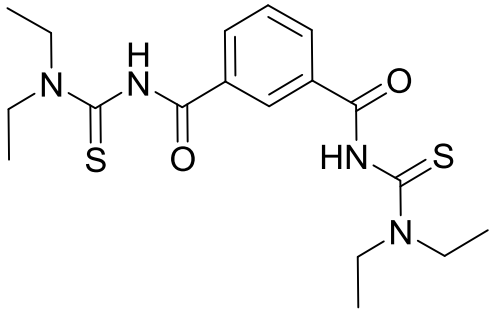

C	14.09045	4.18896	12.09757
C	13.00262	2.79372	10.54651
C	11.43064	-0.11411	8.97949
C	12.47760	1.38345	10.37132
S	14.02991	5.30517	11.17403
N	14.76690	4.34342	13.21487
O	12.91404	3.58298	9.60829
C	11.47629	-1.11083	9.96257
C	12.54329	0.46093	11.39298
C	15.28321	3.23032	14.04304
C	15.25130	5.64544	13.68023
H	11.13529	-1.96047	9.79654
C	12.04221	-0.79747	11.18688
H	12.92295	0.68795	12.21097
H	15.04094	2.37981	13.64444
H	14.89882	3.27149	14.93168
C	16.78351	3.35045	14.12530
H	14.89036	5.83420	14.56021
H	14.95373	6.34186	13.07496
C	16.76376	5.62447	13.73916
H	12.08167	-1.43537	11.86249
H	17.16646	2.59517	14.77937
H	17.20537	3.22502	13.15001
H	17.15596	5.42463	12.76389
H	17.12064	6.57408	14.07940
N	13.54909	2.98556	11.75900
H	12.90247	2.69593	12.46469
H	17.04370	4.31641	14.50492
H	17.08377	4.85987	14.41583
C	11.94336	1.09894	9.17530
H	11.92926	1.83083	8.39489
C	10.78042	-0.38617	7.61025
N	10.74254	0.59012	6.66420
O	10.28973	-1.49921	7.36950
C	10.14179	0.33400	5.403297
S	9.68956	-1.22862	4.98368
N	9.91481	1.43996	4.46189
C	10.65448	1.18392	3.21761
H	10.07722	0.54235	2.58511
H	11.58726	0.71274	3.44765
C	8.47876	1.54436	4.16564
H	8.27249	2.50092	3.73281
H	8.19959	0.77389	3.47764
C	10.91777	2.51722	2.49331
H	11.89305	2.49772	2.05359
H	10.18396	2.65802	1.72741
H	10.85922	3.32229	3.19568
C	7.67301	1.38588	5.46842
H	7.51322	0.34626	5.66474
H	8.21715	1.82253	6.27969
H	6.72883	1.87876	5.36602
H	11.13775	1.48835	6.85654

Table A.65: Coordinates of H_2L^1, conformation C

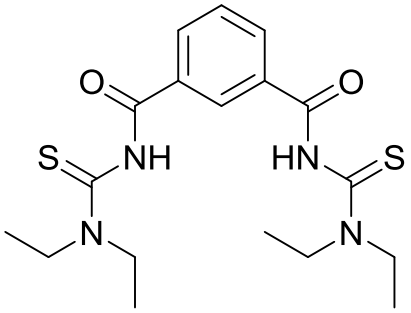

C	14.93539	4.10332	10.25474
C	13.00261	2.79371	10.54651
C	12.92874	-0.75812	9.67411
C	12.47759	1.38344	10.37131
S	14.25616	5.26916	10.78573
N	16.14181	4.26132	9.75534
O	12.23947	3.66691	10.95417
C	11.62732	-1.17020	9.98794
C	11.17660	1.05731	10.68789
C	16.79071	3.31836	8.81663
C	16.92104	5.49012	9.92653
H	11.36158	-2.05217	9.85661
C	10.74807	-0.23015	10.49845
H	10.59700	1.70104	11.02624
H	16.19993	2.57054	8.63585
H	17.60919	2.97391	9.20467
C	17.09736	4.05216	7.53615
H	17.76403	5.28613	10.36017
H	16.43398	6.11209	10.48857
C	17.17827	6.11222	8.57069
H	9.87516	-0.47082	10.71064
H	17.63144	3.40427	6.87291
H	16.18290	4.36049	7.07399
H	16.24484	6.34305	8.10131
H	17.74789	7.00978	8.69238
N	14.29136	2.90504	10.18274
H	14.83028	2.20374	10.64939
H	17.69542	4.91261	7.75261
H	17.72389	5.42355	7.96002
C	13.34838	0.48765	9.88545
H	14.35881	0.76767	9.67208
C	13.94365	-1.74483	9.06751
N	15.20427	-1.33218	8.76725
O	13.61032	-2.91961	8.85211
C	16.13621	-2.24607	8.20807
S	15.77293	-3.88460	8.13280
N	17.42325	-1.75676	7.69329
C	18.52144	-2.39298	8.43497
H	18.72962	-3.35278	8.01030
H	18.23847	-2.51036	9.46018
C	17.53853	-2.08941	6.26607
H	18.31041	-1.49568	5.82268
H	17.78066	-3.12623	6.15993
C	19.77957	-1.50919	8.34765
H	20.29479	-1.52851	9.28524
H	20.42407	-1.88115	7.57878
H	19.49399	-0.50384	8.11826
C	16.19989	-1.80016	5.56181
H	15.55344	-2.64679	5.66293
H	15.73922	-0.94422	6.00907
H	16.37692	-1.60851	4.52411
H	15.47490	-0.38517	8.94026

Table A.66: Coordinates of H_2L^1, conformation D

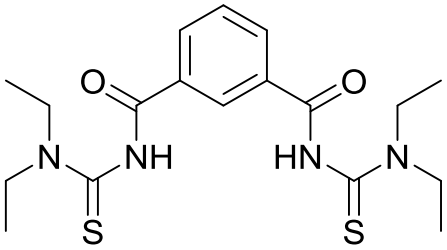

C	14.93539	4.10332	10.25474
C	13.00261	2.79371	10.54651
C	12.92874	-0.75812	9.67411
C	12.47759	1.38344	10.37131
S	14.25616	5.26916	10.78573
N	16.14181	4.26132	9.75534
O	12.23947	3.66691	10.95417
C	11.62732	-1.17020	9.98794
C	11.17660	1.05731	10.68789
C	16.79071	3.31836	8.81663
C	16.92104	5.49012	9.92653
H	11.36158	-2.05217	9.85661
C	10.74807	-0.23015	10.49845
H	10.59700	1.70104	11.02624
H	16.19993	2.57054	8.63585
H	17.60919	2.97391	9.20467
C	17.09736	4.05216	7.53615
H	17.76403	5.28613	10.36017
H	16.43398	6.11209	10.48857
C	17.17827	6.11222	8.57069
H	9.87516	-0.47082	10.71064
H	17.63144	3.40427	6.87291
H	16.18290	4.36049	7.07399
H	16.24484	6.34305	8.10131
H	17.74789	7.00978	8.69238
N	14.29136	2.90504	10.18274
H	14.83028	2.20374	10.64939
H	17.69542	4.91261	7.75261
H	17.72389	5.42355	7.96002
C	13.34838	0.48765	9.88545
H	14.35881	0.76767	9.67208
C	13.94365	-1.74483	9.06751
N	15.20427	-1.33218	8.76725
O	13.61032	-2.91961	8.85211
C	16.13621	-2.24607	8.20807
S	15.77293	-3.88460	8.13280
N	17.42325	-1.75676	7.69329
C	18.52144	-2.39298	8.43497
H	18.72962	-3.35278	8.01030
H	18.23847	-2.51036	9.46018
C	17.53853	-2.08941	6.26607
H	18.31041	-1.49568	5.82268
H	17.78066	-3.12623	6.15993
C	19.77957	-1.50919	8.34765
H	20.29479	-1.52851	9.28524
H	20.42407	-1.88115	7.57878
H	19.49399	-0.50384	8.11826
C	16.19989	-1.80016	5.56181
H	15.55344	-2.64679	5.66293
H	15.73922	-0.94422	6.00907
H	16.37692	-1.60851	4.52411
H	15.47490	-0.38517	8.94026

Table A.67: Coordinates of H_2L^{2a}, conformation A

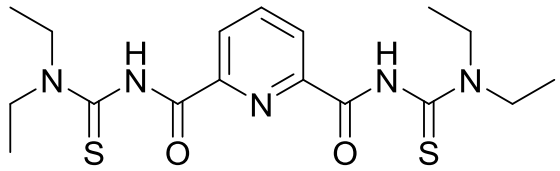

N	13.23268	2.2942	10.74278
C	16.15090	-1.59127	10.69291
C	14.51522	0.23880	10.81290
C	10.55615	6.29028	10.64829
C	11.77069	4.20240	10.82221
C	12.90829	3.46855	10.20576
C	14.22448	1.58622	10.18430
S	15.42819	-2.12239	12.09214
N	17.21865	-2.17018	10.18834
O	13.85571	-0.11994	11.76085
S	9.71713	5.72064	12.0002
N	10.3937	7.49073	10.11501
O	11.16506	3.74254	11.77858
C	13.59979	4.0052	9.11221
C	14.93912	2.04029	9.09699
C	18.14949	-1.52636	9.23416
C	17.71855	-3.46603	10.65451
C	9.36702	8.43833	10.59364
C	11.22133	8.04351	9.04065
H	13.37397	4.83962	8.76799
C	14.62751	3.26079	8.55812
H	15.62406	1.52673	8.73377
H	17.82429	-1.63720	8.32701
H	19.02535	-1.93637	9.29668
C	18.24249	-0.0601	9.57112
H	17.74906	- 4.09139	9.91405
H	17.12199	-3.82452	11.32943
C	19.10568	-3.28797	11.23385
H	8.58858	8.39768	10.01768
H	9.71739	9.34278	10.56697
C	8.98048	8.08452	11.99247
H	11.82779	7.36492	8.70578
H	11.74931	8.78462	9.37643
C	10.30168	8.52267	7.92039
H	15.10151	3.58655	7.82727
H	18.96633	0.40657	8.93616
H	17.28834	0.40104	9.42336
H	19.06388	-2.60404	12.05567
H	19.47386	-4.23305	11.5747
H	9.81761	8.23281	12.64218
H	8.16993	8.70816	12.30711
H	10.88944	8.94674	7.13324
H	9.74103	7.69434	7.54032
N	15.55400	-0.39747	10.20818
N	11.54931	5.37408	10.21168
H	18.53883	0.05292	10.59304
H	8.67701	7.05915	12.03013
H	9.62995	9.26279	8.30237
H	19.7598	-2.90097	10.48068
H	12.10606	5.61323	9.41617
H	15.92122	0.00117	9.36780

Table A.68: Coordinates of H_2L^{2a}, conformation B

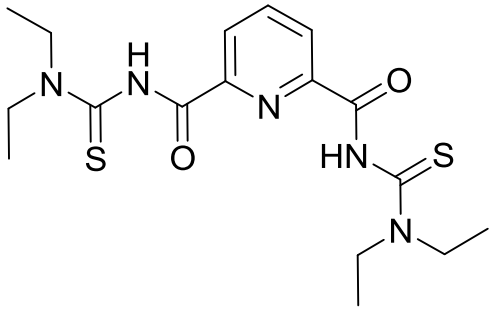

N	0.80609	0.47193	0.89325
C	4.05859	-1.87633	1.03131
C	2.48266	-0.67906	-0.4254
C	-2.51088	2.63922	3.62124
C	-0.77553	1.45904	2.41279
C	-0.31706	1.17439	1.02663
C	1.22403	0.16002	-0.34159
S	4.62087	-2.54226	-0.38383
N	4.55814	-2.30461	2.36815
O	2.88729	-1.02127	-1.51234
S	-1.66614	2.16399	4.96889
N	-3.69918	3.5379	3.6422
O	-0.14498	1.06304	3.38155
C	-1.04386	1.63595	-0.07824
C	0.55346	0.56353	-1.47589
C	3.8326	-2.09394	3.64119
C	5.74322	-3.14791	2.54388
C	-4.30965	4.01548	4.89932
C	-4.35464	4.07955	2.44984
H	-1.81251	2.14757	0.03646
C	-0.58759	1.3104	-1.34443
H	0.87052	0.33344	-2.3193
H	4.03345	-1.21379	3.9961
H	4.10713	-2.75602	4.29342
C	2.35384	-2.21565	3.37552
H	6.3926	-2.68935	3.09913
H	6.15165	-3.32379	1.68239
C	5.33713	-4.45115	3.19819
H	-5.08174	3.47152	5.11685
H	-4.60549	4.93338	4.7924
C	-3.30454	3.93096	6.00111
H	-3.9735	3.68199	1.65165
H	-4.22156	5.03927	2.40514
C	-5.84557	3.76225	2.53209
H	-1.05147	1.59626	-2.09811
H	1.81803	-2.13729	4.29838
H	2.04432	-1.4322	2.71575
H	4.62757	-4.95635	2.57674
H	6.20085	-5.06914	3.3285
H	-2.50359	4.6132	5.80634
H	-3.77128	4.18468	6.92992
H	-6.3441	4.16695	1.67618
H	-5.98363	2.70148	2.55682
N	2.98938	-0.9703	0.80262
N	-1.90138	2.18498	2.42183
H	2.14947	-3.16387	2.92385
H	-2.91877	2.93444	6.0563
H	-6.25401	4.1959	3.42092
H	4.89593	-4.24916	4.15184
H	-2.32997	2.41638	1.54847
H	2.58269	-0.51707	1.59583

Table A.69: Coordinates of H_2L^{2a}, conformation C

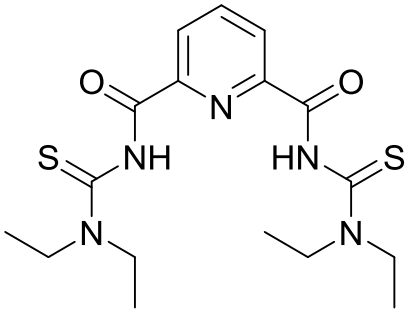

N	12.56192	2.95999	9.79602
C	10.56169	3.32387	13.25922
C	12.77437	3.16951	12.2013
C	9.70873	2.8199	7.00508
C	12.08554	2.69855	7.45300
C	13.05635	2.74169	8.57920
C	13.4038	2.96122	10.83908
S	11.40552	3.19644	14.68539
N	9.24718	3.33648	13.21759
O	13.48507	3.1801	13.17959
S	10.16425	2.5064	5.40811
N	8.45659	2.89714	7.42707
O	12.45633	2.50327	6.30526
C	14.42692	2.56312	8.35195
C	14.76191	2.77571	10.69663
C	8.44329	3.01483	12.01686
C	8.41304	3.4933	14.41177
C	7.30388	2.81792	6.50725
C	8.05697	3.01835	8.83077
H	14.75515	2.43758	7.49042
C	15.27903	2.57856	9.44331
H	15.32064	2.78487	11.43996
H	8.33544	3.807	11.46752
H	7.56398	2.70346	12.27951
C	9.15727	1.94129	11.23592
H	7.83925	4.26853	14.3115
H	8.97550	3.63124	15.18928
C	7.56923	2.25058	14.59917
H	6.98336	3.7099	6.30481
H	6.58205	2.32415	6.92755
C	7.72191	2.13248	5.24757
H	8.83964	3.14425	9.38935
H	7.60490	2.20974	9.11805
C	7.12011	4.21616	8.96450
H	16.19352	2.45634	9.32624
H	8.55467	1.64598	10.40252
H	10.09351	2.32015	10.88263
H	8.20792	1.40038	14.71809
H	6.95827	2.36236	15.47044
H	7.97459	1.11511	5.46207
H	6.91705	2.15916	4.54301
H	6.80332	4.30928	9.98227
H 7	63472	5.10628	8.66827
N	11.42168	3.2908	12.12975
N	10.82758	2.87691	7.87762
H	9.33045	1.09568	11.86826
H	8.57351	2.63220	4.83532
H	6.26564	4.07248	8.33670
H	6.94507	2.11059	13.74142
H	10.67006	3.05752	8.84848
H	11.00578	3.36124	11.22307

Table A.70: Coordinates of H_2L^{2a}, conformation D

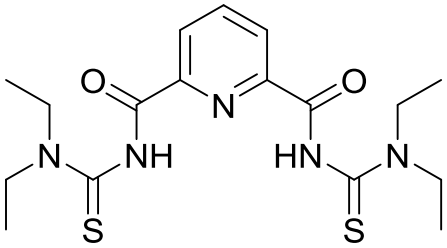

N	14.15056	1.74901	7.38518
C	16.17776	5.10131	7.87578
C	16.34636	2.72081	7.71468
C	10.40136	2.85941	6.70628
C	11.86976	1.02511	7.14258
C	13.31846	0.71531	7.27658
C	15.45796	1.50451	7.55168
S	15.23062	5.94898	8.57354
N	17.34696	5.54161	7.46478
O	17.54286	2.55781	7.94458
S	10.25678	4.07612	7.48166
N	9.47966	2.37681	5.88808
O	11.00576	0.15281	7.32908
C	13.77096	-0.61029	7.28198
C	15.97576	0.22781	7.58428
C	18.15786	4.90241	6.40398
C	17.90586	6.82971	7.88298
C	8.14036	2.98501	5.75588
C	9.67706	1.23541	4.99198
H	13.17566	-1.31789	7.17878
C	15.12696	-0.83859	7.44488
H	16.88846	0.09081	7.69838
H	17.70386	4.11331	6.06908
H	19.01736	4.63181	6.76058
C	18.35376	5.89541	5.28698
H	18.76526	6.69111	8.31018
H	17.31356	7.25201	8.52388
C	18.07286	7.71991	6.67008
H	8.05836	3.41381	4.89058
H	8.01736	3.66001	6.44198
C	7.09866	1.92351	5.89528
H	10.53656	0.82131	5.16578
H	9.66336	1.53221	4.06868
C	8.55336	0.23101	5.23448
H	5.45796	-1.70759	7.45938
H	18.99812	5.47392	4.54398
H	17.40672	6.12869	4.84696
H	17.12027	7.87624	6.20852
H	18.48158	8.66146	6.97226
H	7.12486	1.52631	6.88848
H	6.13334	2.34387	5.70461
H	8.67168	-0.60281	4.57445
H	8.59118	-0.10857	6.24846
N	15.65846	3.87031	7.60968
H	15.32562	4.05002	6.68398
N	11.66626	2.31161	6.82938
H	11.9541	2.69358	5.95117
H	18.79548	6.78849	5.67708
H	7.29159	1.13998	5.1926
H	7.60957	0.70039	5.0505
H	18.73476	7.25126	5.97211

Table A.71: Coordinates of H_2L^{2a}, conformation E

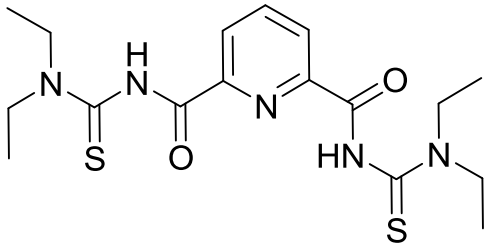

N	13.62753	1.77744	7.37695
C	17.60929	4.26687	6.39716
C	15.51874	3.209	6.87849
C	9.72787	2.01849	8.07329
C	11.6327	0.57812	7.98292
C	13.06791	0.58864	7.59214
C	14.93058	1.82552	7.06621
S	16.88214	5.49386	6.65840
N	18.85199	4.26295	5.96647
O	14.79045	4.18953	7.01704
S	9.58827	3.24848	8.82835
N	8.71531	1.2789	7.64947
O	11.10963	-0.43149	8.48220
C	13.78318	-0.60803	7.45661
C	15.70357	0.69258	6.93175
C	19.49812	3.12102	5.28094
C	19.6941	5.46173	5.95035
C	7.31237	1.58167	7.99760
C	8.84403	0.12142	6.76153
H	13.36671	-1.42991	7.58621
C	15.12551	-0.5345	7.12475
H	16.60482	0.75873	6.71227
H	18.87429	2.38185	5.20729
H	20.26775	2.82155	5.788
C	19.92912	3.56844	3.90757
H	20.49406	5.30763	6.47628
H	19.21266	6.2064	6.34227
C	20.0736	5.78719	4.52154
H	6.84020	1.89827	7.21264
H	7.28471	2.28004	8.67066
C	6.65432	0.34659	8.52012
H	9.78059	-0.08741	6.62152
H	8.44391	0.31797	5.90010
C	8.13408	-1.06501	7.40865
H	15.62947	-1.31082	7.03376
H	20.46209	2.77589	3.42517
H	19.06624	3.82243	3.32806
H	19.18745	5.96482	3.94876
H	20.68936	6.66213	4.50651
H	7.11287	0.06165	9.44382
H	5.61417	0.53803	8.68224
H	8.20267	-1.91644	6.76425
H	8.59729	-1.28943	8.34671
N	16.81798	3.16697	6.5382
H	17.38309	2.66432	7.19241
N	11.04621	1.75827	7.74241
H	10.91676	2.1044	6.81319
H	20.56497	4.42461	3.99458
H	6.76457	-0.44461	7.80814
H	7.10468	-0.82073	7.56857
H	20.61225	4.96467	4.09938

Table A.72: Coordinates of H_2L^{2b}, conformation A

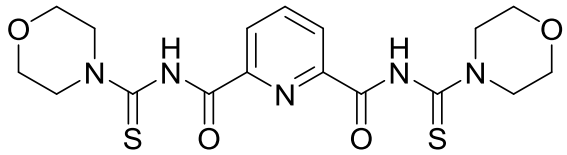

N	13.52763	1.71700	7.43508
C	16.34999	5.57019	7.10853
C	14.92522	3.69721	7.42981
C	10.74107	-2.16026	7.60051
C	12.00650	-0.13358	7.65052
C	13.28761	0.43760	7.15538
C	14.69239	2.25135	7.04188
S	15.28018	6.29391	7.76750
N	17.37294	6.17991	6.55030
O	14.09148	4.37033	8.03216
S	9.73850	-1.37002	8.28818
N	10.56642	-3.40911	7.19834
O	11.19579	0.56059	8.28538
C	14.18838	-0.34796	6.42497
C	15.63521	1.53710	6.33472
C	18.24567	5.57815	5.51702
C	17.66141	7.60188	6.75338
C	9.34315	-4.17719	7.50615
C	11.51664	-4.15901	6.37403
H	13.99006	-1.23309	6.21772
C	15.38071	0.22813	6.02019
H	16.43299	1.93716	6.07339
H	17.95598	4.67274	5.32396
H	19.16095	5.54482	5.83367
C	18.16294	6.42101	4.27008
H	18.55179	7.70634	7.12296
H	17.02652	7.97921	7.38143
C	17.56767	8.32561	5.42715
H	8.82416	-4.30604	6.69783
H	8.79850	-3.68605	8.14147
C	9.72243	-5.50291	8.08059
H	12.33350	-3.64871	6.26114
H	11.13700	-4.32376	5.49683
C	11.81883	-5.48385	7.06959
H	16.00249	-0.26900	5.53938
H	18.76752	6.06036	3.60291
H	17.26310	6.37331	3.91297
O	18.49757	7.78784	4.51343
H	16.67030	8.23623	5.06862
H	17.74709	9.27049	5.55638
H	10.13640	-5.36158	8.94779
H	8.91791	-6.02681	8.21993
O	10.61860	-6.24068	7.25567
H	12.44477	-5.99479	6.53485
H	12.23024	-5.31021	7.93139
N	16.09582	4.23330	7.04525
N	11.87364	-1.42138	7.30627
H	16.81014	3.62563	6.69816
H	12.62327	-1.86688	6.81680

Table A.73: Coordinates of H_2L^{2b}, conformation B

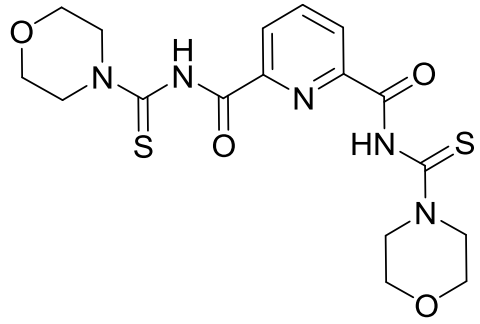

N	14.08989	2.04859	5.86176
C	14.43472	5.94780	6.85062
C	14.92522	3.69721	7.42981
C	12.31120	-1.11219	2.75192
C	13.11154	0.61520	4.19648
C	13.82489	0.79821	5.48888
C	14.69239	2.25135	7.04188
S	14.98512	6.23590	8.16079
N	13.83747	6.86450	6.12070
O	15.43046	4.02915	8.50013
S	11.97654	-0.00903	1.87240
N	12.17212	-2.39065	2.43874
O	12.79106	1.58887	3.49544
C	14.19813	-0.30657	6.26485
C	15.07406	1.21617	7.86763
C	12.89711	6.57417	5.01486
C	13.89053	8.29424	6.43610
C	11.55224	-2.83390	1.17367
C	12.64680	-3.50575	3.26093
H	14.02661	-1.17356	5.97391
C	14.82868	-0.07341	7.47540
H	15.49314	1.38926	8.67956
H	12.79746	5.61534	4.90687
H	13.23704	6.94115	4.18486
C	11.56386	7.19546	5.34431
H	14.26740	8.78149	5.68721
H	14.45836	8.43919	7.20842
C	12.49125	8.79540	6.72301
H	12.22772	-3.21624	0.59326
H	11.15585	-2.07408	0.71864
C	10.50167	-3.85420	1.46801
H	12.97491	-3.17525	4.11154
H	13.37414	-3.96345	2.81122
C	11.48393	-4.46861	3.48667
H	15.08310	-0.78562	8.01667
H	10.95461	7.04995	4.60381
H	11.19295	6.75723	6.12528
O	11.66406	8.59723	5.59816
H	12.12355	8.32008	7.48503
H	12.52055	9.73999	6.94342
H	9.77486	-3.42556	1.94905
H	10.14418	-4.18791	0.63016
O	10.98053	-4.95257	2.23755
H	11.78225	-5.21530	4.02728
H	10.77503	-4.01240	3.96775
N	14.51208	4.62205	6.54688
N	12.90476	-0.68023	3.92508
H	14.25052	4.32478	5.62861
H	13.19091	-1.36284	4.59751

Table A.74: Coordinates of H_2L^{2b}, conformation C

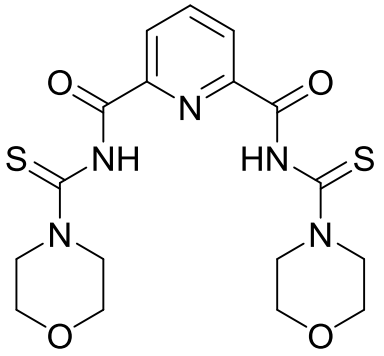

N	15.14282	0.97868	5.43209
C	19.05081	1.83271	4.88544
C	17.29958	1.43434	6.43969
C	13.54662	0.18461	1.88639
C	13.11154	0.61520	4.19648
C	13.82489	0.79821	5.48888
C	15.81045	1.19061	6.57496
S	19.81004	2.17320	6.07293
N	19.51372	2.03635	3.67133
O	18.02642	1.68163	7.39968
S	12.11699	0.37764	1.74013
N	14.38455	-0.00988	0.88044
O	11.87771	0.73388	4.12064
C	13.12687	0.77458	6.70305
C	15.19063	1.19863	7.80577
C	18.67154	2.12741	2.45730
C	20.91098	2.38213	3.39828
C	13.92629	-0.15625	-0.51586
C	15.84276	-0.05500	1.00825
H	12.20937	0.62115	6.72281
C	13.83884	0.98552	7.87180
H	15.68212	1.34566	8.58142
H	17.73792	2.00619	2.69101
H	18.92096	1.43455	1.82733
C	18.87335	3.48546	1.83513
H	21.30180	1.72305	2.80401
H	21.41683	2.38207	4.22534
C	20.97106	3.75188	2.75669
H	14.18044	0.62594	-1.02861
H	12.95921	-0.23230	-0.53753
C	14.54520	-1.37680	-1.11465
H	16.09509	-0.03273	1.94434
H	16.23834	0.71342	0.56804
C	16.34466	-1.34332	0.36121
H	13.40326	0.98241	8.69350
H	18.36081	3.53705	1.01334
H	18.53690	4.16511	2.43878
O	20.24606	3.75400	1.54707
H	20.59731	4.41274	3.36116
H	21.89516	3.99183	2.58300
H	14.18848	-2.16099	-0.66613
H	14.29187	-1.43122	-2.04953
O	15.96583	-1.39551	-1.01781
H	17.30981	-1.38755	0.43428
H	15.97159	-2.10716	0.82969
N	17.79460	1.40316	5.19087
N	13.96088	0.34047	3.19761
H	17.21683	1.04994	4.45506
H	14.93374	0.24410	3.40800

Table A.75: Coordinates of H_2L^{2b}, conformation D

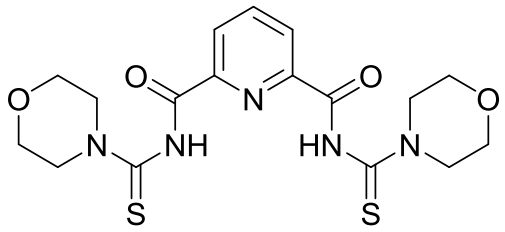

N	14.15055	1.74900	7.38517
C	16.17775	5.10130	7.87577
C	16.34635	2.72080	7.71467
C	10.40135	2.85940	6.70627
C	11.86975	1.02510	7.14257
C	13.31845	0.71530	7.27657
C	15.45795	1.50450	7.55167
S	5.23061	5.94898	8.57354
N	17.34695	5.54160	7.46477
O	17.54285	2.55780	7.94457
S	10.25678	4.07611	7.48165
N	9.47965	2.37680	5.88807
O	11.00575	0.15280	7.32907
C	13.77095	-0.61029	7.28197
C	15.97575	0.22780	7.58427
C	18.15785	4.90240	6.40397
C	17.90585	6.82970	7.88297
C	8.14035	2.98500	5.755877
C	9.67705	1.23540	4.991977
H	13.17565	-1.31789	7.17877
C	15.12695	-0.83859	7.44487
H	16.88845	0.09080	7.69837
H	17.70385	4.11330	6.06907
H	19.01735	4.63180	6.76057
C	18.35375	5.89540	5.28697
H	18.76525	6.69110	8.31017
H	17.31355	7.25200	8.52387
C	18.07285	7.71990	6.67007
H	8.05835	3.41380	4.89057
H	8.01735	3.66001	6.44197
C	7.09865	1.92350	5.89527
H	10.53655	0.82131	5.16572
H	9.66335	1.53220	4.06867
C	8.55335	0.23100	5.23447
H	15.45795	-1.70759	7.45932
H	18.92315	5.50080	4.60817
H	17.49585	6.08940	4.87967
O	18.94295	7.11500	5.73957
H	17.20885	7.87320	6.25557
H	18.43275	8.57920	6.94167
H	7.11535	1.58600	6.80587
H	6.22555	2.31810	5.74317
O	7.27785	0.83430	4.99557
H	8.66725	-0.53039	4.64617
H	8.59585	-0.08689	6.15057
N	15.65845	3.87030	7.60967
H	15.325612	4.05001	6.68397
N	11.66625	2.31160	6.82937
H	11.95410	2.69357	5.95117

Table A.76: Coordinates of H_2L^{2b}, conformation E

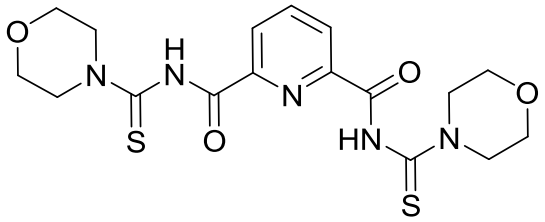

N	13.73513	1.43634	7.03425
C	17.36062	4.47866	6.31439
C	15.52329	3.05678	6.80803
C	9.81832	1.29304	7.65754
C	11.82496	0.02108	7.39923
C	13.2612	0.19224	7.05199
C	15.03562	1.62297	6.76837
S	16.39214	5.53655	6.52748
N	18.56545	4.71188	5.84131
O	14.77945	4.01001	7.02961
S	9.57747	2.37996	8.58656
N	8.86928	0.55775	7.10026
O	11.37007	-1.08735	7.72581
C	14.06439	-0.91625	6.75511
C	5.89167	0.58119	6.48372
C	19.42738	3.69172	5.20273
C	19.12915	6.0591	5.72426
C	7.44285	0.70421	7.45373
C	9.09591	-0.4381	6.05065
H	13.70754	-1.77551	6.74769
C	15.40251	-0.69854	6.47326
H	16.78881	0.7434	6.30031
H	18.9759	2.8332	5.19519
H	20.25418	3.59747	5.69937
C	19.72227	4.12962	3.79085
H	19.95465	6.11426	6.23002
H	18.50722	6.70791	6.08781
C	19.39883	6.36349	4.26615
H	6.96048	1.10331	6.71388
H	7.3539	1.28754	8.22398
C	6.86958	-0.6395	7.76544
H	10.0473	-0.55663	5.90495
H	8.69538	-0.14054	5.21891
C	8.46548	-1.75659	6.49164
H	15.96344	-1.41438	6.27868
H	20.32458	3.49012	3.3798
H	18.8984	4.13313	3.28022
O	20.31213	5.42902	3.73562
H	18.56828	6.32697	3.76548
H	19.76244	7.25911	4.18045
H	7.28082	-0.97432	8.57917
H	5.91884	-0.54431	7.9333
O	7.06314	-1.59175	6.72443
H	8.60377	-2.42686	5.80576
H	8.89582	-2.06467	7.30527
N	16.82791	3.24687	6.5484
N	11.15701	1.17995	7.32538
H	11.01639	1.65436	6.45638
H	17.43297	2.45100	6.52602

Table A.77: Computational results and calculated bond parameters for the structure isomers of $[\{UO_2(L^{2a})(\mu_2\text{-}OMe)\}_2]^{2-}$.

	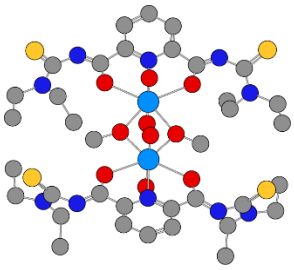	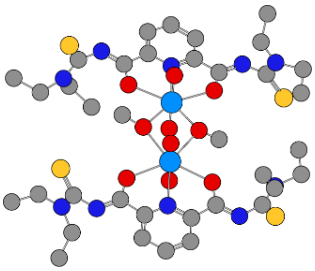	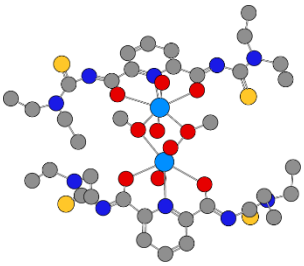
	syn syn	*anti,syn*	*anti,anti*
E[Hartree]	-4400.1782	-4400.1847	-4400.1822
Bond lengths [Å]			
U1–O1	1.796	1.785	1.788
U1–O2	1.781	1.787	1.782
U1–O5	2.463	2.454	2.449
U1–O15	2.480	2.461	2.465
U1–N46	2.613	2.658	2.659
U1–O61	2.393	2.387	2.399
U1–O62	2.404	2.399	2.388
C2–S1	1.701	1.697	1.699
C2–N3	1.359	1.374	1.376
C4–N3	1.308	1.301	1.299
C4–O5	1.283	1.279	1.280
C2–N6	1.361	1.360	1.358
Angles (°)			
O1–U1–O2	176.5	177.4	176.5
O1–U1-N46	88.4	89.9	85.4
O1–U1–O5	89.0	88.8	89.0
O1–U1–O15	87.9	89.3	88.9
O1–U1–O61	90.0	91.3	89.3
O1–U1–O62	91.0	89.4	90.0

Table A.78: Computational results and calculated bond parameters for the structure isomers of $[\{UO_2(L^{2b})(\mu_2\text{-OMe})\}_2]^{2-}$.

	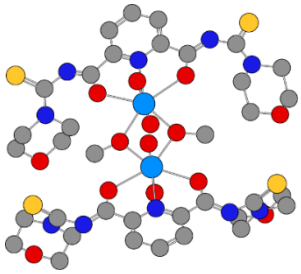	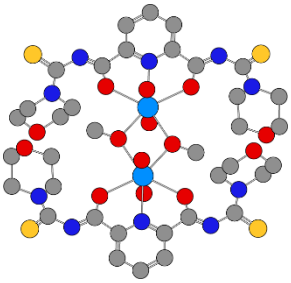	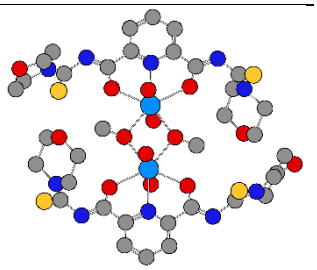
	syn,syn	*anti,syn*	*anti,anti*
E[Hartree]	-4696.2683	-4696.2727	-4696.2751
Bond lengths [Å]			
U1–O1	1.790	1.785	1.787
U1–O2	1.778	1.787	1.784
U1–O5	2.465	2.456	2.458
U1–O15	2.463	2.460	2.462
U1-N46	2.664	2.661	2.658
U1–O61	2.394	2.393	2.393
U1–O62	2.398	2.395	2.399
C2–S1	1.695	1.697	1.698
C2–N3	1.372	1.375	1.370
C4–N3	1.303	1.303	1.299
C4–O5	1.279	1.279	1.280
C2–N6	1.365	1.362	1.364
Angles (°)			
O1–U1–O2	175.5	175.9	176.8
O1–U1-N46	87.6	89.3	89.8
O1–U1–O5	88.9	89.7	88.9
O1–U1–O15	86.9	89.6	92.1
O1–U1–O61	88.8	95.9	95.2
O1–U1–O62	92.8	87.6	90.6